MECHANISMS OF NMDA RECEPTOR INHIBITION
BY MEMANTINE AND KETAMINE

by

Nathan G. Glasgow

Bachelor of Science, University of Toledo, 2010

Submitted to the Graduate Faculty of the

Kenneth P. Dietrich School of Arts and Sciences in partial fulfillment

of the requirements for the degree of

Doctor of Philosophy

University of Pittsburgh

2016

UNIVERSITY OF PITTSBURGH

DIETRICH SCHOOL OF ARTS AND SCIENCES

This dissertation was presented

by

Nathan G. Glasgow

It was defended on

April 21, 2016

and approved by

Dr. Stephen D. Meriney, Professor, Department of Neuroscience

Dr. Anne-Marie Oswald, Assistant Professor, Department of Neuroscience

Dr. Elias Aizenman, Professor, Department of Neurobiology

Dr. Michael S. Gold, Professor, Department of Anesthesiology

Dr. Stephen F. Traynelis, Professor, Department of Pharmacology, Emory University

Dissertation Advisor: Dr. Jon W. Johnson, Professor, Department of Neuroscience

MECHANISMS OF NMDA RECEPTOR INHIBITION
BY MEMANTINE AND KETAMINE

Nathan G. Glasgow, PhD

University of Pittsburgh, 2016

NMDA receptors (NMDARs), a subfamily of ionotropic glutamate receptors, have unique biophysical properties including high permeability to Ca^{2+}. Activation of NMDARs increases the concentration of intracellular Ca^{2+} that can activate a vast array of signaling pathways. NMDARs are necessary for many processes including synaptic plasticity, dendritic integration, and cell survival. Aberrant NMDAR activation is implicated in many central nervous system disorders including neurodegenerative disorders, neuronal loss following ischemia, and neuropsychiatric disorders. Hope that NMDARs may serve as useful therapeutic targets is bolstered by the clinical success of two NMDAR antagonists, memantine and ketamine. Memantine and ketamine act as open channel blockers of the NMDAR-associated ion channel, and exhibit similar IC_{50} values and kinetics. Memantine is approved for treatment of Alzheimer's disease and shows promise in treatments of Huntington's disease, and ischemia. Ketamine was initially approved for use as a general anesthetic, but has recently shown efficacy in treatment of depression and of pain. Notably, memantine is not effective in treatment of depression or pain. In addition, memantine is well tolerated, whereas ketamine induces psychotomimetic side effects. The basis for the divergent clinical profiles of memantine and ketamine is not clear. One recently-proposed hypothesis is that memantine and ketamine inhibit overlapping but distinct subpopulations of NMDARs. However, mechanisms underlying inhibition of distinct NMDAR subpopulations by memantine or by ketamine are not fully understood. We therefore examined and compared

mechanisms of inhibition by memantine and by ketamine. We also describe a novel fast perfusion system optimized for brief synaptic-like glutamate applications to lifted cells. We found that: (1) inhibition by memantine and ketamine exhibit differential dependence on duration of receptor activation and on NMDAR subtype; (2) the dependence of memantine inhibition on duration of NMDAR activation results from stabilization of a Ca^{2+}-dependent desensitized state; (3) the endogenous NMDAR open channel blocker Mg^{2+} slows the binding kinetics of both memantine and ketamine, and, unexpectedly, speeds recovery from memantine inhibition; (4) although inhibition by memantine was thought to be mediated by only the charged form of memantine, the uncharged form of memantine also binds to and inhibits NMDARs, and exhibits surprisingly slow unbinding kinetics.

TABLE OF CONTENTS

LIST OF TABLES

LIST OF FIGURES

xiii

PREFACE

The past six years training at the University of Pittsburgh has been a transformative and uplifting experience. I have benefited immeasurably from the rigorous and supportive environment created by the students, faculty, and staff of the Center for Neuroscience. There are several groups in particular that deserve my gratitude. First, I thank the current and former members of the Johnson lab who lent me their vast experience to help me perform, understand, and teach neurophysiology. Second, I thank my committee, Drs. Elias Aizenman, Anne-Marie Oswald, Michael Gold, my committee chair Dr. Steve Meriney, and my outside examiner Dr. Stephen Traynelis. My committee was always willing to provide essential and timely guidance on scientific and career goals and helped to maintain my focus towards finishing my dissertation. I owe the most to my mentor, Dr. Jon Johnson, whose patience, compassion, and brilliance has been a constant source of inspiration. I hope to be fortunate enough to assimilate much of Jon's character with mine as I continue my scientific career.

I am endlessly indebted to many beyond the Center for Neuroscience. I thank my parents for imbuing in me a sense of curiosity for the world and an appreciation of learning. I also thank my friends for keeping me grounded in this world. Most of all, I thank my fiancé, Nadia Kudla, for her ceaseless love and support, which carried me through many troubles and heightened my joys.

1.0   GENERAL INTRODUCTION

The collection of neurons and glia within our nervous system is responsible for every thought, memory, perception, and emotion we experience. Chemical neurotransmission, the communication between neurons at chemical synapses, is essential for nervous system function. Chemical neurotransmission involves release of a neurotransmitter from a presynaptic neuron and the reception of the neurotransmitter via neurotransmitter receptors present in the membrane of a postsynaptic neuron. Many types of neurotransmitter receptors have associated ion channels, which belong to a larger family of ion channels known as ligand-gated ion channels. Ligand-gated ion channels activate in response to agonist binding and allow the flux of ions across cellular membranes, thereby changing membrane voltage and/or changing the concentrations of ions in the intracellular or extracellular compartments. Changes membrane potential and in ion concentrations within a particular cellular compartment can have profound effects on cellular physiology and result in short or long lasting changes. In relation to the nervous system, ligand-gated ion channels are responsible for exciting or inhibiting postsynaptic neurons, strengthening or weakening synaptic contacts, and inducing or prohibiting gene transcription. The wide functional range of ligand-gated ion channel in the nervous system makes their involvement in central nervous system disorders virtually guaranteed. Therefore, ligand-gated ion channels are excellent targets of pharmacological modulation as potential treatments for central nervous system disorders. The work described in this dissertation focuses on understanding mechanisms

1

of inhibition of one type of neurotransmitter receptor, the *N*-methyl-D-aspartate (NMDA) receptor (NMDAR), by two clinically useful drugs, memantine and ketamine. The remainder of the introduction covers the background relevant understanding the role of NMDARs in nervous system function and in disorders, and how memantine and ketamine might act therapeutically.

1.1   BASIC PROPERTIES OF NMDA RECEPTOR FUNCTION

(Taken from **Appendix A** (Glasgow et al., 2015) with minor revisions)

Glutamate mediates the majority of fast excitatory synaptic transmission in the central nervous system. Glutamate binds to and activates ionotropic glutamate receptors (iGluRs), which open to allow cation flux across the cell membrane. iGluRs are ligand-gated ion channels composed of four subunits organized around a central ion channel. The tertiary structure of all iGluR subunits can be described as several functionally distinct domains: an extracellular N-terminal domain (NTD; or amino-terminal domain, ATD), an extracellular agonist binding domain (ABD; or ligand binding domain, LBD), a transmembrane domain (TMD) made up of 3 transmembrane regions (TMRs; M1, M3, and M4) and a reentrant loop (M2) that forms the selectivity filter, and an intracellular C-terminal domain (CTD) (**Figure 1**) (Traynelis et al., 2010).

There are four classes of iGluRs: AMPA receptors (AMPARs), kainate receptors, NMDA receptors (NMDARs), and δ receptors. Receptors of each class are formed by co-assembly of homologous subunits. Subunit composition defines receptor subtypes within each class of iGluR. Physiological properties, such as agonist potency, maximal channel open probability (P_{open}), and deactivation kinetics, can differ greatly between subtypes of each iGluR class except δ receptors,

which do not form functional receptors (Traynelis et al., 2010). Thus, control of the expression of specific iGluR subtypes can have enormous impact on synaptic function, membrane excitability, and activation of intracellular signaling cascades, each of which more broadly affects the physiology of neuronal circuits and systems. The tight developmental, regional, and subcellular regulation of iGluR subunit expression indicates that iGluR subtypes play distinct physiological roles (Cull-Candy and Leszkiewicz 2004).

NMDARs exhibit several properties that are unique among iGluRs, including: the requirement that both glutamate and a co-agonist, either glycine or D-serine, bind to activate the receptor (Johnson and Ascher 1987; Kleckner and Dingledine 1988; Lerma et al., 1990; Schell et al., 1995); very slow deactivation (Forsythe and Westbrook 1988; Lester et al., 1990; Partin et al., 1996; Swanson and Heinemann 1998; Vicini et al., 1998); high permeability to Ca^{2+} (MacDermott et al., 1986; Burnashev et al., 1992; Burnashev et al., 1995; Schneggenburger 1996); strongly voltage-dependent channel block by physiological concentrations of external Mg^{2+} (Mayer et al., 1984; Nowak et al., 1984; Ascher and Nowak 1988). Flux of Ca^{2+} through NMDARs is essential for many types of synaptic plasticity, learning and memory, and cell survival (Malenka and Bear 2004; Hardingham and Bading 2010). Conversely, aberrant NMDAR activation is implicated in neurodegenerative diseases, schizophrenia, depression, chronic and neuropathic pain, as well as neuronal loss following ischemia or stroke (Lau and Tymianski 2010; Zhou and Sheng 2013).
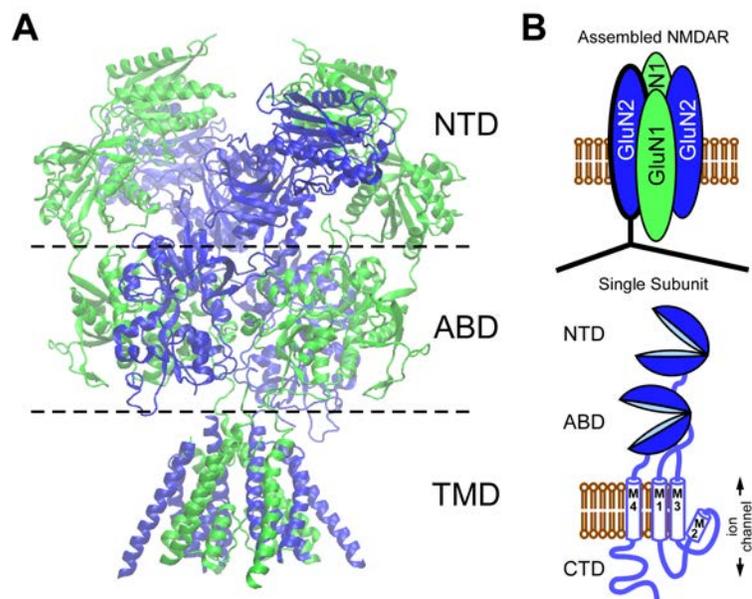
Figure 1. NMDAR structure and assembly.

A, Image of an NMDAR crystal structure of a GluN1/2B receptor (Protein Data Bank (PDB) code 4TLM (Lee et al., 2014)) is shown with GluN1 subunits in green and GluN2B subunits in blue. Dotted lines separate the functional domains of the receptor as denoted by abbreviations to the right, defined in text. **B**, Schematic diagram of an assembled receptor (upper) with an enlarged schematic diagram of a single NMDAR subunit depicting the distinct functional domains (lower). Figure was adapted from Glasgow et al. (2015) (**Appendix A**) and Johnson et al. (2015) (**Appendix B**).

1.1.1 Diversity of NMDAR subtypes

(Taken from **Appendix A** (Glasgow et al., 2015) with minor revisions)

NMDAR subunits are encoded by seven genes. One gene encodes eight GluN1 subunit splice variants, four genes encode the GluN2 subunits (GluN2A, GluN2B, GluN2C, and GluN2D), and two genes encode the GluN3 subunits (GluN3A and GluN3B). Functional NMDARs are obligate heterotetramers thought to be assembled as a combination of two GluN1 subunits and two GluN2 and/or GluN3 subunits. Most diheteromeric NMDARs contain two GluN1 subunits and two GluN2 subunits of the same type. Triheteromeric NMDARs contain two GluN1 subunits and two GluN2 or GluN3 subunits of different identities.

The NMDAR subtype is defined by the subunits present in the receptor, which impart unique properties to each receptor subtype. Most basic studies have focused on diversity of the four diheteromeric NMDAR subtypes defined by the identity of the GluN2 subunits (GluN1/2A, GluN1/2B, GluN1/2C, and GluN1/2D receptors). Many, and possibly most, native NMDARs are triheteromeric NMDAR subtypes (Luo et al., 1997; Al-Hallaq et al., 2007; Rauner and Kohr 2010; Gray et al., 2011; Tovar et al., 2013). However, until recently, few studies have addressed triheteromeric NMDAR properties (Hatton and Paoletti 2005; Rauner and Kohr 2010; Tovar et al., 2013) due to the difficulty of studying them in isolation from other NMDAR subtypes. Recently, exciting new approaches have been developed to study isolated triheteromeric NMDARs (Hansen et al., 2014; Yuan et al., 2014).

Heterologous expression systems, where a single NMDAR subtype can be unambiguously studied by expression of GluN1 and a single type of GluN2 subunits, have allowed extensive characterization of diheteromeric NMDAR subtype-dependent properties (Cull-Candy and Leszkiewicz 2004; Traynelis et al., 2010; Paoletti et al., 2013). Studies in

heterologous systems have revealed great diversity of diheteromeric NMDAR subtype-dependent properties including: deactivation kinetics (Monyer et al., 1992; Monyer et al., 1994; Vicini et al., 1998), agonist potency (Kutsuwada et al., 1992; Priestley et al., 1995; Varney et al., 1996; Erreger et al., 2007; Traynelis et al., 2010), Ca^{2+} permeability (Burnashev et al., 1995; Schneggenburger 1996), voltage dependence of channel gating (Clarke 2006; Clarke and Johnson 2008; Clarke et al., 2013), sensitivity to block by external Mg^{2+} (Monyer et al., 1994; Kuner and Schoepfer 1996), and sensitivity to endogenous inhibitors (Traynelis et al., 1995; Williams 1996; Chen et al., 1997; Paoletti et al., 1997; Traynelis et al., 1998; Paoletti et al., 2013). Expression and subcellular localization of NMDAR subunits varies by developmental stage, brain region, and cell type (Akazawa et al., 1994; Monyer et al., 1994; Sheng et al., 1994). Thus, the expression of specific NMDAR subtypes can be used to tune synapses, neurons, circuits, and systems through the great diversity of NMDAR subtype-dependent properties.

1.1.2   NMDAR desensitization and inactivation

All iGluRs exhibit receptor desensitization or inactivation, which is the reduction in current amplitude until a steady-state is reached in the continuous presence of agonist. Desensitization in NMDARs is much slower and less complete than in AMPARs and kainate receptors (Traynelis et al., 2010). Although some structural correlates of fast AMPAR and kainate receptor desensitization have been identified (Traynelis et al., 2010; Dawe et al., 2013; Meyerson et al., 2014), less is known about the structural determinants of desensitization in NMDARs. Nevertheless, there are several distinct processes that result in NMDAR desensitization have been described, including glycine-dependent desensitization, Ca^{2+}-dependent desensitization (also commonly referred to as Ca^{2+}-dependent inactivation), and glycine- and Ca^{2+}-independent

6

desensitization. Glycine-dependent desensitization results from lowered glycine affinity induced by glutamate binding, and can be avoided by raising the extracellular glycine to saturating concentrations (Mayer et al., 1989; Benveniste et al., 1990; Lerma et al., 1990; Lester et al., 1993). Ca^{2+}-dependent desensitization requires an increase in the intracellular Ca^{2+} concentration near the mouth of the NMDAR channel and results from a complex series of molecular interactions that are not fully understood (Legendre et al., 1993; Rosenmund and Westbrook 1993; Krupp et al., 1996; Medina et al., 1996; Dingledine et al., 1999). It is clear that Ca^{2+}-dependent desensitization is mediated in part through calmodulin binding to the GluN1 CTD (Ehlers et al., 1996; Ehlers et al., 1998; Zhang et al., 1998; Krupp et al., 1999). Calcineurin also plays a role in Ca^{2+}-dependent desensitization and has been shown to bind to the GluN2A CTD (Tong and Jahr 1994; Tong et al., 1995; Raman et al., 1996; Krupp et al., 2002) and may interact with calmodulin binding (Rycroft and Gibb 2004). The actin binding protein α-actinin also competes for binding with calmodulin (Wyszynski et al., 1997; Zhang et al., 1998; Krupp et al., 1999; Rycroft and Gibb 2004). Additionally, Ca^{2+}-dependent desensitization is subtype-dependent; GluN1/2A and GluN1/2D receptors exhibit Ca^{2+}-dependent desensitization, whereas GluN1/2B and GluN1/2C receptors do not (Medina et al., 1995; Krupp et al., 1996). Glycine- and Ca^{2+}-independent desensitization is mediated largely through extracellular regions in a subtype-dependent manner, especially through the NTD (Krupp et al., 1998; Villarroel et al., 1998).

1.1.3   Kinetic models of NMDAR activity

Electrophysiological recordings of ion channel activity can only capture a small fraction of the conformational states available to the channel, generally when current is flowing, or not. The

advent and perfection of single-channel recording has made it possible to analyze the stochastic

behavior of individual receptors in response to agonists and modulators (Neher and Steinbach

1978; Sigworth and Neher 1980; Hamill et al., 1981). To aid interpretation of the extremely

complex nature of single-channel recording data, kinetic schemes were adapted from enzyme

kinetic schemes to describe transitions between discrete channel states (Del Castillo and Katz

1957).

The simplest ion channel model is a two-state model with one closed (C) and one open

(O) state (**Figure 2A**). According to the law of mass action, the rate of any chemical reaction is

proportional to the product of the concentrations of the reactants, thus yielding rate constants (k_+,

k_-; **Figure 2A**) generally with units of s^{-1}. The equilibrium constant (K) is determined as the ratio

of reverse (k_-) to forward (k_+) rate constants by the equation, $K = k_-/k_+$. For Model A, K is

unitless and simply indicates the ratio of closed to open channels at equilibrium. Because

NMDARs are ligand-gated ion channels, the simplest model to describe their activity requires a

state to describe the agonist binding step that precedes channel opening (**Figure 2B**). The

forward rate of agonist-dependent transitions depends on the concentration of agonist and time

(M^{-1} s^{-1}). The agonist equilibrium dissociation constant (K_D), the agonist concentration when

agonist molecules (A) are in equilibrium with receptors bound to agonist (RA), is determined by

the equation $K_D = k_{a-}/k_{a+}$ with units of M (**Figure 2B**). Although agonist binding and channel

opening is all that is necessary to describe the simplest form of ligand-gated ion channel activity,

Model B is not sufficient to recreate the full complexity of NMDAR activity. The inclusion of

multiple agonist binding steps and of one desensitized state are necessary to predict prominent

features of NMDAR single-channel and macroscopic recordings (Clements and Westbrook 1991;

Clements et al., 1992; Edmonds and Colquhoun 1992; Lester and Jahr 1992; Lester et al., 1993)

(**Figure 2C**). Model C still is a vast oversimplification of the available NMDAR conformational states, and more detailed models are needed to relate structural and functional NMDAR states.

Banke et al. (2003) were the first to link multiple pre-open states with specific structural transitions, with GluN1 subunits mediating a fast (RA_2f) and GluN2B subunits mediating a slow (RA_2s) conformational change that preceded channel opening (**Figure 2D**). Cyclic models with structural correlates of NMDAR closed states as presented by Banke et al. (2003) (**Figure 2D**) were reproduced for GluN1/2A receptors sometimes including an additional closed and open state (Auerbach and Zhou 2005; Erreger et al., 2005; Erreger et al., 2005; Schorge et al., 2005). Models with a linear design (**Figure 2E**) without structural correlates of NMDAR closed states were shown to be equally effective in describing single-channel and macroscopic currents of GluN1/2A and GluN1/2B receptors (Popescu et al., 2004; Auerbach and Zhou 2005; Kussius and Popescu 2009; Amico-Ruvio and Popescu 2010). Multiple pre-open states have also been determined for models of GluN1/2C and GluN1/2D receptors (Dravid et al., 2008; Vance et al., 2012; Vance et al., 2013). Furthermore, cyclic and linear models have been used to provide insight into NMDAR modulation by a wide array of molecules including modulation by protons, Zn^{2+}, Ca^{2+}, and inhibition by ifenprodil and other allosteric modulators (Banke et al., 2005; Erreger and Traynelis 2008; Dravid et al., 2010; Amico-Ruvio et al., 2011; Amico-Ruvio et al., 2012; Bhatt et al., 2013; Maki and Popescu 2014).
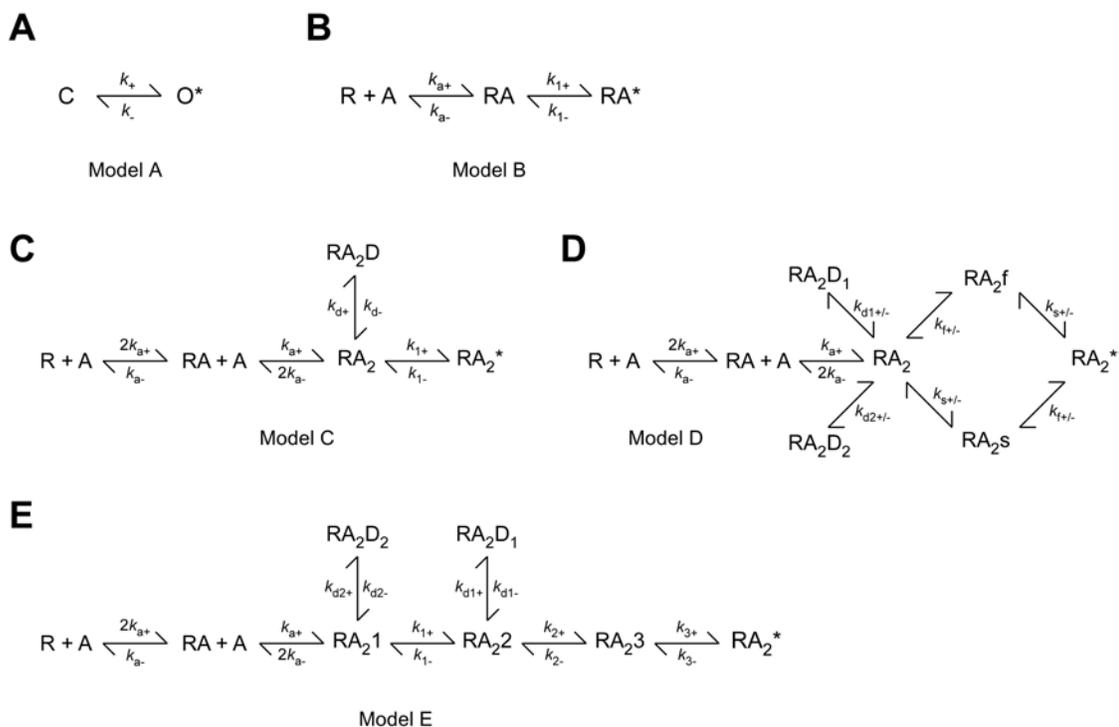
Figure 2. Kinetic models of NMDAR activation.

A, Simplest kinetic model of an ion channel transition from closed (C) to open (O*), with forward rates (k_+) depicted above the arrow and reverse rates (k_-) below the arrow. **B,** Simplest kinetic model of a ligand-gated receptor (R) that exhibits separate agonist (A) binding and opening transitions. * indicates open states. **C-E,** Kinetic models of NMDAR activation referenced in text. RA_2D, RA_2D_1, and RA_2D_2 represent desensitized states. RA_2f, RA_2s, and RA_2N (N = 1-3) represent pre-open closed states.

1.2   ROLE OF NMDA RECEPTORS IN THE CENTRAL NERVOUS SYSTEM

NMDARs are widely expressed in the central nervous system and are critical to many processes including normal development of synapses, many forms of long-term potentiation (LTP) and long-term depression (LTD) thought to be the structural basis of memory, activation of various signaling cascades, and dendritic integration (Traynelis et al., 2010; Paoletti et al., 2013). The role of NMDARs in these myriad processes will be discussed below.

1.2.1   NMDAR expression and localization

Expression of NMDAR subunits varies by age, brain region, and cell type. Obligate GluN1 subunits are expressed ubiquitously throughout life (Monyer et al., 1992; Watanabe et al., 1992; Akazawa et al., 1994; Monyer et al., 1994); however, different GluN1 isoforms have specific developmental and regional expression patterns (Laurie and Seeburg 1994; Paupard et al., 1997). GluN2 subunits follow divergent developmental expression profiles as well; GluN2B and GluN2D subunits are highly expressed embryonically and in early postnatal stages, whereas GluN2A and GluN2C subunit expression increases from birth and peaks about 2 to 3 weeks postnatally (Watanabe et al., 1992; Akazawa et al., 1994; Monyer et al., 1994). Expression of GluN3 subunits also varies regionally and developmentally (Paoletti et al., 2013). The GluN2 subunits also exhibit diverse expression patterns (Paoletti et al., 2013). In the adult cortex and hippocampus, GluN2A and GluN2B subunits are broadly expressed, whereas GluN2C and GluN2D subunit expression is thought to be restricted to interneurons (Monyer et al., 1992; Watanabe et al., 1992; Akazawa et al., 1994; Monyer et al., 1994). GluN2C and GluN2D

subunits are highly expressed in other brain regions, including the cerebellum, thalamus, and olfactory bulb (Akazawa et al., 1994; Monyer et al., 1994).

In addition to regional, developmental, and cell type-specific expression patterns, GluN2 subunits are organized by their subcellular localization. Generally, subcellular localization of NMDARs is divided on the basis of NMDARs being located within synapses (synaptic NMDARs), or outside synapses (extrasynaptic NMDARs) (Hardingham and Bading 2010; Gladding and Raymond 2011; Parsons and Raymond 2014). Some studies have shown in hippocampal and cortical pyramidal cells that GluN2A-containing receptors are predominantly expressed synaptically, whereas GluN2B-containing receptors are predominantly expressed extrasynaptically (Tovar and Westbrook 1999; Groc et al., 2006; Hardingham and Bading 2010; Papouin et al., 2012). However, other reports suggest that the division in GluN2 subunit localization is not as distinct (Thomas et al., 2006; Harris and Pettit 2007; Petralia et al., 2010). Regardless of the localization of specific NMDAR subtypes, differential localization of NMDARs synaptically and extrasynaptically has important implications in downstream signaling (Hardingham and Bading 2010; Gladding and Raymond 2011; Parsons and Raymond 2014).

1.2.2   Role of NMDARs in plasticity and neuronal signaling

NMDARs are critically involved in synaptic plasticity (Collingridge et al., 2004; Malenka and Bear 2004; Shepherd and Huganir 2007). NMDAR-dependent LTP requires the coincident activation of a pre- and postsynaptic neuron. The highly voltage-dependent block by Mg^{2+} of NMDARs allows them to act as coincident detectors: postsynaptic depolarization causes Mg^{2+} to unblock NMDARs. NMDARs are also highly permeable to Ca^{2+}, which is a powerful second messenger that signals through a vast array of signaling cascades. Therefore, unblocked

NMDARs lead to strong Ca^{2+} influx that provides a trigger to activate downstream signaling pathways. The precise amount of Ca^{2+} that enters a cell has a powerful effect on the direction of plasticity: in general, a large influx of Ca^{2+} over a short time mediates synaptic potentiation, whereas a small influx of Ca^{2+} over a long period of time mediates synaptic depression. Thus, precise control over the amount of Ca^{2+} influx in response to a stimulus is determines the direction of plastic change.

Much research over the last two decades has focused on differentiating the function of NMDARs based on their subtype, on their subcellular localization, or both (Hardingham and Bading 2010; Traynelis et al., 2010; Paoletti et al., 2013; Parsons and Raymond 2014). The NMDAR subtype can have a substantial impact on the Ca^{2+} influx during a single synaptic stimulus and during a train of stimuli. Due to subtype-dependent differences in maximal P_{open}, deactivation time course, rate and extent of desensitization, and rate of recovery from desensitization, the charge transfer, and thus the Ca^{2+} influx, differs between GluN1/2A and GluN1/2B receptors depending on the stimulus frequency, glutamate concentration, and duration of glutamate application (Erreger et al., 2005). The location of an NMDAR can also impact the Ca^{2+} influx, as synaptic NMDARs tend to be exposed to glutamate for short durations (1-2 ms) whereas extrasynaptic NMDAR tend to be exposed to glutamate for longer durations (seconds to tonically). Furthermore, the signaling cascades activated by synaptic NMDARs may differ substantially from cascades activated by extrasynaptic NMDARs (Hardingham and Bading 2010; Parsons and Raymond 2014).

Many studies have found that genetic deletion of GluN2A subunits or pharmacological inhibition of GluN2A-containing receptors blocks LTP (Sakimura et al., 1995; Sprengel et al., 1998; Zhao and Constantine-Paton 2007; Papouin et al., 2012). In contrast, deletion of GluN2B

subunits or pharmacological inhibition of GluN2B receptors blocks LTD (Liu et al., 2004; Massey et al., 2004; Brigman et al., 2010). This apparent dichotomy between GluN2A subunits mediating LTP and GluN2B subunits mediating LTD is similar to their proposed dichotomy in subunit localization between the synaptic (GluN2A) and extrasynaptic (GluN2B) compartments (Tovar and Westbrook, 1999; Papouin et al., 2012; see above). In agreement, some studies suggest that synaptic NMDARs are involved in LTP, whereas extrasynaptic NMDARs are involved in LTD induction (Katagiri et al., 2001; Massey et al., 2004; Izumi et al., 2008; Li et al., 2011; Papouin et al., 2012; Liu et al., 2013). However, the subtype and location dependence of LTP and LTD is controversial. Several studies have clearly demonstrated GluN2B subunit involvement in LTP (Barria and Malinow 2005; Berberich et al., 2005; Gardoni et al., 2009; Muller et al., 2009). The inconsistency in the GluN2 subunit dependence of LTP suggests involvement of synaptic triheteromeric GluN1/2A/2B receptors in LTP (Foster et al., 2010; Gray et al., 2011; Delaney et al., 2013; Tovar et al., 2013). Triheteromeric receptors exhibit pharmacology distinct from either GluN1/2A or GluN1/2B diheteromeric receptors (Hatton and Paoletti 2005; Hansen et al., 2014; Stroebel et al., 2014). Altered pharmacology of triheteromeric receptors could reduce subtype-selectivity of diheteromeric subtype-selective inhibitors, whereas genetic manipulations would likely still disrupt subunit-specific CTD interactions necessary for LTP or LTD. These studies suggest that the NMDAR subtype combined with the subcellular location of receptors may determine whether activated NMDARs will induce LTP or LTD.

Consistent with hypotheses of different NMDAR subtypes or differentially localized NMDARs mediating different forms of plasticity, a large literature suggests a dichotomy between signaling mediated by activation of synaptic receptors or GluN2A-containing receptors and signaling mediated by activation extrasynaptic receptors or GluN2B-containing receptors in

14

the context of cell survival and cell death (Hardingham and Bading 2010; Parsons and Raymond 2014). The idea that Ca^{2+} influx through specific subpopulations of NMDARs, defined by the NMDAR subtype or subcellular localization, elicits differential downstream signaling cascades and cellular responses is intriguing. It suggests the possibility of targeting NMDAR subpopulations in treatment of nervous system disorders, a topic that will be considered in greater detail below.

1.3 ROLE OF NMDA RECEPTORS IN CENTRAL NERVOUS SYSTEM DISORDERS

Given the critical role of NMDARs in neurotransmission, development, synaptic plasticity, and cellular signaling, it is not surprising that NMDARs are implicated in many disorders of the central nervous system (Traynelis et al., 2010; Paoletti et al., 2013; Zhou and Sheng 2013). Of particular interest to this dissertation is the involvement of NMDARs in neurodegenerative disorders, such as Alzheimer's disease and Huntington's disease, in neuronal loss following ischemic stroke, and in neuropsychiatric disorders, such as depression. The pathophysiology of each disorder is an area of active research and intense debate, and the precise role that NMDARs play in each disorder is not clearly understood.

1.3.1 NMDAR-mediated excitotoxicity

Excessive NMDAR activation, and thus excessive Ca^{2+} influx, leads to activation of cell death signaling pathways and ultimately to neuronal cell death (Lau and Tymianski 2010). This

process, known as excitotoxicity, also involves other receptors and is thought to be a common feature of neuronal loss following ischemia and in neurodegenerative diseases (Lau and Tymianski 2010; Zhou and Sheng 2013). Cognitive deficits in neurodegenerative diseases are also thought to arise from changes in protein expression, in synaptic contacts, and in the balance of excitatory and inhibitory drive (Zhou and Sheng 2013; Parsons and Raymond 2014). Further work is needed to determine the role of NMDARs in neurodegenerative disorders.

There is a large literature pertaining to the differential influence of synaptic and extrasynaptic NMDARs on excitotoxicity (Hardingham et al., 2002; Leveille et al., 2008; Papadia et al., 2008; Okamoto et al., 2009; Bordji et al., 2010; Leveille et al., 2010; Kaufman et al., 2012; Milnerwood et al., 2012; Papouin et al., 2012; Wroge et al., 2012; Zhou et al., 2013; Zhou et al., 2013). Many studies have relied on pharmacological means to specifically activate synaptic or extrasynaptic NMDARs (Hardingham et al., 2002; Leveille et al., 2008; Papadia et al., 2008; Okamoto et al., 2009; Leveille et al., 2010; Kaufman et al., 2012; Milnerwood et al., 2012; Wroge et al., 2012). Specific activation of synaptic NMDARs in neuronal cultures is achieved through application of 4-aminopyridine (4-AP), a K^+ channel antagonist that increases release of neurotransmitter and frequency of action potentials, and/or bicuculline (bic), a $GABA_A$ receptor antagonist that also increases action potential frequency (Hardingham et al., 2002). Preferential activation of extrasynaptic NMDARs involves initial blockade of synaptic NMDARs during 4-AP and/or bic applications with MK-801, an NMDAR open channel blocker with especially slow unblocking kinetics such that it is unlikely to unblock during the course of the experiments (Huettner and Bean, 1988; but see McKay et al., 2013). After 4-AP and/or bic and MK-801 washout from the bath, NMDA is then bath applied to activate the remaining presumed extrasynaptic NMDARs that were spared from inhibition by MK-801 (Hardingham et al., 2002).

Using these and similar methods, many studies have demonstrated that activation of synaptic NMDARs in neuronal cultures resulted in increased signaling to cell survival pathways and neuroprotection from excitotoxic insults (Hardingham et al., 2002; Leveille et al., 2008; Papadia et al., 2008; Bordji et al., 2010; Leveille et al., 2010). In contrast, activation of extrasynaptic NMDARs in neuronal cultures resulted in decreased cell survival signaling, increased signaling to cell death pathways, and cell death in response to an excitotoxic insult. Notably however, several studies have shown in neuronal cultures or acute slices that synaptic NMDARs are necessary (Zhou et al., 2013; Zhou et al., 2013) and in some studies sufficient (Papouin et al., 2012; Wroge et al., 2012) for excitotoxicity. Additionally, the NMDAR subtype may play a role in excitotoxicity, with GluN2A-containing receptors signaling for cell survival, and GluN2B-containing receptors signaling for cell death (Liu et al., 2007; Martel et al., 2009; Martel et al., 2012; but see von Engelhardt et al., 2007; Papouin et al., 2012; Zhou et al., 2013a). Many studies suggest differential and complicated signaling depending on NMDAR subtype and subcellular localization. In addition, many studies have shown differential signaling of synaptic and extrasynaptic NMDARs in animal models of Alzheimer's disease and Huntington's disease (Okamoto et al., 2009; Bordji et al., 2010; Milnerwood et al., 2010; Kaufman et al., 2012; Milnerwood et al., 2012; Talantova et al., 2013; Dau et al., 2014; Tu et al., 2014). Therefore, targeting subpopulations of NMDARs may be especially effective in the treatment of central nervous system disorders.

1.3.2   NMDARs as targets for drug therapy

The involvement of NMDARs in the pathophysiology of many central nervous system disorders has driven hope that NMDARs would serve as useful targets for pharmacotherapy (Strong et al.,

2014; Johnson et al., 2015; Zhu and Paoletti 2015). Despite much effort, thus far only a few NMDAR antagonists display clinical efficacy, including memantine and ketamine (Lipton 2006; Parsons et al., 2007; Krystal et al., 2013; Johnson et al., 2015; Kavalali and Monteggia 2015). Memantine and ketamine act as NMDAR open channel blockers, which are thought to bind and unbind only when the channel is open, with similar IC_{50} values and kinetics at NMDARs. Mechanisms of NMDAR open channel block by memantine and ketamine are discussed below. This section is focused on the effectiveness of memantine and ketamine on central nervous system disorders and on evidence that memantine and ketamine act primarily on NMDARs.

Memantine is approved for the treatment of Alzheimer's disease, and shows promise in the treatment of other disorders including Huntington's disease, dementia, and ischemia (Witt et al., 2004; Emre et al., 2010; Dau et al., 2014; Kafi et al., 2014). Memantine acts to slow the progression of Alzheimer's disease by about 6 months (Reisberg et al., 2003; Doody et al., 2004; Winblad et al., 2007). How memantine acts to slow the progression of Alzheimer's disease, and how it acts in other disorders, are areas of active research and hotly debated.

Ketamine was initially approved for clinical use as a dissociative anesthetic, and has recently shown efficacy in the treatment of depression and pain (Prommer 2012; Persson 2013; Abdallah et al., 2015; Kavalali and Monteggia 2015). There is great interest in understanding how ketamine elicits rapid relief of the symptoms of major depression, relief that can last up to two weeks from a single sub-anesthetic dose (Abdallah et al., 2015; Kavalali and Monteggia 2015). The rapid antidepressant effects of ketamine are in contrast to traditional antidepressant pharmacotherapy that takes weeks to show an effect on symptoms of depression (Kupfer et al., 2012). A significant drawback to ketamine use is the development of psychotomimetic side effects even at doses similar to those used for antidepressant effects (Krystal et al., 1994; Krystal

18

et al., 2003). Memantine, although relatively free from side effects, is not effective in treating depression or pain (Alviar et al., 2011; Pringle et al., 2012; Sani et al., 2012). How can two drugs that seem to act similarly at the same receptor have such divergent clinical effects?

There are several hypotheses for why memantine and ketamine are able to act similarly at NMDARs while having divergent clinical effects and behavioral effects. These explanations include: (1) differences in pharmacokinetics, since ketamine has much faster pharmacokinetics than memantine; (2) differential action at non-NMDAR targets of memantine and ketamine; (3) differential action of active drug metabolites as a result of degradation; and (4) subtle differences between memantine and ketamine mechanisms of inhibition at NMDARs that result in differential inhibition of subpopulations of NMDARs. The true explanation is likely to be a result of multiple factors, which have been discussed in Johnson et al. (2015) (Appendix B). There we argue that differential clinical and behavioral effects of memantine and ketamine arise largely from inhibition of distinct subpopulations of NMDARs. The work of this dissertation investigates whether, and if so how, memantine and ketamine inhibit distinct subpopulations of NMDARs and how inhibition of NMDARs differs between memantine and ketamine. Thus, the remainder of the introduction focuses on mechanisms of NMDAR inhibition by memantine and ketamine.

1.4   BASIC MECHANISMS OF ACTION OF MEMANTINE AND KETAMINE

1.4.1   Properties of open channel blockers

There is a long history of studying mechanisms of open channel block of ion channels as a means of understanding channel behavior (Hille 2001). In the last few decades interest in open channel blockers has shifted towards use in treatment of central nervous system disorders. Open channel blockers bind within the ion channel and prevent, or block, the flow of ions through the channel. Open channel blockers typically exhibit voltage dependence, a characteristic that is related to the depth of their binding site within the membrane voltage field. Another prominent feature of open channel blockers is their use dependence. In particular, open channel blockers require channel opening in order to bind and unbind. Open channel blockers can generally be categorized as sequential or "foot in the door" blockers (**Figure 3A**), and trapping blockers (**Figure 3B**). When bound, sequential blockers prevent channel closure, and thus upon removal of agonist, the channel must first return to an open unblocked state before drug can unbind, allowing receptor deactivation (**Figure 3A**). In contrast, after trapping blockers bind, the channel is able to close, trapping the blocker inside the channel until the blocked channel opens again and the blocker unbinds (**Figure 3B**).
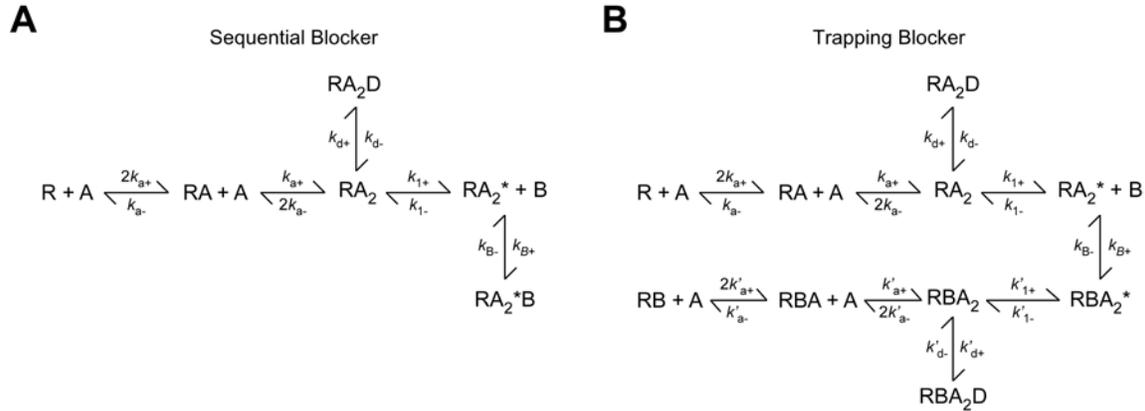
Figure 3. Kinetic models of open channel block of ligand-gated receptors.

A, Kinetic model of a sequential blocker (B), which can bind and unbind only from the channel open state and prevents channel closure while bound. **B**, Kinetic model of a trapping blocker, which can bind and unbind only from the channel open state, but which can be trapped upon channel closing allowing the channel to enter all the closed states available to the receptor. Rates in the presence of blocker are denoted as k'.

The nature of inhibition modeled by simple sequential channel block models predicts features that are experimentally verifiable. First, if agonist is removed when the blocker is bound to the receptor, the blocker must unbind before the channel can deactivate and unbind agonist. Therefore, the receptor must pass through an open state before deactivating, which typically presents as a measurable tail-current. Second, related to the idea that sequential blockers must unbind before agonist can unbind, if agonist was reapplied after a sufficient time for complete unbinding, there should be no evidence of inhibition with a sequential blocker. Third, the IC_{50} of sequential blockers, necessarily depends on P_{open}, with the IC_{50} inversely proportional to P_{open}. Johnson and Qian (2002) derived equations to develop this idea and to develop other quantitative tools to probe the nature of blocker inhibition. Briefly, they derive the equation, $IC_{50} =$

21

$K_d(P_{O+B}/P_{O-B})$, where K_d is the equilibrium dissociation constant of a channel blocker, P_{O+B} is the probability of a channel being open with blocker bound, and P_{O-B} is the probability of a channel being open without blocker bound, or P_{open}. With a sequential blocker, the P_{O+B} is 1, since any blocked channels are necessarily open. Therefore, the IC_{50} must change linearly as a function of the P_{O-B}. For trapping channel blockers the situation is more complicated. A model where the rates in the presence of blocker are identical to the rates in the in absence of blocker are known as symmetrical models. Symmetrical models predict that blockers inhibit current through the channel only by blocking the pore. For symmetrical models, where the presence of blocker has no effect on the rates of channel transitions, P_{O+B} is always equal to P_{O-B}. Therefore, in symmetrical models of trapping block, $IC_{50} = K_d$ regardless of P_{open}. However, if the trapping blocker does alter rates of channel transitions, then P_{O+B} is typically not equal to P_{O-B}, and $IC_{50} \neq K_d$. The direction of change in IC_{50} in relation to K_d depends on whether the presence of blocker increases or decreases P_{O+B} relative to P_{O-B}.

Every NMDAR open channel blocker that has been examined, with the exception of Mg^{2+}, has been shown to alter rates of channel transitions while the blocker was bound (Johnson and Qian 2002; Sobolevskii and Khodorov 2002; Blanpied et al., 2005; Barygin et al., 2009). Therefore, the models are asymmetrical and the mechanism of inhibition of open channel blockers arises in part from changing P_{O+B}, in addition to blocking ion permeation through the pore. The impact a blocker has on stabilizing or destabilizing open states, closed states, or desensitized states is of critical importance to the general mechanism of inhibition by the drug. Uncovering the structural determinants underlying receptor states stabilized or destabilized by the presence of blocker could have broad impact on our understanding of channel gating, the architecture of open, closed, and desensitized states, and on drug design.

1.4.2   Inhibition of NMDARs by memantine and ketamine

Memantine and ketamine are trapping NMDAR open channel blockers. Memantine is classified as a partial trapping blocker, because a fraction of the memantine inhibition recovers in the absence of agonist, whereas ketamine is a nearly full trapping blocker (Blanpied et al., 1997; Sobolevsky et al., 1998; Mealing et al., 1999; Kotermanski et al., 2009). The IC_{50} values of memantine and ketamine are similar and moderate, in the range of 0.5 to 2 μM for memantine and ketamine, with ketamine typically having ~2-fold lower IC_{50} value (Parsons et al., 1995; Kotermanski and Johnson 2009; Kotermanski et al., 2009; Emnett et al., 2013). Binding and unbinding kinetics of memantine and ketamine are also intermediate and similar, with ketamine having slightly slower kinetics (but see Chapter 4). The majority of memantine and ketamine molecules carry a +1 charge at physiological pH (Dravid et al., 2007). Memantine and ketamine are thought to bind to a site overlapping with the Mg^{2+} binding site, referred to here as the deep site (**Figure 4**). Asparagine residues at the tips of the M2 reentrant loop of each subunit that coordinate Mg^{2+} binding, known as the N-site asparagines, are critical for memantine and ketamine binding (Yamakura et al., 1993; Kashiwagi et al., 2002; Chen and Lipton 2005). There is also evidence that memantine binds to a second site on NMDARs (Blanpied et al., 1997; Sobolevsky and Koshelev 1998; Sobolevsky et al., 1998; Chen and Lipton 2005; Kotermanski et al., 2009), and that ketamine can affect channel function without entering the channel from the external side of the membrane (Orser et al., 1997). Nevertheless, due to their positive charge and binding deep within the membrane voltage field, inhibition by memantine and ketamine is highly voltage-dependent (Parsons et al., 2007; Johnson et al., 2015); however, inhibition by memantine and ketamine is less voltage-dependent than inhibition by Mg^{2+} due to its +2 charge

23

(Kotermanski and Johnson 2009; Otton et al., 2011; Nikolaev et al., 2012). Overall, inhibition by

memantine and ketamine exhibit properties expected of trapping blockers.
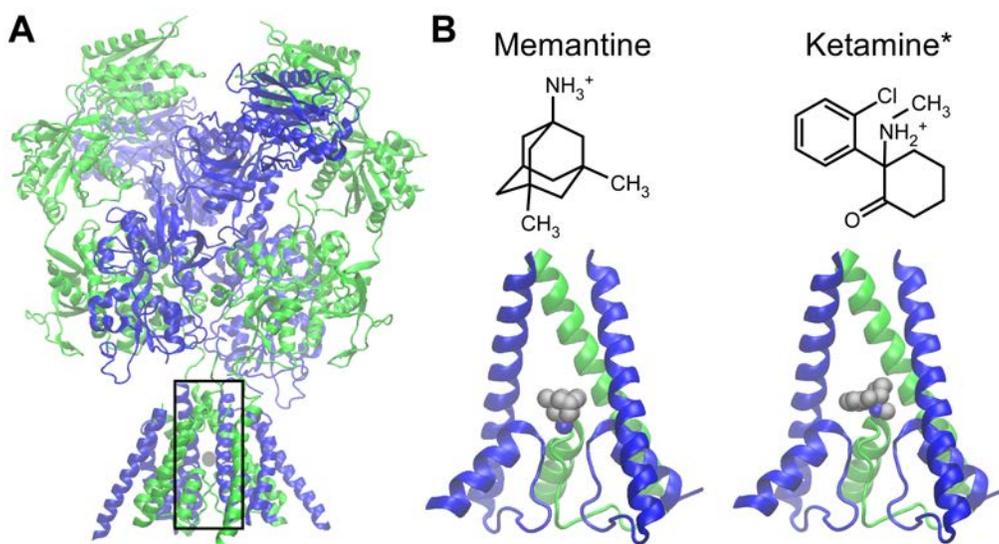
Figure 4. Memantine and ketamine binding at the deep site.

A, NMDAR crystal structure (PDB code 4TLM) is shown with a gray dot at the approximate location of Mg^{2+}, memantine, and ketamine binding sites. GluN1 subunits are in green and GluN2 subunits are in blue. The black box indicates the area of the receptor expanded in **B**. **B**, Top, the structure of memantine (left) and ketamine (right) depicted with charged nitrogen atoms. *, ketamine, which has two enantiomers ((+) and (-)ketamine), is depicted without chirality in this planar representation. Bottom, a view of the channel region of an NMDAR composed of GluN1 and GluN2A subunits with memantine (left) and (-)ketamine (right) blocking the channel. The structure of the NMDAR channel region is based on the homology model from Siegler Retchless et al., (2012); the memantine structure is from www.edinformatics.com; the (-)ketamine structure is from PDB code 4F8H (Pan et al., 2012). Although, the orientation of memantine and ketamine relative to the channel during block is not known, we oriented the drugs with their charged nitrogen atoms (blue) close to the N-site asparagines. Figure adapted from Johnson et al., (2015) (Appendix B).

Many *in vitro* studies of memantine and ketamine have been performed in the absence of Mg^{2+}. However, Mg^{2+} reduces the potency of memantine and ketamine in an NMDAR subtype-dependent manner (Kotermanski and Johnson 2009; Otton et al., 2011; Nikolaev et al., 2012). In $0\ Mg^{2+}$, memantine and ketamine display only weak NMDAR subtype-selectivity (Dravid et al., 2007; Kotermanski and Johnson 2009). The Mg^{2+} binding site overlaps with the memantine and ketamine binding sites. Thus, 1 mM Mg^{2+} increases the memantine and ketamine IC_{50} values through competition for the same binding site. NMDAR subtype dependence of inhibition arises because GluN1/2A and GluN1/2B receptors are more sensitive to block by Mg^{2+} than GluN1/2C and GluN1/2D receptors (Monyer et al., 1994; Kuner and Schoepfer 1996). Therefore, the memantine and ketamine IC_{50} values increase more with GluN1/2A and GluN1/2B receptors than with GluN1/2C and GluN1/2D receptors (Kotermanski and Johnson 2009). Importantly, the Mg^{2+}-induced NMDAR subtype dependence of memantine occurs over the range of memantine concentrations in the serum and cerebrospinal fluid from Alzheimer's disease patients (Parsons et al., 2007). To the best of our knowledge, the ketamine concentration in serum required to achieve rapid antidepressant effects is not known. The finding that Mg^{2+} induces NMDAR subtype-selectivity of memantine and ketamine inhibition suggests that the drugs' beneficial actions in treatment of disease could arise in part through inhibition of GluN2C- and GluN2D-containing receptors.

One clear distinction between memantine and ketamine inhibition of NMDARs is the ability of memantine, but not ketamine, to bind to a second site on NMDARs (Blanpied et al., 1997; Sobolevsky and Koshelev 1998; Sobolevsky et al., 1998; Chen and Lipton 2005; Kotermanski et al., 2009). No NMDAR structures are resolved with an open channel blocker (Karakas and Furukawa 2014; Lee et al., 2014). Mutational studies have identified residues near

the channel gate and the extracellular portion of the M3 TMR that influence inhibition by memantine (Kashiwagi et al., 2002; Chen and Lipton 2005; Limapichat et al., 2013). It is not clear whether these residues interact directly with memantine, since modifications near the channel gate can affect inhibition by other open channel blockers thought only to bind at the deep site (Yuan et al., 2005). Evidence of memantine binding to the second site is not direct, and the consequences of memantine binding at the second site are not well understood.

Multiple lines of evidence support the existence of the second memantine binding site. First, the time course of recovery from inhibition by memantine is slows with increasing concentrations of memantine (Blanpied et al., 1997; Sobolevsky and Koshelev 1998; Sobolevsky et al., 1998; Parsons et al., 2007). Specifically, the weight of the slow exponential component of recovery from inhibition increases with increasing memantine concentration (Sobolevsky and Koshelev 1998; Sobolevsky et al., 1998). This suggests that memantine binds to a lower affinity site than the deep site and that binding to the second site is responsible for slow recovery from inhibition. At low memantine concentrations, inhibition is primarily from the deep site that exhibits a low IC_{50} value, and recovery from inhibition is relatively fast. Memantine exhibits slow recovery from inhibition at high concentrations, where significant binding to the second high IC_{50} site occurs. A site with low affinity and slow unbinding kinetics is paradoxical: as K_d increases, so too should the unbinding rate. Of course, the binding rate could also decrease, but generally binding rates are relatively constant. There is no evidence that the time course of recovery from inhibition by ketamine changes with ketamine concentration. Second, previous reports demonstrate that memantine can bind and unbind in the absence of agonist (Blanpied et al., 1997; Sobolevsky et al., 1998; Kotermanski et al., 2009). This observation led to the hypothesis that the second site is superficial to the channel gate, as opposed to the deep site,

which is internal to the channel gate. Memantine inhibition at this superficial site has a high IC_{50} (IC_{50} ~80 - 180 μM) when measured in the absence of agonist and has relatively slow unbinding kinetics (>2 s or minutes), which is consistent with the effect on unbinding kinetics (Blanpied et al., 1997; Sobolevsky et al., 1998; Kotermanski et al., 2009). Ketamine does not inhibit without NMDAR activation, suggesting that it inhibits NMDARs only at the deep site does not bind to any superficial site (Kotermanski et al., 2009). Third, memantine binding in the absence of agonist at the second site exhibits weaker voltage dependence than binding at the deep site (Blanpied et al., 1997; Kotermanski et al., 2009). However, other studies have concluded that memantine binding at the second site depended strongly on voltage (Sobolevsky and Koshelev 1998; Sobolevsky et al., 1998). The experimental design between studies was quite different, and in principle, strong and weak voltage dependence could be consistent with memantine binding to the same second site. Therefore, through multiple indirect lines of evidence, it is likely that memantine binds to the deep site and a second site on NMDARs, whereas ketamine binds to only the deep site.

Many open questions remain about memantine inhibition, including where the second site is located, how memantine inhibits at the second site, whether memantine inhibition at the second site is NMDAR subtype-dependent, and whether Mg^{2+} affects inhibition at the second site. Answering these questions is essential to understanding the therapeutic role, if any, of memantine binding to the second site. The existence of a second site for memantine, but not for ketamine, remains one of the clearest distinctions between memantine and ketamine inhibition of NMDARs. It is unclear whether this distinction plays a role in the differential clinical and behavioral effects of memantine and ketamine.

1.4.3 Memantine and ketamine inhibit distinct subpopulations of NMDARs

Another distinction between memantine and ketamine may be in their ability to inhibit distinct subpopulations of NMDARs. There has been much interest in the hypothesis that memantine inhibits extrasynaptic NMDARs more potently than synaptic NMDARs (Leveille et al., 2008; Papadia et al., 2008; Okamoto et al., 2009; Milnerwood et al., 2010; Xia et al., 2010; Kaufman et al., 2012; Wild et al., 2013; Dau et al., 2014; Wu and Johnson 2015). Many studies have shown that memantine inhibits synaptic NMDARs less than extrasynaptic NMDARs, leading to the hypothesis that memantine provides therapeutic benefit through differential inhibition of NMDAR subpopulations (Leveille et al., 2008; Papadia et al., 2008; Okamoto et al., 2009; Milnerwood et al., 2010; Xia et al., 2010; Kaufman et al., 2012; Wild et al., 2013; Dau et al., 2014; Wu and Johnson, 2015; but see Wroge et al., 2012; Emnett et al., 2013; Zhou et al., 2013b). This hypothesis in part explains how memantine can provide neuroprotection while producing relatively few side effects. As described above, there is a proposed dichotomy between the consequences of synaptic and extrasynaptic NMDAR activity, with synaptic NMDAR activity promoting cell survival and extrasynaptic NMDAR activity leading to cell death. Accordingly, memantine is hypothesized to inhibit cell-death signaling mediated by extrasynaptic NMDAR activation, while maintaining much of synaptic NMDAR activity for normal neurotransmission and cell survival signaling. In contrast, ketamine is hypothesized to mediate its rapid anti-depressant effects through inhibition of synaptic NMDARs (Autry et al., 2011; Nosyreva et al., 2013; Gideons et al., 2014). It is not clear whether memantine and ketamine inhibit synaptic and extrasynaptic NMDARs differently (Emnett et al., 2013; Gideons et al., 2014). A recent study suggests that in 1 mM Mg^{2+}, but not in 0 Mg^{2+}, a difference between memantine and ketamine inhibition of synaptic NMDARs was revealed (Gideons et al., 2014). In

29

partial agreement, a study comparing inhibition by memantine and ketamine in 0 Mg^{2+} demonstrated no difference between memantine and ketamine inhibition of synaptic or extrasynaptic NMDARs (Emnett et al., 2013). Therefore, it is unclear whether memantine and ketamine exhibit differential inhibition of NMDAR subpopulations. Furthermore, it is unclear by which mechanism memantine or ketamine may differentially inhibit synaptic and extrasynaptic NMDARs.

Of the many potential differences between synaptic and extrasynaptic NMDARs, there are only a few that might serve as a basis for differential inhibition by an open channel blocker. First, as discussed above, the NMDAR subtypes expressed synaptically and extrasynaptically are very likely to differ. Notably, the studies where memantine or ketamine exhibited differential inhibition of synaptic and extrasynaptic NMDARs were conducted in cells that likely only expressed GluN2A and GluN2B subunits (Leveille et al., 2008; Milnerwood et al., 2010; Xia et al., 2010; Kaufman et al., 2012; Dau et al., 2014; Gideons et al., 2014). Since memantine and ketamine NMDAR subtype-selectivity between GluN1/2A and GluN1/2B receptors is weak even in 1 mM Mg^{2+}, NMDAR subtype is not an obvious candidate in differential inhibition. Second, the concentration of glutamate (~1 mM) that activates synaptic NMDARs is likely to differ substantially from the concentration of glutamate (sub-μM to μM) that activates extrasynaptic NMDARs. There are conflicting data about whether inhibition by memantine depends on the concentration of glutamate (Chen et al., 1992; Chen et al., 1997; Gilling et al., 2007; Gilling et al., 2009). To our knowledge, no studies have investigated the impact of glutamate concentration on inhibition by ketamine. Third, the duration of synaptic NMDAR exposure to glutamate is likely to be very brief (~1-2 ms), whereas the duration of extrasynaptic NMDAR exposure to glutamate is likely to be much longer (seconds or tonically). Although no studies have directly

investigated whether the duration of glutamate exposure affects inhibition by NMDAR open channel blockers, a recent report suggests that memantine inhibition increases with increasing intensity of synaptic stimulation (Wild et al., 2013). Whether inhibition by memantine and ketamine depend on these mechanisms is of great importance in understanding how each drug acts.

2.0   WHOLE-CELL PATCH-CLAMP ANALYSIS OF RECOMBINANT NMDA RECEPTOR PHARMACOLOGY USING BRIEF GLUTAMATE APPLICATIONS

Glasgow N. G. and Johnson J. W. (2014). "Whole-cell patch-clamp analysis of recombinant NMDA receptor pharmacology using brief glutamate applications." Methods Mol Biol 1183: 23-41.(in email attachment)

2.1   OVERVIEW

NMDA receptors (NMDARs) are ionotropic glutamate receptors that are essential for synaptic plasticity, learning and memory. Dysfunction of NMDARs has been implicated in many nervous system disorders; therefore, pharmacological modulation of NMDAR activity has great therapeutic potential. However, given the broad physiological importance of NMDARs, modulating their activity often has detrimental side effects precluding pharmaceutical use of many NMDAR modulators. One approach to possibly improve the therapeutic potential of NMDAR modulators is to identify compounds that modulate subsets of NMDARs. An obvious target for modulating NMDAR subsets are the many NMDAR subtypes produced through different combinations of NMDAR subunits. With seven identified genes that encode NMDAR subunits, there are many neuronal NMDAR subtypes with distinct properties and potentially differential pharmacological sensitivities. Study of NMDAR subtype-specific pharmacology is

32

complicated in neurons, however, because most neurons express at least three NMDAR subtypes. Thus, use of an approach that permits study in isolation of a single receptor subtype is preferred. Additionally, the effects of drugs on agonist-activated responses typically depend on duration of agonist exposure. To evaluate drug effects on synaptic transmission, an approach should be used that allows activation of receptor responses as brief as those observed during synaptic transmission, both in the absence and presence of drug. To address these issues, we designed a fast perfusion system capable of (1) delivering brief (~5 ms) and consistent applications of glutamate to recombinant NMDARs of known subunit composition, and (2) easily and quickly (~5 seconds) changing between glutamate applications in the absence and presence of drug.

2.2   INTRODUCTION

There is great interest in pharmacologically modulating ligand-gated ion channels to augment nervous system function or alleviate aberrant activity potentially underlying nervous system disorders. The whole-cell patch-clamp technique is essential in understanding how drugs affect ligand-gated ion channel function, cell physiology, and the nervous system under normal and pathological conditions. Due to the great diversity of subtypes within each ligand-gated ion channel family, pharmacological analysis of a particular ligand-gated ion channel using native cells is complicated. Furthermore, the mechanisms underlying drug actions on ligand-gated ion channels may depend upon the concentration and duration of agonist exposure to receptors. Therefore, expression of recombinant ligand-gated ion channels in mammalian cell lines in conjunction with a fast perfusion system designed to deliver brief agonist applications is very

useful in understanding how drugs affect ligand-gated ion channel function. Here we describe a method for whole-cell patch-clamp analysis of ligand-gated ion channel pharmacology that allows precise control of (1) the receptor subunit composition, (2) the agonist concentration, and (3) the duration of agonist exposure to receptors. Our method also allows brief application of agonist in the absence and presence of drug to the same cell. Here, we demonstrate use of the system to investigate inhibition of recombinant NMDARs during brief glutamate applications.

NMDARs are ionotropic glutamate receptors that exhibit voltage-dependent Mg^{2+} block, are highly Ca^{2+} permeable, and deactivate slowly. These properties contribute to the importance of NMDARs to cell survival, synaptic plasticity, and many forms of learning and memory (Traynelis et al., 2010). Aberrant activation of NMDARs is implicated in neurodegenerative diseases, ischemia, depression, and neuropathic pain (Barnham et al., 2004; Pittenger et al., 2007; Collins et al., 2010; Lau and Tymianski 2010; Autry et al., 2011; Duman and Aghajanian 2012). Pharmacological inhibition of NMDARs is considered to have great therapeutic potential in treating these disorders (Traynelis et al., 2010), although broad inhibition of NMDARs often results in undesirable side effects (Palmer 2001; Lipton 2004). Thus, identification of NMDAR antagonists selective for NMDARs that may be involved in a pathological state while preserving the function of NMDARs underlying normal function may be vital for successful pharmacological therapy (Lipton 2004; Lipton 2006; Paoletti et al., 2013).

NMDARs are heterotetramers composed of two GluN1 subunits either with two GluN2 subunits or with one GluN2 and one GluN3 subunit (Traynelis et al., 2010). There is a single gene that encodes eight splice variants of the GluN1 subunit, four genes that encode four GluN2 subunits (GluN2A, GluN2B, GluN2C and GluN2D), and two genes that encode two GluN3 subunits (GluN3a and GluN3B). Different combinations of GluN1, GluN2, and GluN3 subunits

give rise to NMDAR subtypes with distinct properties. Combinations that include two identical GluN2 subunits form diheteromeric NMDARs (e.g. GluN1/2A) and combinations that include either two different GluN2 subunits, or mixtures of GluN2 and GluN3 subunits, form triheteromeric NMDARs (e.g. GluN1/2A/2B) (Traynelis et al., 2010; Paoletti et al., 2013). In principal cells in the cortex, at least 3 NMDAR subtypes, including GluN1/2A, GluN1/2B, and GluN1/2A/2B, are expressed and can be found postsynaptically (Gladding and Raymond 2011; Paoletti et al., 2013). Consequently, it is difficult to study synaptic NMDAR subtype-specific pharmacology in neurons. Given this difficulty, we emulate synaptic release of glutamate using brief glutamate applications to tsA201 cells expressing recombinant GluN1/2A or GluN1/2B receptors. This approach allows pharmacological assessment of NMDARs with known, uniform subunit compositions. The methods described in this chapter provide a powerful approach to studying ligand-gated ion channel currents in response to brief agonist applications in the absence and presence of many types of drugs.

2.3   MATERIALS

2.3.1   Cell Culture and Transfection

1. tsA201 cell culture medium: DMEM (Life Technologies) supplemented with 10% fetal bovine serum (FBS; Atlanta Biologics) and 1% Glutamax (Life Technologies).

2. Serum-free tsA201 cell culture medium: DMEM supplemented with 1% Glutamax.

3. tsA201 cells (The European Coalition of Cell Cultures, ECACC) are plated on 15 mm glass coverslips (Carolina Biological) in 35 mm petri dishes (BD Falcon).

4. cDNAs encoding the rat GluN1-1a (GenBank X63255 in pCDM8 vector), GluN2A (GenBank M91561 in PCDM8 vector), and GluN2B (GenBank M91562 in pCDNA1 vector) subunits are cotransfected with cDNA for enhanced green fluorescent protein (eGFP) to identify successfully transfected cells.

5. FuGene 6 Transfection Reagent (Promega).

6. D,L-2-amino-5-phosphonopentanoate (AP5) and 7-chlorokynurenic acid (7-CKA), competitive NMDAR antagonists (Tocris).

2.3.2 Fast Perfusion System

1. Solution reservoirs are 30 ml syringes (BD Biosciences) attached to an in-house fabricated height adjustable bracket.

2. Solution flow from reservoirs is controlled by clamping silicone tubing (A-M Systems, Inc.) in solenoid pinch valves (NResearch Inc.).

3. Polyethylene tubing (PE 160, Becton Dickinson) is used to connect silicone pinch valve tubing to 2 to 1 Y connectors (Value Plastics, Inc., Y210-6) (*see* **Note 1**).

4. Polyethylene tubing (PE 50) connects Y connectors (*see* **Note 1**) to silicone tubing (outside diameter 1.2 mm and inside diameter 0.64 mm) that is attached to the back ends of individual square capillary glass (barrels) (Warner Instruments, SG800-5) with outside diameter 0.84 mm and inside diameter 0.6 mm.

5. Four barrels are aligned and glued (Krazy Glue) into an in-house fabricated barrel holder made from a single piece of aluminum, precisely shaped to cup four barrels (*see* **Note 2**).

6. The barrel holder is attached through an in-house fabricated barrel holder arm to the shaft of a stepper motor (Pacific Scientific, Powermax II SIGMAX M21). The barrel holder

arm should give the barrels a ~1" radius from the center of the stepper motor shaft so that stepper motor rotation translates to a nearly linear barrel movement.

7. Stepper motor rotation is controlled by a microstepping power supply (Precision Motor Control, LNII Series) set to 50,000 microsteps/revolution (*see* **Note 3**). Barrel movements are accomplished by smoothly accelerating and decelerating the frequency of brief voltage pulses sent out from a computer parallel port using software (barrel movement software) written in Basic and running in FreeDOS (www.freedos.org) (*see* **Note 4**).

8. Although the fast perfusion system is depicted and described with only two separate solutions flowing through barrel 1, 2, and 3, it is possible to have as many solutions as is experimentally necessary by using an appropriate manifold.

2.3.3 Whole-Cell Recordings

1. The external, control solution contains: 140 mM NaCl, 2.8 mM KCl, 1 mM $CaCl_2$, 10 mM HEPES, 10 μM EDTA, and 100 μM glycine (*see* **Note 5**). Adjust pH to 7.2 ± .05 with NaOH, and adjust osmolality to 290 ± 10 mOsmol/kg with sucrose.

2. The pipette solution contains: 130 mM CsCl, 10 mM BAPTA, 10 mM HEPES. Adjust pH to 7.2 ± 0.05 with CsOH. Osmolality should be 275 ± 10 mOsmol/kg.

3. Recording pipettes are fabricated using borosilicate glass (with filament) with an outer diameter of 1.5 mm and an inner diameter of 0.86 mm (Sutter Instrument Company) pulled on a P-97 Flaming/Brown micropipette puller (Sutter Instrument Company) and lightly fire-polished.

4. Cells are imaged with an inverted fluorescence microscope with an eGFP filter set (Zeiss). Patch-clamp recordings are made while imaging cells and the recording pipette using a Retiga EXi Fast 1394 digital camera (QImaging).

5. Voltage-clamp current recordings are made with an Axopatch 200B amplifier (Molecular Devices) with a CV 203BU headstage (Molecular Devices) attached to a PatchStar micromanipulator (Scientifica) and digitized with a Digidata 1440A A/D converter (Molecular Devices).

2.4   METHODS

Brief synaptic-like agonist applications to recombinant ligand-gated ion channels expressed in tsA201 cells during whole-cell recording can be achieved using the fast perfusion system described in **Section 2.3.2** (*see* **Figure 5**). To emulate synaptic neurotransmitter release, the fast perfusion system must achieve brief agonist applications. Brief agonist applications to the entire cell under study are facilitated by "lifting" cells from the coverslip on which they are cultured. The fast perfusion system must also allow easy changes of the solutions flowing through barrels to allow responses to brief agonist applications in the absence and presence of drug. As an example of fast perfusion system operation we focus on how NMDAR open channel blockers inhibit recombinant NMDAR responses to brief synaptic-like glutamate applications.

NMDAR open channel blockers are a class of use-dependent NMDAR antagonists. One NMDAR open channel blocker, memantine, is currently being used to treat Alzheimer's disease (Witt et al., 2004). Memantine along with another NMDAR open channel blocker, ketamine, have shown promise in the treatment of several other debilitating nervous system disorders

(Pittenger et al., 2007; Collins et al., 2010; Anitha et al., 2011; Autry et al., 2011; Duman and Aghajanian 2012; Prommer 2012). Memantine and ketamine share the same basic mechanism of action and have similar IC_{50} values and kinetics of inhibition at NMDARs (Kotermanski and Johnson 2009; Kotermanski et al., 2009). However, there are subtle kinetic differences in inhibition of NMDARs by memantine and ketamine. These differences demonstrate important considerations when designing experiments to evaluate how drugs affect ligand-gated ion channel currents in response to brief agonist applications. The methods described below explain the steps used to record recombinant NMDAR currents in response to brief glutamate applications in the absence and presence of open channel blockers.

2.4.1 Fast Perfusion System Design
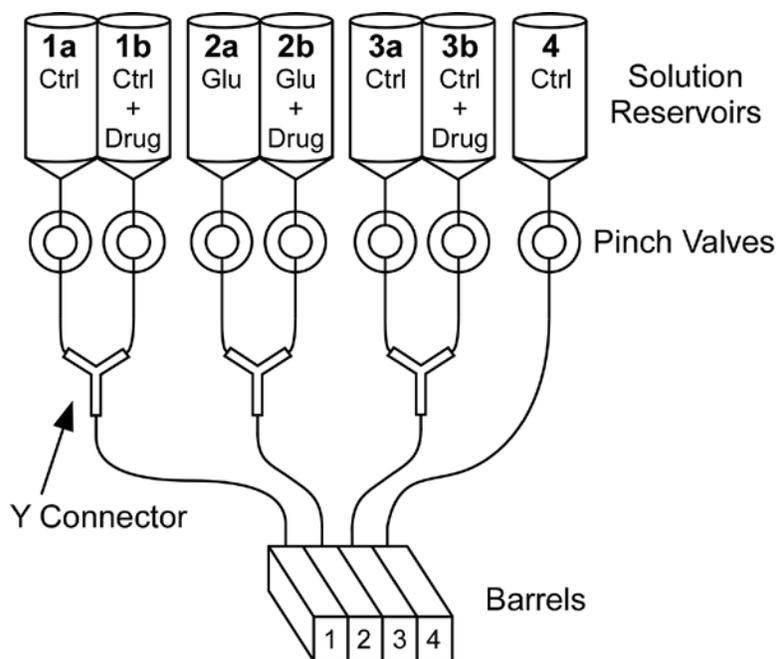
Figure 5. Schematic of fast perfusion system.

Fast perfusion system designed to allow brief applications of 1 mM glutamate (Glu) in control solution (Ctrl) in the absence and presence of a single drug concentration (Drug).

2.4.1.1 Brief Application Strategy

1. Rapid and continuous barrel movement from barrel 1 to barrel 3 (*see* **Figure 6A**), sweeping quickly by barrel 2, delivers brief synaptic-like glutamate applications (~5 ms) to lifted transfected cells.

2. Similar barrel movement from barrel 3 to barrel 1 (*see* **Figure 6A**) delivers another brief synaptic-like glutamate application to lifted transfected cells.

3. With careful calibration, the fast perfusion system can consistently deliver brief, repeated synaptic-like agonist applications to lifted transfected cells.

4. Lifting cells is crucial to ensure complete and rapid exchange of solution during brief agonist applications. Although the duration of agonist application is identical for recordings from attached cells and from lifted cells, the diffusionally-restricted space between the bottom of an attached cell and the coverslip slows solution exchange.

2.4.1.2 Changing Solutions Flowing Through Barrels

1. The Y-connectors described in **Section 2.3** (*see* **Figure 5**) allow one of two solutions to flow through barrels 1, 2, and 3. Importantly, pinch valves 1a, 2a, or 3a are never open concurrently with pinch vales 1b, 2b, or 3b, respectively.

2. Change the solutions flowing through each barrel by closing pinch valves 1a, 2a, and 3a and immediately opening pinch valves 1b, 2b, and 3b.

3. During changes of solution flowing through barrels 1, 2, and 3, it is advisable to move to barrel position 4 to perfuse the cell with control solution (make sure pinch valve 4 is always open). Perfusing the cell with control solution during changes of solutions flowing through barrels helps to avoid (1) releasing gas bubbles onto the cell as a result of opening and closing pinch valves, and (2) contact of the cell with glutamate

40

+ drug-containing solution due to temporary disruptions in solution flow during pinch valve opening and closing.

4   One benefit of this method is that the number of solutions that can be applied to the same cell is limited only by the number of inlets on a manifold that can replace the Y connector.

2.4.2   Transient Transfection of tsA201 Cells

1. tsA201 cells are maintained in culture and plated prior to transfection using standard cell culture procedures (Phelan 2006).

2. 12--24 hours before transfection, 1 x 10^5 tsA201 cells are plated in 1.5 ml of tsA201 cell culture medium on uncoated 15 mm glass coverslips in 35 mm petri dishes (3 coverslips/dish).

3. Warm serum-free tsA201 cell culture medium and FuGene 6 Transfection Reagent to room temperature.

4. The following steps refer to transfection of a single dish of plated cells. If transfecting multiple dishes of plated cells, increase the volume of solutions accordingly.

5. Transfer 95 µl of serum-free tsA201 cell culture medium into a sterilized microcentrifuge tube.

6. Add 3 µl of FuGene 6 Transfection Reagent to the tube, avoiding contact with the tube wall.

7. Vortex the tube for 1 second and incubate at room temperature for 5 minutes.

8. Add 1 µg of cDNA total (2 µl of cDNA at a density of 0.5 µg/µl) to the tube in a ratio of 1:1:2 (eGFP:GluN1:GluN2x) (*see* **Note 6**).

9. Vortex the tube for 1 second and incubate at room temperature for 15 minutes.

10. Transfer 100 μl of medium/FuGene 6 Transfection Reagent/cDNA mixture from the microcentrifuge tube to a petri dish of plated cells (*see* **Note 7**).

11. Add D,L-AP5 (GluN2A or GluN2B, 200 μM; GluN2C or GluN2D, 400 μM) and 7-CKA (200 μM) to the petri dish (*see* **Note 8**).

12. Wait at least 18 hours before recording from transfected cells (*see* **Note 9**)

2.4.3 Performing Brief Glutamate Applications in Control Solution

2.4.3.1 Estimating Duration of Brief Applications

1. Fill solution reservoirs 1a, 1b, 3a, and 3b with control solution and fill solution reservoirs 2a, and 2b with control solution diluted by 10% with deionized H_2O (diluted control solution).

2. Fill a recording pipette with pipette solution, attach to the pipette holder and then apply a small amount of positive pressure (~0.5 PSI) to the side port of the pipette holder (*see* **Note 10**). Lower the pipette into the recording chamber filled with control solution.

3. Position the barrels vertically so they do not touch the bottom of the dish during movement (*see* **Note 11**). Move the pipette into the optimal vertical position for solution application (*see* **Note 12**). Position the pipette in the horizontal plane so that the tip of the pipette is about 50 μm in front of the front edge of the barrels and the tip of the pipette is aligned with the center of barrel 1. Use the barrel movement software to define that location as barrel position 1.

4. Sequentially for each of the remaining three barrels, use the barrel movement software to align the barrel with the tip of the open pipette. Use the barrel movement software to define barrel positions 2, 3, and 4.

5. Make brief solution applications to the open pipette by rapid continuous movements from barrel position 1 to 3 or barrel position 3 to 1, sweeping by the solution in barrel 2 (*see* **Section 2.4.1.1**). With pinch valves 1a, 2a, and 3a open, perform movements from barrel position 1 to 3 and back from barrel position 3 to 1. Measure the duration of solution application with the open pipette by measuring the current in response to the diluted control solution in barrel 2 (*see* **Figure 6B**). Current changes reflect the differing solution osmolality flowing onto the open pipette tip and are used to measure the duration of barrel 2 solution application. We measured the half-width duration of solution application as 4.5 ± 0.6 ms and the solution exchange 10--90% current rise time as < 0.5 ms (*see* **Figure 6B**).

6. Change the solutions flowing through the barrels by closing pinch valves 1a, 2a, 3a and opening pinch valves 1b, 2b, and 3b (*see* **Section 2.4.1.2**). Repeat and evaluate current measurements described in the previous point with pinch valves 1b, 2b, and 3b open.
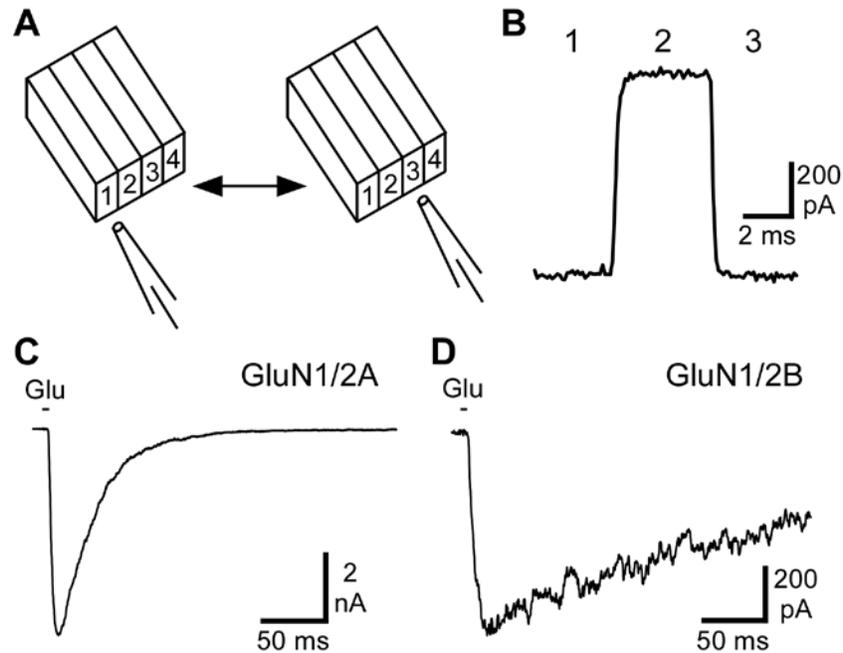
Figure 6. Measuring the duration of glutamate application.

(**A**) Schematic of barrel movement in relation to an open recording pipette. Barrel movements are from barrel position 1 to 3 (and from barrel position 3 to 1), briefly sweeping by barrel 2. (**B**) Example of a current recording from an open recording pipette in response to moving from barrel position 1 to 3, sweeping by barrel 2, which has solution of different osmolality than barrels 1 or 3 (application half-width, 3.7 ms; solution exchange 10--90% current rise times, 1 to 2: 0.26 ms; 2 to 3: 0.22 ms). (**C, D**) Examples of whole-cell voltage-clamp recordings of lifted tsA201 cells expressing GluN1/2A receptors (**C**; 10--90% rise time, 4.0 ms; τ_w, 29.6 ms) or GluN1/2B receptors (**D**; 10--90% rise time, 9.0 ms; τ_w, 421 ms) in response to brief applications of 1 mM glutamate (Glu, black bar). Cells were held at – 65 mV.

44

2.4.3.2 Whole-Cell Recording from Lifted Cells

Patch-clamp recording from lifted cells is similar to patch-clamp recording from attached cells. For more detailed information on standard application of the patch-clamp technique see Hamill et al., 1981 (Hamill et al., 1981).

1. Transfer a coverslip with transfected tsA201 cells to the recording chamber containing room temperature bath solution. Place the recording chamber onto the microscope stage, and then place an efflux tube and reference electrode into the chamber (*see* **Note 13**).

2. Using the fluorescence microscope, identify an isolated eGFP-positive cell (*see* **Note 14**).

3. Position the barrels vertically to ensure that they do not make contact with the coverslip through the full range of barrel movement (*see* **Note 11**). Position the barrels in the horizontal plane so that the front edge of barrel 1 is near the cell, and the center of barrel 1 is aligned with the cell (*see* **Figure 6A**). Then move the barrels axially away from the cell, without changing the alignment of barrel 1 with the cell, to avoid crashing the recording pipette into the barrels (*see* **Note 15**).

4. Position the recording pipette just above the cell. Before forming a gigaohm seal, move the barrels axially towards the cell until about 50 μm from the cell.

5. Lower the recording pipette and form a gigaohm seal. Adjust electrode capacitance, and then achieve a whole-cell configuration.

6. Set whole-cell parameters (cell capacitance and series resistance) and adjust series resistance compensation to ~80%.

7. To lift the cell, apply a constant negative pressure of 1--1.5 PSI to the side port of the pipette holder. Slowly begin to move the pipette straight up from the coverslip. You should see the cell lift from the coverslip. Continue lifting the cell slowly until it is completely free from the coverslip. Move the pipette with the lifted cell into the optimal position for solution application (*see* **Note 12**).

8. Once the lifted cell is positioned, reduce the constant negative pressure to the side port of the pipette holder to 0.3--0.6 PSI. Readjust the whole-cell parameters, as capacitance should have decreased from lifting the cell. Also, the membrane capacitance of lifted cells often decreases throughout experiments, which may require further adjustments to whole-cell parameters.

9. Making an initial glutamate application of about 30 s is recommended to reduce response variability during the rest of the experiment.
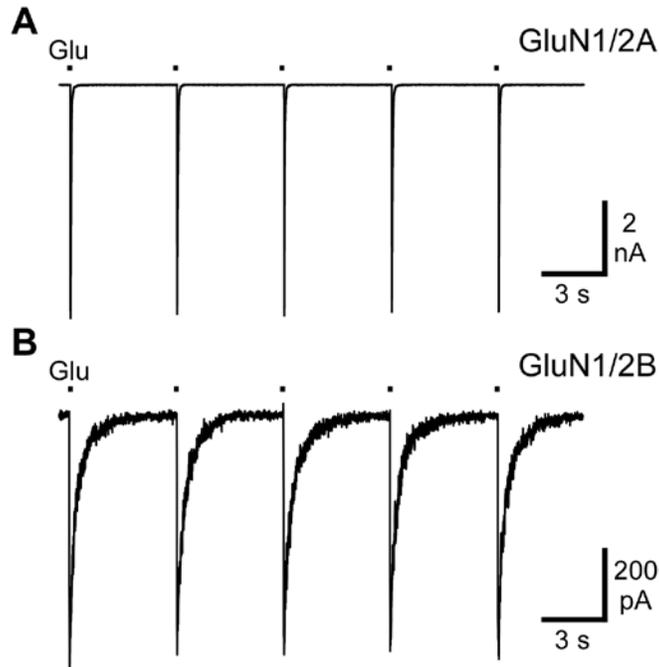
Figure 7. Brief applications of glutamate to lifted cells expressing two different NMDAR subtypes.

(**A, B**) Example whole-cell voltage-clamp recordings of lifted tsA201 cells expressing GluN1/2A receptors (**A**) or GluN1/2B receptors (**B**) in response to 5 brief applications of 1 mM glutamate (Glu, black bars) at a frequency of 0.2 Hz. Cells were held at -65 mV.

2.4.3.3 Quantification of Receptor Response Time Course

1. Fill solution reservoirs 1a, 1b, 3a, and 3b with control solution, and fill solution reservoirs 2a and 2b with control solution containing 1 mM glutamate.

2. Make brief glutamate applications to the lifted cell by rapid continuous movements from barrel position 1 to 3 or barrel position 3 to 1, sweeping by the solution in barrel 2 (*see* **Section 2.4.1.1**).

3. Gauge the similarity to NMDAR-EPSCs of recombinant NMDAR responses by measuring the kinetics of recombinant receptor currents in response to brief glutamate applications.

4. Quantify the activation time course of recombinant NMDAR currents as the 10--90% rise time. We measured a mean 10--90% current rise time in response to brief glutamate applications to GluN1/2A receptors of 4.8 ± 0.6 ms (*see* **Figure 6C**) and in response to brief glutamate applications to GluN1/2B receptors of 12.7 ± 5.6 ms (*see* **Figure 6D**).

5. Quantify the decay time course of recombinant NMDAR currents by fitting the current decay with a double exponential function and determining the weighted time constant of decay ($\tau_w = (\tau_{fast})(fraction_{fast}) + (\tau_{slow})(fraction_{slow})$). We measured a mean τ_w in response to brief glutamate applications to GluN1/2A receptors of 27.5 ± 4.1 ms (*see* **Figure 6C**) and in response to brief glutamate applications to GluN1/2B receptors of 420 ± 34 ms (*see* **Figure 6D**).

6. Compare results to expected EPSC kinetics. The recombinant NMDAR response kinetics we measured are similar to previous measurements of NMDAR-EPSC kinetics and also to results of previous studies using brief glutamate applications to recombinant NMDARs in transfected cells (Vicini et al., 1998; Cull-Candy and Leszkiewicz 2004; Erreger et al., 2005; Tovar et al., 2013).

7. Change the solutions flowing through the barrels by closing pinch valves 1a, 2a, 3a and opening pinch valves 1b, 2b, and 3b (*see* **Section 2.4.1.2**). Repeat and evaluate the kinetic measurements of recombinant NMDAR currents in response to brief glutamate applications (*see* **Note 16**).

8. After finishing an experiment, measure the duration of glutamate application to that specific cell to control for variations in solution flow rate and other potential sources of error, which may lead to exclusion of that experiment from analysis. Turn off series resistance compensation and whole-cell parameters. Return holding potential to 0 mV. Deliver > 2 PSI of positive pressure to the side port of the pipette holder to remove the cell and membrane debris from the tip of the pipette. Dilute the glutamate-containing solutions in reservoirs 2a and 2b (*see* **Figure 5**) with deionized H_2O by at least 10%. Measure changes in pipette current in response to barrel movements with the open pipette (*see* **Section 2.4.3.1**). Make sure to measure solution applications with pinch valves 1a, 2a, and 3a open and also with pinch valves 1b, 2b, and 3b open.

2.4.3.4 Fast Perfusion System Optimization

1. Stepper motor controller power output. Depending on the stepper motor controller, the output power may be adjustable. If so, modifying the output power can change stepper motor operation, either introducing or eliminating oscillations that may result from rapid acceleration and deceleration of the stepper motor. With some power settings, we observed oscillations when monitoring system performance using an open pipette that could have an undesirable impact on brief agonist applications to transfected cells.

2. Weight of barrel holder arm and barrel holder. Due to rapid acceleration and deceleration of the stepper motor, the stepper motor can overshoot desired positions or oscillate. The rotational inertia imposed by the weight of the barrel holder arm and barrel holder can strongly impact stepper motor overshoot and oscillations. The

weight of the barrel holder arm and barrel holder should be minimized to reduce overshoot and oscillations if present.

3. Acceleration of stepper motor. The acceleration and deceleration of the stepper motor should be optimized for system stability and to minimize the duration of agonist application. At more rapid accelerations and decelerations, the stepper motor may overshoot desired positions or oscillate. At slower accelerations and decelerations, the duration of agonist application may be too long.

4. Rate of solution flow. Careful adjustment of the solution flow rate is essential to achieving consistent and brief agonist applications. It is important to maintain similar solution flow rates so that inconsistencies in application duration do not arise (*see* **Note 17**). Also, lifted cells are attached only to the tip of the recording pipette, making them vulnerable to being blown away if the solution flow rate is too fast.

5. Degassing solutions prior to use. Removing gas from solutions prior to starting experiments can help to (1) keep bubbles from destroying cells and (2) keep bubbles from blocking barrels, slowing or stopping solution flow. Gas bubbles can form unpredictably in tubing during experiments, and it can be difficult to determine if solution has stopped flowing from a particular barrel during an experiment. To degas solutions, pour solutions into a vacuum flask and apply negative pressure. Stop negative pressure when few gas bubbles form in solution.

6. Mixing of barrel solutions. It is important to ensure that a cell is exposed almost exclusively to the desired solution at each barrel position. Solution mixing could occur, for example, within the Y connectors, or after solutions leave the barrels if the cell is not properly positioned relative to the barrels. One way to test for mixing is to

fill solution reservoirs 1a, 2a, 3a, and 4 with control solution and solution reservoirs 1b, 2b, and 3b with control solution containing agonist at a concentration orders of magnitude above its EC_{50} for the receptors under study; we use 10 mM glutamate. While whole-cell recording from a lifted cell expressing recombinant receptors, start recording at barrel position 4 with all other pinch valves closed and determine control (in the absence of agonist) holding current. Open pinch valves 1b, 2b, and 3b and be sure that holding current does not change while the cell is in front of barrel 4. Move to barrel position 3 to observe the response to glutamate, and after current has reached steady-state, be sure that there is no further change in current when moving to barrel positions 2 and 1. Move to barrel position 3, close pinch valve 3b, and open pinch valve 3a, and ensure that control holding current is observed. Repeat this procedure for the other barrels, and also change the solution flowing through adjacent barrels to be sure that the cell is exposed only to the solution flowing from the appropriate barrel. If evidence of mixing is observed, identify and correct the source of the problem (e.g., malfunctioning pinch valves or incorrect positioning of the cell relative to the barrels).

2.4.4 Performing Brief Glutamate Applications in Presence of Channel Blockers

1. Use whole-cell patch-clamp recordings from lifted cells expressing GluN1/2A or GluN1/2B receptors to record responses to brief glutamate applications as described in **Section 2.4.3**, with modifications described below.

2. Fill solution reservoirs 1a, 3a, and 4 with control solution and reservoir 2a with control solution containing 1 mM glutamate. Fill solution reservoirs 1b and 3b with control

51

solution + drug and reservoir 2b with control solution containing 1 mM glutamate + drug (*see* **Figure 5**).

3. Choose an appropriate frequency of brief glutamate applications to lifted cells expressing a particular NMDAR subtype. The frequency must be low enough to ensure complete current decay following glutamate application and allow recovery from desensitization before the subsequent glutamate application, yet fast enough to allow for experiments that may require many brief glutamate applications (potentially > 100 applications). We used a glutamate application frequency of 0.2 Hz for both GluN1/2A (*see* **Figure 7A**) and GluN1/2B (*see* **Figure 7B**) receptors.

4. Measure the baseline peak current value in response to brief glutamate applications in the absence of drug (baseline current). We required 10 consecutive, steady glutamate responses to establish that a stable baseline current had been reached, which were then averaged to give the baseline current mean value (*see* **Figure 7A, B**).

5. Add drug to the solutions flowing through the barrels by closing pinch valves 1a, 2a, and 3a and opening pinch valves 1b, 2b, and 3b (*see* **Section 2.4.1.2**). Make sure to allow enough time for complete changes of solutions flowing through the barrels (*see* **Note 18**)

6. Open channel blockers require that the channel be activated to bind and inhibit the channel. The number of brief glutamate applications in the presence of drug needed to reach a steady level of NMDAR inhibition depends on the drug's kinetics and must be determined for each drug and NMDAR subtype. For each successive application of glutamate in the presence of drug, the peak current should be smaller than the previous peak current until reaching a steady level (inhibited current). We required 5 consecutive, steady glutamate responses to establish that a stable inhibited current had been reached,

which were then averaged to give the inhibited current mean value (*see* **Figure 8A, B**). We used memantine and ketamine, two NMDAR open channel blockers with slightly different kinetics, to illustrate differences in the number of glutamate applications in the presence of drug needed to reach steady NMDAR inhibition. We used 20 applications of glutamate in the presence of memantine and 40 applications of glutamate in the presence of ketamine to reach steady levels of NMDAR inhibition with GluN1/2A (data not shown) and GluN1/2B receptors (*see* **Figure 8A, B**).

7. Remove drug from the solutions flowing through the barrels by closing pinch valves 1b, 2b, and 3b, and opening pinch valves 1a, 2a, and 3a (*see* **Section 2.4.1.2**). Make sure to allow enough time for complete changes of solutions flowing through the barrels (*see* **Note 18**).

8. Open channel blockers like memantine and ketamine require channel activation to unbind and allow recovery from inhibition (*see* **Note 19**). The number of brief glutamate applications in the absence of drug following NMDAR inhibition must be determined for each drug and NMDAR subtype. For each successive application of glutamate in the absence of drug following NMDAR inhibition, the peak current should be larger than the previous peak current until reaching a steady level after recovery from inhibition is complete (current after recovery). We required 10 consecutive, steady glutamate responses to establish that a stable current after recovery had been reached, which were then averaged to give the current after recovery mean value (*see* **Figure 8A, B**).We used 20 applications of glutamate in the absence of memantine and 40 applications of glutamate in the absence of ketamine following NMDAR inhibition to reach steady levels

of current after recovery with GluN1/2A (data not shown) and GluN1/2B receptors (*see* **Figure 8A, B**).

9. Measure peak currents in response to brief glutamate applications in the absence and presence of drug as the mean current over a 3 ms window centered at the time of peak current.

10. Calculate the percent inhibition by open channel blockers using the equation: % inhibition = 100 * (1 – (inhibited current)/(0.5 * (baseline current + current after recovery))). We averaged the values for baseline current and current after recovery to account for changes in cell properties during experiments. For **Figure 8**, we used concentrations of memantine and ketamine near their IC_{50} values at NMDARs. We measured percent inhibition of responses to brief glutamate applications to GluN1/2B receptors in the presence of 1 µM memantine as 49% (*see* **Figure 8A**), and in the presence of 0.5 µM ketamine as 56% (*see* **Figure 8B**).
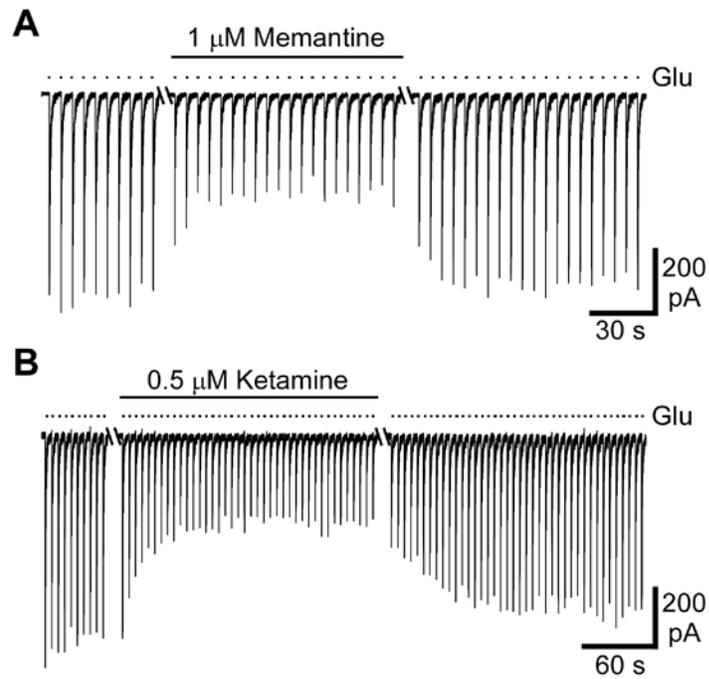
Figure 8. Antagonist kinetics affect the number of brief glutamate applications needed to reach a steady level of current inhibition and a steady level of currents after recovery from inhibition.

(**A**, **B**) Examples of whole-cell voltage-clamp recordings from lifted tsA201 cells expressing GluN1/2B receptors in response to brief applications of 1 mM glutamate (Glu, short black bars) at 0.2 Hz in control solution or in the presence of 1 μM memantine (**A**) or 0.5 μM ketamine (**B**) (long black bars). The average of peak currents from the first 10 glutamate responses shown gives the baseline current mean value, the average the peak currents from the last 5 glutamate responses in the presence of memantine or ketamine gives the inhibited current mean value, and the average of the peak currents from the last 10 glutamate responses gives the current after recovery mean value. Cells were held at -65 mV.

2.5   NOTES

1. Silicone tubing of appropriate size is used to connect PE tubing to Y connectors.

2. Barrels were first cut to length (5 mm) by scoring with a diamond tipped scribe and then both ends were lightly fire-polished. To allow silicone tubing connections to go over the back ends of adjacent barrels, carefully heat individual barrels over a Bunsen burner and bend to a 30 - 60° angle. Only bend two barrels and align them in an alternating pattern of bent then straight barrels to ensure that silicone tubing will attach to the back ends of all the barrels. Glass should be cleaned in 95% ethanol and dried before gluing to the barrel holder. Make sure to align the open edge of the barrels with each other, and ensure that there is no space between barrels.

3. With barrels at a ~1" (~25 mm) radius from the center of the stepper motor shaft, each microstep of stepper motor rotation is translated to ~3 μm of barrel movement. Because the total range of barrel movement is about 2500 μm, less than 1000 microsteps (less than $1/50^{th}$ revolution) are needed for total barrel movement. This translates to nearly linear barrel movement.

4. A compiled version of the stepper motor program is available from the authors by email request.

5. 10 μM EDTA is used to chelate contaminating free Zn^{2+}, which inhibits GluN1/2A receptors in the nM range. The NMDAR coagonist glycine is present in all solutions to saturate the glycine coagonist-sites on NMDARs.

6. The cDNA transfection ratio of 1:1:2 for eGFP:GluN1:GluN2x may vary depending on transfection efficiency with given vectors and subunits.

7. The volume of serum-free tsA201 medium used for transfections depends upon the cDNA solution density. The medium/FuGene 6 Transfection Reagent/cDNA mixture should be at a final volume of 100 μl for transfection of a single dish of plated cells. If the cDNA solution density differs from 0.5 μg/μl, a different volume of cDNA solution should be added to the mixture to reach 1 μg of cDNA; the amount of medium added should be adjusted to reflect this change.

8. NMDARs tonically activated by ambient glutamate present in the culture medium are excitotoxic. Therefore, we add competitive antagonists to the culture medium after transfection of tsA201 cells. Other antagonists, including elevation of the Mg^{2+} concentration of the tsA201 cell culture medium to > 10 mM also may be used.

9. We find that 24--48 hours after transfection offers optimal current amplitudes, cell health, and cell confluency. Depending on current amplitudes, successful recordings from transfected cells can be made up to at least 72 hours after transfection. Vary the time between transfection and recording to optimize protein expression and cell health.

10. We use a 1 ml syringe connected with PE tubing to the side port of the pipette holder and connected in parallel to a pressure gauge. Pressure and suction can be applied by using the plunger of the syringe or by mouth. A stopcock on the end of the syringe can be closed to hold positive and negative pressure in the pipette.

11. The distance between the upper surface of the coverslip and the lowest point on any of the barrels changes slightly when the stepper motor rotates to cause barrel movement (*see* **Note 3**). After positioning the barrels axially so they are near the cell, position the barrels

vertically so they are close to the coverslip, but do not touch the coverslip during movements to each barrel position. The barrels could break if they contact the coverslip during fast movements.

12. Choose the vertical position of the pipette relative to the barrel openings to optimize speed of solution changes. It is best to position the pipette so that it is near the vertical center of the barrel openings. However, note that the barrels should be angled so that they point ~30° below the horizontal plane. The pipette should be positioned vertically so that it sits near the middle of the solution streams flowing from the barrels.

13. To maintain fluid levels in the recording chamber, we siphon solution through a glass efflux tube. The height of solution in the recording chamber is determined by the height of the waste end of the efflux tube.

14. It is important to record only from isolated eGFP-positive tsA201 cells. When recording from lifted cells, it is often difficult to tell if there are thin attachments to other cells, which could drastically alter the recordings.

15. When using lifted cells, it is possible to move the lifted cell to the barrels, even if they are placed relatively far from the starting location of the cell, to simplify barrel positioning. However, aligning the barrels as described minimizes the need to move the cell after lifting, increasing success rate.

16. Make sure that peak current amplitudes and response kinetics in response to brief glutamate applications are similar when pinch valves 1a, 2a, and 3a are open and when pinch valves 1b, 2b, and 3b are open. If significant differences are observed, further optimize the system as described in **Section 2.4.3.4**.

58

17. Differences in the rate of solution flow from barrel 1 and 3 can increase the agonist application duration while moving from barrel position 1 to 3 relative to the agonist application duration while moving from barrel position 3 to 1. Also, differences in solution flow rate from reservoirs 1a and 1b, etc. can have a significant impact on the duration of agonist application in the presence or absence of drug. Such differences could lead to complications in interpreting the effect of a drug.

18. The time required for complete changes of solutions flowing through barrels can be estimated with the following experiment. Fill solution reservoirs 1a, 2a, and 3a with control solution and fill solution reservoirs 1b, 2b, and 3b with diluted control solution. With an open pipette positioned at barrel position 1, measure the time course of current change in response to closing pinch valve 1a and opening pinch valve 1b. The current should change approximately exponentially until reaching a steady level in the presence of the diluted control solution in reservoir 1b. Measure the 10-90% current rise time to estimate the time required for changing the solution flowing through barrel 1. We waited for 5x the 10-90% current rise time after closing pinch valve 1a and opening pinch valve 1b to consider the change of solution flowing through barrel 1 complete. Repeat measurements of current change in response to closing pinch valve a and opening pinch valve b for barrels 2 and 3.

19. Measure recovery in all experiments to ensure that decreases in peak currents in response to brief glutamate applications in the presence of drug are due to the drug itself and not due to other changes in the cell that may decrease peak currents.

3.0   MEMANTINE AND KETAMINE DIFFERENTIALLY ALTER NMDA RECEPTOR DESENSITIZATION KINETICS

3.1   OVERVIEW

Memantine and ketamine are two clinically useful NMDA receptor (NMDAR) open channel blockers. Although memantine and ketamine act at NMDARs with similar IC_{50} values and kinetics, they display vastly different clinical profiles. This discrepancy has been hypothesized to result from inhibition by memantine and ketamine of overlapping but distinct subpopulations of NMDARs. For example, memantine, but not ketamine, may inhibit extrasynaptic more effectively than synaptic NMDARs. However, a mechanistic basis for drugs preferentially inhibiting NMDARs depending on their subcellular location has not been systematically investigated. We integrated whole-cell recordings from transfected cells expressing a single NMDAR subtype with kinetic modeling to demonstrate that memantine and ketamine differentially alter NMDAR desensitization, and that memantine stabilizes a Ca^{2+}-dependent desensitized state. Thus, inhibition by memantine and ketamine depends in part on the intensity and duration of NMDAR activation, as opposed to strictly the location of receptors. Modulation of receptor desensitization is an unexplored mechanism of inhibitory action with the potential to endow drugs with NMDAR selectivity that leads to superior clinical profiles.

3.2 INTRODUCTION

NMDA receptors (NMDARs), a subfamily of ionotropic glutamate receptors, exhibit unique biophysical properties such as high permeability to Ca^{2+} and highly voltage-dependent block by Mg^{2+} at resting membrane potentials (Traynelis et al., 2010; Paoletti et al., 2013; Glasgow et al., 2015). These biophysical features make NMDAR activation particularly relevant to cellular signaling with physiological activation leading to processes such as synaptic plasticity, and pathological activation leading to processes such as excitotoxic cell death (Paoletti et al., 2013; Parsons and Raymond 2014). An emerging literature suggests a dichotomy in cellular signaling arising from the specific subcellular localization of NMDARs: synaptic NMDAR activation leads to processes involved in cell survival, whereas extrasynaptic NMDAR activation leads to processes involved in excitotoxic cell death (Hardingham and Bading 2010; Bading 2013; Parsons and Raymond 2014). However, some studies have demonstrated a clear role of synaptic NMDAR activation in excitotoxic cell death (Papouin et al., 2012; Wroge et al., 2012; Zhou et al., 2013; Zhou et al., 2013). Furthermore, many studies support a role of extrasynaptic NMDARs in normal neuronal physiology (Fellin et al., 2004; Herman and Jahr 2007; Le Meur et al., 2007; Harris and Pettit 2008; Povysheva and Johnson 2012; Riebe et al., 2016). Nevertheless, aberrant activation of extrasynaptic NMDARs is implicated in models of excitotoxicity, Alzheimer's disease, and Huntington's disease particularly relating to the extent of cell death and activation of cell death-related signaling pathways (Hardingham et al., 2002; Leveille et al., 2008; Papadia et al., 2008; Okamoto et al., 2009; Bordji et al., 2010; Leveille et al., 2010; Milnerwood et al., 2010; Kaufman et al., 2012; Talantova et al., 2013; Dau et al., 2014).

The idea that different subpopulations of NMDARs are involved in distinct processes underlies a hypothesis of differential activity by two clinically relevant NMDAR open channel

blockers, memantine and ketamine (Johnson et al., 2015; Kavalali and Monteggia 2015). Memantine is approved for the treatment of moderate to severe Alzheimer's disease and shows promise in the treatment of Huntington's disease, dementia, and ischemia (Witt et al., 2004; Okamoto et al., 2009; Emre et al., 2010; Dau et al., 2014; Kafi et al., 2014). In contrast, ketamine was initially approved for use as an anesthetic, but has recently shown efficacy for rapid and sustained relief of depression symptoms and in treatment of pain (Prommer 2012; Krystal et al., 2013; Persson 2013; Kavalali and Monteggia 2015). Despite their non-overlapping clinical profiles, memantine and ketamine are thought to act primarily as open channel blockers of NMDARs with similar IC_{50} values and kinetics (Lipton 2006; Parsons et al., 2007; Abdallah et al., 2015; Johnson et al., 2015; Kavalali and Monteggia 2015). One hypothesis to explain the divergent clinical profiles of memantine and ketamine is that each drug inhibits overlapping but distinct subpopulations of NMDARs. Memantine is hypothesized to provide neuroprotection through more potent inhibition of extrasynaptic than synaptic NMDARs (Zhao et al., 2006; Leveille et al., 2008; Papadia et al., 2008; Okamoto et al., 2009; Milnerwood et al., 2010; Xia et al., 2010; Kaufman et al., 2012; Dau et al., 2014), but see (Wroge et al., 2012; Emnett et al., 2013; Zhou et al., 2013). In contrast, ketamine is hypothesized to provide rapid anti-depressant effects through inhibition of synaptic NMDARs (Autry et al., 2011; Nosyreva et al., 2013; Gideons et al., 2014; Kavalali and Monteggia 2015), but see (Miller et al., 2014).

It is plausible that the divergent clinical profiles of memantine and ketamine arise from inhibition of overlapping but distinct NMDAR subpopulations. However, there is no clear mechanism by which memantine and ketamine may act to selectively inhibit subpopulations of NMDARs discussed above (Xia et al., 2010; Emnett et al., 2013; Gideons et al., 2014). Thus, we investigated whether inhibition by memantine and ketamine differed depending on three

potential properties or features that are likely to vary between synaptic and extrasynaptic NMDARs.

First, we investigated whether inhibition by memantine and ketamine depended on the NMDAR subtype. NMDARs are four subunit complexes necessarily containing GluN1 and GluN2 subunits. There are four GluN2 subunits, GluN2A – GluN2D, that vary in expression based on the brain region, cell type, and developmental stage (Traynelis et al., 2010; Paoletti et al., 2013; Glasgow et al., 2015). The NMDAR subtype is defined by the specific combination of subunits that a receptor contains. For example, a GluN1/2A contains 2 GluN1 subunits and 2 GluN2A subunits. Memantine and ketamine exhibit subtype-selectivity for GluN1/2C and GluN1/2D receptors over GluN1/2A and GluN1/2B receptors in the presence of 1 mM Mg^{2+}, but not in its absence (Dravid et al., 2007; Kotermanski and Johnson 2009). However, GluN2C and GluN2D subunits are likely not expressed in cell-types (Monyer et al., 1994; Landwehrmeyer et al., 1995) that are particularly relevant for memantine acting as a neuroprotectant in ischemia (Freund et al., 1990; Lipton 1999; Papp et al., 2008) and Huntington's disease (Okamoto et al., 2009; Milnerwood et al., 2010; Kaufman et al., 2012; Dau et al., 2014), or in the context of ketamine as rapid anti-depressant (Autry et al., 2011; Nosyreva et al., 2013; Gideons et al., 2014; Miller et al., 2014; Kavalali and Monteggia 2015). Therefore, we focused on memantine and ketamine inhibition of GluN1/2A and GluN1/2B receptors. Notably, many studies have shown that GluN2A-containing receptors are localized synaptically, whereas GluN2B-containing receptors are localized extrasynaptically (Tovar and Westbrook 1999; Groc et al., 2006; Martel et al., 2009; Papouin et al., 2012), but see (Thomas et al., 2006; Harris and Pettit 2007; Petralia et al., 2010). Second, we investigated whether inhibition by memantine and ketamine depended on the concentration of glutamate to which synaptic and extrasynaptic NMDARs are typically

exposed. Third, we investigated whether inhibition by memantine and ketamine depended on the duration of glutamate to which NMDARs are typically exposed. We found that inhibition by memantine and ketamine depends most strongly upon the NMDAR subtype and the duration of glutamate exposure. Upon further investigation, we discovered that memantine and ketamine differentially alter NMDAR desensitization kinetics and that memantine stabilizes a Ca^{2+}-dependent desensitized state of GluN1/2A receptors.

3.3 MATERIALS AND METHODS

3.3.1 Cell culture and transfection

Experiments were performed on the tsA201 cell line (The European Collection of Authenticated Cell Cultures). tsA201 cells were maintained as previously described (Glasgow and Johnson 2014), in DMEM supplemented with 10% fetal bovine serum and 1% GlutaMAX (Thermo Fisher Scientific). Cells at 1×10^5 cells/dish were plated on 15 mm untreated glass coverslips for experiments using lifted cells and plated on 15 mm glass coverslips treated with poly D-lysine (0.1 mg/ml) and rat-tail collagen (0.1 mg/ml, BD Biosciences) in 35 mm petri dishes for experiments using unlifted cells. 12 to 24 hours after plating, the cells were transiently cotransfected with cDNAs encoding enhanced green fluorescent protein (EGFP) for identification of transfected cells, the rat GluN1-1a subunit (hereafter GluN1; GenBank X63255 in pcDNA3.1), and either the rat GluN2A subunit (GenBank M91561 in pcDNA1) or rat GluN2B subunit (GenBank M91562 in pcDNA1), using FuGENE 6 Transfection Reagent (Promega). Some experiments used cells transfected with GluN1 and a EGFP:pIRES:GluN2A

construct, which was a kind gift from Dr. Kasper Hansen (Hansen, unpublished). Briefly, EGFP was inserted in pIRES (Clontech) under transcriptional control of the CMV promoter, and the open reading frame of rat GluN2A (GenBank D13211) was inserted after the IRES sequence. cDNA ratios of 1 EGFP: 1 GluN1: 1 GluN2A or 1 EGFP: 1 GluN1: 3 GluN2B were used. Immediately proceeding transfection, the culture media was supplemented with the competitive NMDAR antagonists D,L-2-amino-5-phosphonopentanoate (200 μM) and 7-chlorokynurenic acid (200 μM) to prevent NMDAR-mediated cell death.

3.3.2 Electrophysiology

Whole-cell voltage-clamp recordings were performed on transfected tsA201 cells 12 – 48 hours after transfection. Pipettes were pulled from borosilicate capillary tubing (Sutter Instruments) to a resistance of 2 – 5 MΩ on a Sutter Instruments-Flaming Brown P-97 electrode puller and fire polished. Unless otherwise indicated, the extracellular solution contained (in mM): 140 NaCl, 2.8 KCl, 1 $CaCl_2$, 10 HEPES, 0.01 EDTA, and 0.1 glycine, balanced to pH 7.2 ± 0.05 with NaOH and osmolality balanced to 290 ± 10 mOsm with sucrose. Unless other indicated, the intracellular pipette solution contained (in mM): 130 CsCl, 10 HEPES, 10 BAPTA, and 4 MgATP balanced to pH 7.2 ± 0.05 with CsOH and osmolality of 280 ± 10 mOsm. MgATP was added to the intracellular pipette solution to reduce NMDAR current rundown, although some experiments measuring inhibition by memantine and ketamine were performed without addition of MgATP. There was no distinguishable difference in measures of inhibition and therefore data were pooled. Solutions were delivered with an in-house fabricated fast perfusion system described below.

Whole-cell currents were amplified using an Axopatch 200B patch-clamp amplifier (Molecular Devices), low-pas filtered at 5 kHz and sampled at 20 kHz in pClamp10 (Molecular Devices). Series resistance was compensated 85 – 90% with the prediction and correction circuitry in all experiments. An empirically determined liquid junction potential of -6 mV between the pipette solution and extracellular solution was corrected in all experiments *post hoc*.

3.3.3 Fast perfusion system

Solutions were delivered through ten round plastic barrels (recordings from unlifted cells) or through 3 square glass barrels (recordings from lifted cells) with an in-house fabricated fast perfusion system similar to a system described previously(Glasgow and Johnson 2014). Solution changes were achieved by changing the barrel position with a voice-coil linear stage (Equipment Solutions, Inc.) controlled by a custom program described previously(Blanpied et al., 1997). Solution flow rate was controlled by adjusting the height of the solution reservoirs and was typically ~2 ml/min for recordings from unlifted cells and ~1 ml/min for recordings from lifted cells.

Synaptic-like glutamate applications were achieved by quickly changing barrel position from Barrel 1 to Barrel 3 and Barrel 3 to Barrel 1, briefly sweeping by the glutamate-containing Barrel 2 as depicted in **Figure 10A**. Solution exchange across an open pipette during a movement from Barrel 1 to Barrel 3, and a movement from Barrel 3 to Barrel 1, had a 10-90% rise time of < 0.2 ms as measured by the current relaxation of the junction current in response to a solution of different osmolality in Barrel 2 (**Figure 10A**, **B**; **Table 1**). Solution exchange around a lifted whole cell had a 10-90% rise time of ~3 ms and was well fit by a single exponential with a time constant of ~2 ms (**Table 1**). We determined solution exchange around a

whole cell by measuring the time-course of current relaxation following a movement from Barrel 1 containing normal extracellular solution and 1 mM glutamate to Barrel 2 containing extracellular solution with 50% NaCl and 1 mM glutamate. The duration of synaptic-like glutamate applications was determined after each experiment by applying pressure to clear the cell from the tip of the pipette and measuring the duration of junction current change across an open pipette as described above. Synaptic-like glutamate applications were typically ~2-5 ms. Experiments where applications were < 1.5 ms or > 6 ms, or where open pipette tip junction currents displayed multiple peaks were excluded from analysis. Solution exchange around unlifted whole cells measured as described above (**Table 1**).

3.3.4   Kinetic modeling

All model current simulations and model fitting to data were performed in SCoP 3.52 (Simulation Resources), which numerically solves kinetic schemes to determine the probability of entering defined states after a defined stimulus, such as agonist or drug application. Currents were simulated by solving the equation, $I_{NMDA} = NP_{open}\gamma(V_m - V_{rev})$, where N is the number of channels, P_{open} is the probability of being in state $RA_2^\star$, γ is the single-channel conductance of 50 pS, V_m is the membrane voltage of -65 mV, and V_{rev} is the reversal potential of 0 mV. γ and V_{rev} were fixed from previously determined values(Siegler Retchless et al., 2012), whereas N was determined by fitting to data. Models of GluN1/2A receptor function were adapted from previously published models (Model A, Chen et al., (2001), **Figure 12A**; Model B, Erreger et al., (2005), **Figure 13A**). Although we took care to choose models developed under similar experimental conditions (NMDAR subtype, cell type, solution pH, and the extracellular Ca^{2+} concentration), our conditions were not identical, which lead to differences between our data and

current simulations from unmodified models. Therefore, all unblocked arm rates of Model A and Model B, excluding agonist binding and unbinding, were optimized using a PRAXIS algorithm to minimize a least-squares error function with a final tolerance of 2%. To account for differences between cells in desensitization kinetics and other factors that may contribute to channel P_{open}, we averaged current traces from three cells normalized to the peak current during a prolonged application of 1 mM glutamate. Optimization of Model B blocked arm rates were fit to averaged data from the same three averaged cells, although in the presence of memantine.

Model A unblocked arm rates are as follows: k_{a+}, 5 $\mu M^{-1} s^{-1}$; k_{a-}, 25 s^{-1}; k_{1+}, 71 s^{-1}; k_{1-}, 305 s^{-1}; k_{d1+}, 6.9 s^{-1}; k_{d1-}, 0.43 s^{-1}. For Model A and Model B we fixed memantine k_{on} at 30 $\mu M^{-1} s^{-1}$ based on single-channel recordings from our lab (Blanpied, unpublished), and mathematically determined initial memantine k_{off} as 30 s^{-1} so that $K_d = 1$ μM. To mitigate potential confounds from some individual rate changes in Model A causing shifts in memantine IC_{50} (data not shown), we adjusted memantine k_{off} so that the IC_{50} during long glutamate applications was ~1 μM (Table 2). Memantine k_{off} was allowed to vary during fits of Model B blocked arm parameters to data.

3.3.5 Analysis

All data were analyzed with Clampfit 10.3 (Molecular Devices) or Origin 7.0 (OriginLab). Concentration-response relationships for memantine and ketamine (drug) when NMDARs were activated by 1 mM or 0.3 μM glutamate were determined by the following protocol. Glutamate was applied for 10 – 20 s until current reached a steady-state, then glutamate with 0.1, 1, 10, or 100 μM of drug was applied for 10 – 40 s until a steady level of inhibition was reached.

Glutamate in the absence of drug was then reapplied for 20 – 60 s to allow recovery from inhibition. The time needed to reach a steady level of inhibition and to allow recovery from inhibition depended strongly on the glutamate concentration, as expected of open-channel blockers. Cells where recovery from inhibition did not reach 90% of steady-state current preceding drug application were excluded from analysis. Concentration-response data in the presence of drug were log-transformed to determine the IC_{50} value through fits of the following equation, $I_{drug}/I_{control} = 1/(1 + 10^{\wedge}(\log[drug] - \log IC_{50})*n_H)$, where I_{drug} is the mean current during 3 s of steady drug inhibition, $I_{control}$ is the mean current during 3 s of steady-state current preceding drug application and 3 s of steady-state current following recovery from drug inhibition, and n_H is the Hill coefficient. IC_{50} values were statistically compared on the log-scale and transformed for presentation. For graphical representation, concentration-response data were averaged and overlaid with a fit to the mean data.

Fits using single and double exponential functions were made to data to measure NMDAR deactivation time-course (**Table 1**) and the time course of recovery from desensitization (**Figures 14** and **15**). NMDAR deactivation time-course was always best fit by a double exponential function, whereas recovery from desensitization was sometimes better fit by a single exponential function. For comparison with single exponential time constants (τ), double exponential time constants (τ_{fast} and τ_{slow}) were converted to a single weighted time constant (τ_w) by the equation, $\tau_w = (\tau_{fast}*I_{fast} + \tau_{slow}*I_{slow})/(A_{fast} + A_{slow})$, where A_{fast} and A_{slow} are the amplitudes of τ_{fast} and τ_{slow}.

Peak currents (I_{peak}) following synaptic-like glutamate applications were determined by measuring the mean current during a 3 ms window centered on the peak. For comparison across cells, I_{peak} was normalized to the mean I_{peak} in response to the first 10 control synaptic-like

glutamate applications. Steady inhibition ($I_{drug}/I_{control}$) during synaptic-like glutamate applications was measured as the mean I_{peak} in response to the last five synaptic-like glutamate applications in the presence of drug (I_{drug}), divided by the mean I_{peak} in response to the first 10 control synaptic-like glutamate applications and in response to the last 10 synaptic-like glutamate applications following recovery from inhibition ($I_{control}$). $I_{drug}/I_{control}$ during long glutamate applications was measured identically to concentration-response data. Cells where peak or steady-state currents did not display recovery from inhibition of at least 90% of the current preceding drug application were excluded from analysis.

For experiments to determine the time course of recovery from desensitization, I_{peak} in response to long glutamate applications was measured as the mean current during a 30 ms window set 5 ms preceding the time of peak current (**Figures 14** and **15**). A larger window was required to account for current variation not present with I_{peak} in response to synaptic-like glutamate applications. I_{peak}s were normalized to the I_{peak} in response to glutamate after a 200 s Interapplication Interval in order to mitigate effects of current rundown and to empirically determine the maximal current amplitude in the presence of drug. Cells where any normalized I_{peak} value > 1.2 were excluded from analysis, as these cells likely experienced unacceptable NMDAR current rundown or changes to cell properties.

We compared group data with one-way ANOVAs with Tukey's *post hoc* analysis with significance levels as indicated. All error is displayed as ± SEM unless otherwise indicated. Current traces for presentation were refiltered at 1 kHz.

70

3.4   RESULTS

3.4.1   Glutamate concentration does not strongly affect inhibition by memantine or ketamine

The glutamate concentration is likely to differ considerably between the synaptic and extrasynaptic compartments. Synaptic NMDARs briefly are exposed to ~1 mM glutamate following a presynaptic action potential(Clements et al., 1992), whereas extrasynaptic NMDARs experience sub- to low micromolar glutamate(Herman and Jahr 2007; Le Meur et al., 2007) from synaptically released glutamate spillover or from astrocytic glutamate release(Arnth-Jensen et al., 2002; Fellin et al., 2004; Lozovaya 2004; Talantova et al., 2013). It is unclear if NMDAR inhibition by memantine or ketamine depends on the glutamate concentration. Memantine potency has been shown to increase with increasing NMDA concentration(Chen et al., 1992), which may suggest greater inhibition of synaptic NMDARs, but other reports have shown memantine potency to have no dependence on agonist concentration(Gilling et al., 2007; Gilling et al., 2009). Importantly, the NMDAR subtype dependence has not been investigated, as these studies were conducted in cultured neurons(Chen et al., 1992; Gilling et al., 2007) or with only GluN1/2A receptors expressed in HEK293T cells(Gilling et al., 2009). To our knowledge, no studies have investigated whether ketamine potency depends on glutamate concentration. Therefore, we investigated whether a dependence of memantine or ketamine inhibition on the glutamate concentration could underlie preferential inhibition of synaptic or extrasynaptic NMDARs.

To explore the NMDAR subtype dependence and whether memantine or ketamine potency depends on glutamate concentration, we expressed GluN1/2A or GluN1/2B receptors in

tsA201 cells and measured the IC_{50} of memantine or ketamine when NMDARs are activated by either 1 mM or 0.3 µM glutamate. We chose a saturating concentration of 1 mM glutamate to mimic the glutamate concentration at synaptic NMDARs during synaptic transmission and 0.3 µM glutamate, ~10% glutamate EC_{50} for GluN1/2A and GluN1/2B receptors, to represent a lower bounds of detectable NMDAR activation. It is important to compare glutamate concentrations well above and well below the EC_{50}: for channel blockers that exhibit agonist concentration dependence of IC_{50}, blocker IC_{50} should depend on the channel open probability (not on absolute agonist concentration)(Johnson and Qian 2002; Blanpied et al., 2005). Therefore, our experiments are well-suited to detect whether memantine and ketamine potency depends on the concentration of glutamate.

We found that inhibition of GluN1/2A and GluN1/2B receptors by memantine depended slightly, but significantly on glutamate concentration (**Figure 9A**-**D**). The memantine IC_{50} for GluN1/2A receptors when activated by 1 mM glutamate was 1.82 ± 0.07 µM and when activated by 0.3 µM glutamate was 1.33 ± 0.06 µM ($p < 0.05$, one-way ANOVA with Tukey's *post hoc* analysis). The memantine IC_{50} for GluN1/2B receptors when activated by 1 mM glutamate was 0.68 ± 0.04 µM and when activated by 0.3 µM glutamate was 0.99 ± 0.05 µM ($p < 0.05$, one-way ANOVA with Tukey's *post hoc* analysis). In contrast, we found that inhibition of GluN1/2A and GluN1/2B receptors by ketamine did not depend on glutamate concentration (**Figure 9E**-**H**). The ketamine IC_{50} for GluN1/2A receptors when activated by 1 mM glutamate was 0.87 ± 0.05 µM and when activated by 0.3 µM glutamate was 1.03 ± 0.05 µM ($p > 0.05$, one-way ANOVA with Tukey's *post hoc* analysis). The ketamine IC_{50} for GluN1/2B receptors when activated by 1 mM glutamate was 0.42 ± 0.02 µM and when activated by 0.3 µM glutamate was 0.58 ± 0.03 µM ($p > 0.05$, one-way ANOVA with Tukey's *post hoc* analysis). Although memantine

inhibition does depend on glutamate concentration, vastly different glutamate concentrations cause only a small change in memantine inhibition, which is much weaker than the agonist concentration dependence of memantine potency observed previously(Chen et al., 1992). Further, the direction of concentration dependence was opposite for GluN1/2A and GluN1/2B receptors.

Interestingly, we found that inhibition by memantine or ketamine did depend weakly upon the NMDAR subtype with GluN1/2A displaying higher IC_{50} values than previously determined from our lab(Kotermanski and Johnson 2009; Kotermanski et al., 2009) ($p < 0.05$, one-way ANOVA with Tukey's *post hoc* analysis). A potentially important difference in recording conditions is the addition here of 10 μM EDTA to the extracellular solutions to chelate contaminating Zn^{2+} that inhibits GluN1/2A receptors with high nanomolar affinity. Because Zn^{2+} increases NMDAR sensitivity to inhibition by protons, and memantine and ketamine IC_{50} values decrease at lower pH(Dravid et al., 2007), our use of EDTA could have led to the higher memantine and ketamine IC_{50} measurements here.
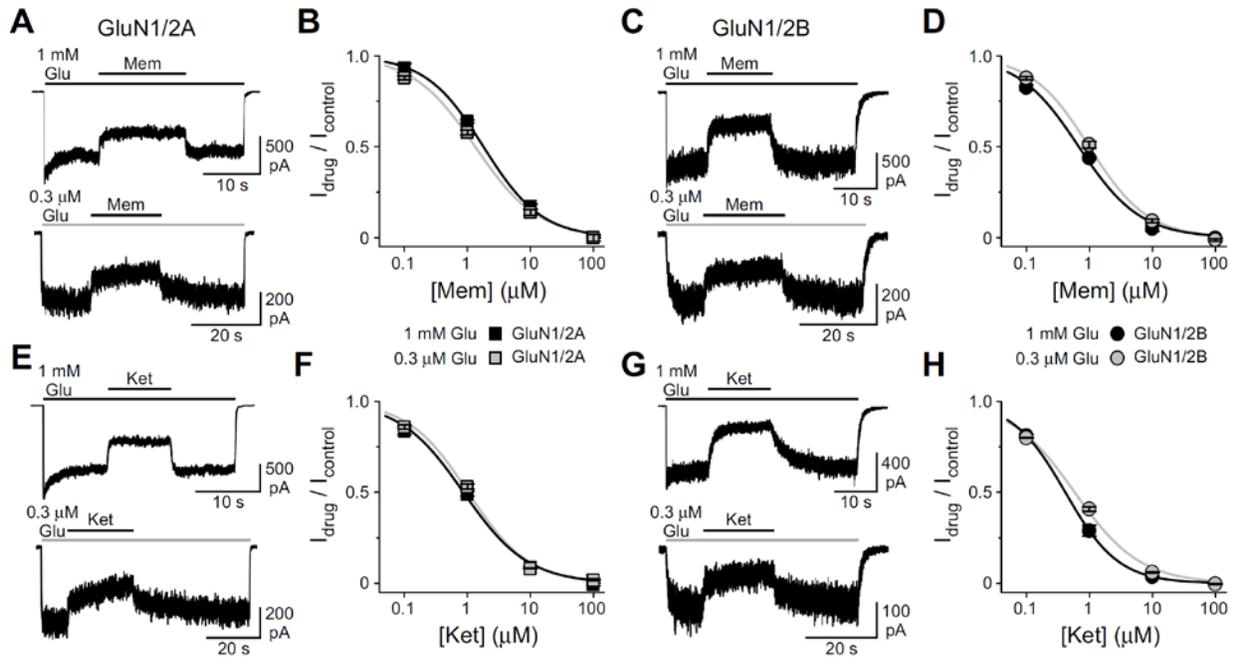
Figure 9. [Glutamate] does not strongly affect inhibition by memantine and ketamine.

A,C,E,G, Representative whole-cell recordings from cells transfected with the indicated NMDAR subtype activated by 1 mM glutamate (Glu, black bar, top) or 0.3 µM glutamate (gray bar, bottom), with application of one concentration (1 µM, black bars) of a four concentration-response curve of memantine (Mem) or ketamine (Ket). **B,D,F,H,** Mean concentration-response curves for Mem and Ket inhibition of GluN1/2A and GluN1/2B receptors, n = 4 – 7 cells.

3.4.2 Inhibition depends on duration of glutamate exposure and on NMDAR subtype

Synaptic NMDARs are transiently exposed to ~1 mM glutamate for ~1-2 ms with very rapid onset and offset kinetics(Clements et al., 1992). In contrast, extrasynaptic NMDARs are likely to be exposed to glutamate for much longer periods or tonically(Fellin et al., 2004; Herman and Jahr 2007; Le Meur et al., 2007; Harris and Pettit 2008; Povysheva and Johnson 2012; Riebe et al., 2016), which allows extrasynaptic NMDARs to reach steady-state activation. Whether inhibition of NMDARs by memantine or ketamine depends on the duration of glutamate exposure is not known, although memantine inhibition of synaptic NMDARs depends on the stimulation frequency, with higher frequency stimulation showing greater inhibition(Wild et al., 2013). To our knowledge, no previous studies have directly examined how the duration of glutamate exposure affects inhibition by any NMDAR open-channel blockers. Therefore, we investigated whether inhibition by memantine or ketamine depends on NMDAR subtype and on the duration of glutamate exposure.

We performed whole-cell recordings from lifted tsA201 cells expressing GluN1/2A or GluN1/2B receptors held at -65 mV. Open channel blockers like memantine and ketamine require channel opening in order to bind to the receptor. Therefore, steady levels of inhibition are reached through coapplication of agonist in the presence of drug for a sufficiently long time to reach equilibrium at a particular drug concentration. We measured steady levels of inhibition by memantine and ketamine during long glutamate applications (>45 s) by standard protocols (**Figure 11A-D**).

We achieved brief, synaptic-like glutamate applications (~2-5 ms, Table 1, Methods) through the following means. We performed recordings from lifted transfected cells to ensure rapid and complete solution exchange for synaptic-like glutamate applications (**Figure 10**; **Table 1**). The time course of currents activated by synaptic-like glutamate applications to cells expressing GluN1/2A or GluN1/2B receptors (**Figure 10C**-**D**) were consistent with outside-out patch currents recorded from HEK293 cells expressing the same NMDAR subtype activated by brief glutamate applications(Erreger et al., 2005). The time course of responses to synaptic-like glutamate applications (**Figure 10C**-**D**) were also consistent with EPSCs recorded from cultured neurons expressing predominantly the same NMDAR subtype(Gray et al., 2011; Tovar et al., 2013). Synaptic-like glutamate applications were delivered at 0.2 Hz to allow receptor deactivation between applications and to prevent apparent receptor desensitization (**Figure 10C**-**D**).

To measure inhibition of peak NMDAR currents in response to synaptic-like glutamate applications, we developed the following protocol (**Figure 11A**-**D**). We delivered 10 synaptic-like glutamate applications in the absence of drug to determine the control peak current amplitude (control), followed by synaptic-like glutamate applications in the continuous presence of memantine or ketamine until reaching a steady level of inhibition (drug; 20 applications for memantine and 40 applications for ketamine), then we delivered synaptic-like glutamate applications in the absence of memantine or ketamine to allow for recovery from inhibition (recovery; 20 applications for memantine and 40 applications for ketamine). The number of applications required to reach a steady level of inhibition and to allow for recovery from inhibition were empirically determined. We compared inhibition during synaptic-like and long glutamate applications at a single drug concentration (1 μM memantine and 0.5 μM ketamine)

near the IC_{50} values for GluN1/2A and GluN1/2B receptors. Because the drug concentration near the IC_{50} value is on the linear part of the sigmoidal curve, any change in potency should be reflected by a difference in fractional current. Only cells where paired measurements of inhibition during synaptic-like glutamate applications and during long glutamate applications were included.
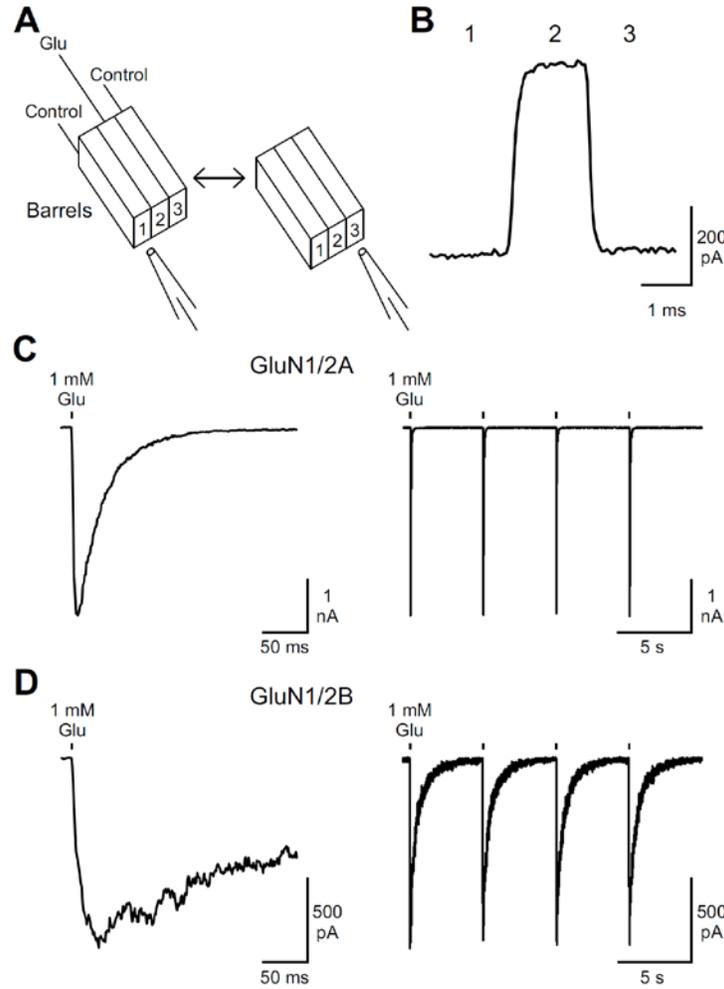
Figure 10. Synaptic-like glutamate applications to lifted transfected cells.

A, Schematic of fast perfusion system depicting three fused square glass barrels, containing normal extracellular solution (Control) or with 1 mM glutamate (Glu) added. Arrows indicate movement of barrels, which are attached to a linear motor, from barrel position 1 to barrel position 3 (or barrel position 3 to barrel position 1) in relation to a fixed recording pipette. **B**, Open pipette recordings of junction current relaxation during movement of barrels as in a, where barrel 2 contains a solution of ~50% osmolarity. **C,D**, Representative whole-cell recordings from lifted cells expressing GluN1/2A (**C**) or GluN1/2B receptors (**D**) when activated by synaptic-like applications of 1 mM glutamate (black bars) by moving as depicted in a. Traces on left are the first synaptic-like application shown on the right with repeated synaptic-like glutamate applications at 0.2 Hz.

Table 1. Kinetics of solution exchange and NMDAR activation and deactivation.

Solution exchange was measured as described in Methods. SD is standard deviation. No significant differences between the absence and presence of memantine or ketamine were observed for NMDAR activation or deactivation kinetics as determined by comparison with one-way ANOVA with Tukey's *post hoc* analysis, $p > 0.05$. n = 6 for all groups.

Solution Exchange	Condition	10-90% Rise Time (ms)		τ (ms)	
		Average	± SD	Average	± SD
Open Pipette		0.18	0.05	0.09	0.03
Whole-Cell	Lifted Cell	3.37	0.65	2.02	0.35
Whole-Cell	Unlifted Cell	150	35.3	27.4	6.65
		10-90% Rise Time (ms)		τ_w (ms)	
NMDAR Subtype	Condition	Average	± SEM	Average	± SEM
GluN1/2A	Control	4.50	0.34	31.5	3.85
	Memantine	4.63	0.49	28.5	3.25
	Recovery	4.72	0.41	33.3	3.73
	Control	4.13	0.32	31.8	3.02
	Ketamine	4.24	0.41	31.6	3.81
	Recovery	4.11	0.37	34.8	3.39
GluN1/2B	Control	17.6	2.38	400	47.2
	Memantine	21.0	1.66	361	53.0
	Recovery	17.4	2.45	369	43.5
	Control	24.0	3.41	456	60.3
	Ketamine	25.3	3.12	423	63.5
	Recovery	18.3	3.34	425	64.6

We found that memantine and ketamine inhibition during synaptic-like glutamate applications can differ significantly from inhibition during long glutamate applications, but this difference depends on the NMDAR subtype (**Figure 11E**). 1 μM memantine inhibited GluN1/2A receptors significantly less during synaptic-like glutamate applications than during long glutamate applications, whereas 1 μM memantine inhibited GluN1/2B receptors similarly during synaptic-like and long glutamate applications (**Figure 11A**, **B**, **E**). 0.5 μM ketamine inhibited GluN1/2A receptors significantly less during synaptic-like glutamate applications than during long glutamate applications, whereas 0.5 μM ketamine inhibited GluN1/2B receptors significantly more during synaptic-like glutamate applications than during long glutamate applications (**Figure 11C**-**E**). Therefore, inhibition by both memantine and ketamine depends on the duration of glutamate exposure and on the NMDAR subtype.

We also examined whether memantine or ketamine affected the time course of responses to synaptic-like glutamate applications. We found that neither memantine nor ketamine significantly alters activation or deactivation kinetics of GluN1/2A or GluN1/2B receptors (Table 1). Our findings are in contrast to a study that investigated differences between inhibition of memantine and ketamine in cultured hippocampal neurons(Emnett et al., 2013), which contain a mixed population of GluN2A- and GluN2B-containing receptors(Tovar and Westbrook 1999; Groc et al., 2006; Thomas et al., 2006; Harris and Pettit 2007; Martel et al., 2009; Petralia et al., 2010). The authors found that NMDAR EPSC deactivation kinetics were significantly more rapid in the presence of memantine or ketamine(Emnett et al., 2013). Since GluN2A-containing receptors display deactivation kinetics 5 – 10 fold faster than GluN2B-containing receptors(Vicini et al., 1998), the ability of memantine and ketamine to quicken NMDAR EPSC deactivation kinetics could reflect preferential inhibition of GluN2B-containing receptors. This is

consistent with our finding that both memantine and ketamine inhibit GluN1/2B receptors significantly more than GluN1/2A receptors during synaptic-like glutamate applications (**Figure 11E**).
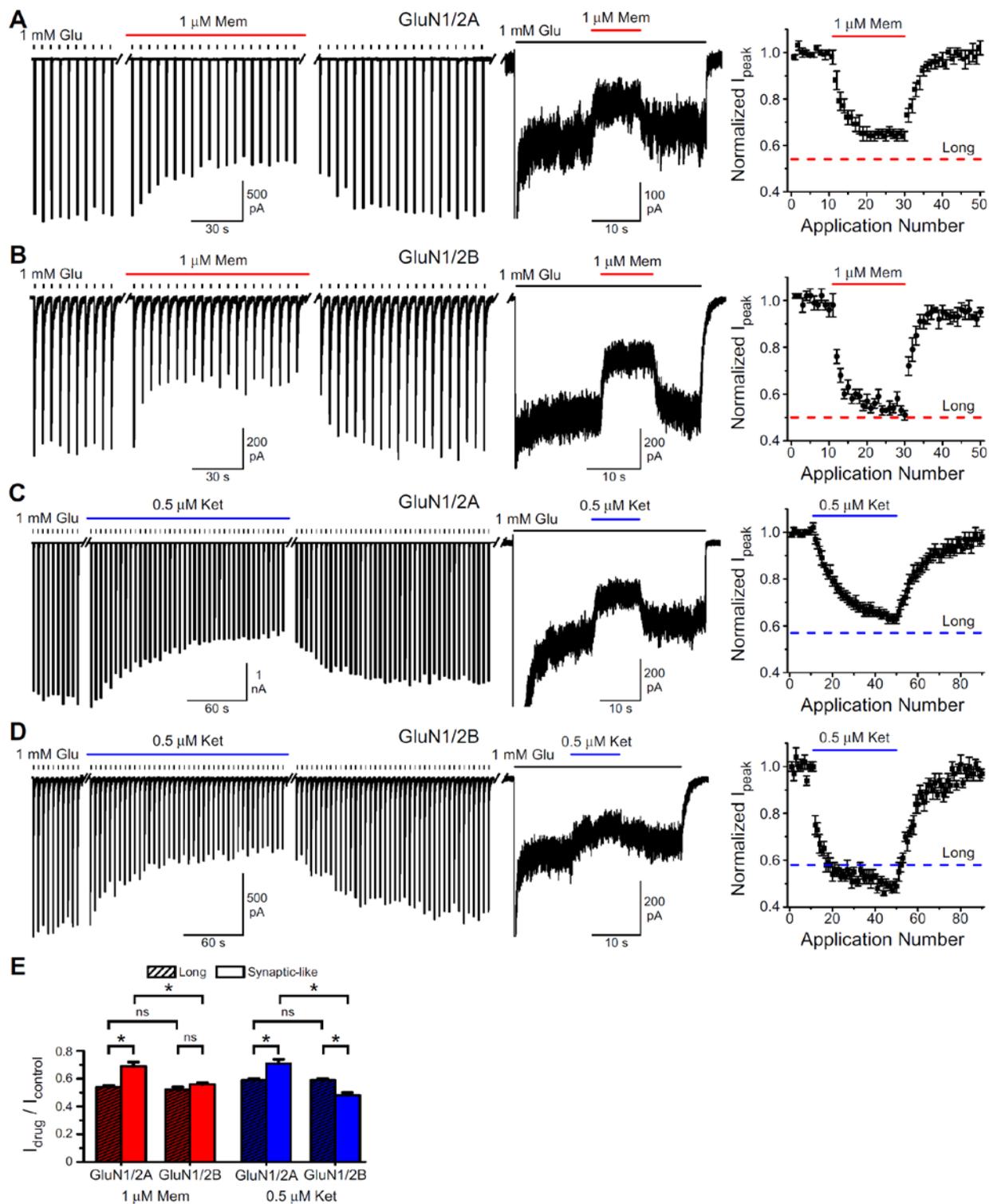
Figure 11. Inhibition by memantine and ketamine depends on duration of glutamate exposure in an NMDAR subtype-dependent manner.

82

A, Representative whole-cell recording of a lifted cell expressing GluN1/2A receptors in response to synaptic-like (left) or long (center) glutamate applications (black bars) in the absence or presence of memantine (red bars). Right, plot of mean I_{peak} (black symbols) during synaptic-like glutamate applications normalized to the average of the I_{peak} in response to the first 10 synaptic-like glutamate applications. Red dashed line indicates mean memantine inhibition during long glutamate applications. **B-D**, Same as a, except for cells expressing the indicated NMDAR subtype and for ketamine (blue bars, blue dashed lines, **C-D**). Inhibition during synaptic-like and long glutamate applications are paired, n = 6 cells for each group. e, Mean $I_{drug}/I_{control}$ for memantine and ketamine inhibition of GluN1/2A and GluN1/2B receptors during synaptic-like or long glutamate applications. Groups were compared by one-way ANOVA with Tukey's *post hoc* analysis; *, $p < 0.05$ and ns, $p > 0.05$.

3.4.3   Memantine enhances desensitization of GluN1/2A receptors

We next focused on the drug-receptor subtype combination with the largest discrepancy between inhibition of responses to synaptic-like and to long glutamate applications, inhibition by memantine of GluN1/2A receptors. We used kinetic models to investigate mechanisms by which inhibition by a channel blocker could depend on the duration of glutamate exposure. Due to memantine's relatively slow kinetics and because memantine inhibits current flow, it is not practical to determine blocked arm rates of kinetic models from single-channel recordings in the presence of memantine. Since complex open channel blocker models have a large number of states and adjustable parameters, we first used a simple kinetic model(Clements and Westbrook 1991) with the fewest closed and open states while still being able to account for agonist binding, channel opening, and receptor desensitization (Model A; **Figure 12A**). In our model, only glutamate (agonist, A) binding is depicted, as all of our experiments were conducted in the continuous presence of a saturating concentration of glycine. Memantine and ketamine are at

83

least partially trapping open-channel blockers(Blanpied et al., 1997; Chen and Lipton 1997; Sobolevsky et al., 1998; Mealing et al., 1999; Kotermanski et al., 2009). Like "foot-in-the-door" open-channel blockers, trapping open-channel blockers can only bind and unbind from the receptor when the channel is open. Unlike "foot-in-the-door" blockers, the channel is able to close with a trapping blocker bound, thereby trapping the blocker in the channel(Johnson and Kotermanski 2006). Presumably, closed receptors blocked by drug can access all the states available to unblocked receptors. The inhibitory properties of many open channel blockers depend not only on block of current flow, but also on alteration of transition rates between states while the blocker is bound in the channel (Johnson and Qian 2002; Johnson et al., 2015). Therefore, we examined the hypothesis that memantine acts in part by altering transitions between receptor states thereby causing the observed dependence of memantine inhibition on the duration of glutamate exposure.

We used optimized rates of Model A (**Figure 12B**, **Section 3.3.4**) to simulate our experiment where we measured inhibition during synaptic-like and long glutamate applications (**Table 2**). When Model A is symmetrical, where all rates in the blocked arm are equal to the rates in the unblocked arm, current simulations predicted that inhibition during synaptic-like glutamate applications should be identical to inhibition during long glutamate applications (**Table 2**). The prediction of the symmetrical model does not match our experimental results. This suggests that memantine is altering the transition between receptor states. Therefore, we simulated inhibition during synaptic-like and long glutamate applications when each blocked arm rate was increased or decreased by 5-fold (**Table 2**). For ease of comparison, we calculated the ratio of inhibition during synaptic-like glutamate applications to inhibition during long applications (Synaptic-like/Long Ratio; **Table 2**). Changes to three rate constants caused the

Synaptic-like/Long Ratio to change in a similar direction and magnitude to our data (**Table 2**). Therefore, our modeling suggests that the dependence of memantine inhibition on duration of glutamate application is due to memantine altering one or more of the rates of receptor state transitions identified in **Table 2**.
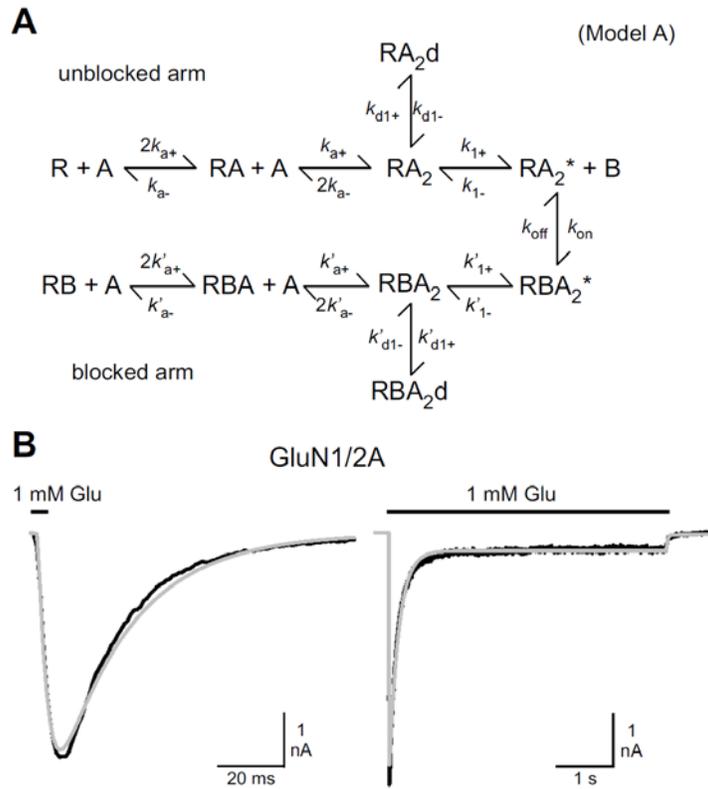
Figure 12. Model A.

A, GluN1/2A receptor trapping block model (Model A) used to describe inhibition by memantine (blocker, B). The unblocked arm describes receptor function in the absence of memantine, whereas the blocked arm allows memantine binding and trapping and describes any changes memantine imparts on channel function. **B**, Current traces (black lines) of GluN1/2A receptors activated by synaptic-like (left) or long (right) applications of 1 mM glutamate (black bars) in the absence of memantine, with simulations (gray lines) of Model A overlaid.

86

Table 2. Model A blocked arm rates affect memantine inhibition.

Model A blocked arm rates were individually increased (up arrow) or decreased (down arrow) 5-fold (5x) from the unblocked arm rates (Methods). $I_{drug}/I_{control}$ of Model A simulations (not shown) are measured as described in Methods. Model A blocked arm rates that produced a Synaptic-like/Long ratio qualitatively similar to experimental results are in bold text.

Model A Blocked Arm Rates	k_{off} (s^{-1})	$I_{drug}/I_{control}$		Ratio Synaptic-like/Long
		Synaptic-like	Long	
Experimental	-	0.65	0.54	**1.20**
Symmetrical	30	0.50	0.50	1.01
k'_{a+} ↑ 5x	30	0.51	0.50	1.02
k'_{a+} ↓ 5x	30	0.47	0.50	0.95
k'_{a-} ↑ 5x	30	0.30	0.50	0.60
k'_{a-} ↓ 5x	30	0.75	0.50	**1.51**
k'_{1+} ↑ 5x	6	0.48	0.49	0.99
k'_{1+} ↓ 5x	150	0.52	0.50	1.03
k'_{1-} ↑ 5x	150	0.52	0.50	1.04
k'_{1-} ↓ 5x	6	0.48	0.49	0.98
k'_{d1+} ↑ 5x	150	0.81	0.52	**1.57**
k'_{d1+} ↓ 5x	6	0.21	0.44	0.47
k'_{d1-} ↑ 5x	6	0.21	0.44	0.47
k'_{d1-} ↓ 5x	150	0.80	0.55	**1.44**

Model A is unable to capture more complex aspects of NMDAR activation, including multiple desensitized states. Because Model A identified rates of desensitization to be potentially involved in memantine inhibition, we used a more sophisticated kinetic model (Banke and Traynelis 2003; Erreger et al., 2005) that contains multiple desensitized and pre-open states (Model B, **Figure 13A**). Model B contains an additional desensitized state (RA_2D_2) as well as 2 additional pre-open states (RA_21 and RA_22) between the fully liganded closed state, RA_2, and the open state, RA_2^*. Model B has the disadvantage of an increased number of adjustable rates in the blocked arm. As the number of adjustable rates increases, the accuracy and validity of the model decreases. Model A was therefore used to constrain the number of adjustable parameters in Model B, thereby improving the accuracy and validity of its prediction. Model A rates that did not predict dependence on duration of glutamate application were fixed in the blocked arm of Model B. The additional pre-open states in Model B were equated to the single opening rates in Model A. Based on results from Model A (**Table 2**), we let either the agonist unbinding rate (k'_{a-}), the desensitization rates ($k'_{d1+/-}$ and $k'_{d2+/-}$), or k'_{a-}, $k'_{d1+/-}$, and $k'_{d2+/-}$ to vary and performed fits to our experimental data (**Table 3**). The memantine unbinding rate, k_{off}, was varied in each fit because the value of k_{off} is not known and is estimated to approximate the apparent affinity (IC_{50}; **Section 3.3.5**). When Model B is symmetrical (Model B1), it predicts poor agreement with our experimental data (**Figure 13B**-**D**; **Table 3**). Fits where only k_{a-} and k_{off} varied never converged by our criteria (Methods). Models where $k_{d1+/-}$, $k_{d2+/-}$, and k_{off} varied (Model B2), or where k_{a-}, $k_{d1+/-}$, $k_{d2+/-}$, and k_{off} varied (Model B3) both fit our experimental data better than symmetrical Model B1 (**Figure 13B-D**; **Table 3**). Model B2 and Model B3 are similar in how well they fit experimental data, however, Model B2 contains one fewer free parameter, suggesting that allowing k_{a-} to vary does not greatly benefit the goodness of fit. Our kinetic modeling suggests

that memantine preferentially inhibits NMDAR responses activated by long glutamate applications primarily by increasing occupancy of desensitized states.
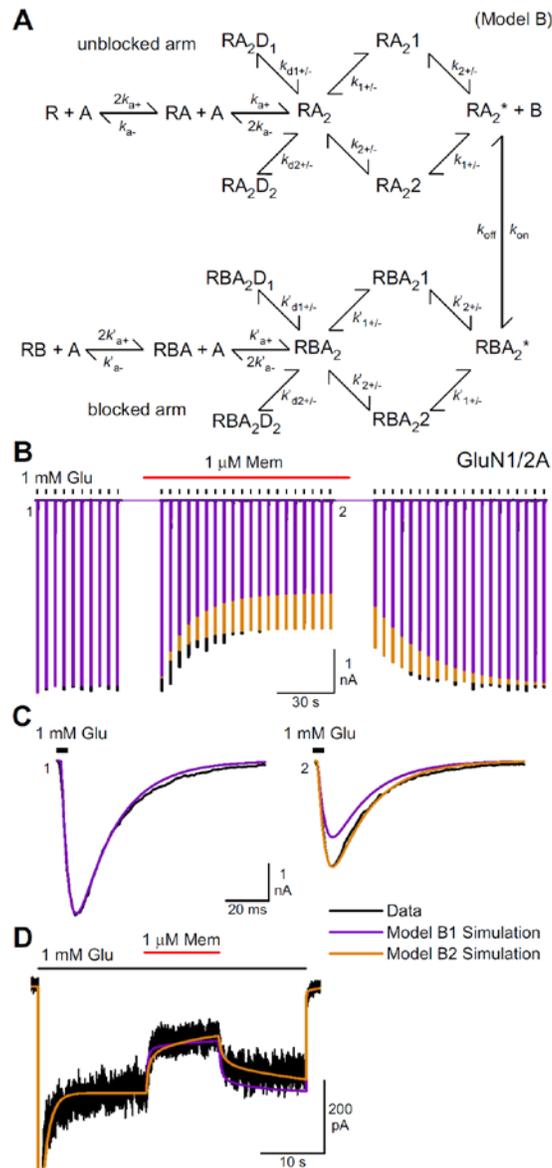
Figure 13. Model B predicts that memantine increases occupancy of desensitized states of GluN1/2A receptors.

A, GluN1/2A receptor trapping block model (Model B) used for fitting to current traces in the presence of memantine (red bars). **B-D**, Current traces (black lines) of GluN1/2A receptors activated by synaptic-like (**B**, **C**) or long (**D**) applications of 1 mM glutamate (black bars) in the absence or presence of memantine (red lines) overlaid with simulations of Model B1 (purple lines) or Model B2 (orange lines). Current traces and simulations in **C** show individual responses to synaptic-like applications of glutamate indicated in **B** with a shorter time-base.

90

Table 3. Model B predicts that memantine affects desensitization rates of GluN1/2A receptors.

Model B blocked arm rates allowed to vary during fits to data are indicated by [f] for Model B2 and Model B3. All other rates were fixed during fits to data. Red text indicates rates that decreased more than 1.5-fold and blue text indicates rates that increased more than 1.5-fold. Final sums of squared error (SSE) for the least squares fits are shown. Model B1 allowed no blocked arm rates to vary to establish the baseline SSE predicted.

Rate Constant	Units	Model B1, B2, B3 Unblocked Arm	Model B1 Blocked Arm	Model B2 Blocked Arm	Model B3 Blocked Arm
k_{a+}	$\mu M^{-1}s^{-1}$	31.6	31.6	31.6	31.6
k_{a-}	s^{-1}	1010	1010	1010	550[f]
k_{1+}	s^{-1}	2155	2155	2155	2155
k_{1-}	s^{-1}	198	198	198	198
k_{2+}	s^{-1}	109	109	109	109
k_{2-}	s^{-1}	185	185	185	185
k_{d1+}	s^{-1}	72.5	72.5	207[f]	142[f]
k_{d1-}	s^{-1}	1.96	1.96	0.45[f]	0.36[f]
k_{d2+}	s^{-1}	76.7	76.7	130[f]	85[f]
k_{d2-}	s^{-1}	0.24	0.24	0.08[f]	0.07[f]
k_{on}	$\mu M^{-1}s^{-1}$	30	30	30	30
k_{off}	s^{-1}	30	30	92[f]	71[f]
K_d	μM	1	1	3.07	2.37
SSE	-	-	10,830,465	6,483,686	6,470,443

91

3.4.4 Memantine stabilizes a Ca^{2+}-dependent desensitized state of GluN1/2A receptors

Next, we experimentally tested the validity of our kinetic modeling results. Our modeling suggests that memantine inhibits in part through increasing occupancy of desensitized states. We used Model B2 to predict the time course of recovery from desensitization in the absence and presence of memantine. Model B2 predicts that in the presence of 3 μM memantine (a concentration at which memantine is bound to ~70% of receptors) the time course of recovery from desensitization, as measured by a fitting with a double exponential function, should be ~4-fold slower than in the absence of memantine (compare Control and Mem in **Figure 14C**). We tested the Model B2 prediction in cells expressing GluN1/2A receptors by measuring the time course of recovery from desensitization in the absence and presence of 3 μM memantine.

To determine the time course of recovery from desensitization we used the following protocol. We applied 1 mM glutamate to GluN1/2A-expressing tsA201 cells held at -65 mV for 30 s to allow receptors to reach steady-state level of activation, then reapplied 1 mM glutamate for 30 s after an increasing interval from 0.2 – 200 s (Interapplication Interval) (**Figure 14A-B**). We measured the peak current (I_{peak}) following reapplication of glutamate and normalized it to the I_{peak} following the longest Interapplication Interval of 200 s. Measurement of the time course of recovery from desensitization was performed in the absence and the presence of 3 μM memantine. We found that 3 μM memantine significantly slows the time course of recovery from desensitization (Control, τ_w = 5.46 ± 1.71 s; Mem, τ_w = 47.2 ± 8.50 s, $p < 0.05$, one-way ANOVA; **Figure 14C** and **Figure 15E**). Our experimental results display greater slowing of

recovery from desensitization than predicted by Model B2 (Control Simulation, τ_w = 2.48 s; Mem Simulation, τ_w = 9.78 s; **Figure 14C**). This discrepancy reflects a limitation of our modeling. Nevertheless, our results qualitatively support the conclusions of our kinetic modeling: memantine stabilizes and slows the rate of exit from one or more desensitized states of NMDARs.

Next, we investigated whether memantine affects a particular type of NMDAR desensitization. GluN1/2A receptor-mediated currents typically decay slowly during prolonged exposure to a constant concentration of agonists via multiple pathways that have been referred to as desensitization or inactivation (Traynelis et al., 2010). There are at least three separable types of NMDAR desensitization or inactivation (Dingledine et al., 1999): (1) glycine-dependent desensitization, which involves a glutamate-induced decrease of glycine affinity that due to our use of a saturating glycine concentration, we do not observe; (2) Ca^{2+}-dependent inactivation, which is thought to be controlled by Ca^{2+} influx-dependent activation of intracellular signaling pathways that act on the C-terminal domains of NMDAR subunits; and (3) glycine- and Ca^{2+}-independent desensitization. Unless otherwise specified, we will use desensitization to refer generally to decreases in current in the continuous presence of agonist. To determine whether memantine stabilizes a Ca^{2+}-dependent desensitized state, we measured the time course of recovery from desensitization in the absence and presence of 3 μM memantine in 0.1 mM external Ca^{2+} ($[Ca^{2+}]_o$), a $[Ca^{2+}]_o$ that does not display Ca^{2+}-dependent desensitization (Legendre et al., 1993). We found that in 0.1 mM $[Ca^{2+}]_o$, the time course of recovery from desensitization was slightly, but not significantly faster in the absence of memantine and was no different in the presence of memantine (Control, τ_w = 1.93 ± 0.25 s; Mem, τ_w = 1.28 ± 0.35 s, p > 0.05; **Figure**

14D). Our results suggest that memantine specifically stabilizes a Ca^{2+}-dependent desensitized state.

If memantine inhibits GluN1/2A receptors in part through stabilization of a Ca^{2+}-dependent desensitized state, then the memantine IC_{50} should depend on the $[Ca^{2+}]_o$. Therefore, we compared memantine IC_{50} in 0.1 mM $[Ca^{2+}]_o$ to the IC_{50} in 1 mM $[Ca^{2+}]_o$ with reduced intracellular Ca^{2+} buffering capacity using 1 mM EGTA instead of 10 mM BAPTA in the intracellular pipette solution. Consistent with our finding that memantine stabilizes a Ca^{2+}-dependent desensitized state, we found that memantine IC_{50} was significantly higher with 0.1 mM $[Ca^{2+}]_o$ (2.41 ± 0.12 µM) than with 1 mM $[Ca^{2+}]_o$ and 1 mM intracellular EGTA (1.22 ± 0.06 µM; $p < 0.0001$, Student's t-test). Interestingly, the memantine IC_{50} in 1 mM $[Ca^{2+}]_o$ and 10 mM intracellular BAPTA is intermediate to these two conditions (1.82 µM; **Figure 9**). The memantine IC_{50} in 0.1 mM $[Ca^{2+}]_o$ is similar to the K_d ($K_d = k_{off}/k_{on}$) predicted by Model B2 and B3 (**Table 3**). Because $K_d = IC_{50}$ in a symmetrical model, a similar K_d to IC_{50} in 0.1 mM $[Ca^{2+}]_o$ suggests that the presence of memantine in the GluN1/2A receptor channel only alters receptor state transitions in the presence of Ca^{2+}. The observed Ca^{2+} dependence is likely due to action of Ca^{2+} on intracellular signaling molecules, however we cannot rule out an effect of Ca^{2+} on the channel itself (Ascher and Nowak 1988; Maki and Popescu 2014).
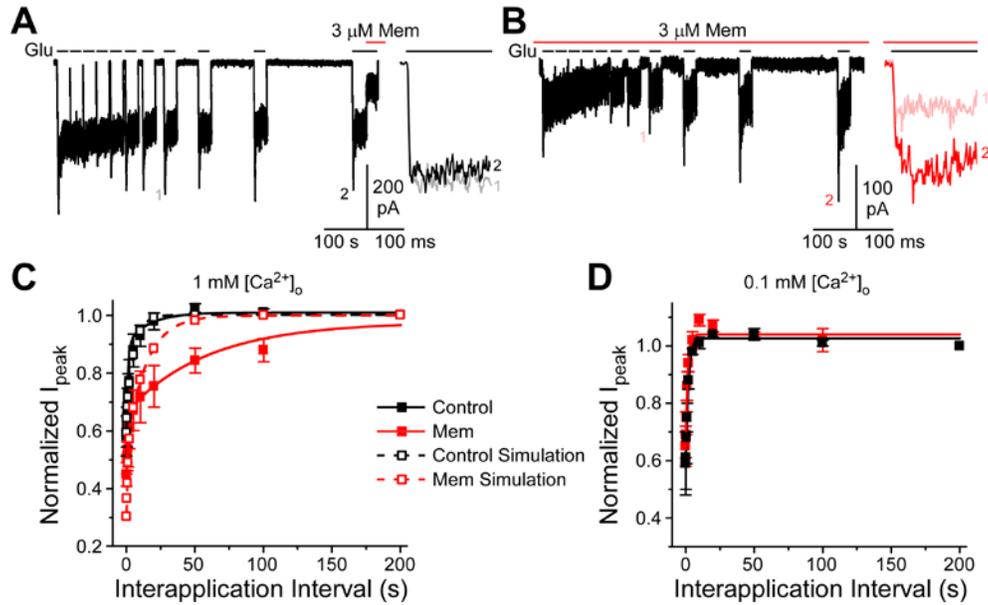
Figure 14. Memantine slows recovery from desensitization of GluN1/2A receptors in a Ca^{2+}-dependent manner.

A,B, Representative current traces of GluN1/2A receptors activated by 1 mM glutamate (black bars) during the recovery from desensitization protocol in the absence (**A**) or presence of 3 μM memantine (**B**, red bars). Insets at right show I_{peak} responses at two Interapplication Intervals indicated at left, with shortened time-base, in the absence (black and gray lines) and presence of memantine (red and pink lines). **C-D,** Closed squares display mean I_{peak} normalized to I_{peak} at 200 s of GluN1/2A receptors in 1 mM $[Ca^{2+}]_o$ (**C**) or in 0.1 mM $[Ca^{2+}]_o$ (**D**) in the absence (Control) or presence of memantine (Mem). Open squares display the normalized I_{peak} simulated by Model B2 in the absence and presence of memantine. Solid and dashed lines show single or double exponential fits to the mean time course of recovery from desensitization. n = 5 cells for each group.

95

3.4.5 Memantine and ketamine differentially alter desensitization kinetics of NMDARs

Next we compared the effects of memantine and ketamine on recovery from desensitization of GluN1/2A and GluN1/2B receptors. As described above, we measured the time course of recovery from desensitization in the absence and presence of 3 μM memantine or an approximately equipotent concentration of ketamine, 1.5 μM. To increase the success rate of our experiments we removed two Interapplication Intervals, 0.2 and 0.5 s, as these intervals provided little additional information. We found that unlike memantine, ketamine had no significant effect on the time course of recovery from desensitization of GluN1/2A receptors (**Figure 15A, C, E**). The normalized I_{peak} for memantine was significantly less than for ketamine and control at each Interapplication Interval (except at 200 s), whereas normalized I_{peak} for ketamine and control were not significantly different at any Interapplication Interval (**Figure 15C**). Additionally, recovery from desensitization of GluN1/2A receptors in the presence of ketamine was well fit by a single exponential function, instead of a double exponential function for memantine. This suggests that ketamine and memantine have distinct effects on GluN1/2A receptor state transitions (**Figure 15E**). For GluN1/2B receptors we found that the presence of memantine had no significant effect on recovery from desensitization. In contrast, ketamine recovery from desensitization was ~3.5-fold faster than control and was well fit by a single exponential (**Figure 15B, D, E**). The normalized I_{peak} for memantine was not significantly different from control at any Interapplication Interval, but the normalized I_{peak} was significantly less than ketamine at 10 s, whereas the normalized I_{peak} for ketamine was significantly greater than control at several

96

Interapplication Intervals (**Figure 15D**). Our findings suggest that memantine and ketamine differentially alter rates of transitions from desensitized states in a subtype-dependent manner.
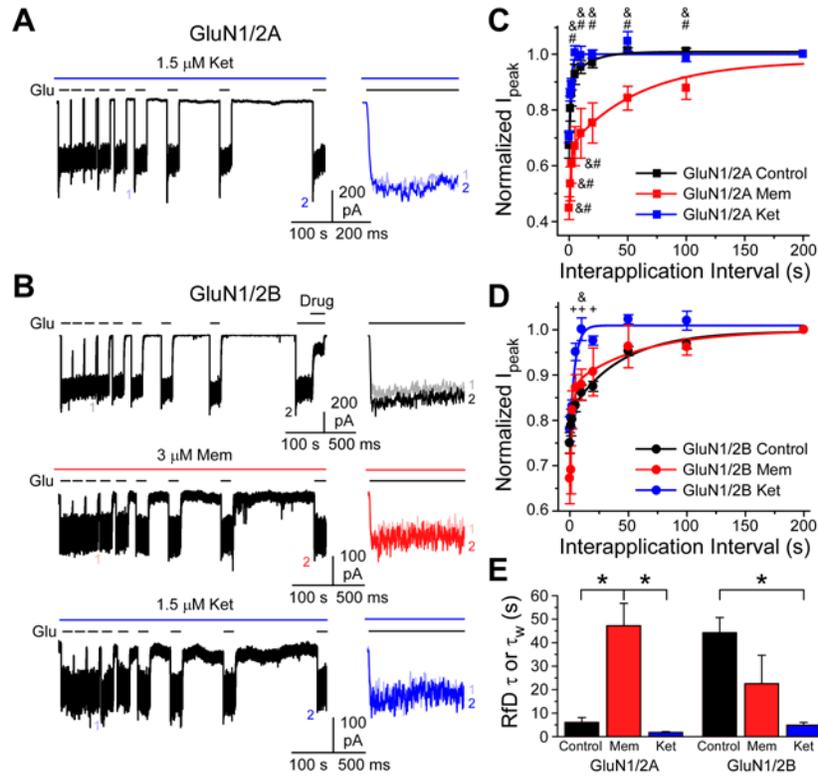
Figure 15. Memantine and ketamine differentially alter NMDAR desensitization kinetics.

A,B, Representative current traces of GluN1/2A (**A**) or GluN1/2B (**B**) receptors activated by 1 mM glutamate (black bars) during the recovery from desensitization protocol in the presence of 1.5 μM ketamine (**A**, **B**, bottom; Ket, blue bars), absence of drug (**B**, top) or presence of 3 μM memantine (**B**, middle; Mem, red bars). Insets at right show I_{peak} responses at two Interapplication Intervals indicated at left, with shortened time-base, in the absence of drug (**B**, top; black and gray lines) presence of memantine (b, middle; red and pink lines) or presence of ketamine (**A**, **B**, bottom; blue and light blue lines). **C,D**, Closed symbols display the mean normalized I_{peak} of GluN1/2A (**C**) and GluN1/2B (**D**) receptors in the absence (Control) or presence of memantine or ketamine. Lines show single or double exponential fits to the mean time course of recovery from desensitization. Control data for GluN1/2A receptors from **Figure 14** was combined with Controls for ketamine in **C**, and data of GluN1/2A Mem from **Figure 14** is replotted. Mean I_{peak} at each Interapplication Interval was compared by one-way ANOVA with Tukey's *post hoc* analysis. # indicates $p < 0.05$ between Control and Mem, + indicates $p < 0.05$ between Control and Ket, and & indicates $p < 0.05$ between Mem and Ket. n = 5 – 6 cells in each group. e, mean τ or τ_w from

fits of the time course of recovery from desensitization (RfD). * indicates $p < 0.05$ by one-way ANOVA with Tukey's *post hoc* analysis.

3.5   DISCUSSION

Recent work suggests that memantine and ketamine inhibit overlapping but distinct subpopulations of NMDARs, and that this feature may be related to their divergent clinical profiles. Here we have uncovered subtle mechanistic differences in NMDAR inhibition by memantine and ketamine that likely underlie their ability to inhibit distinct subpopulations of NMDARs. In a reduced system, we investigated whether inhibition by memantine and ketamine depended on three properties or features that are likely to vary between synaptic and extrasynaptic compartments: the NMDAR subtype, the concentration of glutamate activating receptors, and the duration of glutamate receptors are exposed to. We found that inhibition by both memantine and ketamine depended on the duration of glutamate exposure in an NMDAR subtype-dependent manner. Using kinetic modeling, we further investigated the basis of memantine inhibition dependence on the duration of glutamate application and found that memantine increases occupancy of a Ca^{2+}-dependent desensitized state of NMDARs. These findings have broad implications for the action of memantine as a neuroprotectant. Specifically, our results suggest that memantine is neuroprotective in part through increased inhibition of highly activated NMDARs (e.g. receptors where the intracellular concentration of Ca^{2+} is elevated), as opposed to inhibition of specifically synaptic or extrasynaptic NMDARs. This difference could underlie discrepancies in the literature highlighting the involvement of synaptic NMDARs (Papouin et al., 2012; Wroge et al., 2012; Zhou et al., 2013) or extrasynaptic

99

NMDARs (Hardingham et al., 2002; Leveille et al., 2008; Papadia et al., 2008; Okamoto et al., 2009; Bordji et al., 2010; Milnerwood et al., 2010; Kaufman et al., 2012; Dau et al., 2014) in cell death. Furthermore, we found that memantine and ketamine differentially alter desensitization kinetics of NMDARs. Our study highlights the modulation of desensitization as an unexplored mechanism of inhibition for activation-selective NMDAR blockers.

The hypothesis that memantine inhibits extrasynaptic NMDARs more potently than synaptic NMDARs was supported directly and indirectly by several different groups and in several different preparations (Zhao et al., 2006; Leveille et al., 2008; Papadia et al., 2008; Okamoto et al., 2009; Milnerwood et al., 2010; Xia et al., 2010; Wild et al., 2013; Wu and Johnson 2015; Vyklicky et al., 2016). Despite memantine's modest selectivity for extrasynaptic NMDARs (2- to 5-fold over synaptic NMDARs), it is increasingly being used as a tool to selectively inhibit extrasynaptic NMDAR activity (Wills et al., 2012; Ferrario et al., 2013; Joe et al., 2014; Garcia-Munoz et al., 2015; Iizuka et al., 2015; Lo et al., 2015; Riebe et al., 2016). Our data argue that memantine is not truly selective for synaptic or extrasynaptic NMDARs. Instead memantine inhibition depends upon the intensity of NMDAR activation (both duration and glutamate concentration) and on the NMDAR subtypes present. In addition, our results suggest that it is not necessarily the subcellular location that determines the degree of inhibition, but rather the duration of glutamate exposure that determines whether the NMDAR will likely reach Ca^{2+}-dependent desensitized states.

Notably, Ca^{2+}-dependent desensitization of NMDARs is subtype-dependent. GluN1/2A and GluN1/2D receptors do display Ca^{2+}-dependent desensitization, whereas GluN1/2B and GluN1/2C receptors do not (Medina et al., 1995; Krupp et al., 1996). Memantine shows a similar pattern of NMDAR subtype dependence, where GluN1/2A receptors display an effect and

100

GluN1/2B receptors do not, in two of our experiments: (1) whether inhibition depends on the duration of glutamate exposure, and (2) whether the time course of recovery from desensitization is affected by the presence of memantine. Our data suggest a causal link between these two phenomena; memantine stabilizes a Ca^{2+}-dependent desensitized state of GluN1/2A receptors, which causes memantine to slow recovery from desensitization and thus inhibition increases with long durations of glutamate exposure. In contrast, since GluN1/2B receptors do not enter a Ca^{2+}-dependent desensitized state, memantine cannot stabilize this state, memantine does not slow the recovery from desensitization, and inhibition does not depend on the duration of glutamate exposure. Inhibition by ketamine follows a similar, but more complicated pattern of NMDAR subtype dependence. Ketamine does not significantly affect the time course of recovery from desensitization of GluN1/2A receptors, but inhibition does depend on the duration of glutamate exposure. In contrast, and similar to the pattern with memantine, ketamine speeds recovery of desensitization of GluN1/2B receptors and inhibition decreases with long durations of glutamate exposure. It is possible that ketamine did not reach a steady level of inhibition during synaptic-like glutamate applications to GluN1/2A receptors. It is also likely that ketamine affects another unidentified aspect of channel function that we did not consider here. For instance, our data suggest that in the presence of ketamine, the time course of recovery from desensitization follows a single exponential time course. This could mean that receptors cannot access all the closed states while bound to ketamine, which we did not consider in our modeling. Also, ketamine has been reported to have a second site of action accessible from the membrane or intracellular space (Orser et al., 1997). Overall, a drug's effect on desensitization kinetics seems to predict whether inhibition will depend on the duration of glutamate exposure.

Memantine stabilizing a Ca^{2+}-dependent desensitized state of GluN1/2A receptors presents a novel, rational mechanism of neuroprotection: increased inhibition of highly activated receptors with increased Ca^{2+}-influx, while leaving receptors not experiencing as intense activation relatively spared from inhibition. To evaluate the plausibility of this mechanism, we must consider several physiological factors we have not investigated. First, triheteromeric NMDARs may make up a majority of synaptic and extrasynaptic receptors (Paoletti et al., 2013), yet we do not know how memantine and ketamine affect desensitization kinetics of triheteromeric GluN1/2A/2B receptors. Methods have only recently been developed to study triheteromeric NMDARs in isolation and the role of Ca^{2+}-dependent desensitization on these subtypes is not known (Hansen et al., 2014; Stroebel et al., 2014). Second, we do not know how the presence of physiological concentrations of extracellular Mg^{2+} may affect our findings. Mg^{2+} competes with memantine and ketamine for binding, thus lowering each drug's potency (Kotermanski and Johnson 2009), but how Mg^{2+} interacts with their effects on desensitization kinetics is not known. A recent study has shown that presence of Mg^{2+} reveals differential inhibition of synaptic NMDARs activated by spontaneous EPSCs by memantine and ketamine (Gideons et al., 2014), which supports the need to further investigate mechanisms of action in the presence of Mg^{2+}. Also, specific GluN2B subunit deletion in cortical pyramidal neurons mimicked and occluded the antidepressant effects of ketamine in a rodent model of depression (Miller et al., 2014), suggesting that ketamine's NMDAR subtype dependence can be maintained in the presence of Mg^{2+} and native triheteromeric NMDARs. Lastly, whether memantine and ketamine alter desensitization kinetics of NMDARs in neurons has not been investigated. Despite these open questions, our study serves as an important first step in identifying key

differences in the action of memantine and ketamine that underlie their preferential inhibition of distinct subpopulations of NMDARs.

4.0   EFFECTS OF EXTERNAL MG^{2+} ON NMDA RECEPTOR INHIBITION BY MEMANTINE AND BY KETAMINE

4.1   OVERVIEW

Physiological concentrations of external Mg^{2+} decrease the potency of NMDAR open channel blockers. Mg^{2+} is thought to lower the potency of NMDAR open channel blockers through competition for overlapping binding sites deep within the NMDAR channel. Studies must therefore be conducted in the presence of a physiological concentration of Mg^{2+} for complete understanding of the mechanisms of NMDAR inhibition *in vivo*. Here we characterized the effect of external Mg^{2+} on NMDAR inhibition by two open channel blockers, memantine and ketamine, by investigating their macroscopic kinetics in 0 and 1 mM Mg^{2+}. Our results demonstrate that Mg^{2+} slows drug binding kinetics, as expected if bound Mg^{2+} prevents drug from accessing its binding site. Also, Mg^{2+} does not speed unbinding of ketamine, as expected if only drug or Mg^{2+} can bind, but surprisingly, Mg^{2+} speeds unbinding of memantine. The mechanistic basis of Mg^{2+}-induced speeding of memantine unbinding is not clear and requires further investigation

4.2 INTRODUCTION

In Chapter 3, we demonstrated that memantine can inhibit in part by increasing occupancy of desensitized states of NMDARs, whereas ketamine can decrease occupancy of desensitized states. We linked the effects of memantine on desensitization to the observation that inhibition depends on the duration of glutamate exposure. These findings have broad implications for how memantine and ketamine may be acting *in vivo*, in particular how channel blockers may act differentially at synaptic and extrasynaptic NMDARs (Parsons and Raymond 2014; Johnson et al., 2015; Kavalali and Monteggia 2015). A limitation of our findings is that our experiments were conducted in the absence of Mg^{2+}. Thus, the inhibition *in vivo* may be complicated due to strong voltage-dependent inhibition of NMDARs by physiological concentrations of Mg^{2+} (~1 mM Mg^{2+}) (Mayer et al., 1984; Nowak et al., 1984). Interestingly, a recent study showed that spontaneous NMDAR excitatory postsynaptic currents exhibited differential inhibition by memantine and ketamine only in 1 mM Mg^{2+} (Gideons et al., 2014). This study highlights how Mg^{2+} can impart differences in the mechanisms of inhibition by open channel blockers.

Most basic investigations of NMDAR open channel blockers have been conducted in the absence of external Mg^{2+}. Inhibition by Mg^{2+} is thought to occur when Mg^{2+} binds to a site within the channel pore. Asparagine residues at the tip the M2 re-entrant loop, known as the N-site, of each NMDAR subunit are critical for Mg^{2+} block (Burnashev et al., 1992; Kuner and Schoepfer 1996; Kashiwagi et al., 2002; Glasgow et al., 2015). Many NMDAR open channel blockers are also thought to bind at or near the N-site within the channel pore (Yamakura et al., 1993; Kashiwagi et al., 2002; Johnson et al., 2015). It is therefore not surprising that several recent studies have shown that 1 mM Mg^{2+} reduces the potency of NMDAR open channel blockers, including memantine and ketamine (Kotermanski and Johnson 2009; Otton et al., 2011;

Nikolaev et al., 2012). These studies suggest that the Mg^{2+}-induced reduction in memantine and ketamine potency likely arises from a simple competition model. Interestingly, a simple competition model of inhibition does not apply to all NMDAR open channel blockers (Nikolaev et al., 2012). A recent study also showed that 1 mM Mg^{2+} was able to speed the recovery from inhibition by another open channel blocker, MK-801, which typically exhibits extremely slow unbinding kinetics (Huettner and Bean 1988; McKay et al., 2013). This study suggests a complex interaction between open channel blockers and Mg^{2+} that is not well understood. Furthermore, whether Mg^{2+} affects the unbinding kinetics of open channel blockers other than MK-801 has not been explored.

Whether Mg^{2+} alters the mechanisms of NMDAR inhibition by memantine and ketamine is essential to understanding the differential effects of each drug works *in vivo*. Studies have well characterized how the presence of Mg^{2+} alters steady-state memantine and ketamine potency. However, it is unclear whether Mg^{2+} alters the kinetics of memantine and ketamine inhibition. Therefore, we have investigated the macroscopic binding and unbinding kinetics of memantine and ketamine in the absence and presence of 1 mM Mg^{2+}.

4.3   MATERIALS AND METHODS

4.3.1   Cell culture and transfection

Experiments were performed on the tsA201 cell line (The European Collection of Authenticated Cell Cultures). tsA201 cells were maintained as previously described (Glasgow and Johnson 2014), in DMEM supplemented with 10% fetal bovine serum and 1% GlutaMAX (Thermo

Fisher Scientific). Cells at 1 x 10^5 cells/dish were plated on 15 mm untreated glass coverslips for experiments using lifted cells and plated on 15 mm glass coverslips treated with poly D-lysine (0.1 mg/ml) and rat-tail collagen (0.1 mg/ml, BD Biosciences) in 35 mm petri dishes for experiments using unlifted cells. 12 to 24 hours after plating, the cells were transiently cotransfected with cDNAs encoding enhanced green fluorescent protein (EGFP) for identification of transfected cells, the rat GluN1-1a subunit (hereafter GluN1; GenBank X63255 in pcDNA3.1), and either the rat GluN2A subunit (GenBank M91561 in pcDNA1) or rat GluN2B subunit (GenBank M91562 in pcDNA1), using FuGENE 6 Transfection Reagent (Promega). For some experiments we used cells transfected with GluN1 and an EGFP:pIRES:GluN2A construct, which was a kind gift from Dr. Kasper Hansen (Hansen, unpublished). Briefly, EGFP was inserted in pIRES (Clontech) under transcriptional control of the CMV promoter, and the open reading frame of rat GluN2A (GenBank D13211) was inserted after the IRES sequence. cDNA ratios of 1 EGFP: 1 GluN1: 1 GluN2A or 1 EGFP: 1 GluN1: 3 GluN2B were used. Immediately after transfection, the culture medium was supplemented with the competitive NMDAR antagonists DL-2-amino-5-phosphonopentanoate (200 μM) and 7-chlorokynurenic acid (200 μM) to prevent NMDAR-mediated cell death.

4.3.2   Solutions

The extracellular bath solution contained (in mM): 140 NaCl, 2.8 KCl, 1 $CaCl_2$, 10 HEPES, 0.01 EDTA, and 0.1 glycine, balanced to pH 7.2 ± 0.05 with NaOH and osmolality balanced to 290 ± 10 mOsm with sucrose. L-glutamate, $MgCl_2$, memantine, and (±)ketamine (hereafter, ketamine) were added to the extracellular solution as indicated from frozen concentrated stock solutions on the same day as experiments. The intracellular pipette solution contained (in mM): 130 CsCl, 10

HEPES, 10 BAPTA, and 4 MgATP balanced to pH 7.2 ± 0.05 with CsOH and solution osmolality was 280 ± 10 mOsm. Frozen aliquots of pipette solution were thawed and kept on ice until loaded into pipettes immediately before starting an experiment.

4.3.3   Electrophysiology

Experiments were performed 12 – 48 hours after tsA201 cells were transiently transfected with NMDAR subunits. Pipettes were pulled from borosilicate capillary tubing (Sutter Instruments) to a resistance of 2 – 5 MΩ on a Sutter Instruments-Flaming Brown P-97 microelectrode puller and fire polished on an in-house fabricated forge. Whole-cell recordings were made from cells expressing EGFP identified by epifluroescence illumination on an inverted Zeiss Axioscop microscope. All cells were held at a membrane potential (V_m) of -65 mV corrected for an empirically determined liquid junction potential between the extracellular and intracellular solution of -6 mV. Whole-cell currents were amplified using an Axopatch 200B patch-clamp amplifier (Molecular Devices), low-pass filtered at 5 kHz and sampled at 20 kHz in pClamp10 (Molecular Devices). Series resistance was compensated with the prediction and correction circuitry to at least 85% in all experiments.

Solutions were delivered through a ten barrel, voice-coil linear stage-driven fast perfusion system described previously (**Section 3.3.3**). Solution flow rate was typically ~1 ml/min for recordings from lifted cells and ~2 ml/min for recordings from unlifted cells. Solution exchange was measured previously with a 10–90% rise time of < 0.2 ms for an open pipette, ~3 ms around a lifted whole-cell, and ~150 ms around an unlifted whole-cell (**Section 3.3.3**).

4.3.4 Analysis

All data were analyzed with Clampfit 10.3 (Molecular Devices) or Origin 7.0 (OriginLab). Macroscopic memantine or ketamine binding and unbinding kinetics were determined from drug concentration-response experiments. Some concentration-response data were collected for drug IC_{50} measurements presented in Chapter 3. Briefly, glutamate was applied for $10 - 20$ s (until current reached a steady level), then glutamate with 1, 10, 100, or 1000 μM memantine or ketamine was applied for $10 - 40$ s until a steady level of inhibition was reached. Glutamate without drug was then reapplied for $20 - 60$ s to allow recovery from inhibition. The time necessary to reach a steady level of inhibition and to allow recovery from inhibition depended strongly on the glutamate concentration. Recordings were obtained in a constant concentration of 0 or 1 mM Mg^{2+}. Cells were excluded from analysis if recovery from inhibition did not reach 90% of steady-state current preceding drug application. Cells with NMDAR currents > 2 nA were excluded from kinetic analysis due to atypical binding and unbinding kinetics.

Macroscopic drug binding and unbinding kinetics were measured by performing least-squares fits of single or double exponential functions to data using Clampfit 10.3. The number of components in the exponential was determined by visual examination, using the fewest components required to obtain a satisfactory fit. To compare single exponential time constants (τ) with double exponential time constants (τ_{fast} and τ_{slow}), we converted τ_{fast} and τ_{slow} to a single weighted time constant (τ_w) using the equation: $\tau_w = (\tau_{fast}*A_{fast} + \tau_{slow}*A_{slow})/(A_{fast} + A_{slow})$, where A_{fast} and A_{slow} are the amplitudes of τ_{fast} and τ_{slow}.

Individual pair-wise comparisons were made by two-tailed Student's t-test with significance levels as indicated. Group data were compared by one-way ANOVA with Tukey's

post hoc analysis with significance values as indicated. All error is displayed as ± standard error of the mean (SEM). Current traces for presentation were refiltered offline in Clampfit 10.3 at 200 Hz.

4.4   RESULTS

To determine whether 1 mM external Mg^{2+} affects the time course of inhibition (macroscopic binding kinetics) or recovery from inhibition (macroscopic unbinding kinetics) of memantine and ketamine, we first measured memantine and ketamine kinetics in the absence of Mg^{2+}. We used three memantine and ketamine concentrations, 1, 10 and 100 μM, in 0 Mg^{2+} to assess the macroscopic binding and unbinding kinetics for each drug for GluN1/2A or GluN1/2B receptors. Drug concentrations below 1 μM were not used, as the amount of inhibition did not produce reliable kinetic measurements. We initially measured kinetics in the presence of saturating glutamate (1 mM glutamate). All experiments were conducted in saturating glycine (100 μM). For experiments in 1 mM Mg^{2+} we used three memantine and ketamine concentrations, 10, 100, and 1000 μM, to measure macroscopic binding and unbinding kinetics for each drug. 1 mM Mg^{2+} causes ~10-fold increases in the IC_{50} values of memantine and ketamine with GluN1/2A and GluN1/2B receptors (Kotermanski and Johnson 2009). Therefore, the fractional current at each drug concentration in 1 mM Mg^{2+} is similar to the fractional current at the 10-fold lower concentration in 0 Mg^{2+}. Macroscopic kinetics were assessed by comparing time constants of single (τ) or double exponential (τ_w) fits to the time course of macroscopic binding and unbinding kinetics of memantine and ketamine (**Section 4.3.4**).

4.4.1 Memantine unbinding kinetics exhibit strong concentration dependence

We found in 0 Mg^{2+} that memantine exhibited strongly concentration-dependent unbinding kinetics (**Figure 16A**, **C**; **Table 4**). The unbinding τ_w with 100 μM memantine was 13.9-fold slower than with 1 μM memantine for GluN1/2A receptors and 4.9-fold slower for GluN1/2B receptors (**Figure 16A**, **C**, **E**; **Table 4**). A memantine concentration-dependent slowing of unbinding τ_w may be consistent with previous reports of memantine binding to two sites on NMDARs (Blanpied et al., 1997; Sobolevsky and Koshelev 1998; Sobolevsky et al., 1998; Chen and Lipton 2005; Kotermanski et al., 2009). These studies suggest a model in which memantine binds to two sites: the deep site, which is near N-site asparagine residues, that exhibits a lower IC_{50} (~1 μM) and faster kinetics; and the second site, which may or may not be within the channel pore, that exhibits a higher IC_{50} (~100 μM) and slower kinetics. As memantine concentration increases, occupation of the second site increases, thereby increasing the fraction of the slow component of unbinding (Sobolevsky and Koshelev 1998; Sobolevsky et al., 1998). In our hands, the fraction and the duration of the slow component of unbinding increase with increasing memantine concentrations, but in complicated ways (**Table 4;** see Unbinding Kinetics: $Frac_{slow}$, τ_{slow}). This is likely due to macroscopic exponential components describing the average of multiple kinetically similar microscopic components. To avoid these complications, we focus primarily on the τ_w, which captures changes in both $Frac_{slow}$ and τ_{slow}.

There is a significant increase in memantine unbinding τ_w for GluN1/2A and GluN1/2B receptors between 10 and 100 μM memantine, but not between 1 and 10 μM memantine, which suggests the second site has an IC_{50} closer to 100 than to 10 μM (**Figure 16E**). This observation is consistent with previous estimates of the memantine IC_{50} at the second binding site (80 – 180

μM) (Blanpied et al., 1997; Kotermanski et al., 2009). Also consistent with previous investigations of the second site, our results display paradoxical apparent low affinity binding with relatively slow unbinding kinetics (Blanpied et al., 1997; Sobolevsky and Koshelev 1998; Sobolevsky et al., 1998; Kotermanski et al., 2009). This observation is paradoxical because the speed of unbinding generally increases as affinity decreases. It is not clear how memantine unbinds more slowly from the second site than from the deep site. Nevertheless, our findings provide further evidence of memantine binding to the second site.

We also determined whether unbinding τ_w depends on the NMDAR subtype. Unbinding τ_w was significantly faster from GluN1/2A than from GluN1/2B receptors at each concentration (e.g. 1 μM for GluN1/2A vs. 1 μM for GluN1/2B) in 0 and 1 mM Mg^{2+} (**Figure 16E**; **Table 4**). This is not surprising, as both the binding and unbinding kinetics of open channel blockers depend on the probability of a channel being open (P_{open}), and GluN1/2A receptors exhibit higher P_{open} than GluN1/2B receptors (Glasgow et al., 2015).

Next, we investigated memantine kinetics in the presence of 1 mM Mg^{2+}. We found that 1 mM Mg^{2+} significantly speeds memantine unbinding τ_w with 100 μM memantine in GluN1/2A and GluN1/2B receptors (**Figure 16B**, **D**, **E**; **Table 4**). Memantine exhibited concentration-dependence of unbinding in 1 mM Mg^{2+}. The unbinding τ_w with 1000 μM memantine was 6.5-fold slower than with 10 μM memantine for GluN1/2A receptors and 4.5-fold slower for GluN1/2B receptors (**Figure16B**, **C**, **E**; **Table 4**). These data suggest that Mg^{2+} shifts the concentration-dependence of memantine unbinding, potentially by competing with memantine binding to the second site, as well as to the deep site. However, it is not clear whether Mg^{2+} affects memantine binding at the second site through direct competition or through a complex interaction involving memantine binding at the deep site as well.

We also analyzed memantine binding kinetics in 0 and 1 mM Mg^{2+}. As expected, because binding rates depend on the concentration of blocker, memantine binding τ_w increased in a concentration-dependent manner in 0 and 1 mM Mg^{2+} (**Table 4**). Mg^{2+} is thought to compete for binding with memantine, resulting in decreased speed with which memantine binds. Indeed, 1 mM Mg^{2+} slowed the binding τ_w with 10 and 100 µM memantine compared to 0 Mg^{2+} (**Table 4**; Student's t-test, $p < 0.01$).
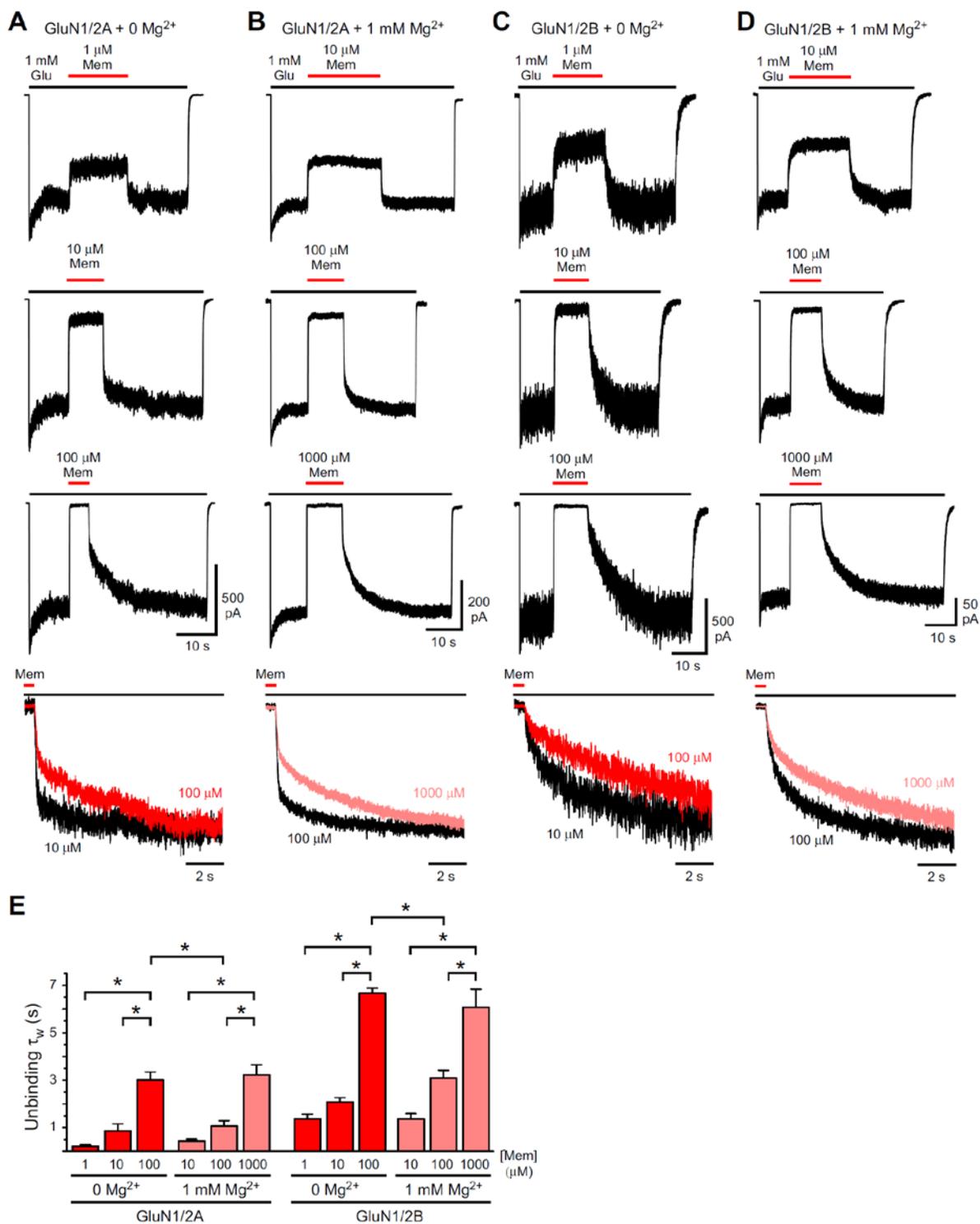
Figure 16. Mg^{2+} shifts the concentration dependence of memantine unbinding kinetics.

A-D, Representative current traces used for measuring memantine binding and unbinding kinetics of

GluN1/2A (**A**, **B**) and GluN1/2B receptors (**C**, **D**) in the absence (**A**, **C**) and presence of 1 mM Mg^{2+} (**B**,

114

D), when activated by 1 mM glutamate (Glu, black bars). Memantine (Mem, red bars) was applied at the indicated concentrations. Traces within each column are from the same cell. The bottom row of traces in **A**-**D** illustrate memantine concentration dependence of unbinding kinetics. The memantine unbinding traces are taken from above at the memantine concentrations indicated, aligned at the time of memantine removal, and scaled to the change in current amplitude during recovery from inhibition. Dark red traces were recorded in 0 Mg^{2+}; light red traces were recorded in 1 mM Mg^{2+}. **E**, Mean unbinding τ_w values compared across groups. * indicates $p < 0.05$ by one-way ANOVA with Tukey's *post hoc* analysis, n = 4 – 6 cells for each group.

Table 4. Memantine binding and unbinding kinetics with unlifted cells.

Values represent means ± SEM, n = 4 – 6 cells per group.

| | | | | Memantine Macroscopic Binding Time Constant Components | | | | | | | | | |
Subtype	[Glu] (µM)	[Mg^{2+}] (mM)	[Drug] (µM)	τ_{Fast} (ms)	± SEM	Frac$_{Fast}$	± SEM	τ_{Slow} (ms)	± SEM	Frac$_{Slow}$	± SEM	τ_w (ms)	± SEM
GluN1/2A	0.3	0	1	138	31.0	0.60	0.02	7587	321	0.40	0.02	3145	213
			10	33.0	3.38	0.86	0.01	3593	656	0.15	0.01	556	112
			100	13.7	2.01	0.90	0.08	415	147	0.11	0.08	23.7	1.78
	1000	0	1	37.2	6.50	0.66	0.11	940	337	0.34	0.11	210	92.2
			10	29.3	0.89	0.87	0.06	821	309	0.13	0.06	89.7	31.1
			100	16.1	2.19	0.98	0.00	811	414	0.02	0.00	31.2	10.2
	1000	1	10	80.0	10.8	0.82	0.04	985	176	0.18	0.04	291	86.6
			100	31.5	1.46	0.94	0.01	762	87.7	0.06	0.01	76.9	7.92
			1000	17.1	0.91	0.83	0.12	999	456	0.17	0.12	34.9	4.49
GluN1/2B	0.3	0	1	256	21.1	0.65	0.06	12584	3280	0.35	0.06	4918	1638
			10	68.0	6.09	0.88	0.01	3096	1023	0.12	0.01	376	93.3
			100	19.4	4.26	0.87	0.08	1360	769	0.13	0.08	83.4	37.3
	1000	0	1	123	26.5	0.55	0.03	1012	197	0.45	0.03	491	60.2
			10	42.2	6.97	0.67	0.03	229	18.8	0.33	0.03	102	6.99
			100	16.4	1.38	0.94	0.01	184	31.2	0.06	0.01	25.6	1.49
	1000	1	10	223	30.2	0.70	0.03	1302	275	0.30	0.03	532	84.6
			100	47.5	3.83	0.73	0.03	276	37.9	0.27	0.03	107	9.04
			1000	18.6	1.37	0.94	0.01	149	23.4	0.06	0.01	27.4	3.59

| | | | | Memantine Macroscopic Unbinding Time Constant Components | | | | | | | | | |
Subtype	[Glu] (µM)	[Mg^{2+}] (mM)	[Drug] (µM)	τ_{Fast} (ms)	± SEM	Frac$_{Fast}$	± SEM	τ_{Slow} (ms)	± SEM	Frac$_{Slow}$	± SEM	τ_w (ms)	± SEM
GluN1/2A	0.3	0	1	128	26.6	0.60	0.07	6538	1613	0.40	0.07	3022	1056
			10	95.8	19.7	0.43	0.03	10945	2363	0.57	0.03	6506	1681
			100	90.6	13.8	0.29	0.03	16580	1764	0.71	0.03	11928	1657
	1000	0	1	66.2	6.83	0.66	0.09	567	163	0.34	0.09	217	61.8
			10	105	2.75	0.75	0.06	2740	541	0.25	0.06	853	308
			100	115	7.73	0.42	0.03	5046	475	0.58	0.03	3010	337
	1000	1	10	117	11.5	0.76	0.04	1397	117	0.24	0.04	433	76.7
			100	113	5.70	0.67	0.04	2849	579	0.33	0.04	1063	232
			1000	137	11.0	0.42	0.04	5871	1080	0.58	0.04	3223	436
GluN1/2B	0.3	0	1	260	68.4	0.48	0.02	10501	2609	0.52	0.02	5592	1449
			10	367	57.3	0.44	0.03	10126	2025	0.56	0.03	5950	1360
			100	482	82.3	0.24	0.03	11555	1321	0.76	0.03	8917	1103
	1000	0	1	296	49.2	0.32	0.05	1920	292	0.68	0.05	1370	198
			10	332	43.3	0.42	0.03	3403	310	0.58	0.03	2085	180
			100	289	41.2	0.22	0.03	8470	334	0.78	0.03	6671	210
	1000	1	10	401	72.5	0.54	0.09	3135	730	0.46	0.09	1362	230
			100	424	20.9	0.56	0.03	6498	738	0.44	0.03	3093	327
			1000	366	43.1	0.31	0.00	8690	1064	0.69	0.00	6082	754

4.4.2 Ketamine unbinding kinetics are independent of concentration

Next we examined the kinetics of inhibition by ketamine in the absence and presence of 1 mM Mg^{2+}. We found that unlike memantine, ketamine unbinding kinetics were not concentration-dependent, in 0 or 1 mM Mg^{2+} (**Figure 17**; **Table 5**). This is consistent with ketamine binding only to a single site on NMDARs (Johnson et al., 2015). At several ketamine concentrations in 0 Mg^{2+}, unbinding kinetics were well fit by a single exponential function, whereas in 1 mM Mg^{2+}, ketamine unbinding kinetics were always best fit by a double exponential (**Table 5**). This suggests that Mg^{2+} may be interacting in with ketamine. Although 1 mM Mg^{2+} did not cause any significant speeding of ketamine unbinding kinetics, there was a trend towards faster unbinding (**Figure 17E**; **Table 5**). Therefore, it is possible that Mg^{2+} has a small impact on ketamine unbinding kinetics, which is not consistent with our current understanding of Mg^{2+} interactions with open channel blockers.

We also measured ketamine binding kinetics in 0 and 1 mM Mg^{2+}. As with memantine, ketamine binding was concentration-dependent in 0 and 1 mM Mg^{2+} (**Table 5**). As expected, 1 mM Mg^{2+} significantly slowed the binding τ_w with 10 and 100 mM ketamine compared to 0 Mg^{2+} (**Table 5**; Student's t-test, $p < 0.05$).

Figure 17. Ketamine unbinding kinetics are independent of concentration.

A-D, Representative current traces used for measuring ketamine binding and unbinding kinetics of GluN1/2A (**A**, **B**) and GluN1/2B receptors (**C**, **D**) in the absence (**A**, **C**) and presence of 1 mM Mg^{2+} (**B**, **D**), when activated by 1 mM

glutamate (black bars). Ketamine (Ket, blue bars) was applied at the indicated concentrations. Traces within each column are from the same cell. The bottom row of traces in **A**-**D** illustrate ketamine concentration independence of unbinding kinetics. The ketamine unbinding traces are taken from above at the ketamine concentrations indicated, aligned at the time of ketamine removal, and scaled to the change in current amplitude during recovery from inhibition. Dark blue traces were recorded in 0 Mg^{2+}; light blue traces were recorded in 1 mM Mg^{2+}. **E**, Mean unbinding τ_w values compared across groups. ns indicates $p > 0.05$ by one-way ANOVA with Tukey's *post hoc* analysis , n = 4 – 6 cells for each group.

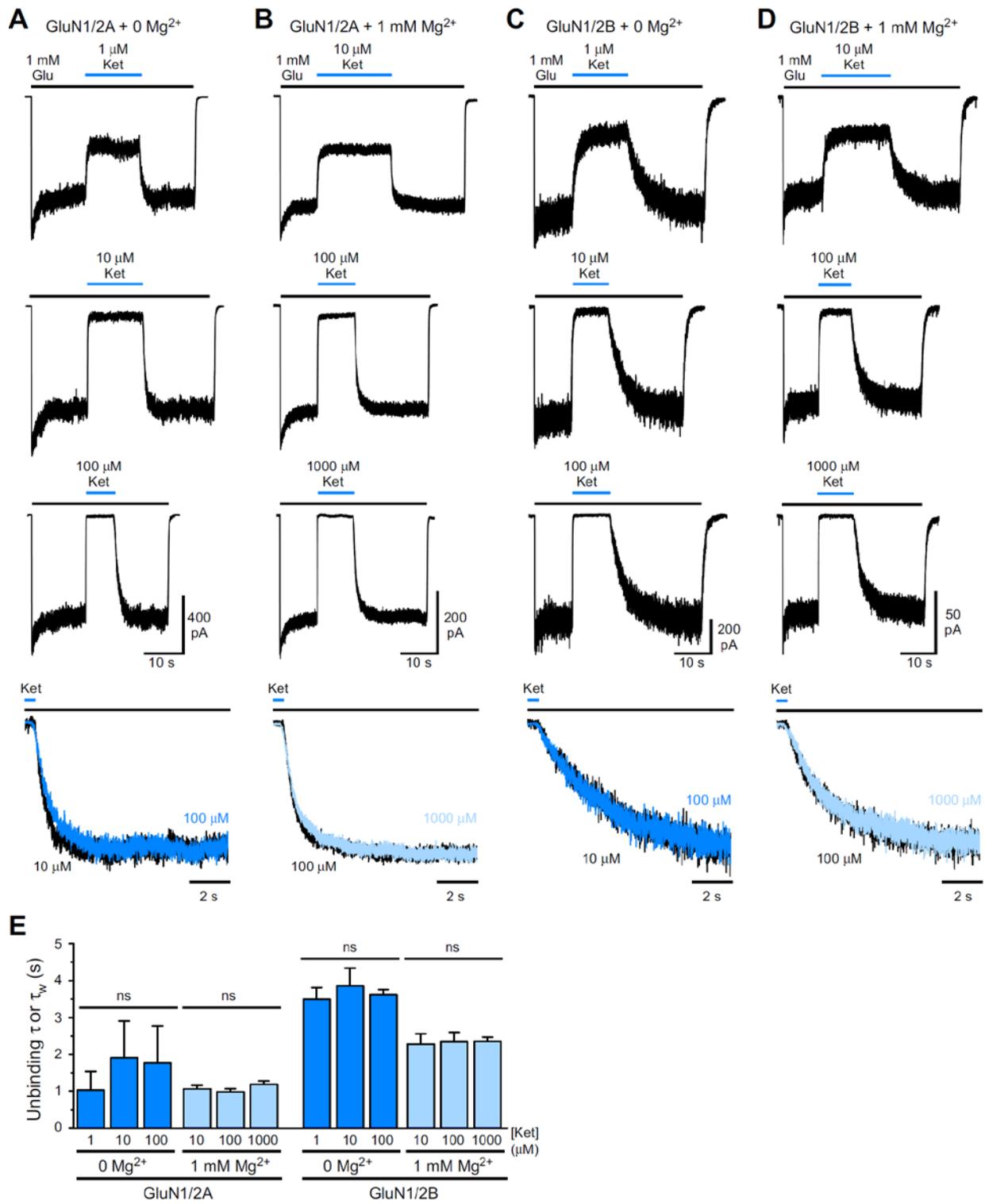**Table 5. Ketamine binding and unbinding kinetics with unlifted cells.**

Values represent means ± SEM, n = 4 – 6 cells per group.

| | | | | Ketamine Macroscopic Binding Time Constant Components | | | | | | | | | |
Subtype	[Glu] (μM)	[Mg^{2+}] (mM)	[Drug] (μM)	τ_{Fast} (ms)	± SEM	Frac$_{Fast}$	± SEM	τ_{Slow} (ms)	± SEM	Frac$_{Slow}$	± SEM	τ_w (ms)	± SEM
GluN1/2A	0.3	0	1	259	78.2	0.37	0.02	15002	2871	0.63	0.02	9717	2069
			10	81.7	7.12	0.73	0.01	7520	331	0.27	0.01	2115	170
			100	34.1	3.63	0.96	0.00	2935	1246	0.04	0.00	171	74.6
	1000	0	1	180	35.3	0.75	0.07	2356	1025	0.25	0.07	668	344
			10	61.2	12.2	0.92	0.02	1606	1045	0.08	0.02	232	157
			100									24.3	1.35
	1000	1	10	166	10.8	0.73	0.03	1087	157	0.27	0.03	404	26.5
			100	58.4	2.88	0.95	0.01	990	377	0.05	0.01	93.2	9.24
			1000	20.5	1.30	0.99	0.01	306	58.7	0.01	0.01	24.1	2.66
GluN1/2B	0.3	0	1	492	63.1	0.58	0.04	10752	1473	0.42	0.04	4563	368
			10	126	2.50	0.87	0.01	3393	430	0.13	0.01	551	47.0
			100	34.4	2.08	0.97	0.00	1387	143	0.03	0.00	71.3	2.89
	1000	0	1									1313	80.7
			10	121	45.3	0.64	0.12	684	290	0.36	0.12	235	37.0
			100	26.0	1.31	0.82	0.03	138	13.0	0.18	0.03	46.5	4.95
	1000	1	10	349	99.4	0.54	0.14	2288	799	0.46	0.14	859	130
			100	110	5.17	0.88	0.03	578	83.3	0.12	0.03	159	8.38
			1000	29.3	1.42	0.96	0.01	388	98.6	0.04	0.01	46.5	7.04

| | | | | Ketamine Macroscopic Unbinding Time Constant Components | | | | | | | | | |
Subtype	[Glu] (μM)	[Mg^{2+}] (mM)	[Drug] (μM)	τ_{Fast} (ms)	± SEM	Frac$_{Fast}$	± SEM	τ_{Slow} (ms)	± SEM	Frac$_{Slow}$	± SEM	τ_w (ms)	± SEM
GluN1/2A	0.3	0	1	298	71.2	0.31	0.05	22773	2916	0.69	0.05	16062	2592
			10	671	144	0.25	0.02	20022	1387	0.75	0.02	15291	1388
			100	865	94.3	0.30	0.01	25426	764	0.70	0.01	18118	667
	1000	0	1	287	136	0.47	0.05	2913	1785	0.53	0.05	1024	512
			10	430	54.0	0.59	0.05	3166	1743	0.41	0.05	1901	1010
			100									1763	1004
	1000	1	10	293	38.6	0.58	0.09	2724	761	0.42	0.09	1060	99.2
			100	423	39.5	0.64	0.07	2129	383	0.36	0.07	976	90.3
			1000	559	60.1	0.61	0.04	2221	237	0.39	0.04	1186	96.5
GluN1/2B	0.3	0	1	783	93.8	0.35	0.03	39526	7220	0.65	0.03	26571	5382
			10	872	157	0.33	0.03	25835	3201	0.67	0.03	17616	2235
			100	1387	356	0.30	0.03	33400	5847	0.70	0.03	23128	3630
	1000	0	1									3496	325
			10									3864	472
			100									3611	150
	1000	1	10	720	153	0.40	0.09	3450	502	0.60	0.09	2284	274
			100	987	182	0.53	0.14	5534	1692	0.47	0.14	2343	252
			1000	1184	136	0.54	0.09	4258	653	0.46	0.09	2355	118

4.4.3 Memantine and ketamine kinetics with a low concentration of glutamate

Thus far, we have presented memantine and ketamine kinetic measurements determined in saturating concentrations of glutamate and glycine. We wondered whether at a low concentration of glutamate relative to EC_{50} (0.3 μM, ~0.1 glutamate EC_{50}), and thus at a much lower NMDAR P_{open}, the memantine concentration dependence of memantine unbinding kinetics would be diminished. Therefore, we measured binding and unbinding kinetics of memantine and ketamine in the absence of Mg^{2+}, when GluN1/2A or GluN1/2B receptors are activated by 0.3 μM glutamate.

We found that GluN1/2A, but not GluN1/2B receptors, activated by 0.3 μM glutamate maintain significant memantine concentration dependence of memantine unbinding τ_w (**Figure 18A-B**, **E**; **Table 4**). The unbinding τ_w with 100 μM memantine was 3.9-fold slower than with 1 μM memantine for GluN1/2A receptors, whereas there was a non-significant change for GluN1/2B receptors (**Figure 18E**; **Table 4**). Therefore, at a low glutamate concentration, the memantine concentration dependence of unbinding is occluded for GluN1/2B, but not for GluN1/2A, receptors.

We found that ketamine unbinding kinetics were not concentration dependent for GluN1/2A and GluN1/2B receptors activated by 0.3 μM glutamate (**Figure 18C-D**, **F**; **Table 5**). Ketamine unbinding kinetics were significantly slower at each ketamine concentration when activated by 0.3 μM glutamate than by 1 mM glutamate, except for 10 μM ketamine with GluN1/2B receptors.

Memantine and ketamine binding τ_w were significantly slowed at 1 and 10 μM when activated by 0.3 μM glutamate compared to activation by 1 mM glutamate (**Tables 4** and **5**;

Student's t-test, p < 0.01). Surprisingly, except with ketamine for GluN1/2B receptors, 100 μM memantine or ketamine binding τ_w was not significantly different when activated by 0.3 μM or 1 mM glutamate (**Tables 4** and **5**; Student's t-test, p > 0.05). One possible explanation for this observation is that our measurements of the fastest kinetic components may be limited by our fast perfusion system and recording configuration. It is possible that by recording from unlifted cells, which have a 10 – 90% solution exchange time of ~150 ms (**Table 1**; **Section 3.3.3**) we underestimated the fastest kinetic components. Therefore, we explored memantine and ketamine kinetics using lifted cells, which have a 10 – 90% solution exchange time of ~3 ms (**Table 1**; **Section 3.3.3**).
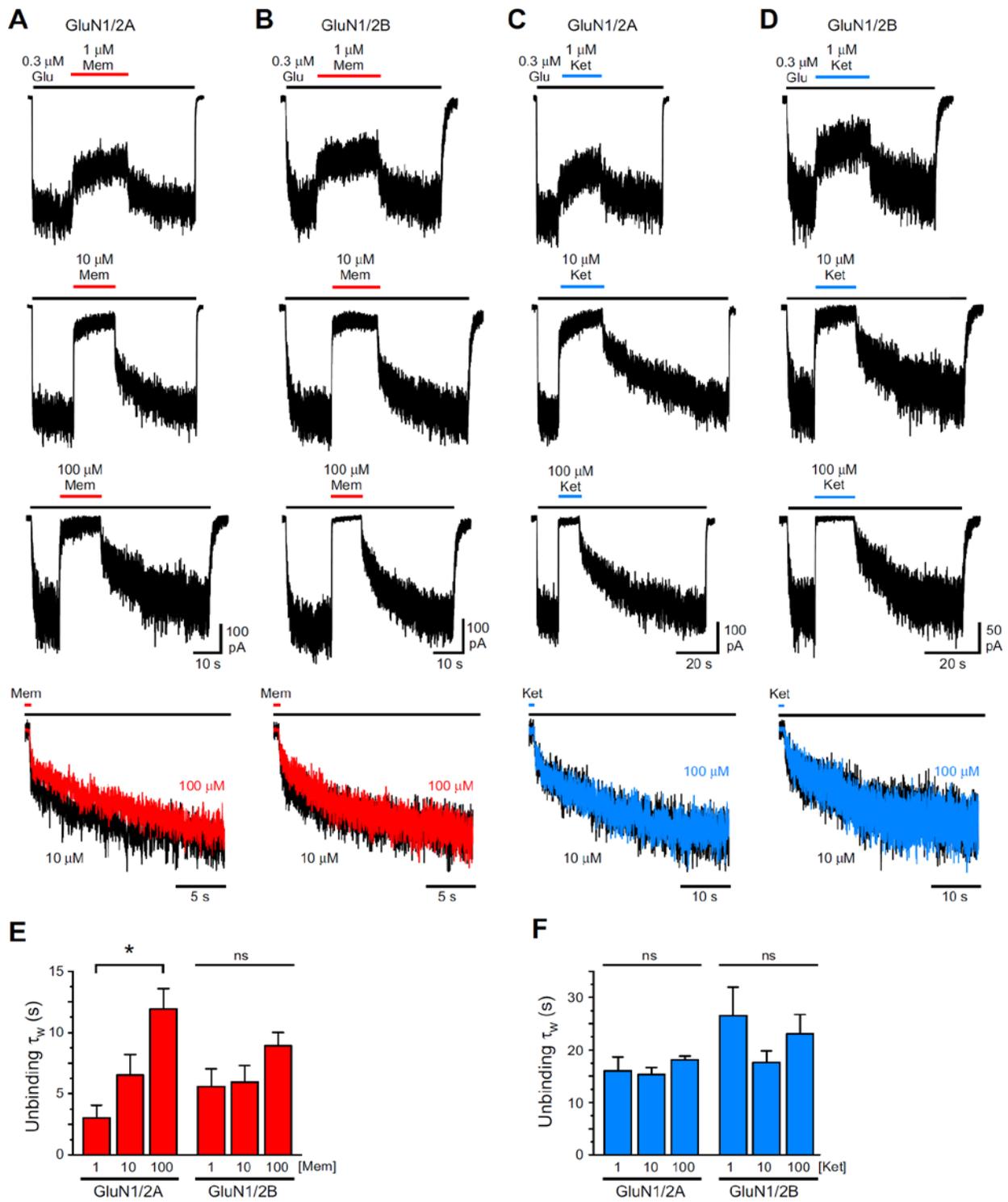
Figure 18. Memantine and ketamine unbinding kinetics when activated by 0.3 μM glutamate.

A-D, Representative current traces used for measuring memantine (**A**, **B**) and ketamine (**C**, **D**) binding and unbinding kinetics of GluN1/2A (**A**, **C**) and GluN1/2B receptors (**B**, **D**) in the absence of Mg^{2+}, when activated by

123

0.3 μM glutamate (black bars). Memantine (red bars) or ketamine (blue bars) were applied at the indicated concentrations. Traces within each column are from the same cell. The bottom row of traces in **A**-**D** illustrate the extent of memantine or ketamine concentration dependence of unbinding kinetics. The drug unbinding traces are taken from above at the concentrations indicated, aligned at the time of drug removal, and scaled to the change in current amplitude during recovery from inhibition. **E**, **F**, Mean unbinding τ_w values compared across groups for memantine (**E**) and ketamine (**F**). * indicates $p < 0.05$ and ns indicates $p > 0.05$ by one-way ANOVA with Tukey's *post hoc* analysis, n = 4 – 6 cells for each group.

4.4.4 Recordings from lifted cells reveal significantly faster memantine kinetics

Next, we wanted to test whether solution exchange time is a limiting factor in determining memantine and ketamine binding and unbinding kinetics. We used lifted cells to achieve rapid and complete solution exchange not possible when recording from unlifted cells. As a strict test, we measured memantine and ketamine kinetics in the same cell before and after lifting. We found that the unbinding τ_w following inhibition with 100 μM memantine quickened after lifting by ~4-fold, whereas the unbinding τ following inhibition with 100 μM ketamine quickened by ~1.5-fold (**Figure 4A**). Due to the greater lifting-induced kinetic changes, we focus on memantine kinetics here. The extent to which memantine unbinding kinetics quickened due to lifting was surprising. We wanted to ensure that memantine concentration dependence of unbinding was not the result of inaccuracies from the relatively slow solution exchange around unlifted cells. Therefore, we repeated measurements of memantine kinetics using lifted cells expressing GluN1/2A receptors.

We found that even from lifted cells, memantine unbinding τ_w was concentration dependent, both in 0 and 1 mM Mg^{2+} (**Figure 19B**-**D**; **Table 6**). In 0 Mg^{2+}, the unbinding τ_w with

124

100 μM memantine was 7.3-fold slower than with 1 μM memantine (**Figure 19B, D**; **Table 6**). In 1 mM Mg^{2+}, the unbinding τ_w with 1000 μM memantine was 3.9-fold slower than with 10 μM memantine and increased 3.9-fold in 1 mM Mg^{2+} from 10 to 1000 μM memantine (**Figure 19C, D**; **Table 6**). Importantly, 1 mM Mg^{2+} significantly quickened memantine unbinding τ_w at 100 μM memantine, consistent with our results with unlifted cells (**Figure 16E** and **19D**). As expected, unbinding τ_{fast} from lifted cells quickened ~2- to 3-fold at each memantine concentration compared to unlifted cells (**Table 6**). Surprisingly, unbinding τ_{slow} with 100 μM from lifted cells also quickend by 2.8-fold compared to unlifted cells (**Tables 4** and **6**). It is not clear how the unbinding τ_{slow}, which is ~20-fold slower than the time course of solution exchange of unlifted cells, could be affected by quicker solution exchange.

Binding τ_w in 0 Mg^{2+}, but not in 1 mM Mg^{2+}, was significantly quickened with 10 μM and 100 μM memantine from lifted cells compared to unlifted cells (**Table 6**). Therefore, the effect of Mg^{2+} on slowing memantine binding kinetics is greater than we previously measured (**Table 4**). It will be important to determine in lifted cells whether the effects of Mg^{2+} on ketamine binding differs greatly from the effects of Mg^{2+} on memantine binding.
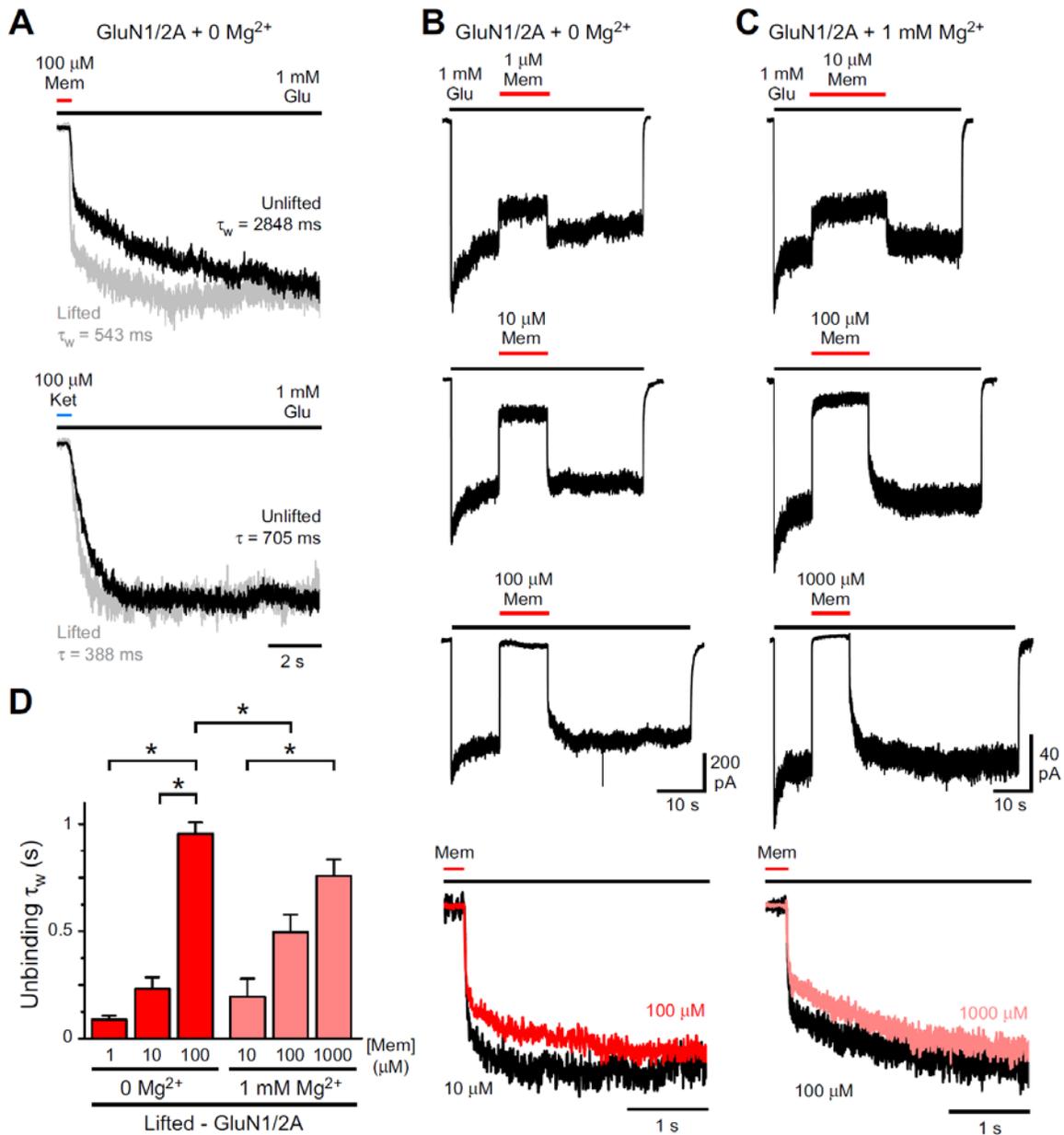
Figure 19. Lifted cells reveal faster unbinding kinetics.

A, Representative current traces of memantine (top, red bar) and ketamine (bottom, blue bar) unbinding kinetics of GluN1/2A receptors activated by 1 mM glutamate (black bars). All traces in **A** are from the same cell before lifting (Unlifted, black traces) and after lifting (Lifted, gray traces) in 0 Mg^{2+}. Current traces were aligned at the time of drug removal and scaled to the change in current amplitude during recovery from inhibition. **B**, **C**, Representative traces used for measuring memantine binding and unbinding kinetics of GluN1/2A receptors in 0 (**B**) and 1 mM Mg^{2+} (**C**), when activated by 1 mM glutamate (black bars). Memantine (red bars) was applied at the indicated

126

concentrations. Traces within each column are from the same cell. The bottom traces illustrate metamine concentration dependence of unbinding kinetics. The memantine unbinding traces are taken from above at the memantine concentrations indicated, aligned at the time of memantine removal, and scaled to the change in current amplitude during recovery from inhibition. Dark red traces were recorded in 0 Mg^{2+}; light red traces were recorded in 1 mM Mg^{2+}. **D**, Mean unbinding τ_w values compared across groups. * indicates $p < 0.05$ by one-way ANOVA with Tukey's *post hoc* analysis, n = 3 cells for each group.

Table 6. Memantine binding and unbinding kinetics from lifted cells.

Values represent means ± SEM, n = 3 cells per group.

	[Glu]	[Mg^{2+}]	[Drug]	τ_{Fast}				τ_{Slow}				τ_w	
							Memantine Macroscopic Binding Time Constant Components						
Subtype	(μM)	(mM)	(μM)	(ms)	± SEM	Frac$_{Fast}$	± SEM	(ms)	± SEM	Frac$_{Slow}$	± SEM	(ms)	± SEM
GluN1/2A	1000	0	1	23.0	3.41	0.77	0.05	1161	587	0.23	0.05	208	55.5
			10	6.70	0.28	0.91	0.00	209	67.6	0.09	0.00	26.3	7.22
			100	1.63	0.12	0.92	0.02	106	58.1	0.08	0.02	6.73	2.41
	1000	1	10	19.3	3.23	0.68	0.02	2582	856	0.32	0.02	854	286
			100	7.86	0.64	0.83	0.02	670	116	0.17	0.02	124	33.4
			1000	2.79	0.38	0.92	0.03	293	123	0.08	0.03	22.1	5.53
	[Glu]	[Mg^{2+}]	[Drug]	τ_{Fast}				Memantine Macroscopic Unbinding Time Constant Components τ_{Slow}				τ_w	
Subtype	(μM)	(mM)	(μM)	(ms)	± SEM	Frac$_{Fast}$	± SEM	(ms)	± SEM	Frac$_{Slow}$	± SEM	(ms)	± SEM
GluN1/2A	1000	0	1	20	5.28	0.79	0.06	355	73.3	0.21	0.06	88.8	17.3
			10	22.3	4.74	0.72	0.01	793	207	0.28	0.01	231	54.8
			100	58.3	23.2	0.57	0.04	2228	319	0.43	0.04	955	52.8
	1000	1	10	21.0	4.61	0.72	0.04	581	245	0.28	0.04	195	84.2
			100	28.2	2.23	0.65	0.03	1328	145	0.35	0.03	496	82.1
			1000	22.7	1.73	0.52	0.03	1532	86.3	0.48	0.03	758	78.5

4.5 DISCUSSION

In this study we investigated whether the presence of 1 mM Mg^{2+} affects the kinetics of inhibition or recovery from inhibition by memantine and ketamine in tsA201 cells expressing GluN1/2A or GluN1/2B receptors. Our data show that memantine, but not ketamine, unbinding

kinetics slow with increasing concentration of drug. These data are consistent with hypotheses that memantine binds to multiple sites on the NMDAR receptor, and ketamine binds to a single site (Blanpied et al., 1997; Sobolevsky and Koshelev 1998; Sobolevsky et al., 1998; Chen and Lipton 2005; Parsons et al., 2007; Kotermanski et al., 2009; Johnson et al., 2015). Importantly, we show that the presence of Mg^{2+} does not alter the memantine concentration dependence of unbinding, or the ketamine concentration independence of unbinding. Importantly, Mg^{2+} significantly quickens unbinding kinetics of 100 μM memantine, which suggests that Mg^{2+} affects memantine binding at the second site, as well as at the deep site. Further work is needed to understand the mechanistic basis of the memantine binding at two sites, in addition to how Mg^{2+} interacts with binding at both sites.

Several previous studies have proposed that there are two binding sites for memantine on NMDARs (Blanpied et al., 1997; Sobolevsky and Koshelev 1998; Sobolevsky et al., 1998; Chen and Lipton 2005; Kotermanski et al., 2009). Our data support this hypothesis, but differ from previous studies in several key ways. First, our experiments were conducted in a heterologous expression system as opposed to neurons (Blanpied et al., 1997; Sobolevsky and Koshelev 1998; Sobolevsky et al., 1998), which contain a heterogeneous population of NMDAR subtypes (Glasgow et al., 2015). Our data support the notion that the presence of multiple NMDAR subtypes with differential kinetic components could obfuscate interpretation of experiments in the context of two memantine binding sites. Second, our experiments with unlifted cells yielded unbinding kinetic components that were ~2- to 10-fold faster than previous measurements. Faster components could have arisen from the use of a saturating concentration of the full agonist glutamate, rather than a low or intermediate concentrations of the partial agonist NMDA used in some other studies (Blanpied et al., 1997; Kotermanski et al., 2009). In addition, to prevent

NMDAR current rundown, we included ATP in the intracellular solution, which has generally not been present in the intracellular solutions used in other studies. Besides maintaining a higher NMDAR P_{open} (Tong and Jahr 1994), ATP may have yet unknown effects on memantine or ketamine inhibition. Our findings from Chapter 3 suggest that Ca^{2+}-mediated effects are involved in the mechanism of action of memantine, and it is conceivable that ATP is also indirectly or directly involved in the Ca^{2+}-mediated process. Third, we examined whether Mg^{2+} interferes with binding at one or both memantine binding sites, which has not been explored previously. It is not clear from our data or earlier studies how memantine interacts with the two memantine binding sites in the absence of Mg^{2+}. Therefore, how Mg^{2+} interacts with memantine binding at one or both sites is in need of further investigation.

Our experiments from lifted cells revealed that memantine unbinding kinetics are much faster than previously appreciated, and highly dependent on the rate of solution exchange. Most kinetic studies of memantine and ketamine have been performed on unlifted cells, which yield fast components that are limited by the rate of solution exchange. One study investigated kinetics of memantine inhibition and recovery from inhibition from outside-out patches of oocytes, which yielded kinetic measurements that were still ~3- to 8-fold slower than our data from lifted cells (Parsons et al., 2008). Interestingly, we found that even the slow component of memantine unbinding depends on whether a cell is lifted or not. This finding suggests that either memantine is particularly difficult to wash out from diffusionally restricted spaces (between the cell and the coverslip), or that lifting cells causes structural changes to NMDARs that somehow result in significantly faster memantine unbinding. It will be important for future studies to determine why lifting cells speeds the slow component of memantine unbinding, and whether lifting cells changes NMDAR properties. Overall, our results suggest caution in extrapolating from

macroscopic kinetic data alone, as the data are highly dependent on the experimental conditions (e.g. ion concentrations, presence of metabolic components, rate of solution exchange).

Our data further support a model of memantine inhibition in which memantine binds with higher affinity to the deep site and binds with lower affinity to a second site, which may or may not be within the channel pore (Blanpied et al., 1997; Sobolevsky and Koshelev 1998; Sobolevsky et al., 1998; Chen and Lipton 2005; Kotermanski et al., 2009). The second, lower affinity site exhibits paradoxically slow memantine unbinding, as observed previously (Blanpied et al., 1997; Sobolevsky and Koshelev 1998; Sobolevsky et al., 1998; Kotermanski et al., 2009). However, our data in 1 mM Mg^{2+} suggest that in addition to competing with memantine inhibition at the deep site, Mg^{2+} also may affect inhibition at the second memantine binding site. To understand the mechanism of action of memantine, further work is needed to investigate memantine's interaction with the second site in the absence and presence of Mg^{2+}.

5.0   EFFECTS OF UNCHARGED MEMANTINE ON NMDA RECEPTORS

5.1   OVERVIEW

Over the last two decades, several studies have demonstrated that memantine can inhibit NMDARs through binding at two sites, the deep site and the second site. Based on mutations that affect memantine binding, the deep site overlaps the Mg^{2+} binding site near the middle of the membrane voltage field. In contrast, the location of the second site is likely somewhere in the external portion of the M3 TMR. Thus far, evidence of memantine binding to the second site is through indirect measures. Mutations to occlude memantine binding to the second site have been difficult to assess. Therefore, the physiological role of memantine binding at the second site is not clear. A deeper understanding of memantine inhibition at the second site is thus warranted. To address memantine binding to the second site, we develop and test the hypothesis that uncharged memantine binds to the second site. At physiological pH, > 99% of memantine carries a positive charge. Changing the solution pH from 7.2 to 9 with a constant concentration of memantine increases the concentration of uncharged memantine ~60-fold. Comparing the same concentrations of memantine at pH 7.2 and 9, we find that established properties of inhibition at the second site are enhanced. Identification of uncharged memantine as the molecular species that binds to the second site improves our understanding of several unique features of memantine inhibition. Furthermore, use of pH manipulation as a tool to test memantine inhibition at the

131

second site will be useful in driving further investigation into the mechanisms of NMDAR inhibition by memantine.

5.2   INTRODUCTION

In Chapter 4 we showed that the time course of recovery from inhibition by memantine, but not by ketamine, depended strongly on the drug concentration. Our data are consistent with the hypotheses that memantine binds to at least two sites on NMDARs (Blanpied et al., 1997; Sobolevsky and Koshelev 1998; Sobolevsky et al., 1998; Chen and Lipton 2005; Kotermanski et al., 2009), whereas ketamine binds to only one site (Parsons et al., 2007; Kotermanski et al., 2009; Johnson et al., 2015; but see Orser et al., 1997). The approximate location of the deep site for memantine binding is thought to overlap with the Mg^{2+} binding site. Memantine is coordinated by asparagine residues at the tips of the M2 reentrant loops of each NMDAR subunit (Kashiwagi et al., 2002; Chen and Lipton 2005). Indeed, 1 mM Mg^{2+} slows the macroscopic memantine binding rate, and decreases memantine potency 10- to 20-fold (Chapter 4; Kotermanksi and Johnson, 2009). Mutational studies have identified regions in the extracellular portion of the M3 TMR that may correspond to approximate location of the memantine binding at the second site (Chen and Lipton 2005).

Interestingly, our data in Chapter 4 suggest that in addition to competing with memantine binding at the deep site, Mg^{2+} may compete for binding at the second site. The ability of Mg^{2+} to interfere with binding at the second site suggests that the second site is somewhere in the proximity of the deep site, or of memantine bound at the deep site. However, previous studies suggest that memantine binds to a shallow or superficial second site that was both accessible

when NMDARs are closed and exhibited weak apparent V_m dependence (Blanpied et al., 1997; Chen and Lipton 2005; Kotermanski et al., 2009). However, one study suggests that memantine can bind to a second site deep in the voltage field, presumably within the channel pore (Sobolevsky et al., 1998). Therefore, it is unclear where the second memantine binding site is located, and how Mg^{2+} can compete for binding at this site.

Irrespective of precisely where memantine binds to the second site, previous work has identified several unusual properties associated with memantine inhibition at the second site, including the ability of memantine to bind and unbind without NMDAR activation and paradoxical high IC_{50} with relatively slow unbinding kinetics. These properties are not consistent with our current understanding of inhibition by open channel blockers. Therefore, a deeper understanding of memantine binding to the second site and of how Mg2+ affects binding at this site is necessary.

5.3   MATERIALS AND METHODS

5.3.1   Cell culture and transfection

Experiments were performed on the tsA201 cell line (The European Collection of Authenticated Cell Cultures). tsA201 cells were maintained as previously described (Glasgow and Johnson 2014), in DMEM supplemented with 10% fetal bovine serum and 1% GlutaMAX (Thermo Fisher Scientific). Cells at 1 x 10^5 cells/dish were plated on 15 mm glass coverslips treated with poly D-lysine (0.1 mg/ml) and rat-tail collagen (0.1 mg/ml, BD Biosciences) in 35 mm petri dishes. 12 to 24 hours after plating, the cells were transiently cotransfected using FuGENE 6

Transfection Reagent (Promega) with cDNAs encoding enhanced green fluorescent protein (EGFP) for identification of transfected cells, either the rat GluN1-1a subunit (hereafter GluN1; GenBank X63255 in pcDNA3.1) or GluN1(N616R) subunit, and the rat GluN2A subunit (GenBank M91561 in pcDNA1). The GluN1(N616R) mutant (residue numbering starting from initiating methionine) cDNA was a kind gift from Dr. Pierre Paoletti. Cells transfected with GluN1 and a EGFP:pIRES:GluN2A construct, which was a kind gift from Dr. Kasper Hansen (Hansen, unpublished), were used in some experiments. Briefly, EGFP was inserted in pIRES (Clontech) under transcriptional control of the CMV promoter, and the open reading frame of rat GluN2A (GenBank D13211) was inserted after the IRES sequence. cDNA ratios of 1 EGFP: 1 GluN1: 1 GluN2A. Immediately after transfection, the culture media was supplemented with the competitive NMDAR antagonists DL-2-amino-5-phosphonopentanoate (200 µM) and 7-chlorokynurenic acid (200 µM) to prevent NMDAR-mediated cell death.

5.3.2 Solutions

The extracellular bath solution contained (in mM): 140 NaCl, 2.8 KCl, 1 $CaCl_2$, 10 HEPES, 0.01 EDTA, and 0.1 glycine, balanced to pH 7.2 ± 0.05 with NaOH and osmolality balanced to 290 ± 10 mOsm with sucrose. For experiments performed at pH 9, NaOH was added to bring the pH to 9 ± 0.05. L-glutamate, $MgCl_2$, memantine, and ($\pm$)ketamine were added to the extracellular solution as indicated from frozen concentrated stock solutions on the same day as experiments. The intracellular pipette solution contained (in mM): 130 CsCl, 10 HEPES, 10 BAPTA, and 4 MgATP balanced to pH 7.2 ± 0.05 with CsOH and solution osmolality was 280 ± 10 mOsm. Frozen aliquots of pipette solution were thawed and kept on ice until loaded into pipettes immediately before starting an experiment.

5.3.3 Electrophysiology

Experiments were performed 12 – 48 hours after tsa201 cells were transiently transfected with NMDAR subunits. Pipettes were pulled from borosilicate capillary tubing (Sutter Instruments) to a resistance of 2 – 5 MΩ on a Sutter Instruments-Flaming Brown P-97 microelectrode puller and fire polished. Whole-cell recordings were made from cells expressing EGFP identified by epifluroescence illumination on an inverted Zeiss Axioscop microscope. Unless otherwise indicated, all recordings were made from unlifted cells held at a membrane potential (V_m) of -65 mV corrected for an empirically determined liquid junction potential between the extracellular and intracellular solution of -6 mV. Whole-cell currents were amplified using an Axopatch 200B patch-clamp amplifier (Molecular Devices), filtered at 5 kHz and samples at 20 kHz in pClamp10 (Molecular Devices). Series resistance was compensated with the prediction and correction circuitry to at least 85% in all experiments.

Solutions were delivered through a ten barrel, voice-coil linear stage-driven fast perfusion system described previously (**Section 3.3.3**). Solution flow rate was typically ~2 ml/min for recordings from unlifted cells. Solution exchange was measured previously with a 10–90% rise time of < 0.2 ms for an open pipette and ~150 ms around an unlifted whole-cell.

5.3.4 Analysis

All data were analyzed with Clampfit 10.3 (Molecular Devices) or Origin 7.0 (OriginLab). To measure macroscopic drug unbinding kinetics during NMDAR activation after drug trapping, we developed the following protocol (**Figures 20** and **23**). We applied glutamate for 20 s (I_{cont1}), then applied 100 μM of drug with glutamate for 10 s, then washed off glutamate in the

continuous presence of 100 μM drug for 5 s to maintain inhibition during NMDAR deactivation, before returning to normal extracellular solution for 25 s. Glutamate was then reapplied for 20 s to measure macroscopic drug unbinding kinetics after trapping (I_{trap}). This glutamate reapplication was followed by a 40 s wash with normal extracellular solution, and then another 20-s glutamate application (I_{cont2}), which was used to ensure there was not significant current rundown. To take into account current rundown, we aligned peak currents at the times of glutamate application and determined the ratio of current after trapping to control current at every time point by the equation, trapped unbinding = I_{trap}/I_{cont}, where $I_{cont} = ((I_{cont1} + I_{cont2})/2)$. Trapped unbinding is a ratio value as a function of time for a 20 s duration of glutamate application. To determine the time course of unbinding following the trapping protocol (trapped unbinding kinetics) by fitting trapped unbidning with a single or double exponential function in Clampfit 10.3. The number of components in the exponential was determined by visual examination, using the fewest components necessary for a satisfactory fit. For simple comparison of double exponential time constants (τ_{fast} and τ_{slow}) with single exponential time constants (τ), we converted τ_{fast} and τ_{slow} to a single weighted time constant (τ_w) by the equation: $\tau_w = (\tau_{fast}*A_{fast} + \tau_{slow}*A_{slow})/(A_{fast} + A_{slow})$, where A_{fast} and A_{slow} are the amplitudes of τ_{fast} and τ_{slow}. We measured fractional recovery after trapping as the mean trapped unbinding over a 5 ms window at the start of the exponential fit. Trapped drug unbinding was then compared to unbinding from steady drug inhibition in the continuous presence of glutamate (steady-state unbinding) in the same cells. Some drug trapping experiments were conducted in the continuous presence of 1 mM Mg^{2+} with a memantine or ketamine concentration of 1000 μM.

Concentration-response relations for memantine inhibition of GluN1(N616R)/2A receptors were measured using the following protocol. 1 mM glutamate was applied for 20 s

until current reached a steady-state amplitude, then 1 mM glutamate plus the lowest concentration of memantine (50, 200, 1000, and 2000 μM memantine) was applied for 20 s before applying the next highest concentration of memantine with glutamate. After 20 s of 2000 μM memantine with glutamate, glutamate in the absence of memantine was reapplied for 30 s to allow recovery from inhibition. Cells where recovery from inhibition did not reach 80% of steady-state current preceding memantine application were excluded from analysis. Concentration-response data for individual cells were then log-transformed to determine the IC_{50} value through fits of the following equation, $I_{memantine}/I_{control} = 1/(1 + 10\char`^(\log[memantine] - \log(IC_{50}))*n_H)$, where $I_{memantine}$ is the mean current during 3 s of steady memantine inhibition at each memantine concentration, $I_{control}$ is the mean current during 3 s of steady-state current preceding drug application and 3 s of steady-state current following recovery from drug inhibition, and n_H is the Hill coefficient. $Log(IC_{50})$ and n_H were the free parameters in the fits. The $logIC_{50}$ value for each cell was transformed to IC_{50} and values averaged across cells for presentation. For graphical representation, $I_{memantine}/I_{control}$ were averaged at each memantine concentration, plotted, and overlaid with the fit determined as described above.

We determined the voltage dependence of memantine inhibition of GluN1(N616R)/2A receptors by fitting IC_{50} values at -105, -65 and -25 mV to the following equation, $IC_{50}(V_m) = IC_{50}(0 \text{ mV})*e\char`^(V_m/V_o)$, where $IC_{50}(V_m)$ is the IC_{50} value at membrane voltage V_m, $IC_{50}(0 \text{ mV})$ is the IC_{50} value at 0 mV, and V_o is the number of mV for an e-fold change in IC_{50}, which quantifies voltage dependence.

The extent of closed channel inhibition (CCI) was measured using the following protocol (**Figures 21** and **23**). 1 mM glutamate was applied for 20 s (I_{cont1}), followed by normal extracellular solution for at least 9 s to allow for full deactivation of receptors, then 100 μM

memantine in the absence of glutamate was applied for 30 s. Memantine was washed away briefly by a 1 s application of normal extracellular solution before glutamate was reapplied for 20 s (I_{CCI}). We chose a 1 s wash to allow for full solution exchange while still maintaining substantial CCI (CCI washout $\tau > \sim 2$ s (Kotermanski et al., 2009)). The 20 s reapplication of 1 mM glutamate (I_{CCI}) was followed by a wash in normal extracellular solution for at least 40 s, and then glutamate was reapplied for 20 s (I_{cont2}) to compare to I_{cont1} to ensure there was not significant current rundown. Fractional inhibition after CCI was measured by comparing I_{cont} and I_{cont2} to I_{CCI} by the following equation; fractional response after CCI = I_{CCI}/I_{cont}, where $I_{cont} = ((I_{Cont1} + I_{Cont2})/2)$ (see **Figures 21** and **23**). Peak currents were measured as the mean current over a 30 ms window centered on the mean time to peak for I_{cont1} and I_{cont2} in each cell to account for the possibility that NMDAR activation kinetics may be altered after CCI, which could affect accurate measurement of I_{CCI}.

Macroscopic memantine binding and unbinding kinetics were analyzed from drug concentration-response experiments, as described in Chapters 3 and 4. Briefly, 1 mM glutamate was applied for 10 – 20 s until current reached steady-state amplitude, then glutamate with 1, 10, 100, or 1000 μM memantine was applied for 10 – 40 s until a steady level of inhibition was reached. Glutamate without drug was then reapplied for 20 – 60 s to allow recovery from inhibition. Recordings were performed in 0 or 1 mM Mg^{2+} for the duration of the experiment. Cells were excluded from analysis if recovery from inhibition did not reach 80% of steady-state current preceding drug application.

Individual pair-wise comparisons were made by two-tailed Student's t-test with a level of significance as indicated. Group data were compared by one-way ANOVA with Tukey's *post*

hoc analysis with a significance level as indicated. All error is displayed as ± SEM. Current traces for presentation were refiltered offline in Clampfit 10.3 at 200 Hz.

5.4   RESULTS

5.4.1   Memantine unbinds from the second site without NMDAR activation

In Chapter 4, we showed that the unbinding τ_w of memantine, but not ketamine, was concentration-dependent. The memantine concentration dependence of unbinding τ_w resulted from increases in the duration and fraction of the slow component of unbinding. Presumably, memantine binding at the second site, which exhibits a high IC_{50} site and slow unbinding kinetics, is responsible for the increase in the duration and fraction of the slow component of unbinding. Results of previous studies support the hypothesis that memantine is able to bind and unbind from the second site without NMDAR activation (Blanpied et al., 1997; Sobolevsky et al., 1998; Kotermanski et al., 2009). If memantine bound to the second site is responsible for slow unbinding, and if memantine is able to unbind from the second site without NMDAR activation, then slow unbinding should be absent after a protocol that allows memantine unbinding without NMDAR activation. Therefore, we measured the kinetics of memantine unbinding after a trapping protocol previously used to demonstrate that memantine could unbind without NMDAR activation.

We used a drug trapping protocol (**Figure 20A**; **Section 5.3.4**) to inhibit GluN1/2A with 100 μM memantine, which exhibits an unbinding τ_{slow} of ~5 s and $Frac_{slow}$ of ~0.6 (**Figure 16**; **Table 7**). If memantine is able to unbind from the second site without NMDAR activation, then

the duration and fraction of the slow component of unbinding should decrease significantly. The kinetics of open channel blockers depend strongly on P_{open}, and due to desensitization, peak P_{open} is much higher than P_{open} during steady-state activation. Comparisons of memantine unbinding kinetics measured at peak P_{open} to kinetics measured at steady-state P_{open} require a conversion to account for the difference in P_{open} between the two conditions. Therefore, we determined the ratio of current during glutamate applications following memantine trapping (I_{trap}) to the current during control glutamate applications (I_{cont}, I_{cont1}, and I_{cont2}; **Section 5.3.4**). We then determined the trapped unbinding kinetics (**Section 5.3.4**) by fitting the trapped ratio with exponential functions (**Figure 20B**, **C**). We also measured ketamine unbinding kinetics after trapping. Ketamine serves as a control for our method of comparing unbinding kinetics during peak and steady-state activation and as a control for how an open channel blocker without two binding sites might unbind after trapping. We also examined whether 1 mM Mg^{2+} affected unbinding kinetics after drug trapping.

We found that the trapped memantine unbinding τ_w was ~40-fold faster than the steady-state unbinding τ_w in both 0 and 1 mM Mg^{2+} (**Figure 20B**, **D**; **Table 7**). In contrast, the trapped ketamine unbinding τ_w was ~4-fold faster than the steady-state ketamine unbinding τ_w in both 0 and 1 mM Mg^{2+} (**Figure 20C**, **D**; **Table 7**). Faster ketamine unbinding after trapping is likely a result of higher P_{open} at peak than at steady-state activation. In contrast, faster memantine unbinding after trapping is likely a result of higher P_{open} at peak than at steady-state activation and a result of memantine unbinding from the second site. Further analysis of unbinding kinetics demonstrate that the fraction of the slow component of memantine unbinding decreases to < 0.1 in trapped unbinding from ~0.6 in steady-state unbinding in both 0 and 1 mM Mg^{2+} (**Table 7**).

These results suggest that faster memantine unbinding τ_w after trapping is due to memantine unbinding from the second site without NMDAR activation.

Consistent with memantine either escaping from a closed channel or inhibiting at a site outside the channel gate, we found that the fractional recovery, also referred to as partial trapping (the fraction of receptors not bound by drug immediately following glutamate application) of memantine was significantly greater than the fractional recovery of ketamine, consistent with previous results (Kotermanski et al., 2009) (**Figure 20E**). Interestingly, our data exhibit more fractional recovery for memantine and ketamine than previous reports (Mealing et al., 1999; Kotermanski et al., 2009). This could result from higher agonist concentration, higher P_{open} (due to various sources), or differences in the drug concentrations used in the trapping protocol. Importantly, these data do not reveal whether the second site is internal or external to the channel gate. However, if the second site is more intracellular than the channel gate, then memantine must be able to unbind from the second site by passing through or around the closed channel gate.
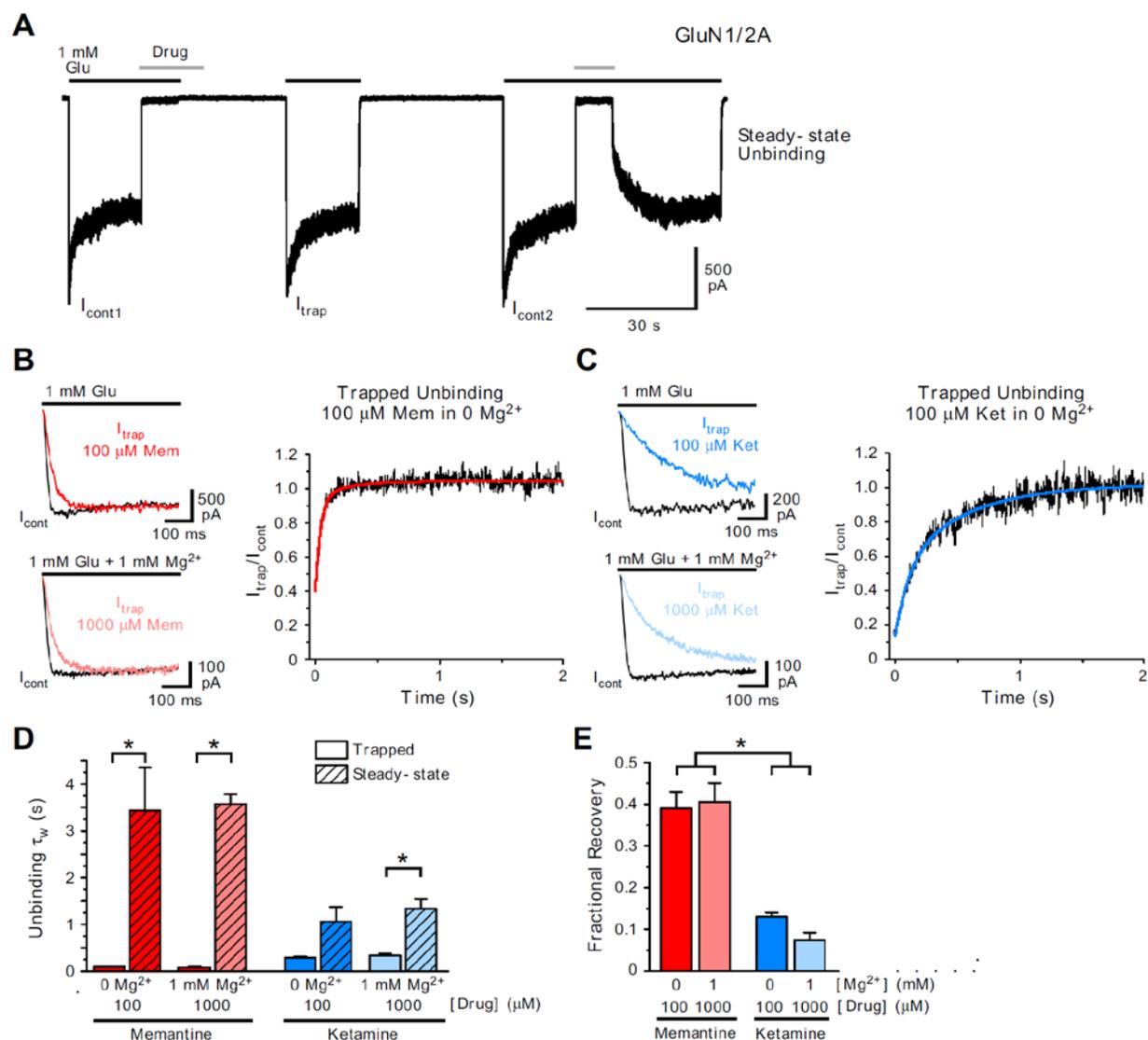
Figure 20 Memantine unbinds from the second site without NMDAR activation

A, Representative current trace of the trapping protocol (see Materials and Methods) with 100 μM memantine. Applications of 1 mM glutamate (Glu, black bars) and applications of memantine or ketamine (Drug, gray bars). **B**, Left, representative current traces of peak current alignments of control (I_{cont}, black traces) and after memantine trapping (I_{trap}, red traces) in 0 (left, top, dark red traces) and 1 mM Mg^{2+} (left, bottom, light red traces). Right, double exponential fit (red line) of trapped unbinding to determine unbinding kinetics after trapping with 100 μM memantine in 0 Mg^{2+}. **C**, same as **B**, except with ketamine (blue traces, and blue fit line). **D**, Mean trapped and steady-state unbinding τ_w across groups. **E**, Mean fractional recovery after trapping across groups. * indicates p < 0.05 by one-way ANOVA with Tukey's *post hoc* analysis within drug groups, n = 3 cells per group.

142

Table 7 Kinetics of recovery from trapped and steady-state inhibition of GluN1/2A receptors.

Values represent means ± SEM, n = 3 cells per group.

				Memantine Unbinding Kinetics After Trapping or Steady-State Inhibtion									
Inhibition Protocol	pH	$[Mg^{2+}]$ (mM)	[Drug] (µM)	τ_{Fast} (ms)	± SEM	$Frac_{Fast}$	± SEM	τ_{Slow} (ms)	± SEM	$Frac_{Slow}$	± SEM	τ_W (ms)	± SEM
Trapping	7.2	0	100	46.4	2.73	0.93	0.01	691	23.9	0.07	0.01	93.9	6.72
Steady-State	7.2	0	100	131	20.6	0.45	0.05	5789	1391	0.55	0.05	3437	1085
Trapping	7.2	1	1000	47.4	2.33	0.97	0.01	1197	382	0.03	0.01	79.8	20.2
Steady-State	7.2	1	1000	96.4	11.2	0.33	0.05	5294	297	0.67	0.05	3573	209
Trapping	9	0	100	29.6	3.14	0.79	0.11	1326	679	0.21	0.11	181	99.8
Steady-State	9	0	100	47.0	8.54	0.05	0.00	9402	675	0.95	0.00	8915	676
				Ketamine Unbinding Kinetics After Trapping or Steady-State Inhibtion									
Inhibition Protocol	pH	$[Mg^{2+}]$ (mM)	[Drug] (µM)	τ_{Fast} (ms)	± SEM	$Frac_{Fast}$	± SEM	τ_{Slow} (ms)	± SEM	$Frac_{Slow}$	± SEM	τ_W (ms)	± SEM
Trapping	7.2	0	100	87	17.0	0.47	0.07	473	46	0.53	0.07	291	30
Steady-State	7.2	0	100									1060	313
Trapping	7.2	1	1000	145	12.6	0.71	0.13	1275	421	0.29	0.13	334	44.1
Steady-State	7.2	1	1000	570	34.7	0.73	0.02	3550	799	0.27	0.02	1340	202

5.4.2 Memantine deep site mutation effects inhibition at the second site

Next, we attempted to isolate memantine binding at the second site by mutating one of the N-site asparagines, amino acid residues at the outer tip of the M2 reentrant loop that are critical for memantine binding at the deep site. We mutated the GluN1 N-site to an arginine (GluN1(N616R)), which has previously been shown to severely decrease memantine potency (Kashiwagi et al., 2002; Chen and Lipton 2005; Limapichat et al., 2013). Consistent with these previous studies, we found that the memantine IC_{50} of GluN1(N616R)/2A receptors at -65 mV was 459 ± 24.3 µM (**Figure 21A**, **B**). We also determined that GluN1(N616R)/2A receptors exhibit relatively voltage-independent inhibition with a V_o of 118 mV, compared to V_o of 30 – 35 mV in wild-type receptors (Blanpied et al., 1997; Parsons et al., 2007; Kotermanski and Johnson 2009) (**Figure 21A**, **B**). Therefore, memantine inhibition is ~5-fold less potent at mutant

receptors than at the memantine superficial site (IC_{50} ~80 – 180 μM) (Blanpied et al., 1997; Kotermanski et al., 2009) and is 2- to 3-fold less voltage-dependent than wild-type GluN1/2A receptors (V_o ~30-35 mV for deep site inhibition, Parsons et al. (2007); and V_o = 67.2 mV for superficial site inhibition, Blanpied et al. (1997)). These data suggest that mutation of the deep site may disrupt memantine inhibition at the second site.

To more directly assess memantine inhibition at the second site in GluN1(N616R)/2A receptors, we measured second site inhibition in the absence of agonist, which is a prominent property of memantine inhibition at the second site (Blanpied et al., 1997; Sobolevsky et al., 1998; Kotermanski et al., 2009). From here on, we will refer to second site inhibition in the absence of agonist as closed channel inhibition (CCI). We measured CCI of wild-type and mutant receptors with a CCI protocol (**Figure 21C**, **D**; **Section 5.3.4**) using 500 μM memantine, which is near the fully effective concentration of CCI in wild-type receptors (Blanpied et al., 1997; Kotermanski et al., 2009). As expected, we found that 500 μM memantine exhibited robust CCI in wild-type receptors (Fractional response after CCI = 0.43 ± 0.05; **Figure 21C**). Surprisingly, 500 μM memantine exhibited only marginal CCI in GluN1(N616R)/2A receptors (Fractional response after CCI = 0.91 ± 0.02; **Figure 21D**). These findings suggest that CCI, and thus memantine binding at the second site, requires memantine binding at the deep site. However, it is possible that the positive charge of the arginine at the deep site interferes with memantine binding at the second site. Nevertheless, GluN1(N616R)/2A receptors exhibit lower memantine potency and lower voltage dependency than expected. Furthermore, GluN1(N616R)/2A receptors exhibit lower CCI, which is a characteristic of memantine binding at the second site. Therefore, the mutant seems ill-suited for investigation of memantine binding at the second site.

144
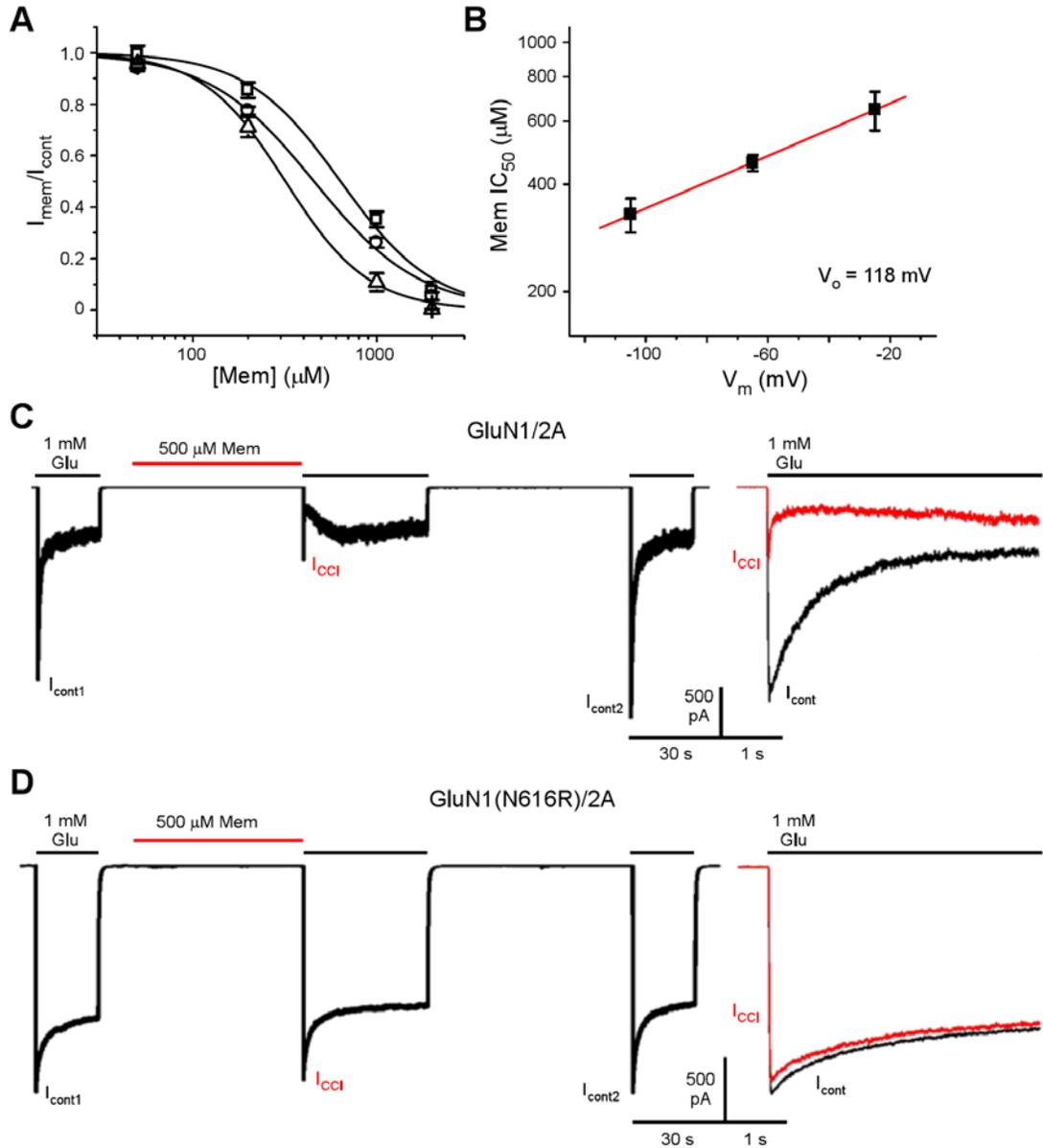
Figure 21. Memantine deep site mutation effects inhibition at the second site.

A, Memantine concentration-response curves for GluN1(N616R)/2A receptors at -105 mV (open triangles), -65 mV (open circles), and -25 mV (open squares). **B**, Memantine IC_{50} values (filled squares) fit by the voltage dependence equation (red line; **Section 5.3.4**). **C**, **D**, Representative current traces of CCI protocol (**Section 5.3.4**) with GluN1/2A receptors (**C**) and GluN1(N616R)/2A receptors (**D**). Applications of 1 mM glutamate (black bars) and 500 μM memantine (red bars). Right, Aligned currents at time of glutamate applications of control (I_{cont}, black traces) and after CCI (I_{CCI}, red traces). n = 3 – 5 cells per group.

145

5.4.3   Uncharged memantine binds to the second site

Inhibition by memantine of GluN1(N616R)/2A receptors at both the deep site and the second site was severely disrupted. However, strikingly, the weak remaining inhibition by memantine was nearly insensitive to voltage. This observation suggests an intriguing hypothesis: the uncharged species of memantine binds NMDARs at the second memantine binding site. At physiological pH, the amine group of memantine, which has a pKa of 10.3 (Freudenthaler et al., 1998) is protonated at a ratio of ~1200 charged to 1 uncharged memantine. Therefore, at 100 μM memantine, the concentration of uncharged memantine is close to 80 nM. Interestingly, consistent with previous findings, we demonstrated in Chapter 4 that memantine binding at the second site exhibits a high IC_{50} (~100 μM) with paradoxically slow unbinding kinetics (Blanpied et al., 1997; Sobolevsky and Koshelev 1998; Sobolevsky et al., 1998; Kotermanski et al., 2009). However, if the species of memantine binding at the second binding site is uncharged memantine, then the IC_{50} would be closer to the 100 nM range, and memantine would exhibit expectedly slow unbinding kinetics. Uncharged memantine binding at the second site also presents a plausible mechanism for binding and unbinding without NMDAR activation; uncharged memantine should be much more hydrophobic than charged memantine, and could potentially associate and disassociate through the membrane, between transmembrane helices, or through the closed gate. Therefore, we tested whether uncharged memantine is responsible for inhibition at the second site.

To increase the concentration of uncharged memantine, we increased the pH of our extracellular solution to pH 9. We avoided raising pH higher than 9 due to the lack of receptor characterization at a pH much greater than 8 (Traynelis and Cull-Candy 1990; Vyklicky et al.,

1990; Traynelis and Cull-Candy 1991; Traynelis et al., 1995; Banke et al., 2005; Schorge et al., 2005; Erreger and Traynelis 2008; Kussius and Popescu 2009). At pH 9, the calculated ratio is ~20 charged to 1 uncharged memantine, resulting in more than a 60-fold increase in the relative concentration of uncharged memantine compared to pH 7.2. We measured the memantine IC_{50} and kinetics of inhibition and recovery from inhibition of GluN1/2A receptors at pH 9. Consistent with previous work on the proton sensitivity of NMDAR open channel blockers (Dravid et al., 2007), we found that in 0 Mg^{2+} the memantine IC_{50} at pH 9 ($IC_{50} = 3.43 \pm 0.61$ μM) increased ~2-fold compared to the IC_{50} at pH 7.2 (**Figure 9**; **Table 7**). We found that in 0 Mg^{2+}, memantine unbinding τ_w at pH 9 was 5- to 10-fold slower than at pH 7.2 at each memantine concentration (**Table 4**; **Figure 22A**, **C**, **E**; **Table 8**). Memantine unbinding kinetics also exhibited concentration dependence at pH 9, as the unbinding τ_w with 100 μM memantine was 8.5-fold slower than with 1 μM memantine (**Figure 22E**; **Table 8**). Further investigation of memantine unbinding kinetics at pH 9 demonstrated that the weight of the fast component of unbinding ($Frac_{fast}$) decreased from 0.55 to 0.03 in a memantine concentration-dependent manner (**Table 8**), suggesting that the second site is near full occupation at 100 μM memantine. These data support the hypothesis that uncharged memantine binds to the second site.

Next, we determined whether 1 mM Mg^{2+} affects memantine inhibition at pH 9. We found that 1 mM Mg^{2+} at pH 9 increases the memantine IC_{50} 6.9-fold compared to 0 Mg^{2+}, compared to a 16.7-fold increase from the absence to presence of 1 mM Mg^{2+} at pH 7.2 (Kotermanski and Johnson 2009). Although the memantine concentration dependence of unbinding kinetics was maintained in 1 mM Mg^{2+} at pH 9, the unbinding τ_w was significantly faster than in 0 Mg^{2+} (**Figure 22B**, **C**, **E**; **Table 8**). Interestingly, in 1 mM Mg^{2+} the unbinding τ_w at pH 9 and at pH 7.2 were not significantly different at any of the memantine concentrations

147

tested (**Figure 22E**). These findings suggest that Mg^{2+} strongly interferes with uncharged memantine binding to the second site, as well as memantine binding to the deep site.

We also investigated memantine binding kinetics at pH 9. Surprisingly, memantine at pH 9 revealed a slow binding component that was much slower than at pH 7.2 (**Table 4**; **Figure 22A**; **Table 8**). About 14% of the inhibition by 100 µM at pH 9 is due to the slow component of binding (**Table 8**), compared to only 2% at pH 7.2 (**Table 4**). Slow binding may suggest that uncharged memantine binding to the second site inhibits NMDARs in part through changes in rates of receptor state transitions. Interestingly, slow binding and unbinding kinetics are consistent with the kinetics predicted by Model B2, where memantine increases occupancy desensitized states of NMDARs (**Figure 13**). However, the origin of the much slower memantine binding component at pH 9 is not clear.
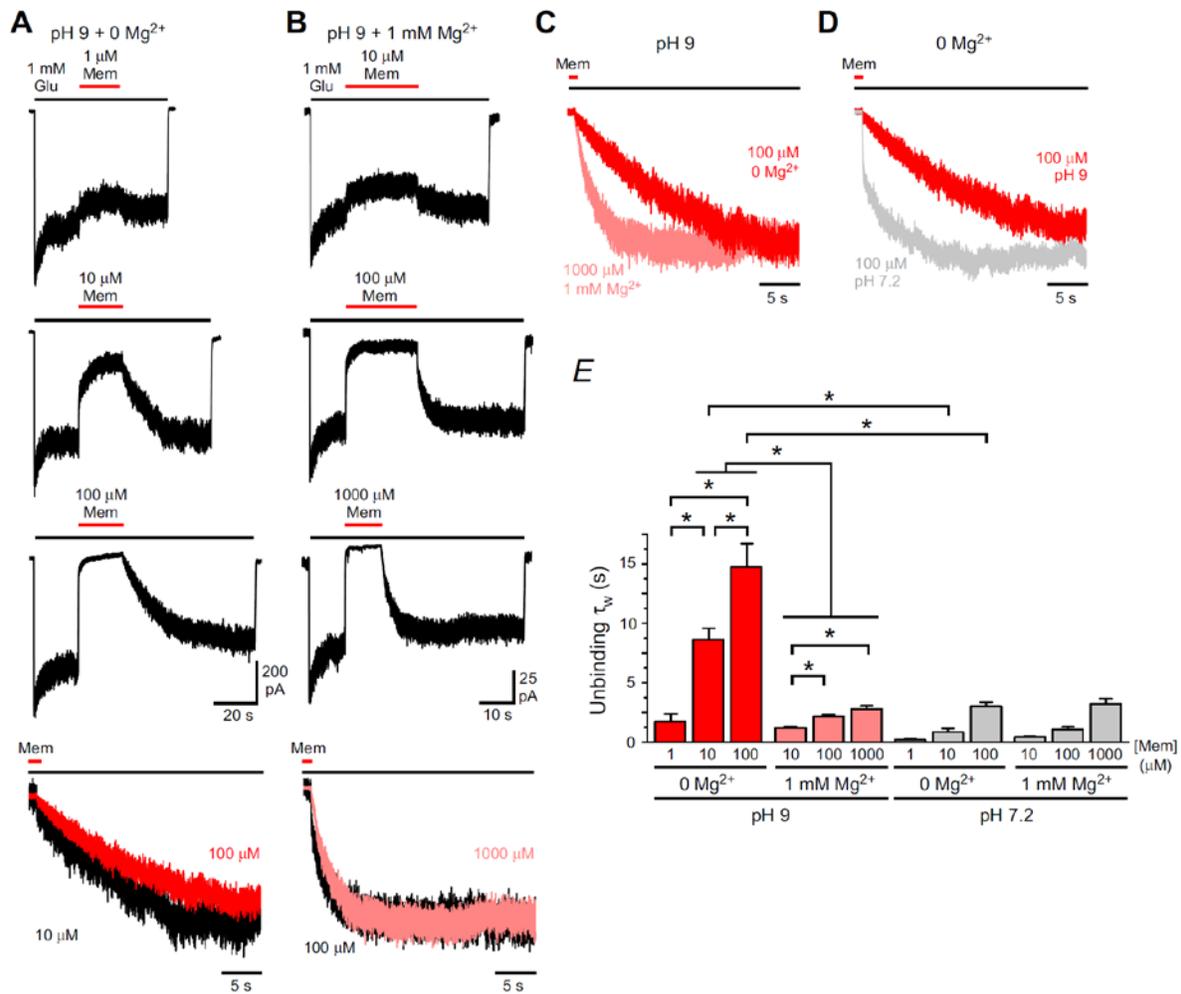
Figure 22. Uncharged memantine binds to the second site.

A, **B**, Representative current traces used for measuring binding and unbinding kinetics of GluN1/2A receptors at pH 9 in 0 Mg^{2+} (**A**) and 1 mM Mg^{2+} (**B**), when activated by 1 mM glutamate (black bars). Memantine was applied at the indicated concentrations (red bars). Traces within a column are from the same cell. The bottom traces illustrate memantine concentration dependence of unbinding kinetics. The memantine unbinding traces are taken from above at the memantine concentrations indicated, aligned at the time of memantine removal, and scaled to the change in current amplitude during recovery from inhibition. Dark red traces are in 0 Mg^{2+}; light red traces are in 1 mM Mg^{2+}. **C**, Representative current traces to show the difference in memantine unbinding at pH 9 in 0 Mg^{2+} (dark red trace, scaled and replotted from **A**) and 1 mM Mg^{2+} (light red trace, scaled and replotted from **B**). **D**, Representative current traces to show the difference in memantine unbinding in 0 Mg^{2+} at pH 9 (dark red trace, scaled and replotted

from **A**) and at pH 7.2 (gray trace, scaled and replotted from **Figure 16A**). **E**, Mean unbinding τ_w across groups with data at pH 7.2 replotted from **Figure 16E**. * indicates $p < 0.05$ by one-way ANOVA, n = 4 – 6 cells per group.

Table 8. Memantine kinetics at pH 9 with unlifted cells.

Values represent means ± SEM, n = 4 cells per group.

				Memantine Macroscopic Binding Time Constant Components									
	[Glu]	[Mg^{2+}]	[Drug]	τ_{Fast}				τ_{Slow}				τ_w	
Subtype	(μM)	(mM)	(μM)	(ms)	± SEM	Frac$_{Fast}$	± SEM	(ms)	± SEM	Frac$_{Slow}$	± SEM	(ms)	± SEM
GluN1/2A	1000	0	1	89.6	28.1	0.39	0.03	13886	3883	0.61	0.03	8328	2416
			10	74.0	9.67	0.62	0.04	3630	480	0.38	0.04	1498	312
			100	42.0	4.18	0.86	0.01	2387	528	0.14	0.01	392	99
	1000	1	10	201	105	0.41	0.05	5909	123	0.59	0.05	3554	265
			100	54.9	9.84	0.57	0.05	2007	331	0.43	0.05	886	163
			1000	23.3	0.87	0.89	0.02	533	78.3	0.11	0.02	73.0	3.59
				Memantine Macroscopic Unbinding Time Constant Components									
	[Glu]	[Mg^{2+}]	[Drug]	τ_{Fast}				τ_{Slow}				τ_w	
Subtype	(μM)	(mM)	(μM)	(ms)	± SEM	Frac$_{Fast}$	± SEM	(ms)	± SEM	Frac$_{Slow}$	± SEM	(ms)	± SEM
GluN1/2A	1000	0	1	112	36.3	0.55	0.12	3377	365	0.45	0.12	1734	645
			10	47.9	14.0	0.15	0.02	10202	1217	0.85	0.02	8623	954
			100	31.1	12.4	0.03	0.01	15241	2058	0.97	0.01	14750	1957
	1000	1	10	71.6	26.9	0.41	0.03	2028	135	0.59	0.03	1226	103
			100	60.4	11.8	0.28	0.02	3009	207	0.72	0.02	2172	157
			1000	1067	145	0.31	0.04	3608	391	0.69	0.04	2790	277

5.4.4   Uncharged memantine can access the second site without NMDAR activation

To further investigate the hypothesis that uncharged memantine binds to the second site, we determined whether uncharged memantine could bind and unbind in the absence of agonist. Previously, we demonstrated that memantine that had bound to the second site during agonist application could unbind without NMDAR activation (**Figure 20**). Using the trapping protocol illustrated in **Figure 20A**, we found that at pH 9, the trapped unbinding τ_w of 100 μM memantine was 50-fold faster than the steady-state unbinding τ_w (**Figure 23A**, **Table 7**). Importantly, the trapped unbinding τ_w at pH 7.2 and 9 are not significantly different (**Table 7**; Student's t-test, p =

150

0.51), whereas steady-state unbinding at pH 7.2 and 9 are significantly different (**Table 7**; Student's t-test, p = 0.02). This suggests that elevating pH does not severely disrupt memantine inhibition at the deep site and that the slowing of unbinding kinetics results primarily from an increased concentration of uncharged memantine binding to the second site. These results support our conclusion that at pH 7.2 memantine bound to the second site is able to unbind without NMDAR activation, and also further support the hypothesis that uncharged memantine binds to the second site.

Next, we determined whether uncharged memantine could bind at the second site without NMDAR activation by measuring the extent of CCI at pH 7.2 and pH 9, both in 0 and in 1 mM Mg^{2+}. We used a similar CCI protocol as in **Figure 21C**, **D**, except to be able to detect an increase or decrease in CCI, we used 100 μM memantine, which is near the CCI IC_{50} at pH 7.2 (Blanpied et al., 1997; Kotermanski et al., 2009). At pH 7.2 in 0 Mg^{2+}, the fractional response after CCI was 0.63 ± 0.02 (**Figure 23B**, **F**). If CCI is dependent on binding of uncharged memantine to the second site, then CCI should increase at pH 9, resulting in a reduced fractional response after CCI. Indeed, at pH 9 fractional response after CCI with 100 μM memantine decreased 5.6-fold to 0.11 ± 0.01 (**Figure 23C**, **F**). Our data support the hypothesis that uncharged memantine binds to the second site, and also supports the hypothesis that uncharged memantine is able to bind to the second site without NMDAR activation. These findings are consistent with previous data that demonstrated that at physiological pH, memantine can bind to and unbind from the second site without NMDAR activation (Blanpied et al., 1997; Sobolevsky et al., 1998; Kotermanski et al., 2009).

We also evaluated CCI in 1 mM Mg^{2+}. Surprisingly, at both pH 7.2 and pH 9, Mg^{2+} strongly occluded CCI (**Figure 23D**-**F**). These data suggest that Mg^{2+} prevents memantine

binding at the second site without NMDAR activation. Importantly, it is not clear from these experiments where the second memantine binding site is located relative to the channel gate. It is plausible that the second site is truly external to the channel gate and Mg^{2+} happens to compete for binding at the second site as well as the deep site. Therefore, we designed a modified CCI protocol to test the hypothesis that memantine and Mg^{2+} compete for the same external binding site.

The modified CCI protocol was similar to the CCI protocol performed in 0 Mg^{2+}, except that we co-applied 1 mM Mg^{2+} and 100 μM memantine. Thus, the modified CCI protocol involved application of the following sequence of solutions: 1 mM glutamate for 20 s; normal extracellular solution for 9 s; 1 mM Mg^{2+} plus 100 μM memantine in the absence of glutamate for 30 s; normal extracellular solution for 1 s; 1 mM glutamate for 20 s. We found that the fractional response after modified CCI was not significantly different than after CCI in 0 Mg^{2+}, but was significantly different than the fractional response after CCI in 1 mM Mg^{2+} at pH 7.2 and at pH 9 (**Figure 23F**). These data suggest that memantine and Mg^{2+} do not compete for the same external binding site. Instead our results suggest that Mg^{2+} trapped inside the channel inhibits memantine binding at the second site in the absence of glutamate. Regardless the interaction of Mg^{2+}, these data support the hypothesis that uncharged memantine binds at the second memantine binding site, and that this site is accessible without NMDAR activation.
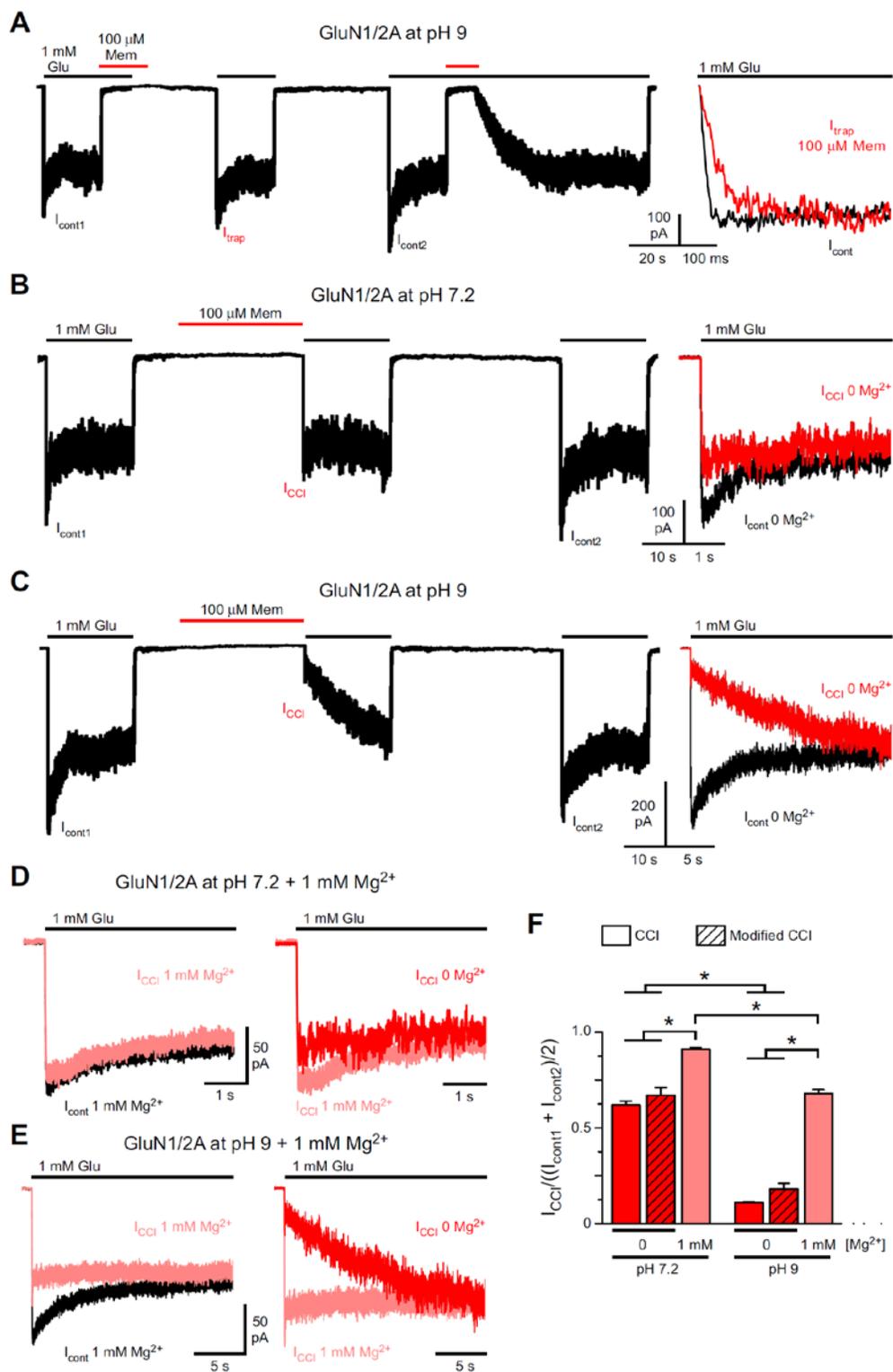
Figure 23. Uncharged memantine can access the second site without NMDAR activation.

A, Representative current traces at pH 9 of the memantine trapping protocol (left) and the aligned currents at time of glutamate applications (right) of the control (I_{cont}, black trace) and I_{trap} (red trace). Applications of 1 mM glutamate

153

(black bars) and 100 μM memantine (red bars). **B**, **C**, Representative current traces of the CCI protocol (left) in 0 Mg^{2+} at pH 7.2 (**B**) and pH 9 (**C**) and currents aligned at time of glutamate applications (right) of control and I_{CCI} (red traces). **D**, **E**, left, Representative current traces of the currents aligned to the time of glutamate applications of control and I_{CCI} following inhibition with 100 μM memantine in 1 mM Mg^{2+} in normal CCI protocol. **D**, **E**, right, Representative current traces of currents aligned to the time of glutamate applications of I_{CCI} following inhibition with 100 μM memantine in 0 Mg^{2+} (dark red traces) and 1 mM Mg^{2+} in normal CCI protocol (light red traces) at pH 7.2 (**D**) and pH 9 (**E**). **F**, Mean fractional response after CCI across groups. For the modified CCI protocol, 1 mM Mg^{2+} only was co-applied with 100 μM memantine; for the CCI protocol the $[Mg^{2+}]$ was constant throughout the experiment. * indicates $p < 0.05$ by one-way ANOVA with Tukey's *post hoc* analysis, n = 3 cells per group.

5.5   DISCUSSION

In the experiments described in this chapter we investigated how memantine interacts with a second site on GluN1/2A receptors. Our results build on work presented in Chapter 4, as well as on work from our lab and others that probed memantine binding at a second site (Blanpied et al., 1997; Sobolevsky and Koshelev 1998; Sobolevsky et al., 1998; Chen and Lipton 2005; Kotermanski et al., 2009). We provide multiple lines of evidence in support of the hypothesis that the uncharged species of memantine binds to the second site. Uncharged memantine binding at the second site contributes to several properties linked to memantine inhibition at the second site, including high IC_{50} with paradoxically slow unbinding kinetics, and the ability to bind and unbind without NMDAR activation. Further, our results suggest a complex interaction between Mg^{2+} and memantine at both binding sites. Additional experiments are necessary to understand the mechanistic basis of memantine binding at the second site and the interaction between Mg^{2+} and memantine. For the first time, our data demonstrate that raising the pH from physiological

154

levels is an effective method to shift memantine inhibition towards occupation of the second site. This method could prove useful in further investigation of the mechanisms of inhibition by memantine. However, significant caveats should be considered when interpreting experiments performed using extracellular solutions with modified pH.

First, NMDARs exhibit proton inhibition below pH of ~9 (Tang et al., 1990; Traynelis and Cull-Candy 1990; Vyklicky et al., 1990; Traynelis and Cull-Candy 1991; Traynelis et al., 1995). With decreasing pH, NMDAR P_{open} decreases due to changes in rates of NMDAR state transitions (Banke et al., 2005; Dravid et al., 2007; Erreger and Traynelis 2008). NMDAR properties are well characterized up to a pH of ~8, in a pH-dependent manner (Erreger et al., 2005; Schorge et al., 2005; Erreger and Traynelis 2008; Kussius and Popescu 2009; Amico-Ruvio and Popescu 2010). However, at pH levels > 8 NMDAR properties are relatively unexplored. Second, one basis of pH sensitivity of proteins, including NMDARs, is due to changing ionization states of the amino acid residue backbone and their side chains (Yuan et al., 2015). Some amino acid residues lining the NMDAR channel pore and the second memantine binding site are likely to have pKa values between 7 and 10. Within this range of pKa values, the percent of protonation of some residues would change drastically between pH 7.2 and 9. Thus, in addition to shifting the ratio of charged to uncharged memantine, an increase in pH from 7.2 to 9 could change residue ionization states that normally interact with memantine. Memantine inhibition may be altered without regard to charged or uncharged memantine binding. Indeed, the inhibition of many open channel blockers, including memantine, is altered by increased pH over a range wherein the drug ionization is relatively unchanged (Dravid et al., 2007).

Despite concerns that elevating pH may affect memantine action via unanticipated mechanisms, memantine inhibition at the second site exhibited similar characteristics at pH 7.2

155

and pH 9. For instance, at pH 9 and at pH 7.2 memantine exhibited concentration dependence of unbinding kinetics, and unbinding kinetics were faster in 1 mM Mg^{2+} (**Figure 23**; **Table 8**). It is important to have multiple approaches for independently characterizing inhibition by memantine at the deep site and the second site. Presently, the only other approach to isolate memantine inhibition at the second site is through indirect measure, CCI, and through mutation of the deep site. Although we anticipated that the N to R mutation at the GluN1 N-site would selectively affect memantine binding at the deep site, the mutation also strongly affected memantine binding at the second site (**Figure 21**). Therefore, with the use of proper and careful controls, elevating pH is a plausible approach to increase memantine occupation of the second site.

Mutation of the GluN1 N-site to R, gives a 2+ charge at the deep site, which is similar to Mg^{2+} binding at the deep site in wild-type receptors. Interestingly, mutation at the deep site alters memantine inhibition in two ways that are consistent with how 1 mM Mg^{2+} alters inhibition at the second site. First, the deep site mutation increases the memantine IC_{50} higher than measurements of memantine CCI IC_{50} in wild-type receptors (Blanpied et al., 1997; Kotermanski et al., 2009). Similarly, 1 mM Mg^{2+} shifts concentration dependence of memantine unbinding kinetics, which suggests that the memantine IC_{50} at the second site is also higher in 1 mM than 0 Mg^{2+}. Second, the deep site mutation unexpectedly decreases CCI to a degree similar to the degree that 1 mM Mg^{2+} unexpectedly decreases CCI. In combination with our other findings, these observations support two alternative models of memantine inhibition (**Figure 24**). Model 1 has two binding sites, the deep site and the second site within the channel; memantine binding at the second site requires memantine to be bound at the deep site (**Figure 24A**). Model 2 instead has only a single binding site that can bind either of the two species of memantine: charged or uncharged memantine (**Figure 24B**). Each model supports various aspects of what is known

156

about memantine inhibition at the deep site and at the second site. It is possible that a combination of Models 1 and 2, or other models may more accurately and completely describe memantine inhibition. More experiments are needed to test the validity of each model.

Given the dearth of information regarding the mechanism of interaction of memantine and Mg^{2+} at the second site, the therapeutic implications of memantine binding at the second site are not yet clear. By manipulating memantine's charge, we now have an additional tool to investigate memantine interaction with the second binding site and its impact on the broader mechanism of action of memantine. Understanding the role of memantine binding at the second site in the basic and therapeutic mechanisms of NMDAR inhibition by memantine could also impact understanding of mechanisms of NMDAR inhibition by other open channel blockers. For instance, one key mechanistic difference between memantine and ketamine action is that memantine binds to a second site and ketamine does not (Johnson et al., 2015). The therapeutic impact of this difference has yet to be determined.
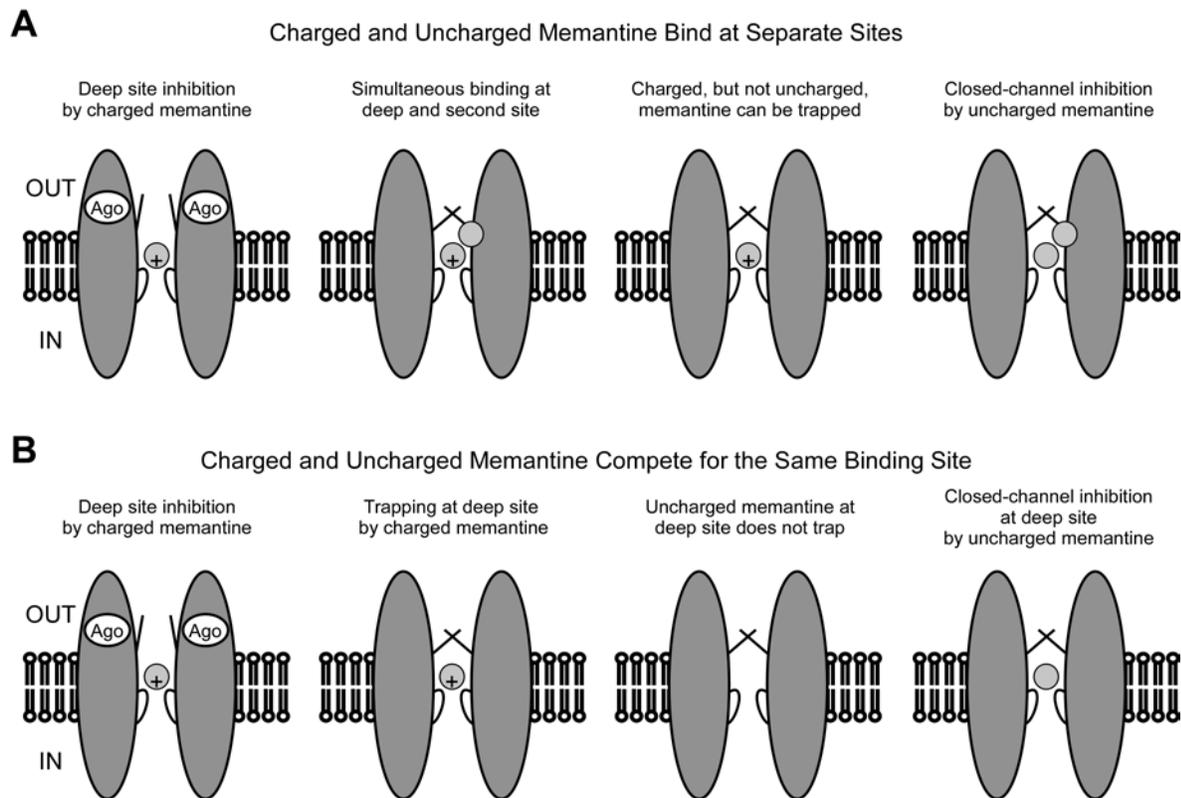
Figure 24. Two models of charged and uncharged memantine binding to NMDARs.

A, Model depicting memantine binding at two separate sites under a range of conditions. The M2 re-entrant loops are represented by curved lines in the middle of the membrane and the channel gate is represented by straight lines at the top of the membrane. Presence of agonist (Ago) and channel gate being open represents NMDAR activation. Charged memantine (gray circle with +) binds to the deep site at the tips of the M2 re-entrant loops and uncharged memantine (plain gray circle) binds to a second site near charged memantine. Closed channel inhibition requires uncharged memantine binding at the deep site. **B**, Model depicting charged or uncharged memantine binding at the deep site under a range of conditions. Only one species of memantine can bind to NMDARs at one time. The validity of these models assumes that uncharged memantine is able to access its binding site when the channel is closed, whereas charged memantine can only access its binding site when the channel is open (**Figure 23**).

6.0   GENERAL DISCUSSION

The work presented in this dissertation focused on the basic mechanisms of NMDAR inhibition by the clinically useful open channel blockers memantine and ketamine. Specifically, we investigated whether memantine and ketamine inhibition depended on features that likely differ between synaptic and extrasynaptic compartments; we investigated the effects of 1 mM Mg^{2+} on the characteristics of inhibition by memantine and ketamine; we investigated possible mechanisms that underlie memantine inhibition at a second site on NMDARs. Our primary conclusions are that memantine or ketamine cause a differential effect on NMDAR desensitization kinetics (Chapter 3), that 1 mM Mg^{2+} speeds recovery from inhibition by memantine, but not by ketamine (Chapter 4), and that uncharged memantine binds to the second memantine binding site (Chapter 5). This discussion focuses on the implications of our findings for understanding basic features of NMDAR structure and function, and for the therapeutic utility of memantine or ketamine.

6.1 RELATION BETWEEN MEMANTINE EFFECTS ON DESENSITIZATION AND ABILITY TO BIND AT TWO SITES

In Chapter 3 we found that memantine and ketamine differentially altered desensitization kinetics. The presence of 3 μM memantine increased the extent of desensitization and slowed the time course of recovery from desensitization for GluN1/2A, but not for GluN1/2B receptors. Furthermore, we found that the increased extent of desensitization and slowed recovery from desensitization for GluN1/2A receptors was Ca^{2+}-dependent. Although we did not test the Ca^{2+} dependence of the interaction between memantine and GluN1/2B receptors, our observations were consistent with GluN1/2A, but not GluN1/2B receptor, sensitivity to Ca^{2+}-dependent desensitization (Medina et al., 1995; Krupp et al., 1996). Our kinetic model (Model B2), which exhibited increased occupation of desensitized states, predicted that recovery from desensitization for GluN1/2A receptors would slow in 3 μM memantine compared to control. We found that recovery from desensitization for GluN1/2A receptors slowed in 3 μM memantine substantially more than Model B2 predicted. Therefore, Model B2 likely underestimated the extent of a memantine-induced increase in the occupancy of desensitized states. However, Model B2 also predicted that the time course of recovery from inhibition in the continuous presence of 1 mM glutamate should exhibit a relatively slow component of unbinding (Model B2, τ_{slow} = 9.1 s). This predicted slow component was either not present or not fully resolved in our recordings from GluN1/2A receptors. Interestingly, the predicted slow component is kinetically similar to the time course of memantine unbinding from the second site. Is memantine binding to the second site related to increased occupancy of desensitized states?

We presume that with 3 μM memantine at pH 7.2, the occupancy of the second site is very low. However, we do not fully understand the interaction between the deep site and the second site. For instance, mutation of the GluN1 N-site asparagine would be expected to affect only inhibition at the deep site, but inhibition at the second site was also affected (**Figure 21**). Mutational studies have identified residues in the external portion of the M3 TMR that increase memantine IC_{50} values ~5 -fold (Kashiwagi et al., 2002; Limapichat et al., 2013). Interestingly, a study investigating the location of the second memantine site identified a region in the external portion of the M3 TMR to be important for memantine binding to the second site (Chen and Lipton 2005). It is not clear whether mutations in the external portion of the M3 TMR affect memantine inhibition a the deep site, memantine inhibition at the second site, or both. However, these studies and our data (**Figure 21** and **23**) may suggest that memantine binding to the second site requires binding at the deep site, and that binding at the deep site may be affected by binding at the second site. An alternative explanation is that only memantine binding to the second site requires binding at the deep site, whereas inhibition at the deep site may be affected by conformational changes in the external portion of the M3 TMR, irrespective of binding at the second site.

Ketamine is able to alter desensitization kinetics presumably by binding to only the deep site. Many trapping blockers are thought to bind to only one site yet still affect rates of receptor state transitions thereby stabilizing closed, open, or desensitized states (Dilmore and Johnson 1998; Johnson and Qian 2002; Sobolevskii and Khodorov 2002). Therefore, in principle memantine binding only at the deep site is capable of increasing the occupancy of desensitized states.

If memantine binding to the second site is not involved in memantine-induced increases in the occupancy of desensitized states, what other factors can account for the discrepancy between our observed binding kinetics and the prediction of Model B2? NMDAR desensitization is a complex process involving several separable components (Dingledine, et al., 1999; Traynelis et al., 2010; **Section 1.1.2**). Ca^{2+}-dependent desensitization itself likely involves components sensitive to calmodulin, calcineurin, and α-actinin (**Section 1.1.2**) The conformational changes underlying any form of Ca^{2+}-dependent desensitization, or any other form of NMDAR desensitization, are not well understood. Nevertheless, it seems unlikely that calmodulin and calcineurin induce similar conformational changes to result in desensitized states, as calmodulin and calcineurin alter desensitization in qualitatively distinct ways (Tong and Jahr 1994; Krupp et al., 1996; Krupp et al., 2002). Furthermore, it seems unlikely that memantine increases occupancy of all Ca^{2+}-dependent states equally. Therefore, in the presence of memantine, Ca^{2+}-dependent desensitized states that are not affected by memantine are likely to recover due to memantine limiting Ca^{2+} influx. If there is substantial overlap of the time courses of memantine increasing occupancy of desensitized states, and of unaffected desensitized states recovering from desensitization, a kinetic component related to increased occupancy of desensitized states would not be resolved. This could explain why we did not observe slow components of recovery from memantine inhibition in our data that are similar to Model B2 predictions. This could also explain why recovery from desensitization was much slower in our data than predicted by Model B2. Nevertheless, the mechanisms responsible for memantine increasing occupancy of desensitized states will need to be investigated further.

6.2   EFFECTS OF OPEN CHANNEL BLOCKERS ON NMDAR STRUCTURE

The effects of memantine and ketamine described in this dissertation (altering desensitization and uncharged memantine binding to the second site) have the potential to deepen our understanding of conformational changes during receptor state transitions and of the structure of the channel itself. It is not surprising that the presence of memantine or ketamine in the channel can influence the stability of desensitized states (Johnson and Qian 2002; Sobolevskii and Khodorov 2002). However, it is interesting that memantine specifically increases the occupancy of a Ca^{2+}-dependent desensitized state, as opposed to other closed or desensitized states. This suggests that the conformations of regions that interact with memantine in a Ca^{2+}-dependent desensitized state do not closely resemble their conformations in other closed states. Furthermore, it is surprising that the same conformational state is absent in GluN1/2B receptors as GluN2A and GluN2B subunits vary by only four residues within the TMR α-helices (Siegler Retchless et al., 2012).

Not much is known about conformational changes at the level of the TMD during desensitization in NMDARs or other iGluRs. Although several structures of AMPARs and kainate receptors have been solved in various closed states and desensitized states, those studies have focused mainly on changes in the better resolved NTD and ABD regions (Sobolevsky et al., 2009; Chen et al., 2014; Durr et al., 2014; Meyerson et al., 2014; Yelshanskaya et al., 2014). Two NMDAR structures have also recently been solved (Karakas and Furukawa 2014; Lee et al., 2014), and hopefully soon more structures will follow that will allow comparison of various receptor states. Lee et al. (2014) utilized the NMDAR open channel blocker, MK-801 to help stabilize the crystal structure, but unfortunately MK-801 was not fully resolved inside the channel pore. Memantine might be useful to stabilize the desensitized state and aid in

crystallizing the receptors to solve structures of Ca^{2+}-dependent desensitized states. In contrast, ketamine might be useful to solve structures of non-desensitized states. However, Ca^{2+}-dependent desensitized states of NMDARs functionally require the CTD (Krupp et al., 1996; Krupp et al., 2002), which no iGluR structures have included thus far. Memantine binding to the second site may also complicate interpretation of structures solved in the presence of memantine. Nevertheless, open channel blockers with well characterized functional effects could serve as tools to aid interpretation of NMDAR structures.

It is unclear how uncharged memantine is able to bind and unbind without NMDAR activation. Previous studies identified a second shallow binding site on NMDARs that corresponded with sequential block by open channel blockers (Antonov and Johnson 1996; Bolshakov et al., 2003). However, uncharged memantine seems able to bind without the need for open channels, which is inconsistent with sequential block. Furthermore, unlike a sequential blocker, memantine IC_{50} depends only slightly on the agonist concentration, and in the opposite direction expected for a sequential blocker (Johnson and Qian 2002), although we did not measure the agonist concentration dependence of memantine IC_{50} at pH 9. Still, it is unlikely that uncharged memantine inhibits as a sequential blocker at the second site. Since only Mg^{2+} trapped in the channel was able to occlude closed channel inhibition by uncharged memantine, the second site is likely internal to the channel gate. How is uncharged memantine able to enter and exit a closed channel? Previous studies have reported that the lipophilicity of a blocker is unrelated to the extent of drug trapping in the channel, suggesting that the molecules tested do not exit the channel through a hydrophobic pathway (Mealing et al., 2001; Bolshakov et al., 2005). However, these studies and others (Mealing et al., 1999; Bolshakov et al., 2003) measured the degree of blocker trapping as the amount of unblock following a long period in the absence

of agonist, as in (**Figure 20**). The difference between fast unblocking and partial trapping is particularly hard to estimate with this method (Sobolevsky and Yelshansky, 2000; **Figure 20**). Furthermore, the ability of drugs to enter closed channels depending on lipophilicity was not assessed (Mealing et al., 2001; Bolshakov et al., 2005). Structural understanding of how uncharged memantine is able to enter and exit closed channels could be useful in identifying a functional hydrophobic pathway between the lipid membrane and the channel pore (also known as fenestrations) as found in Na^+ channels and possibly in K^+ channels (Payandeh et al., 2011; Lenaeus et al., 2014).

It is also surprising that 1 mM Mg^{2+} is able to occlude closed channel inhibition, irrespective of which species of memantine binds or how it binds to closed channels. Because the microscopic rates of Mg^{2+} binding to and unbinding from open NMDAR channels are very fast, it is difficult to determine the use dependence of Mg^{2+} (Ascher and Nowak 1988; Antonov and Johnson 1999; Sobolevsky and Yelshansky 2000; Johnson and Qian 2002; Qian et al., 2002). Most evidence suggests that NMDARs can access all states in Mg^{2+} and that gating rates are not affected in Mg^{2+} (Nowak et al., 1984; Ascher and Nowak, 1988; Jahr and Stevens, 1990; Benveniste and Mayer, 1995; Sobolevsky and Yelshansky, 2000; Qian and Johnson, 2002; but see Kampa et al., 2004; Vargas-Caballero and Robinson, 2004). However, trapping block by Mg^{2+} likely cannot be explicitly demonstrated because the rate of Mg^{2+} unblock from open channels is much faster than the rate of NMDAR channel opening (Mayer and Westbrook 1987; Stout et al., 1996; Antonov and Johnson 1999; Qian et al., 2002). If Mg^{2+} does not trap, it may be due to unblock to the intracellular side of the membrane. Estimates of Mg^{2+} unbinding rates from open channels to the intracellular side of the membrane in neurons near resting potential suggest that Mg^{2+} should unblock to the inside in an average of 4 ms (Antonov and Johnson 1999; Qian

et al., 2002). Even if estimates of unbinding were 1000-fold slower, Mg^{2+} should unbind to the intracellular side within 20 s of channel closure. It is unclear if conformational changes at the level of the Mg^{2+} binding site, which could alter unbinding rates to the inside, occur when the channel closes. The ability of Mg^{2+} to occlude closed channel inhibition suggests that Mg^{2+} remains trapped in the channel and that the conformation of the pore constricts with channel closure.

6.3   LIMITATIONS OF KINETIC MODELING

Careful determination of kinetic model rates can substantially improve the interpretation of complicated electrophysiological data and can aid development and testing of novel hypotheses. The utility of kinetic models is limited by the number of adjustable parameters that are not constrained by data. When considering models of trapping open channel blockers, and with Mg^{2+}, the number of adjustable rates increases dramatically. For instance, when starting from a model of a trapping blocker, addition of another model arm to describe trapping block by Mg^{2+} increases the number of adjustable rates and channel states by 50%. Instead, if memantine binding at the second site does not depend on memantine binding at the deep site, then the number of rates and channel states doubles, with four total arms: an unblocked arm, a deep site blocked arm, a deep site blocked and second site blocked arm, and second site blocked arm, all without Mg^{2+}. It is unclear if kinetic models of memantine inhibition with the second site and/or in the presence of Mg^{2+} will be useful in data interpretation or hypothesis generation.

Simultaneous fits of our models to peak and steady-state NMDAR responses over long time scales present another limitation of our kinetic modeling. The modeling described in

Chapter 3 required fitting to data sets spanning ~335 s (~290 s for inhibition during synaptic-like glutamate applications and ~45 s for inhibition during long glutamate applications). In principle, a recording duration of 335 s should not present a limitation. However, because we were interested in modeling non-equilibrium peak currents that occur in ~10 ms, our data set also required a high sampling frequency of 1 kHz, with ~335,000 total data points. For GluN1/2A receptors, full activation and deactivation was complete within ~100 ms following a synaptic-like glutamate application. For 50 responses to synaptic-like glutamate applications, we were only truly interested in ~5000 data points, or < 2% of data points during synaptic-like glutamate applications. We tried several weighting methods to improve fits to responses to synaptic-like glutamate applications, but remarkably none were superior to unweighted data sets. Although the resulting fits were satisfactory, they required enormous effort and precision to achieve reliable simulations that matched the data set. Larger data sets required for modeling synaptic-like vs. long inhibition by ketamine (> 500 s) or for modeling recovery from desensitization (> 700 s) were not easily amenable to fitting due again to the few salient data points spread over thousands of steady-state or baseline data points. Therefore, due to the nature of modeling non-equilibrium and steady-state responses over long time scales, our kinetic modeling was limited.

6.4   THERAPEUTIC IMPACT OF MEMANTINE AND KETAMINE STABILIZATION OF DESENSITIZED STATES

Our results support the idea that memantine and ketamine can, under certain circumstances, preferentially inhibit distinct subpopulations of NMDARs. However, the subpopulations of NMDARS are not as well defined as previously hypothesized. Subpopulations are defined either

by NMDAR subtype or by subcellular localization (Hardingham and Bading, 2010; Parsons and Raymond, 2014; **Section 1.4.3**). For example, it is clear that memantine inhibition of GluN1/2A receptors depends in part on Ca^{2+}-dependent desensitization, which requires an increase in intracellular Ca^{2+} concentration near the NMDAR CTD. With low stimulation frequency, synaptic NMDARs are unlikely to accumulate in Ca^{2+}-dependent desensitized states, whereas with high frequency stimulation, Ca^{2+}-dependent desensitization can become evident (Tong et al., 1995; Raman et al., 1996). Consistent with these observations and with the dependence of memantine inhibition on Ca^{2+}-dependent desensitization, a recent report showed that memantine inhibition increased with increasing stimulation intensity (frequency and number of stimulations) (Wild et al., 2013). It is likely that extrasynaptic NMDARs can be relatively spared from Ca^{2+}-dependent desensitization if the glutamate concentration activating the receptors is quite low. In contrast, sustained glutamate at high concentrations will likely drive Ca^{2+}-dependent desensitization of NMDARs, as is seen with exogenous application of high glutamate concentrations (Legendre et al., 1993; Medina et al., 1996). Therefore, the precise circumstances by which NMDARs are activated, regardless of their location, may determine whether they are inhibited more or less by memantine, or by ketamine.

Emnett et al., (2013) using hippocampal microisland cultures where recordings were made from single cells that form autapses, compared inhibition of neuronal NMDARs by memantine and ketamine. In clear disagreement with our findings, Emnett et al., (2013) found that inhibition did not vary under the tested conditions, including inhibition of synaptic or inhibition of extrasynaptic NMDARs. However, their cells likely contained GluN2A and GluN2B subunits comprising GluN1/2A, GluN1/2B, and GluN1/2A/2B receptors. As pointed out in Chapter 3, they found a quickening of NMDAR EPSC in the presence of memantine and

ketamine. This suggests preferential inhibition of GluN1/2B receptors, which is consistent with our observation that both memantine and ketamine inhibited GluN1/2B more than GluN1/2A receptor responses to synaptic-like glutamate applications. Although not direct evidence of subtype-dependent inhibition, the findings from Emnett et al. (2013) are suggestive that memantine and ketamine can preferentially inhibit different NMDAR subtypes during synaptic activation of neuronal NMDARs.

Our findings are in general agreement with studies that support memantine preferential inhibition of extrasynaptic receptors (Leveille et al., 2008; Okamoto et al., 2009; Xia et al., 2010) and with studies that support memantine preferential inhibition synaptic NMDARs (Wroge et al., 2012; Emnett et al., 2013) that are in clear conflict with one another. Consistent with our results, memantine exhibits more potent inhibition of extrasynaptic NMDARs activated by long applications of high agonist concentrations than of synaptic NMDARs activated by low frequency stimulation (Xia et al., 2010; Wild et al., 2013; Wu and Johnson 2015). Also consistent with our results, memantine inhibition of synaptic NMDARs is more effective when the synaptic stimulation intensity is high (Wild et al., 2013) and during oxygen-glucose deprivation, which was shown to cause strong activation of synaptic NMDARs (Wroge et al., 2012). In acute hippocampal slices, Papouin et al., (2012) show that synaptic, but not extrasynaptic NMDARs, activated by a high concentration of NMDA are necessary and sufficient for cell death. Although the authors did not investigate the effects of memantine on cell death, other studies with a similar method of NMDA-induced cell death have shown memantine to be neuroprotective (Leveille et al., 2008; Okamoto et al., 2009; Kaufman et al., 2012; Milnerwood et al., 2012). These results suggest that memantine effectively inhibits strongly activated synaptic NMDARs. It is difficult to compare our findings to other studies where

169

synaptic NMDAR activation leads to cell survival and neuroprotection (Hardingham et al., 2002; Leveille et al., 2008; Papadia et al., 2008; Leveille et al., 2010; Kaufman et al., 2012; Milnerwood et al., 2012). These studies activated synaptic NMDARs pharmacologically by addition of 4-aminopyridine and/or bicuculline (4-AP and/or bic) to the extracellular solution (**Section 1.3.1**). Because addition of 4-AP and/or bic increases the overall synaptic release probability, it is unclear how frequently individual synapses, and thus synaptic NMDARs, are activated. It is therefore difficult to assess how often synaptic NMDARs activated by this method enter into Ca^{2+}-dependent desensitized states, whereas extrasynaptic NMDARs activated by application of a high concentration of NMDA are likely to enter Ca^{2+}-dependent desensitized states. Nevertheless, studies using 4-AP and/or bic posit that extrasynaptic, but not synaptic NMDARs, are necessary and sufficient for cell death and that memantine inhibits extrasynaptic more potently than synaptic NMDARs and is neuroprotective (Leveille et al., 2008; Okamoto et al., 2009; Kaufman et al., 2012; Milnerwood et al., 2012). In contrast, studies using other means of inducing cell death come to the opposite conclusions: that synaptic, but not extrasynaptic, NMDAR activation is necessary and sufficient for cell death (Papouin et al., 2012; Wroge et al., 2012), and that memantine is neuroprotective (Wroge et al., 2012). Our results suggest that the conflicting results of these studies are due to differences in the intensity of NMDAR activation, and thus differences in accumulation of NMDARs in Ca^{2+}-dependent desensitized states. Therefore, our results support a unifying hypothesis: memantine inhibition increases with increasing strength of NMDAR activation, irrespective of the subcellular localization. These studies suggest that NMDAR-mediated cell death requires the accumulation of intracellular Ca^{2+} irrespective of the subcellular localization (Zhou et al., 2013).

170

Our findings highlight the possibility that new drugs designed to modulate NMDAR desensitization may exhibit improved neuroprotective properties. Every NMDAR open channel blocker adequately characterized, with the exception of Mg^{2+}, alters rates of receptor state transitions (Johnson and Qian 2002). Other drugs have also been shown to modulate desensitization, including the endogenous NMDAR modulator pregnanolone sulfate, which increases occupancy of desensitized states (Kussius et al., 2009). The membrane cholesterol also strongly modulates NMDAR desensitization (Korinek et al., 2015). Therefore, modulation of desensitization is likely possible through several distinct routes. The comparison of inhibition in high vs. low concentrations of Ca^{2+} should serve as an effective means to screen new compounds in their ability to increase occupancy of Ca^{2+}-dependent desensitized states of NMDARs. It will be important to determine how the extent of modulating NMDAR desensitization correlates with neuroprotection offered by new compounds.

6.5 FUTURE DIRECTIONS

The research described in this dissertation has increased our understanding of mechanisms of NMDAR inhibition by memantine and ketamine. There are still many basic questions about NMDAR inhibition by memantine and ketamine that have not been explored. The sections above alluded to some important gaps in knowledge that are addressed specifically here.

It will be important to determine whether memantine binds to two sites of NMDARs and of memantine and ketamine effects on desensitization are subtype dependent. Two memantine binding sites have been studied in neurons or with GluN1/2A and GluN1/2B receptors in transfected cells (Blanpied et al., 1997; Sobolevsky and Koshelev 1998; Sobolevsky et al., 1998;

Chen and Lipton 2005; Kotermanski et al., 2009). Therefore, there is a need to explore whether memantine binds to two sites on GluN1/2C and GluN1/2D receptors. Effects on these subtypes could have important structural and therapeutic implications for memantine inhibition. Further, whether 1 mM Mg^{2+} speeds memantine unbinding kinetics in GluN1/2C and GluN1/2D receptors, which are less sensitive to Mg^{2+} block, could have important implications for the interaction of Mg^{2+} with memantine in the pore. Investigating effects of memantine and ketamine on desensitization of GluN1/2C and GluN1/2D receptors is also necessary. Results of these experiments could impact our understanding of how memantine and ketamine act in brain regions and cell-types with high expression of GluN2C and GluN2D. Since memantine and ketamine are selective for GluN1/2C and GluN1/2D receptors in 1 mM Mg^{2+}, these findings could have important therapeutic implications. This leaves the problem of triheteromeric NMDARs. New methods allow investigation of triheteromeric GluN1/2A/2B receptors in transfected cells (Hansen et al., 2014; Stroebel et al., 2014). However, these methods rely on modifications to the GluN2 subunit CTDs. The Ca^{2+}-dependent effects of memantine may require specific interactions between the GluN2A CTD and other intracellular proteins, which could be disrupted in CTD-modified GluN2A subunits needed for isolation of triheteromeric receptors. Indeed, it is not known whether GluN1/2A/2B receptors exhibit Ca^{2+}-dependent desensitization. The effects of memantine and ketamine on desensitization of GluN1/2A/2B receptors are still worth investigating, albeit with proper controls.

Further investigations of memantine increasing occupancy of Ca^{2+}-dependent desensitized states of NMDARs could help identify structural determinants of NMDAR desensitization. As described in Chapter 1, Ca^{2+}-dependent desensitization involves a complex process of several CTD protein-protein interactions (**Section 1.1.2**). How memantine is involved

172

with effects of these CTD elements, individually or in concert, could have significant impact on our understanding of the structural determinants underlying Ca^{2+}-dependent desensitized states of NMDARs. These insights could also impact drug design, by identifying specific intracellular targets through which memantine binding might partially depend. Further investigation of the NMDAR subtype dependence of memantine's effects on desensitization could also deepen our understanding of structural-functional differences between GluN1/2A, GluN1/2B, GluN1/2C, and GluN1/2D receptors. Overall, investigating the mechanisms by which memantine increases occupancy of Ca^{2+}-dependent desensitized states of NMDARs could deepen our understanding of open channel block and of NMDAR structure in general.

APPENDIX A

MOLECULAR BASES OF NMDA RECEPTOR SUBTYPE-DEPENDENT PROPERTIES

Glasgow NG, Siegler Retchless B, and Johnson JW (2015) Molecular bases of NMDA receptor subtype-dependent properties. J Physiol 593: 83-95.

JPn

Neuroscience

The Journal of Physiology

TOPICAL REVIEW

Molecular bases of NMDA receptor subtype-dependent properties

Nathan G. Glasgow, Beth Siegler Retchless and Jon W. Johnson

Department of Neuroscience and Center for Neuroscience, University of Pittsburgh, Pittsburgh, PA 15260, USA

Abstract NMDA receptors (NMDARs) are a class of ionotropic glutamate receptors (iGluRs) that are essential for neuronal development, synaptic plasticity, learning and cell survival. Several features distinguish NMDARs from other iGluRs and underlie the crucial roles NMDARs play in nervous system physiology. NMDARs display slow deactivation kinetics, are highly Ca^{2+} permeable, and require depolarization to relieve channel block by external Mg^{2+} ions, thereby making them effective coincidence detectors. These properties and others differ among NMDAR subtypes, which are defined by the subunits that compose the receptor. NMDARs, which are heterotetrameric, commonly are composed of two GluN1 subunits and two GluN2 subunits, of which there are four types, GluN2A–D. 'Diheteromeric' NMDARs contain two identical GluN2 subunits. Gating and ligand-binding properties (e.g. deactivation kinetics) and channel properties (e.g. channel block by Mg^{2+}) depend strongly on the GluN2 subunit contained in diheteromeric NMDARs. Recent work shows that two distinct regions of GluN2 subunits control most diheteromeric NMDAR subtype-dependent properties: the N-terminal domain is responsible for most subtype dependence of gating and ligand-binding properties; a single residue difference between GluN2 subunits at a site termed the GluN2 S/L site is responsible for most subtype dependence of channel properties. Thus, two structurally and functionally distinct regions underlie the majority of subtype dependence of NMDAR properties. This topical review highlights recent studies of recombinant diheteromeric NMDARs that uncovered the involvement of the N-terminal domain and of the GluN2 S/L site in the subtype dependence of NMDAR properties.

Abbreviations   ABD, agonist-binding domain; AMPAR, AMPA receptor; CTD, C-terminal domain; iGluR, ionotropic glutamate receptor; MTS, methanethiosulfonate; NMDAR, NMDA receptor; NTD, N-terminal domain; NTD+L, NTD and NTD-ABD linker; PDB, Protein Data Bank; P_{open}, open probability; TMD, transmembrane domain; TMR, transmembrane region.

Introduction

Glutamate mediates the majority of fast excitatory synaptic transmission in the central nervous system. Glutamate binds to and activates ionotropic glutamate receptors (iGluRs), which open to allow cation flux across the cell membrane. iGluRs are ligand-gated ion channels composed of four subunits organized around a central ion channel. The tertiary structure of all iGluR subunits can be described as several functionally distinct domains: an extracellular N-terminal domain (NTD; or amino-terminal domain, ATD), an extracellular agonist-binding domain (ABD; or ligand-binding domain, LBD), a transmembrane domain

Nathan Glasgow is a PhD candidate in the Center for Neuroscience at the University of Pittsburgh. He received a BS in Biology from the University of Toledo in 2010. He is currently a graduate student working in Jon Johnson's lab studying the structure and pharmacology of NMDARs. **Jon Johnson** is a Professor of Neuroscience at the University of Pittsburgh. He was an undergraduate at MIT, graduate student at Stanford, and postdoc with Philippe Ascher at the Ecole Normale Supérieure. He and his colleagues employ electrophysiological, molecular, optical, pharmacological and computational approaches to study the physiology, structure and regulation of glutamate receptors.

(TMD) made up of three transmembrane regions (TMRs; M1, M3 and M4) and a re-entrant pore-lining loop termed the p-loop (or M2 region) that forms the selectivity filter, and an intracellular C-terminal domain (CTD) (Fig. 1*A*) (Traynelis *et al.* 2010).

There are four classes of iGluRs: AMPA receptors (AMPARs), kainate receptors, NMDA receptors (NMDARs) and δ receptors. Receptors of each class are formed by co-assembly of homologous subunits. Subunit composition defines receptor subtypes within
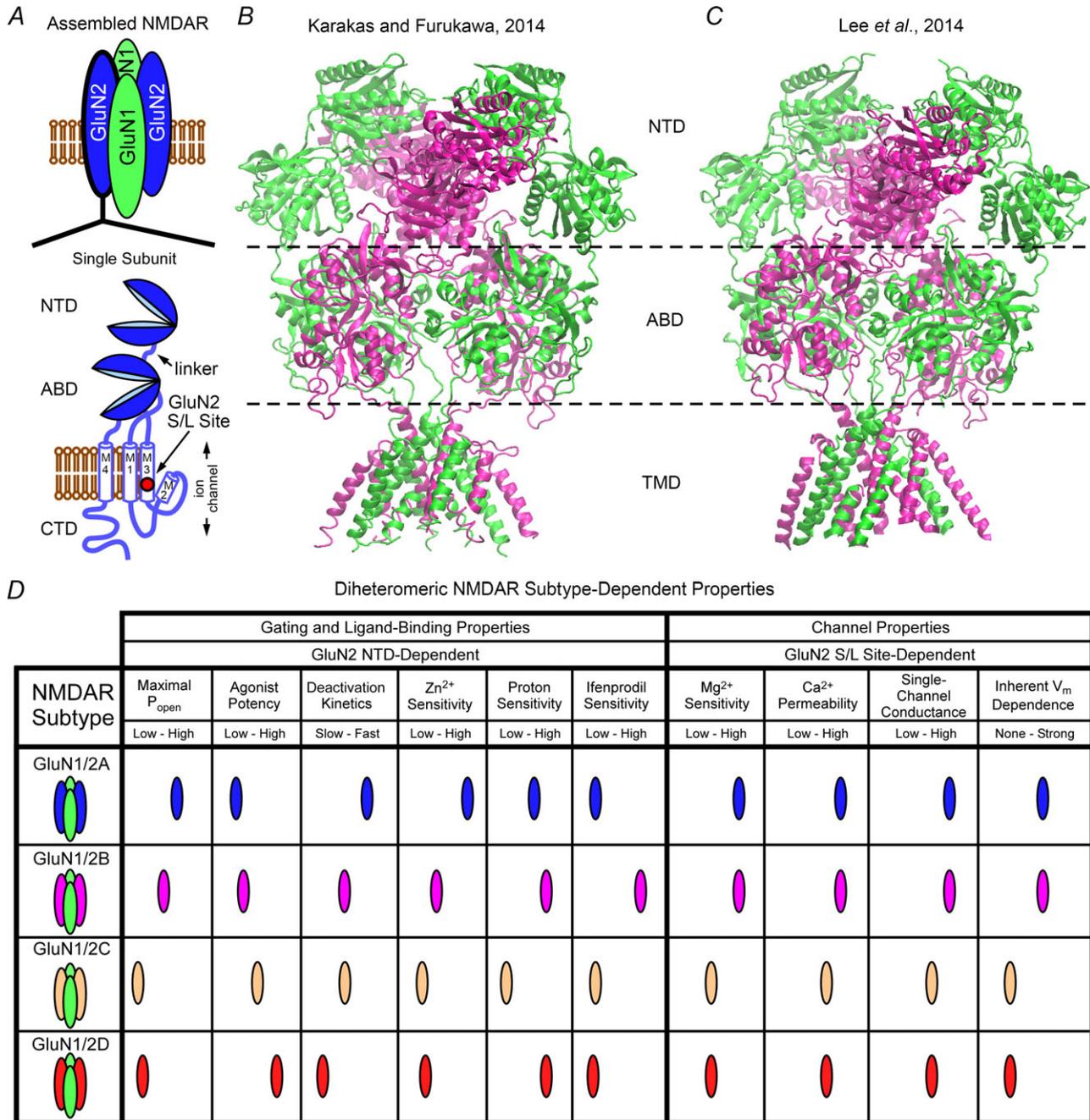
Figure 1. NMDAR schematic diagram, crystal structures and subtype-dependent properties
A, schematic diagram of an assembled diheteromeric NMDAR (upper) with an enlarged schematic diagram of a single NMDAR subunit depicting the distinct functional domains (lower). The location of the GluN2 S/L site is indicated with a red filled circle in the M3 TMR. *B* and *C*, crystal structures of GluN1/2B NMDARs. Images in *B* (Protein Data Bank (PDB) ID: 4PE5 (Karakas & Furukawa 2014)) and in *C* (PDB ID: 4TLL (Lee *et al.* 2014)) were created using the molecular visualization program VMD (Humphrey *et al.* 1996). GluN1 subunits are shown in green and GluN2B subunits are shown in magenta. *D*, comparison of relative values of NMDAR subtype-dependent properties.

each class of iGluR. Physiological properties, such as agonist potency, maximal channel open probability (P_{open}), and deactivation kinetics, can differ greatly between subtypes of each iGluR class except δ receptors, which seem not form functional receptors (Traynelis *et al.* 2010). Thus, control of the expression of specific iGluR subtypes can have enormous impact on synaptic function, membrane excitability, and activation of intracellular signalling cascades, each of which more broadly affects the physiology of neuronal circuits and systems. The tight developmental, regional and subcellular regulation of iGluR subunit expression indicates that iGluR subtypes play distinct physiological roles (Cull-Candy & Leszkiewicz, 2004).

NMDARs exhibit several properties that are unique among iGluRs, including: the requirement that both glutamate and a co-agonist, either glycine or D-serine, bind to activate the receptor (Johnson & Ascher, 1987; Kleckner & Dingledine, 1988; Lerma *et al.* 1990; Schell *et al.* 1995); very slow deactivation (Forsythe & Westbrook, 1988; Lester *et al.* 1990; Partin *et al.* 1996; Swanson & Heinemann, 1998; Vicini *et al.* 1998); high permeability to Ca^{2+} (MacDermott *et al.* 1986; Burnashev *et al.* 1992, 1995; Schneggenburger, 1996); and strongly voltage-dependent channel block by physiological concentrations of external Mg^{2+} (Mayer *et al.* 1984; Nowak *et al.* 1984; Ascher & Nowak, 1988). Flux of Ca^{2+} through NMDARs is essential for many types of synaptic plasticity, learning and memory, and cell survival (Malenka & Bear, 2004; Hardingham & Bading, 2010). Conversely, aberrant NMDAR activation is implicated in neurodegenerative diseases, schizophrenia, depression, chronic and neuropathic pain, as well as neuronal loss following ischaemia or stroke (Lau & Tymianski, 2010; Zhou & Sheng, 2013).

Diversity of NMDAR subtypes

NMDAR subunits are encoded by seven genes. One gene encodes eight GluN1 subunit splice variants, four genes encode GluN2 subunits (GluN2A, GluN2B, GluN2C and GluN2D), and two genes encode GluN3 subunits (GluN3A and GluN3B). Functional NMDARs are obligate heterotetramers thought to be assembled as a combination of two GluN1 subunits and two GluN2 and/or GluN3 subunits. Most diheteromeric NMDARs contain two GluN1 subunits and two GluN2 subunits of the same type. Triheteromeric NMDARs contain two GluN1 subunits and two GluN2 or GluN3 subunits of different identities.

The NMDAR subtype is defined by the subunits present in the receptor, which impart unique properties to each receptor subtype. This review focuses on the well-characterized diversity of the four diheteromeric NMDAR subtypes defined by the identity of the GluN2 subunits (GluN1/2A, GluN1/2B, GluN1/2C and

GluN1/2D receptors; Fig. 1*D*). Many, and possibly most, native NMDARs are triheteromeric NMDAR subtypes (Luo *et al.* 1997; Al-Hallaq *et al.* 2007; Rauner & Kohr, 2010; Gray *et al.* 2011; Tovar *et al.* 2013). However, until recently, few studies have addressed triheteromeric NMDAR properties (Hatton & Paoletti, 2005; Rauner & Kohr, 2010; Tovar *et al.* 2013) due to the difficulty of studying them in isolation from other NMDAR subtypes. Very recently, exciting new approaches have been developed to study isolated triheteromeric NMDARs (Hansen *et al.* 2014; Yuan *et al.* 2014), a topic outside the scope of this review.

Heterologous expression systems, where a single NMDAR subtype can be unambiguously studied by expression of GluN1 and a single type of GluN2 subunits, have allowed extensive characterization of diheteromeric NMDAR subtype-dependent properties (Cull-Candy & Leszkiewicz, 2004; Traynelis *et al.* 2010; Paoletti *et al.* 2013). Studies in heterologous systems have revealed great diversity of diheteromeric NMDAR subtype-dependent properties including: deactivation kinetics (Monyer *et al.* 1992, 1994; Vicini *et al.* 1998), agonist potency (Kutsuwada *et al.* 1992; Priestley *et al.* 1995; Varney *et al.* 1996; Erreger *et al.* 2007; Traynelis *et al.* 2010), Ca^{2+} permeability (Burnashev *et al.* 1995; Schneggenburger, 1996), voltage dependence of channel gating (Clarke, 2006; Clarke & Johnson, 2008; Clarke *et al.* 2013), sensitivity to block by external Mg^{2+} (Monyer *et al.* 1994; Kuner & Schoepfer, 1996), and sensitivity to endogenous inhibitors (Traynelis *et al.* 1995; Williams, 1996; Chen *et al.* 1997; Paoletti *et al.* 1997, 2013; Traynelis *et al.* 1998). Expression and subcellular localization of NMDAR subunits varies by developmental stage, brain region and cell type (Akazawa *et al.* 1994; Monyer *et al.* 1994; Sheng *et al.* 1994). Thus, the expression of specific NMDAR subtypes can be used to tune synapses, neurons, circuits and systems through the great diversity of NMDAR subtype-dependent properties.

Despite in-depth characterization of NMDAR subtype-dependent properties (for comprehensive reviews see Cull-Candy & Leszkiewicz, 2004; Traynelis *et al.* 2010; Paoletti *et al.* 2013), for many of these properties little was known about the mechanisms that underlie their subtype dependence until recently. Here we highlight recent major advances in our understanding of the molecular bases of functional diversity among NMDAR subtype-dependent properties.

Two categories of NMDAR subtype-dependent properties

Prior to the work described in this review, there was no clear justification for dividing the long list of NMDAR properties that depend on receptor subtype into two categories. However, recent work provides strong evidence

that nearly all diheteromeric NMDAR subtype-dependent properties can be structurally and functionally divided into two categories: (1) gating and ligand-binding properties and (2) channel properties (Fig. 1*D*).

Two congruent studies in 2009 revealed that the GluN2 NTD controls the NMDAR subtype dependence of gating and ligand-binding properties (Gielen *et al.* 2009; Yuan *et al.* 2009). These two studies identified the following NTD-dependent properties: maximal P_{open}, agonist potency, deactivation kinetics, and sensitivity to the endogenous inhibitors Zn^{2+} and protons. Other studies identified inhibition by ifenprodil (Fig. 1*D*) (Perin-Dureau *et al.* 2002; Malherbe *et al.* 2003; Ng *et al.* 2008; Karakas *et al.* 2009) and voltage- and glycine-independent potentiation by polyamines (Gallagher *et al.* 1997; Masuko *et al.* 1999; Han *et al.* 2008; Mony *et al.* 2011) as additional NTD-dependent ligand-binding properties that differ among NMDAR sub-types. In contrast, the residue at a single site near the intracellular end of the M3 region of GluN2 subunits, a serine (S) in GluN2A (S632; residue numbering used here begins at the start methionine) or GluN2B (S633) and a leucine (L) in GluN2C (L643) or GluN2D (L657) (the GluN2 S/L site; Fig. 1*A*), controls diheteromeric NMDAR subtype-dependent channel properties (Siegler Retchless *et al.* 2012; Clarke *et al.* 2013). The GluN2 S/L site was shown to control the subtype dependence of the following properties: Mg^{2+} sensitivity, Ca^{2+} permeability, single-channel conductance, and inherent voltage dependence of channel gating (Fig. 1*D*). Unlike gating and ligand-binding properties, channel properties of GluN1/2A and GluN1/2B receptors are very similar, channel properties of GluN1/2C and GluN1/2D receptors are very similar, but channel properties of GluN1/2A and GluN1/2B receptors differ strongly from those of GluN1/2C and GluN1/2D receptors (Fig. 1*D*). The residue at the GluN2 S/L site determines whether the channel properties of an NMDAR resemble properties of GluN1/2A and GluN1/2B receptors (GluN1/2A-like) or resemble properties of GluN1/2C and GluN1/2D receptors (GluN1/2D-like) (Siegler Retchless *et al.* 2012; Clarke *et al.* 2013).

The GluN2 NTD controls gating and ligand-binding properties

Diheteromeric NMDARs display wide functional variation in gating and ligand-binding properties. For instance, GluN1/2A receptors have a maximal P_{open} of ~0.5, GluN1/2B receptors have a maximal P_{open} of ~0.1, and GluN1/2C and GluN1/2D receptors have a maximal P_{open} of ~0.01 (Wyllie *et al.* 1998; Chen *et al.* 1999; Erreger *et al.* 2005; Dravid *et al.* 2008). Gielen *et al.* (2009) and Yuan *et al.* (2009) demonstrated that the NMDAR sub-type dependence of maximal P_{open} and other gating and

ligand-binding properties is largely due to variation at the GluN2 NTD and the linker region that connects the GluN2 NTD to the ABD (NTD-ABD linker). Both studies took advantage of mutant receptors containing GluN2 subunits with either the NTD deleted (ΔNTD) or the NTD and NTD-ABD linker deleted (ΔNTD+L), as well as chimeric receptors containing GluN2 subunits in which the GluN2 NTD, or the NTD and NTD-ABD linker (NTD+L), was replaced with the NTD or NTD+L of another GluN2 sub-unit (Fig. 2*A*).

Gielen *et al.* (2009) showed that the dependence of maximal P_{open} on NMDAR subtype was abolished in GluN2(ΔNTD) subunit-containing receptors. Examination of GluN1/2B(2A-NTD) and GluN1/2A(2B-NTD) receptors revealed that exchanging NTDs does not result in an exchange of maximal P_{open} (Gielen *et al.* 2009). However, examination of GluN1/2B(2A-NTD+L) and GluN1/2A(2B-NTD+L) receptors revealed that exchanging the NTD+L does result in an exchange of maximal P_{open} (Fig. 2*B*).

Yuan *et al.* (2009) examined the influence of the GluN2 NTD+L on steady-state P_{open} in saturating agonist concentrations using mutant GluN2 subunits in which the NTD+L were removed, as opposed to just the NTD. A distinction of this study from Gielen *et al.* (2009) is the investigation of differences between GluN1/2A and GluN1/2D receptors, which exhibit much greater differences in gating and ligand-binding properties than GluN1/2A and GluN1/2B receptors. GluN1/2A(2D-NTD+L) receptors displayed P_{open} values in saturating agonist concentrations far lower than wild-type GluN1/2A receptors and similar to wild-type GluN1/2D receptors, whereas GluN1/2D(2A-NTD+L) receptors displayed P_{open} values nearly 5-fold greater than wild-type GluN1/2D receptors, although still far below wild-type GluN1/2A receptor values (Yuan *et al.* 2009). Interestingly, there were intermediate effects on P_{open} when only the NTD-ABD linker was interchanged between GluN2A and GluN2D subunits. These studies argue strongly for a fundamental role of the NTD and the NTD-ABD linker in determining maximal P_{open}. Importantly, Yuan *et al.* (2009) demonstrated that the presence or identity of the NTD+L did not affect single-channel conductance.

The identity of the GluN2 NTD+L also affects agonist potency and deactivation kinetics (Yuan *et al.* 2009). The glutamate potency of all receptors that contained a GluN2(ΔNTD+L) subunit were indistinguishable from wild-type receptors (Fig. 2*C*). The glycine potency of GluN1/2A and GluN1/2A(ΔNTD+L) did not differ, whereas the glycine potency of GluN1/2B(ΔNTD+L), GluN1/2C(ΔNTD+L), and GluN1/2D(ΔNTD+L) receptors was lower than for corresponding wild-type receptors. The time constant of deactivation following rapid removal of glutamate (τ)

also differed between wild-type receptors and receptors containing GluN2(ΔNTD+L) subunits. Importantly, for glutamate EC_{50}, glycine EC_{50} and τ values, chimeric GluN1/2A(2D-NTD+L) receptors resembled GluN1/2D more closely than GluN1/2A receptors, and chimeric GluN1/2D(2A-NTD+L) receptors resembled GluN1/2A more closely than GluN1/2D receptors (Fig. 2*C* and *D*) (Yuan *et al.* 2009).

Gielen *et al.* (2009) also investigated NMDAR subtype dependence of sensitivity to the endogenous allosteric inhibitors Zn^{2+} and protons. Zn^{2+} inhibits GluN1/2A receptors with high affinity (in the nanomolar range) and inhibits GluN1/2B receptors in the micromolar range (Fig. 1*D*) (Williams, 1996; Chen *et al.* 1997; Paoletti

et al. 1997; Traynelis *et al.* 1998; Rachline *et al.* 2005). A Zn^{2+} binding site is in the bilobed cleft of both the GluN2A and GluN2B NTDs, where binding of Zn^{2+} stabilizes a closed cleft conformation of the NTD (Choi & Lipton, 1999; Fayyazuddin *et al.* 2000; Low *et al.* 2000; Paoletti *et al.* 2000; Choi *et al.* 2001; Rachline *et al.* 2005; Karakas *et al.* 2009; Stroebel *et al.* 2011). Crystallography of Zn^{2+} bound to the GluN2B NTD showed that Zn^{2+} directly contacts a histidine and a glutamate residue in the GluN2B NTD (Karakas *et al.* 2009). The two homologous residues in the GluN2A NTD (a histidine and an asparagine residue) are thought to coordinate Zn^{2+}, along with at least one additional histidine residue, and possibly a lysine and a glutamate residue (Choi & Lipton,
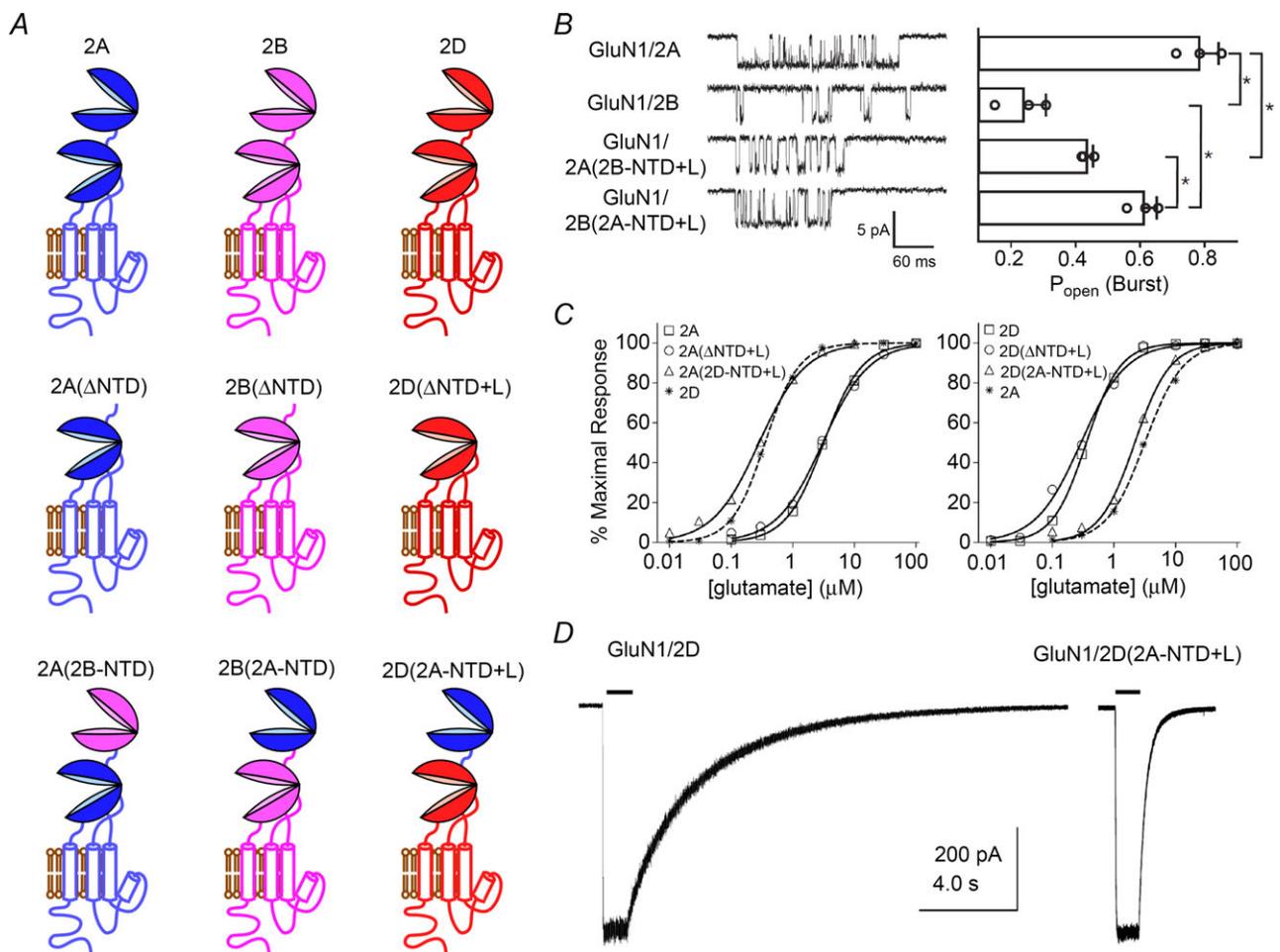
Figure 2. The GluN2 NTD and adjacent linker region control gating and ligand-binding properties
A, schematic diagrams of wild-type GluN2 subunits (upper), examples of GluN2 subunits with deletions (middle), and examples of chimeric GluN2 subunits with domains interchanged between GluN2 subunits (lower). Colours of domains correspond to the GluN2 subunits (upper). *B*, single-channel records of wild-type or chimeric GluN2 subunit-containing receptors (left) and the P_{open} during bursts of channel openings, which was used as an estimate of maximal P_{open} (right). Panel was modified from Gielen *et al.* (2009). *C*, glutamate concentration–response relations of wild-type, GluN2(ΔNTD+L), and chimeric GluN2(NTD+L) subunit-containing receptors. Panel was modified from Yuan *et al.* (2009), with permission. *D*, whole-cell recording of wild-type and chimeric GluN1/2D(2A-NTD+L) receptors showing the time course of deactivation following 1 s applications of 1 mM glutamate (black bars). Panel was modified from Yuan *et al.* (2009), with permission.

1999; Fayyazuddin *et al.* 2000; Low *et al.* 2000). The additional GluN2A NTD residues interacting with Zn^{2+} are thought to be responsible for the higher affinity of GluN1/2A receptors for Zn^{2+}. In contrast to the Zn^{2+} binding site, the location of the proton sensor is not known. Several mutations in the NTD, ABD and pore regions have been shown to affect proton sensitivity (Low *et al.* 2003; Gielen *et al.* 2008); however, interpretation of mutant studies is complicated because high affinity Zn^{2+} inhibition enhances proton sensitivity (Low *et al.* 2000; Erreger & Traynelis, 2008). Nevertheless, protons are thought to mediate their inhibitory effect through associations with regions near the channel gate (Low *et al.* 2003; Traynelis *et al.* 2010).

Chimeric GluN1/2D(2A-NTD+L) and GluN1/2B(2A-NTD+L) receptors exhibited Zn^{2+} sensitivity nearly identical to wild-type GluN1/2A receptors (Gielen *et al.* 2009). Surprisingly, GluN1/2B(2A-NTD) receptors were significantly more sensitive to Zn^{2+} than GluN1/2A receptors, suggesting that the GluN2B NTD-ABD linker facilitates NTD cleft closure. Sensitivity to protons was unexpectedly affected by the identity of the GluN2 NTD. GluN1/2A(ΔNTD) and GluN1/2B(ΔNTD) receptors did not display NMDAR subtype dependence of proton sensitivity as displayed in wild-type GluN1/2A and GluN1/2B receptors. Furthermore, examination of GluN1/2A(2B-NTD+L) and GluN1/2B(2A-NTD+L) receptors revealed that exchanging the NTD+L results in exchanged proton sensitivity. These data support the role of the GluN2 NTD and NTD-ABD linker in mediating the effect of Zn^{2+} on channel gating (Erreger & Traynelis, 2008) and the accessibility of protons to the proton sensor (Gielen *et al.* 2009).

The GluN2 NTD also confers sensitivity to the synthetic allosteric modulator ifenprodil and its derivatives, such as Ro 25-6981, which display >100-fold selectivity for GluN1/2B receptors over other diheteromeric NMDAR subtypes (Williams, 1993; Traynelis *et al.* 2010). Like high affinity Zn^{2+} binding to the GluN2A NTD, ifenprodil sensitivity is conferred by the GluN2B NTD (Perin-Dureau *et al.* 2002; Malherbe *et al.* 2003; Ng *et al.* 2008; Karakas *et al.* 2011). However, unlike Zn^{2+}, which binds in the cleft of the NTD (Karakas *et al.* 2009), a recent crystal structure showed that ifenprodil binds to the interface between the GluN1 and GluN2B NTDs (Karakas *et al.* 2011). Interestingly, only a single residue (an isoleucine (I) in GluN2B and a methionine (M) in GluN2A) differs between the GluN2B NTD (I111) and the GluN2A NTD (M112) in the ifenprodil binding pocket. Receptors containing mutated GluN2B(I111M) or GluN2A(M112I) subunits do not exhibit abolished or augmented ifenprodil sensitivity compared to the mutant receptors, respectively (Karakas *et al.* 2011). Therefore, the mechanism of ifenprodil selectivity of GluN1/2B receptors over GluN1/2A receptors is still not fully understood.

To investigate the mechanism by which ligands that bind to the NTD influence NMDAR gating and ligand-binding properties, Gielen *et al.* (2009) introduced cysteine residues deep into the NTD cleft, creating GluN2A(Y281C) and GluN2B(Y282C) subunits. Cysteine modification by methanethiosulfonate (MTS) reagents of varying size was then used to lock open the NTD cleft. Potentiation of GluN1/2B(Y282C) receptor currents by MTS reagent modification increased with increasing MTS reagent size. A similar, but lesser increase in potentiation of GluN1/2A(Y281C) receptor currents by MTS reagent modification was seen with increasing MTS reagent size. Based on these data, Gielen *et al.* (2009) proposed a model in which oscillation of GluN2 NTDs between open and closed conformations in the absence of NTD ligands determines the maximal P_{open} of a receptor. GluN1/2A receptors were hypothesized to exhibit a higher maximal P_{open} than GluN1/2B receptors because of higher occupancy by the GluN2A NTD of the open cleft conformation. An alternative possibility is that the GluN2A NTD might adopt a more open conformation than the GluN2B NTD when no ligand is bound, and MTS reagent modification may lead to greater than normal NTD opening. In contrast to the NTD, when the bilobed ABD cleft of GluN2A subunits (Furukawa *et al.* 2005) is locked closed using disulfide bridges, maximal P_{open} of GluN1/2A receptors increases (Kussius & Popescu, 2010).

The gating and ligand-binding properties of receptors containing chimeric GluN2(NTD+L) subunits created by Gielen *et al.* (2009) and Yuan *et al.* (2009) were not fully converted to the properties of subtypes containing the GluN2 subunits that contributed the NTD+L. In addition, results with truncated receptors were unpredictable; truncation had no significant effect on some receptor properties, while strongly modifying other receptor properties. These and other data indicate that regions other than the NTD+L contribute significantly to the NMDAR subtype dependence of gating and ligand-binding properties. Another NMDAR domain that appears likely to contribute is the ABD (Erreger *et al.* 2007; Chen *et al.* 2008), whereas the CTD appears unlikely to contribute (Maki *et al.* 2012; Martel *et al.* 2012; Punnakkal *et al.* 2012; Ryan *et al.* 2013). Nevertheless, Gielen *et al.* (2009) and Yuan *et al.* (2009) demonstrate the critical importance of the GluN2 NTD and NTD-ABD linker in controlling diheteromeric NMDAR subtype dependence of gating and ligand-binding properties.

During final revisions of this review, two separate crystal structures of intact diheteromeric GluN1/2B receptors were published within weeks of one another (Fig. 1*B* and *C*) (Karakas & Furukawa, 2014; Lee *et al.* 2014). Both structures revealed NMDAR subunit arrangement and organization similar to the homomeric GluA2 AMPAR crystal structure (Sobolevsky *et al.* 2009). However, the shape of the GluN1/2B NMDAR crystal structures differed

from the GluA2 AMPAR crystal structure, with, for example, the NTD and ABD much more closely associated in the GluN1/2B NMDAR crystal structures (Sobolevsky *et al.* 2009; Karakas & Furukawa, 2014; Lee *et al.* 2014). The close association of the NTD and ABD in the GluN1/2B NMDAR crystal structures suggests that ligand binding to the NTD may affect the ABD through multiple contacts in addition to the NTD-ABD linker (Karakas & Furukawa, 2014; Lee *et al.* 2014). Assessment of NTD-ABD interactions in the GluN1/2B NMDAR crystal structures may be complicated by modifications designed to increase NMDAR stability. Of note, deletions were made within the GluN2B NTD-ABD linker, and cysteine residues introduced in GluN2B NTDs formed intersubunit cross-links that nearly eliminated receptor activity (Karakas & Furukawa, 2014; Lee *et al.* 2014). However, the GluN1/2B NMDAR crystal structures represent a fundamental advance that will be invaluable in determining how the NTD influences NMDAR gating and ligand-binding properties.
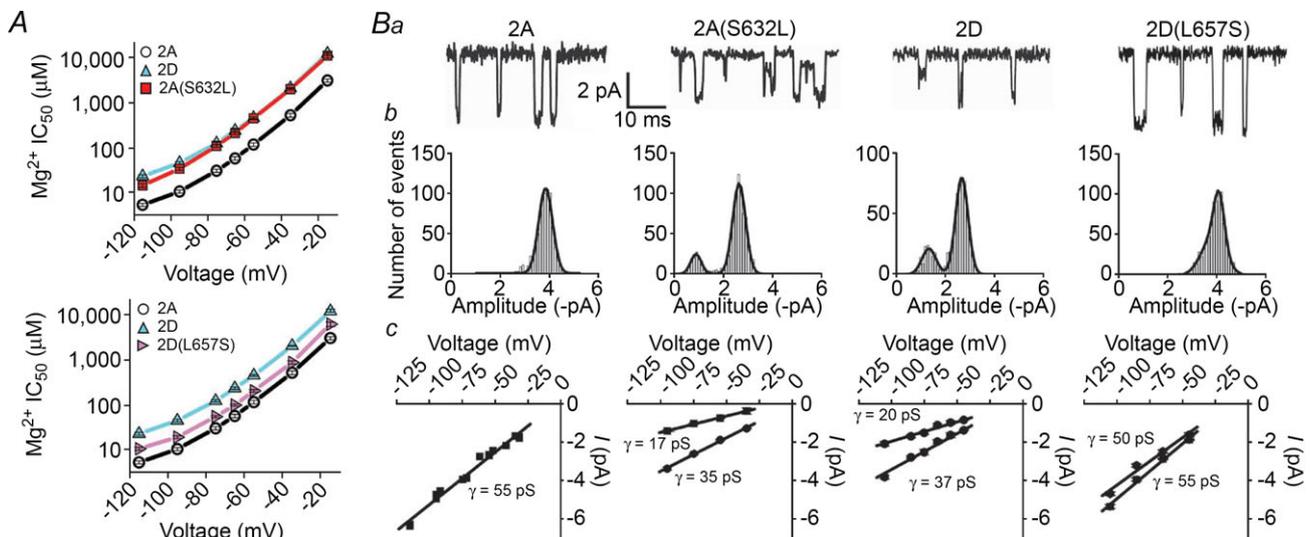
The GluN2 S/L site controls channel properties

The identity of the GluN2 NTD+L does not affect single-channel conductance (Yuan *et al.* 2009), and whether the identity of the GluN2 NTD or NTD+L affects other channel properties was not investigated. Therefore,

NMDAR subtype dependence of channel properties may be controlled by other regions of the receptor.

Previous studies that mostly utilized chimeric subunits implicated the TMD and the ABD in controlling the NMDAR subtype dependence of channel properties (Kuner & Schoepfer, 1996; Wrighton *et al.* 2008; O'Leary & Wyllie, 2009). Kuner & Schoepfer (1996) investigated the role of the entire TMD, subregions of the TMD, and part of the ABD in the NMDAR subtype dependence of Mg^{2+} sensitivity. They found that parts of the M1, M2, M3 and M4 regions in GluN2 subunits all contribute to the subtype dependence of Mg^{2+} sensitivity. Wrighton *et al.* (2008) found that the M1–M3 regions, and to a lesser extent the ABD, were responsible for determining subtype dependence of Mg^{2+} sensitivity. O'Leary & Wyllie (2009) showed that the M1–M3 regions determine subtype dependence of single-channel conductance in addition to Mg^{2+} sensitivity. Therefore, multiple structural elements were found to contribute to NMDAR subtype dependence of channel properties.

Siegler Retchless *et al.* (2012) investigated the structural determinants of GluN1/2A-like and GluN1/2D-like channel properties by mutating single residues. Mutations were introduced at sites within the TMD where GluN2A and GluN2B subunits express the same residue, GluN2C and GluN2D subunits express the same residue, but the GluN2A and GluN2B subunit residue differs from the GluN2C and GluN2D subunit residue.

Figure 3. The GluN2 S/L site controls channel properties
A, voltage dependence of Mg^{2+} IC_{50} values of wild-type receptors and receptors with a mutation at the GluN2 S/L site (see Fig. 1*A*). Mg^{2+} IC_{50} values of GluN1/2A(S632L) receptors resembled those of GluN1/2D receptors, whereas Mg^{2+} IC_{50} values of GluN1/2D(L657S) receptors resembled those of GluN1/2A receptors. *B*, single-channel records (*a*), current amplitude histograms (*b*), and current–voltage relations (*c*) of wild-type receptors and receptors with a mutation at the GluN2 S/L site. Slopes of single-channel current–voltage relations were used to determine single-channel conductance (γ) in *c*. Single-channel current amplitude histograms and γ values of GluN1/2A(S632L) receptors resembled those of GluN1/2D receptors, whereas single-channel current amplitude histograms and γ values of GluN1/2D(L657S) receptors resembled those of GluN1/2A receptors. Panels were taken from Siegler Retchless *et al.* (2012).

Mutations of residues at a single site, the GluN2 S/L site, were found to control NMDAR subtype dependence of channel properties. GluN1/2A(S632L) receptors, in which the residue at the GluN2 S/L site is changed from the GluN2A S to the GluN2D L, exhibit NMDAR channel properties that are GluN1/2D-like (Fig. 3*A* and *B*). Conversely, GluN1/2D(L657S) receptors, in which the GluN2D L at the GluN2 S/L site is changed to the GluN2A S, exhibit NMDAR channel properties that are GluN1/2A-like (Fig. 3*A* and *B*) (Siegler Retchless *et al.* 2012; Clarke *et al.* 2013). The single residue at the GluN2 S/L site was found to control NMDAR subtype dependence of: Mg^{2+} sensitivity (Fig. 3*A*); Ca^{2+} permeability; single-channel conductance, including the conductance of subconductance states (Fig. 3*B*); and inherent voltage-dependent gating of NMDARs (Siegler Retchless *et al.* 2012; Clarke *et al.* 2013). Kinetic analysis of single-channel recordings from GluN1/2A(S632L) receptors did not reveal significant differences from GluN1/2A receptors, consistent with the conclusion that the GluN2 NTD controls NMDAR subtype dependence of gating kinetics.

Although the GluN2 S/L site powerfully affects NMDAR subtype-dependent channel properties, inter-conversion of channel properties between GluN1/2D-like and GluN1/2A-like by GluN2 S/L site substitutions was incomplete. Thus, regions in addition to the GluN2 S/L site influence NMDAR subtype dependence of channel properties. As noted above, other parts of the TMD and the ABD were found to contribute to NMDAR subtype dependence of Mg^{2+} sensitivity (Kuner & Schoepfer, 1996; Wrighton *et al.* 2008; O'Leary & Wyllie, 2009). Taken together, studies that examined the NMDAR subtype dependence of channel properties suggest that the GluN2 S/L site is the major determinant of subtype dependence, with other parts of the TMD, and the ABD, playing smaller roles.

Because the GluN2 S/L site is located at the base of the M3 TMR, it is unlikely to interact directly with ions in the pore. Therefore, the GluN2 S/L site probably affects NMDAR subtype-dependent channel properties through interactions with residues that are closer to the pore.

The GluN2 S/L site controls channel properties through subunit–subunit interactions

Until recently, neither an intact NMDAR crystal structure nor a crystal structure of the NMDAR TMD had been published. Therefore, to aid in understanding the mechanism by which the GluN2 S/L site controls NMDAR subtype-dependent channel properties, Siegler Retchless *et al.* (2012) created homology models of the GluN1/2A M2 p-loop and M3 TMR (GluN1/2A M2–M3; Fig. 4). Homology models take advantage of structural homology of previously crystallized proteins with a protein of inter-

est that has not yet been crystallized. Homology models allow prediction of the structure of the protein of interest based on sequence alignment and hypothesized structural homologies.

In 2009, the first nearly complete iGluR crystal structure was published (Sobolevsky *et al.* 2009). The GluA2 AMPAR crystal structure led to many breakthroughs concerning the function and structural organization of iGluRs, including NMDARs (e.g. Traynelis *et al.* 2010; Salussolia *et al.* 2011; Riou *et al.* 2012). However, despite the utility of the GluA2 AMPAR crystal structure for answering structural and functional questions, the extended region of the M2 p-loop was not resolved (Sobolevsky *et al.* 2009). Siegler Retchless *et al.* (2012) therefore utilized crystal structures of more distantly related ion channels as a basis for a GluN1/2A M2–M3 homology model. Several earlier studies had based NMDAR channel homology models on the crystal structure of the bacterial potassium channel KcsA (Doyle *et al.* 1998), and predictions of the homology models had been validated with physiological experiments (Wood *et al.* 1995; Panchenko *et al.* 2001; Tikhonov, 2007). Another crystallized channel, the cyclic nucleotide-gated channel NaK, shares great sequence homology and structural similarity with potassium channels (Shi *et al.* 2006), but, like NMDARs, is permeable to Na^+, K^+ and Ca^{2+} (Shi *et al.* 2006; Alam *et al.* 2007). Siegler Retchless *et al.* (2012) chose to base their GluN1/2A M2–M3 homology model on the NaK channel structure. Karakas & Furukawa (2014) and Lee *et al.* (2014) found that homologous portions of the TMDs of their GluN1/2B NMDAR crystal structures displayed high structural similarity to corresponding regions of the KcsA channel, further supporting the use of potassium and related channel structures for NMDAR homology modelling.
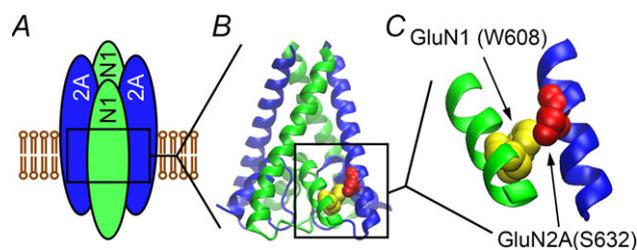
Figure 4. NaK channel-based GluN1/2A M2–M3 homology model
A, schematic diagram of an assembled NMDAR. *B*, all four subunits of the NaK-based GluN1/2A M2–M3 homology model (Siegler Retchless *et al.*, 2012) magnified from the NMDAR schematic diagram in *A*. Regions of GluN1 are shown in green, and regions of GluN2A are shown in blue. One of the two GluN1(W608) residues is shown as space-filling model in yellow, and the adjacent GluN2A(S632) residue is shown as space-filling model in red. *C*, enlarged view of GluN2 S/L site interaction with W608 in the GluN1 M2 region.

The NaK channel-based GluN1/2A M2–M3 homology model was developed with a GluN1-GluN2A-GluN1-GluN2A arrangement around the pore based on Sobolevsky *et al.* (2009), an arrangement that subsequently has been further supported (Rambhadran *et al.* 2010; Salussolia *et al.* 2011; Riou *et al.* 2012; Karakas & Furukawa, 2014; Lee *et al.* 2014). The NaK channel-based GluN1/2A M2–M3 model predicted that GluN2A(S632) is very close to two tryptophan residues in the adjacent GluN1 sub-unit: GluN1(W608) and GluN1(W611), which are in the α-helical portion of the GluN1 M2 p-loop (Fig. 4*B* and *C*) (Siegler Retchless *et al.* 2012). Using mutant cycle analyses (Hidalgo & MacKinnon, 1995; Schreiber & Fersht, 1995), Siegler Retchless *et al.* (2012) demonstrated coupling between GluN2A(S632) and GluN1(W608), but not between GluN2A(S632) and GluN1(W611). Thus, the authors concluded that the identity of the residue at the GluN2 S/L site is likely to control NMDAR subtype-dependent channel properties through a subunit–subunit interaction between the GluN2 M3 and GluN1 M2 α-helices (Fig. 4*C*) (Siegler Retchless *et al.* 2012).

Siegler Retchless *et al.* (2012) also developed a GluN1/2A M2–M3 homology model based on the GluA2 AMPAR crystal structure. Importantly, the AMPAR-based GluN1/2A M2–M3 homology model did not predict close proximity of the GluN2 S/L site to GluN1(W608) (Siegler Retchless *et al.* 2012). In the NaK channel-based GluN1/2A M2–M3 homology model, the side chains of GluN1(W608) and GluN2A(S632) have a minimum separation of 3.5 Å (Fig. 4*C*). In the AMPAR-based GluN1/2A M2–M3 homology model, the side chains of GluN1(W608) and GluN2A(S632) have a minimum separation of 12.2 Å. Although mutant cycle analysis provides only an indirect gauge of proximity of residues, coupling is likely to occur only for residues with side chains separated by less than 7 Å (Schreiber & Fersht, 1995). Thus, the mutant cycle data are more consistent with the NaK channel-based than the AMPAR-based model. Possible explanations for why the distantly related NaK channel may better model the GluN1/2A M2–M3 regions than the more closely related AMPAR include: (1) the structure of the M2–M3 regions of NMDARs simply may resemble more closely membrane regions of potassium channels and closely-related channels than AMPARs; (2) the limited resolution of the M2 region of homomeric GluA2 AMPAR crystal structure may have led to inaccurate placement of the M2 α-helix.

The pore-lining regions in the recently published GluN1/2B NMDAR crystal structures, like the GluA2 AMPAR crystal structure, were not well resolved. However, Lee *et al.* (2014) were able to position residues in the majority of the TMD, including the M2 p-loops, in their structure 2 (PDB ID: 4TLM). We measured the minimum separation between GluN1(W608) and the GluN2B residue homologous to GluN2A(S632) in structure 2. The result, 7.5 Å, is between the minimum separation in the NaK channel-based (3.5 Å) and the AMPAR-based (12.2 Å) GluN1/2A M2–M3 homology models. As Lee *et al.* (2014) were careful to point out, atom positioning in the pore region was not precise; measurements of distances between residues near the pore therefore are subject to substantial uncertainty. The limited resolution of the pore regions of currently available iGluR crystal structures suggest that high-resolution NaK and related channel crystal structures remain valuable resources for modelling the TMD of iGluRs.

Conclusion

The functional properties of diheteromeric NMDAR sub-types depend on the identity of the GluN2 subunits present in the receptor. Recent studies provide strong evidence for grouping diheteromeric NMDAR subtype-dependent properties into two categories based on distinct structural determinants and functional characteristics. Gating and ligand-binding properties are primarily controlled by the identity of the GluN2 NTD and NTD-ABD linker (Gallagher *et al.* 1997; Perin-Dureau *et al.* 2002; Gielen *et al.* 2009; Yuan *et al.* 2009; Mony *et al.* 2011), whereas channel properties are primarily controlled by the identity of the residue at the GluN2 S/L site (Siegler Retchless *et al.* 2012; Clarke *et al.* 2013). Previous work has suggested that subunit–subunit interactions have profound effects on gating and ligand-binding properties (Monyer *et al.* 1994; Vicini *et al.* 1998; Regalado *et al.* 2001; Schorge *et al.* 2005; Vance *et al.* 2012). Similarly, the influence of the GluN2 S/L site on channel properties depends on a subunit–subunit interaction between the GluN2 M3 TMR and the GluN1 M2 p-loop. Thus, NMDAR subunit–subunit interactions are critically important in determining diheteromeric NMDAR subtype-dependent properties. Use of receptor crystal structures (e.g. Karakas & Furukawa, 2014; Lee *et al.* 2014) and structural models will be essential to our understanding of the interdomain and intersubunit interactions that play fundamental roles in NMDAR subtype-dependent properties, and most other aspects of iGluR function.

References

Akazawa C, Shigemoto R, Bessho Y, Nakanishi S & Mizuno N (1994). Differential expression of five *N*-methyl-D-aspartate receptor subunit mRNAs in the cerebellum of developing and adult rats. *J Comp Neurol* **347**, 150–160.

Alam A, Shi N & Jiang Y (2007). Structural insight into Ca^{2+} specificity in tetrameric cation channels. *Proc Natl Acad Sci U S A* **104**, 15334–15339.

Al-Hallaq RA, Conrads TP, Veenstra TD & Wenthold RJ (2007). NMDA di-heteromeric receptor populations and associated proteins in rat hippocampus. *J Neurosci* **27**, 8334–8343.

Ascher P & Nowak L (1988). The role of divalent cations in the *N*-methyl-D-aspartate responses of mouse central neurones in culture. *J Physiol* **399**, 247–266.

Burnashev N, Schoepfer R, Monyer H, Ruppersberg JP, Gunther W, Seeburg PH & Sakmann B (1992). Control by asparagine residues of calcium permeability and magnesium blockade in the NMDA receptor. *Science* **257**, 1415–1419.

Burnashev N, Zhou Z, Neher E & Sakmann B (1995). Fractional calcium currents through recombinant GluR channels of the NMDA, AMPA and kainate receptor subtypes. *J Physiol* **485**, 403–418.

Chen N, Luo T & Raymond LA (1999). Subtype-dependence of NMDA receptor channel open probability. *J Neurosci* **19**, 6844–6854.

Chen N, Moshaver A & Raymond LA (1997). Differential sensitivity of recombinant *N*-methyl-D-aspartate receptor subtypes to zinc inhibition. *Mol Pharmacol* **51**, 1015–1023.

Chen PE, Geballe MT, Katz E, Erreger K, Livesey MR, O'Toole KK, Le P, Lee CJ, Snyder JP, Traynelis SF & Wyllie DJ (2008). Modulation of glycine potency in rat recombinant NMDA receptors containing chimeric NR2A/2D subunits expressed in *Xenopus laevis* oocytes. *J Physiol* **586**, 227–245.

Choi Y, Chen HV & Lipton SA (2001). Three pairs of cysteine residues mediate both redox and Zn^{2+} modulation of the NMDA receptor. *J Neurosci* **21**, 392–400.

Choi YB & Lipton SA (1999). Identification and mechanism of action of two histidine residues underlying high-affinity Zn^{2+} inhibition of the NMDA receptor. *Neuron* **23**, 171–180.

Clarke RJ (2006). NMDA receptor NR2 subunit dependence of the slow component of magnesium unblock. *J Neurosci* **26**, 5825–5834.

Clarke RJ, Glasgow NG & Johnson JW (2013). Mechanistic and structural determinants of NMDA receptor voltage-dependent gating and slow Mg^{2+} unblock. *J Neurosci* **33**, 4140–4150.

Clarke RJ & Johnson JW (2008). Voltage-dependent gating of NR1/2B NMDA receptors. *J Physiol* **586**, 5727–5741.

Cull-Candy SG & Leszkiewicz DN (2004). Role of distinct NMDA receptor subtypes at central synapses. *Sci STKE* **2004**, re16.

Doyle DA, Morais Cabral J, Pfuetzner RA, Kuo A, Gulbis JM, Cohen SL, Chait BT & MacKinnon R (1998). The structure of the potassium channel: molecular basis of K^+ conduction and selectivity. *Science* **280**, 69–77.

Dravid SM, Prakash A & Traynelis SF (2008). Activation of recombinant NR1/NR2C NMDA receptors. *J Physiol* **586**, 4425–4439.

Erreger K, Dravid SM, Banke TG, Wyllie DJ & Traynelis SF (2005). Subunit-specific gating controls rat NR1/NR2A and NR1/NR2B NMDA channel kinetics and synaptic signalling profiles. *J Physiol* **563**, 345–358.

Erreger K, Geballe MT, Kristensen A, Chen PE, Hansen KB, Lee CJ, Yuan H, Le P, Lyuboslavsky PN, Micale N, Jorgensen L, Clausen RP, Wyllie DJ, Snyder JP & Traynelis SF (2007). Subunit-specific agonist activity at NR2A-, NR2B-, NR2C-, and NR2D-containing *N*-methyl-D-aspartate glutamate receptors. *Mol Pharmacol* **72**, 907–920.

Erreger K & Traynelis SF (2008). Zinc inhibition of rat NR1/NR2A *N*-methyl-D-aspartate receptors. *J Physiol* **586**, 763–778.

Fayyazuddin A, Villarroel A, Le Goff A, Lerma J & Neyton J (2000). Four residues of the extracellular N-terminal domain of the NR2A subunit control high-affinity Zn^{2+} binding to NMDA receptors. *Neuron* **25**, 683–694.

Forsythe ID & Westbrook GL (1988). Slow excitatory postsynaptic currents mediated by *N*-methyl-D-aspartate receptors on cultured mouse central neurones. *J Physiol* **396**, 515–533.

Furukawa H, Singh SK, Mancusso R & Gouaux E (2005). Subunit arrangement and function in NMDA receptors. *Nature* **438**, 185–192.

Gallagher MJ, Huang H, Grant ER & Lynch DR (1997). The NR2B-specific interactions of polyamines and protons with the *N*-methyl-D-aspartate receptor. *J Biol Chem* **272**, 24971–24979.

Gielen M, Le Goff A, Stroebel D, Johnson JW, Neyton J & Paoletti P (2008). Structural rearrangements of NR1/NR2A NMDA receptors during allosteric inhibition. *Neuron* **57**, 80–93.

Gielen M, Siegler Retchless B, Mony L, Johnson JW & Paoletti P (2009). Mechanism of differential control of NMDA receptor activity by NR2 subunits. *Nature* **459**, 703–707.

Gray JA, Shi Y, Usui H, During MJ, Sakimura K & Nicoll RA (2011). Distinct modes of AMPA receptor suppression at developing synapses by GluN2A and GluN2B: single-cell NMDA receptor subunit deletion in vivo. *Neuron* **71**, 1085–1101.

Han X, Tomitori H, Mizuno S, Higashi K, Full C, Fukiwake T, Terui Y, Leewanich P, Nishimura K, Toida T, Williams K, Kashiwagi K & Igarashi K (2008). Binding of spermine and ifenprodil to a purified, soluble regulatory domain of the *N*-methyl-D-aspartate receptor. *J Neurochem* **107**, 1566–1577.

Hansen KB, Ogden KK, Yuan H & Traynelis SF (2014). Distinct functional and pharmacological properties of triheteromeric GluN1/GluN2A/GluN2B NMDA receptors. *Neuron* **81**, 1084–1096.

Hardingham GE & Bading H (2010). Synaptic *versus* extrasynaptic NMDA receptor signalling: implications for neurodegenerative disorders. *Nat Rev Neurosci* **11**, 682–696.

Hatton CJ & Paoletti P (2005). Modulation of triheteromeric NMDA receptors by N-terminal domain ligands. *Neuron* **46**, 261–274.

Hidalgo P & MacKinnon R (1995). Revealing the architecture of a K^+ channel pore through mutant cycles with a peptide inhibitor. *Science* **268**, 307–310.

Humphrey W, Dalke A & Schulten K (1996). VMD: Visual molecular dynamics. *J Molecular Graphics* **14**, 33–38.

Johnson JW & Ascher P (1987). Glycine potentiates the NMDA response in cultured mouse brain neurons. *Nature* **325**, 529–531.

Karakas E & Furukawa H (2014). Crystal structure of a heterotetrameric NMDA receptor ion channel. *Science* **344**, 992–997.

Karakas E, Simorowski N & Furukawa H (2009). Structure of the zinc-bound amino-terminal domain of the NMDA receptor NR2B subunit. *EMBO J* **28**, 3910–3920.

Karakas E, Simorowski N & Furukawa H (2011). Subunit arrangement and phenylethanolamine binding in GluN1/GluN2B NMDA receptors. *Nature* **475**, 249–253.

Kleckner NW & Dingledine R (1988). Requirement for glycine in activation of NMDA-receptors expressed in *Xenopus* oocytes. *Science* **241**, 835–837.

Kuner T & Schoepfer R (1996). Multiple structural elements determine subunit specificity of Mg^{2+} block in NMDA receptor channels. *J Neurosci* **16**, 3549–3558.

Kussius CL & Popescu GK (2010). NMDA receptors with locked glutamate-binding clefts open with high efficacy. *J Neurosci* **30**, 12474–12479.

Kutsuwada T, Kashiwabuchi N, Mori H, Sakimura K, Kushiya E, Araki K, Meguro H, Masaki H, Kumanishi T, Arakawa M & Mishina M (1992). Molecular diversity of the NMDA receptor channel. *Nature* **358**, 36–41.

Lau A & Tymianski M (2010). Glutamate receptors, neurotoxicity and neurodegeneration. *Pflugers Arch* **460**, 525–542.

Lee C-H, Lu W, Michel JC, Goehring A, Du J, Song X & Gouaux E (2014). NMDA receptor structures reveal subunit arrangement and pore architecture. *Nature* **511**, 191–197.

Lerma J, Zukin RS & Bennett MV (1990). Glycine decreases desensitization of *N*-methyl-D-aspartate (NMDA) receptors expressed in *Xenopus* oocytes and is required for NMDA responses. *Proc Natl Acad Sci U S A* **87**, 2354–2358.

Lester RA, Clements JD, Westbrook GL & Jahr CE (1990). Channel kinetics determine the time course of NMDA receptor-mediated synaptic currents. *Nature* **346**, 565–567.

Low CM, Lyuboslavsky P, French A, Le P, Wyatte K, Thiel WH, Marchan EM, Igarashi K, Kashiwagi K, Gernert K, Williams K, Traynelis SF & Zheng F (2003). Molecular determinants of proton-sensitive *N*-methyl-D-aspartate receptor gating. *Mol Pharmacol* **63**, 1212–1222.

Low CM, Zheng F, Lyuboslavsky P & Traynelis SF (2000). Molecular determinants of coordinated proton and zinc inhibition of *N*-methyl-D-aspartate NR1/NR2A receptors. *Proc Natl Acad Sci U S A* **97**, 11062–11067.

Luo J, Wang Y, Yasuda RP, Dunah AW & Wolfe BB (1997). The majority of *N*-methyl-D-aspartate receptor complexes in adult rat cerebral cortex contain at least three different subunits (NR1/NR2A/NR2B). *Mol Pharmacol* **51**, 79–86.

MacDermott AB, Mayer ML, Westbrook GL, Smith SJ & Barker JL (1986). NMDA-receptor activation increases cytoplasmic calcium concentration in cultured spinal cord neurones. *Nature* **321**, 519–522.

Maki BA, Aman TK, Amico-Ruvio SA, Kussius CL & Popescu GK (2012). C-terminal domains of *N*-methyl-D-aspartic acid receptor modulate unitary channel conductance and gating. *J Biol Chem* **287**, 36071–36080.

Malenka RC & Bear MF (2004). LTP and LTD: an embarrassment of riches. *Neuron* **44**, 5–21.

Malherbe P, Mutel V, Broger C, Perin-Dureau F, Kemp JA, Neyton J, Paoletti P & Kew JN (2003). Identification of critical residues in the amino terminal domain of the human NR2B subunit involved in the RO 25-6981 binding pocket. *J Pharmacol Exp Ther* **307**, 897–905.

Martel M-A, Ryan TJ, Bell KFS, Fowler JH, McMahon A, Al-Mubarak B, Komiyama NH, Horsburgh K, Kind PC, Grant SGN, Wyllie DJA & Hardingham GE (2012). The subtype of GluN2 C-terminal domain determines the response to excitotoxic insults. *Neuron* **74**, 543–556.

Masuko T, Kashiwagi K, Kuno T, Nguyen ND, Pahk AJ, Fukuchi J, Igarashi K & Williams K (1999). A regulatory domain (R1-R2) in the amino terminus of the *N*-methyl-D-aspartate receptor: effects of spermine, protons, and ifenprodil, and structural similarity to bacterial leucine/isoleucine/valine binding protein. *Mol Pharmacol* **55**, 957–969.

Mayer ML, Westbrook GL & Guthrie PB (1984). Voltage-dependent block by Mg^{2+} of NMDA responses in spinal cord neurones. *Nature* **309**, 261–263.

Mony L, Zhu S, Carvalho S & Paoletti P (2011). Molecular basis of positive allosteric modulation of GluN2B NMDA receptors by polyamines. *EMBO J* **30**, 3134–3146.

Monyer H, Burnashev N, Laurie DJ, Sakmann B & Seeburg PH (1994). Developmental and regional expression in the rat brain and functional properties of four NMDA receptors. *Neuron* **12**, 529–540.

Monyer H, Sprengel R, Schoepfer R, Herb A, Higuchi M, Lomeli H, Burnashev N, Sakmann B & Seeburg PH (1992). Heteromeric NMDA receptors: molecular and functional distinction of subtypes. *Science* **256**, 1217–1221.

Ng FM, Geballe MT, Snyder JP, Traynelis SF & Low CM (2008). Structural insights into phenylethanolamines high-affinity binding site in NR2B from binding and molecular modeling studies. *Mol Brain* **1**, 16.

Nowak L, Bregestovski P, Ascher P, Herbet A & Prochiantz A (1984). Magnesium gates glutamate-activated channels in mouse central neurones. *Nature* **307**, 462–465.

O'Leary T & Wyllie DJ (2009). Single-channel properties of *N*-methyl-D-aspartate receptors containing chimaeric GluN2A/GluN2D subunits. *Biochem Soc Trans* **37**, 1347–1354.

Panchenko VA, Glasser CR & Mayer ML (2001). Structural similarities between glutamate receptor channels and K^+ channels examined by scanning mutagenesis. *J Gen Physiol* **117**, 345–360.

Paoletti P, Ascher P & Neyton J (1997). High-affinity zinc inhibition of NMDA NR1-NR2A receptors. *J Neurosci* **17**, 5711–5725.

Paoletti P, Bellone C & Zhou Q (2013). NMDA receptor subunit diversity: impact on receptor properties, synaptic plasticity and disease. *Nat Rev Neurosci* **14**, 383–400.

Paoletti P, Perin-Dureau F, Fayyazuddin A, Le Goff A, Callebaut I & Neyton J (2000). Molecular organization of a zinc binding N-terminal modulatory domain in a NMDA receptor subunit. *Neuron* **28**, 911–925.

Partin KM, Fleck MW & Mayer ML (1996). AMPA receptor flip/flop mutants affecting deactivation, desensitization, and modulation by cyclothiazide, aniracetam, and thiocyanate. *J Neurosci* **16**, 6634–6647.

Perin-Dureau F, Rachline J, Neyton J & Paoletti P (2002). Mapping the binding site of the neuroprotectant ifenprodil on NMDA receptors. *J Neurosci* **22**, 5955–5965.

Priestley T, Laughton P, Myers J, Le Bourdelles B, Kerby J & Whiting PJ (1995). Pharmacological properties of recombinant human *N*-methyl-D-aspartate receptors comprising NR1a/NR2A and NR1a/NR2B subunit assemblies expressed in permanently transfected mouse fibroblast cells. *Mol Pharmacol* **48**, 841–848.

Punnakkal P, Jendritza P & Kohr G (2012). Influence of the intracellular GluN2 C-terminal domain on NMDA receptor function. *Neuropharmacology* **62**, 1985–1992.

Rachline J, Perin-Dureau F, Le Goff A, Neyton J & Paoletti P (2005). The micromolar zinc-binding domain on the NMDA receptor subunit NR2B. *J Neurosci* **25**, 308–317.

Rambhadran A, Gonzalez J & Jayaraman V (2010). Subunit arrangement in *N*-methyl-D-aspartate (NMDA) receptors. *J Biol Chem* **285**, 15296–15301.

Rauner C & Kohr G (2010). Triheteromeric NR1/NR2A/NR2B receptors constitute the major *N*-methyl-D-aspartate receptor population in adult hippocampal synapses. *J Biol Chem* **286**, 7558–7566.

Regalado MP, Villarroel A & Lerma J (2001). Intersubunit cooperativity in the NMDA receptor. *Neuron* **32**, 1085–1096.

Riou M, Stroebel D, Edwardson JM & Paoletti P (2012). An alternating GluN1-2-1-2 subunit arrangement in mature NMDA receptors. *PLoS One* **7**, e35134.

Ryan TJ, Kopanitsa MV, Indersmitten T, Nithiananthatarajah J, Afinowi NO, Pettit C, Stanford LE, Sprengel R, Saksida LM, Bussey TJ, O'Dell TJ, Grant SG & Komiyama NH (2013). Evolution of GluN2A/B cytoplasmic domains diversified vertebrate synaptic plasticity and behaviour. *Nat Neurosci* **16**, 25–32.

Salussolia CL, Prodromou ML, Borker P & Wollmuth LP (2011). Arrangement of subunits in functional NMDA receptors. *J Neurosci* **31**, 11295–11304.

Schell MJ, Molliver ME & Snyder SH (1995). D-Serine, an endogenous synaptic modulator: localization to astrocytes and glutamate-stimulated release. *Proc Natl Acad Sci U S A* **92**, 3948–3952.

Schneggenburger R (1996). Simultaneous measurement of Ca^{2+} influx and reversal potentials in recombinant *N*-methyl-D-aspartate receptor channels. *Biophys J* **70**, 2165–2174.

Schorge S, Elenes S & Colquhoun D (2005). Maximum likelihood fitting of single channel NMDA activity with a mechanism composed of independent dimers of subunits. *J Physiol* **569**, 395–418.

Schreiber G & Fersht AR (1995). Energetics of protein-protein interactions: analysis of the barnase-barstar interface by single mutations and double mutant cycles. *J Mol Biol* **248**, 478–486.

Sheng M, Cummings J, Roldan LA, Jan YN & Jan LY (1994). Changing subunit composition of heteromeric NMDA receptors during development of rat cortex. *Nature* **368**, 144–147.

Shi N, Ye S, Alam A, Chen L & Jiang Y (2006). Atomic structure of a Na^+- and K^+-conducting channel. *Nature* **440**, 570–574.

Siegler Retchless B, Gao W & Johnson JW (2012). A single GluN2 subunit residue controls NMDA receptor channel properties via intersubunit interaction. *Nat Neurosci* **15**, 406–413.

Sobolevsky AI, Rosconi MP & Gouaux E (2009). X-ray structure, symmetry and mechanism of an AMPA-subtype glutamate receptor. *Nature* **462**, 745–756.

Stroebel D, Carvalho S & Paoletti P (2011). Functional evidence for a twisted conformation of the NMDA receptor GluN2A subunit N-terminal domain. *Neuropharmacology* **60**, 151–158.

Swanson GT & Heinemann SF (1998). Heterogeneity of homomeric GluR5 kainate receptor desensitization expressed in HEK293 cells. *J Physiol* **513**, 639–646.

Tikhonov DB (2007). Ion channels of glutamate receptors: structural modeling. *Mol Membr Biol* **24**, 135–147.

Tovar KR, McGinley MJ & Westbrook GL (2013). Triheteromeric NMDA receptors at hippocampal synapses. *J Neurosci* **33**, 9150–9160.

Traynelis SF, Burgess MF, Zheng F, Lyuboslavsky P & Powers JL (1998). Control of voltage-independent zinc inhibition of NMDA receptors by the NR1 subunit. *J Neurosci* **18**, 6163–6175.

Traynelis SF, Hartley M & Heinemann SF (1995). Control of proton sensitivity of the NMDA receptor by RNA splicing and polyamines. *Science* **268**, 873–876.

Traynelis SF, Wollmuth LP, McBain CJ, Menniti FS, Vance KM, Ogden KK, Hansen KB, Yuan H, Myers SJ & Dingledine R (2010). Glutamate receptor ion channels: Structure, regulation, and function. *Pharmacol Rev* **62**, 405–496.

Vance KM, Hansen KB & Traynelis SF (2012). GluN1 splice variant control of GluN1/GluN2D NMDA receptors. *J Physiol* **590**, 3857–3875.

Varney MA, Jachec C, Deal C, Hess SD, Daggett LP, Skvoretz R, Urcan M, Morrison JH, Moran T, Johnson EC & Velicelebi G (1996). Stable expression and characterization of recombinant human heteromeric *N*-methyl-D-aspartate receptor subtypes NMDAR1A/2A and NMDAR1A/2B in mammalian cells. *J Pharmacol Exp Ther* **279**, 367–378.

Vicini S, Wang JF, Li JH, Zhu WJ, Wang YH, Luo JH, Wolfe BB & Grayson DR (1998). Functional and pharmacological differences between recombinant *N*-methyl-D-aspartate receptors. *J Neurophysiol* **79**, 555–566.

Williams K (1993). Ifenprodil discriminates subtypes of the *N*-methyl-D-aspartate receptor: selectivity and mechanisms at recombinant heteromeric receptors. *Mol Pharmacol* **44**, 851–859.

Williams K (1996). Separating dual effects of zinc at recombinant *N*-methyl-D-aspartate receptors. *Neurosci Lett* **215**, 9–12.

Wood MW, VanDongen HMA & VanDongen AMJ (1995). Structural conservation of ion conduction pathways in K channels and glutamate receptors. *Proc Natl Acad Sci U S A* **92**, 4882–4886.

Wrighton DC, Baker EJ, Chen PE & Wyllie DJ (2008). Mg^{2+} and memantine block of rat recombinant NMDA receptors containing chimeric NR2A/2D subunits expressed in *Xenopus laevis* oocytes. *J Physiol* **586**, 211–225.

Wyllie DJ, Behe P & Colquhoun D (1998). Single-channel activations and concentration jumps: comparison of recombinant NR1a/NR2A and NR1a/NR2D NMDA receptors. *J Physiol* **510**, 1–18.

Yuan H, Hansen KB, Vance KM, Ogden KK & Traynelis SF (2009). Control of NMDA receptor function by the NR2 subunit amino-terminal domain. *J Neurosci* **29**, 12045–12058.

Yuan H, Hansen KB, Zhang J, Pierson TM, Markello TC, Fajardo KV, Holloman CM, Golas G, Adams DR, Boerkoel CF, Gahl WA & Traynelis SF (2014). Functional analysis of a de novo GRIN2A missense mutation associated with early-onset epileptic encephalopathy. *Nat Commun* **5**, 3251.

Zhou Q & Sheng M (2013). NMDA receptors in nervous system diseases. *Neuropharmacology* **74**, 69–75.

Additional information

Competing interests

The authors have no competing interests.

Funding

APPENDIX B

RECENT INSIGHTS INTO THE MODE OF ACTION OF MEMANTINE AND KETAMINE

Johnson JW, Glasgow NG, and Povysheva NV (2015) Recent insights into the mode of action of memantine and ketamine. Curr Opin Pharmacol 20: 54-63.

Recent insights into the mode of action of memantine and ketamine

Jon W. Johnson, **Nathan G. Glasgow**, and **Nadezhda V. Povysheva**
Department of Neuroscience and Center for Neuroscience, University of Pittsburgh, Pittsburgh PA, 15260, USA

Jon W. Johnson: jjohnson@pitt.edu; Nathan G. Glasgow: ngglasgow@gmail.com; Nadezhda V. Povysheva: nvp1@pitt.edu

Abstract

The clinical benefits of the glutamate receptor antagonists memantine and ketamine have helped sustain optimism that glutamate receptors represent viable targets for development of therapeutic drugs. Both memantine and ketamine antagonize *N*-methyl-ᴅ-aspartate receptors (NMDARs), a glutamate receptor subfamily, by blocking the receptor-associated ion channel. Although many of the basic characteristics of NMDAR inhibition by memantine and ketamine appear similar, their effects on humans and to a lesser extent on rodents are strongly divergent. Some recent research suggests that preferential inhibition by memantine and ketamine of distinct NMDAR subpopulations may contribute to the drugs' differential clinical effects. Here we review studies that shed light on possible explanations for differences between the effects of memantine and ketamine.

Introduction

The strikingly broad involvement of *N*-methyl-ᴅ-aspartate receptors (NMDARs) in nervous system disorders has led to persistent hope that pharmacological NMDAR modulators will provide a rich source of pharmaceuticals. However, many NMDAR-focused drug development efforts have ended with failed clinical trials. Although the failures resulted in part from weaknesses in trial design [1-3], an important implication is that nonspecific NMDAR inhibition is unlikely to yield successful treatments, probably because NMDARs play many fundamental physiological roles. Optimism endures that NMDARs may be a fruitful pharmaceutical target using drugs that select for receptor subpopulations based on NMDAR subtype, location, and/or mechanism of activation. The encouraging but divergent clinical effects of the NMDAR antagonists memantine and ketamine have helped motivate continuing efforts to develop new drugs based on NMDAR modulation. Understanding the mechanistic bases of the beneficial effects of these drugs may help guide development of

Corresponding author: Jon W. Johnson, Office phone number: (412) 624-4295.

189

more effective therapies based on NMDAR modulation. Here we review research that sheds light on the similarities and differences in memantine and ketamine actions, focusing where possible on research that compares memantine and ketamine directly.

NMDARs and their inhibition by memantine and ketamine

NMDARs are tetrameric ionotropic glutamate receptors found at nearly all vertebrate excitatory synapses. NMDARs are centrally involved in fundamental nervous system functions including learning and memory [3,4]. NMDAR dysfunction has been implicated in nervous system disorders including Alzheimer's disease, Huntington's disease, depression, schizophrenia, chronic and neuropathic pain, epilepsy, and neuron death following stroke [5-7]. NMDARs are obligate heterotetramers composed of GluN1 subunits in combination with GluN2 and/or GluN3 subunits [3,4,8]. The GluN1 subunit is encoded by a single gene; four genes encode the GluN2 subunits (GluN2A, GluN2B, GluN2C, and GluN2D); two genes encode the GluN3 subunits (GluN3A and GluN3B). Most NMDARs are composed of two GluN1 subunits and two GluN2 subunits, and their activation requires binding of agonists to all four subunits. The principal endogenous agonists that bind to the GluN1 subunit are glycine and D-serine, whereas the principal endogenous agonist that binds to GluN2 subunits is glutamate. The open channel of NMDARs mediates permeation predominantly of Na^+, K^+, and Ca^{2+}; the influx of Ca^{2+} ions through NMDAR channels is critical to both the physiological and the pathological effects of receptor activation. Many endogenous substances modulate NMDAR activity, including Mg^{2+}, Zn^{2+}, H^+, polyamines, neurosteroids, and fatty acids [3]. Mg^{2+} is a physiologically crucial modulator that blocks the channel of NMDARs, conferring strong voltage dependence to NMDAR-mediated conductance.

Both memantine and ketamine inhibit NMDARs by occupying the NMDAR's ion channel and occluding current flow. Both drugs are open channel blockers: when the channel is closed, the drugs have little or no ability to enter an unblocked channel or to unbind after blocking the channel. Both drugs exhibit voltage dependence, entering the channel more quickly, leaving the channel more slowly, and inhibiting more effectively as a cell's membrane potential is hyperpolarized. The basic characteristics of NMDAR inhibition by memantine and ketamine, including IC_{50}, kinetics, and voltage dependence, do not differ strongly [9-12]. Many studies report that ketamine inhibits NMDAR channels with slightly lower IC_{50} and slower kinetics than memantine; however, the differences are small (generally less than a factor of 2). However, ketamine is used in most experiments as a racemic mixture of two enantiomers, S- and R-ketamine; each enantiomer has somewhat different pharmacological properties [13,14]. Voltage dependence of memantine and ketamine are similar, although memantine's has been reported to be slightly greater [15]. Because both memantine's and ketamine's binding site in the NMDAR channel (Figure 1) overlaps with the Mg^{2+} binding site, Mg^{2+} competes with both drugs for binding to NMDAR channels. As a result, physiological concentrations of Mg^{2+} (~1 mM) substantially increase the IC_{50}, modify the voltage dependence, and alter the NMDAR subtype-selectivity of both memantine and ketamine [16-18].

Despite their many similarities, the clinical effects of memantine and ketamine, and to a lesser extent the behavioral effects in rodents, are surprisingly distinct.

Clinical, behavioral, and circuit effects of memantine and ketamine

Human studies

There are clear differences between the clinical effects of memantine and ketamine. Memantine is the only glutamate receptor ligand that is approved for treatment of Alzheimer's disease (AD). The clinical benefits of memantine in AD patients are modest but broad, and include positive effects on communication, comprehension, memory, and activities of daily living. Memantine is very well tolerated and appears to have no abuse potential [19-21]. Ketamine, in contrast, is a drug of abuse that produces schizophrenia-like symptoms in healthy adults and exacerbates symptoms in schizophrenics [11,22,23].

Ketamine also has demonstrated impressive beneficial effects in clinical studies. Along with its well-established utility as a general anesthetic, ketamine has been found useful in the treatment of several disorders, including depression and pain. A single ketamine infusion has been found to alleviate rapidly and for an extended period the symptoms of major depressive disorder [6,24]. Ketamine also is effective in pain management [25,26]. Memantine, however, does not appear to be effective in treating either depression [27,28] or pain [29]. Thus, the differences between the effects of memantine and ketamine in humans appear robust and consistent.

Rodent studies

Based in part on the ability of ketamine to produce schizophrenia-like symptoms in humans, ketamine administration has been widely used to produce rodent models of schizophrenia [30,31]. Although memantine generally is not used to model schizophrenia, comparisons of the behavioral effects of memantine and ketamine in rodents reveal similarities as well as differences, with differences weaker than in human studies. Especially at lower doses (very approximately, and depending on route of administration, below 20 mg/kg), memantine and ketamine have broadly similar effects on locomotor and exploratory activity, stereotypic behavior, impulsive choice, and attention [32-37]. Several of those studies also found similar tendencies for memantine and ketamine to impair memory function, although low doses of memantine can improve memory [38-40], an observation not reported for ketamine. Both memantine and ketamine decrease ethanol ingestion by alcohol-preferring rats, but only the effect of ketamine is blocked by mTOR (mammalian target of rapamycin) inhibition [41]. Differences at low doses between the effects of memantine and ketamine were reported for aggressive behavior when combined with alcohol ingestion [42], and striking differences in antidepressant-like effects were observed [43]. At higher doses, a wide variety of differences between the locomotor and cognitive effects of memantine and ketamine emerged [33,36]. When memantine and ketamine were compared in drug discrimination studies, ketamine displayed complete substitution for PCP or MK-801, and memantine displayed complete [44] or partial [11,45] substitution.

Many NMDAR channel blockers have been found to exhibit properties thought to be associated with activation of brain circuits. Ketamine powerfully increases gamma (∼30 –

90 Hz) oscillations in cortex (for review, see [46]) and delta ($\sim$0.5 – 4 Hz) oscillations in multiple brain regions [47]. Although the effects of memantine on oscillations have been less extensively studied, a recent article showed that memantine as well as ketamine increased gamma oscillations in rat cortex, whereas ketamine but not memantine increased delta oscillations [48]. Both memantine and ketamine increased 2-deoxyglucose (2-DG) uptake, a marker of neuronal activation [49]. Ketamine has been hypothesized to disinhibit cortical circuits [12,50,51], a process that may underlie increases in gamma oscillations and 2-DG uptake. Similarly, memantine inhibition of NMDARs was proposed to produce cognitive improvements in AD patients through disinhibition [52], although memantine's ability to mediate disinhibition has not been directly assessed. Ketamine reduces expression of the important GABAergic interneuron markers parvalbumin (a Ca^{2+} binding protein) and GAD67 (a GABA synthetic enzyme) in rodents, thereby compromising inhibitory neuron function [53-55]. The relation of decreased interneuron function to increased oscillations, however, has been questioned [56,57]. Memantine and ketamine also have been proposed to inhibit a subpopulation of interneurons (but see [58]) as a result of the drugs' selectivity in physiological Mg^{2+} for GluN2C and GluN2D subunit-containing NMDARs [16]. Because GluN2D subunits are expressed predominantly by inhibitory neurons in mature cortex and hippocampus [59,60], preferential inhibition of GluN2D-containing receptors could mediate disinhibition.

Both memantine and ketamine have been shown to be neuroprotective using many in vivo and in vitro paradigms, and their neuroprotective actions are thought to contribute to their clinical benefits (for reviews, see [10,61,62]). There has been very limited comparison of the neuroprotective properties of memantine and ketamine. In one direct comparison of their ability to reduce the effects of oxygen-glucose deprivation in cultured hippocampal slices at equal concentrations, ketamine was found to be slightly more effective than memantine [63].

Thus, the effects of memantine and ketamine in rodent studies demonstrate both strong similarities and clear differences; in human studies, the drugs' effects differ conspicuously.

Mechanistic bases for differential effects of memantine and ketamine

Pharmacological differences between memantine and ketamine

We will consider several possible explanations for the differential effects of memantine and ketamine noted above.

Drugs with the same site of action can differ in their clinical and behavioral effects because of pharmacokinetic differences. The increase in serum and brain concentration, and subsequent elimination, is much faster for ketamine than memantine in both humans and rodents, a difference that could be responsible for the drugs' differential effects (see [9,10,36,64,65]). Several lines of evidence argue against the hypothesis that pharmacokinetic differences between memantine and ketamine are the principal explanation for their differential clinical and behavioral effects. First, numerous studies of ketamine action in humans have involved drug infusion protocols (e.g., [66,67]), some of which have been demonstrated to maintain a steady serum concentration [68]. Nevertheless, the effects of infused ketamine differed strongly from the effects of memantine, which is maintained at

stable levels in patients treated by oral administration due to its slow pharmacokinetics [10]. Second, phencyclidine, an analog of ketamine, has much slower pharmacokinetics than ketamine [69], but greater psychotomimetic effects [70]. Third, a recent study compared in rats the behavioral effects of memantine and ketamine at two time points: 15 min after i.p. injection, when ketamine concentration should be near peak but memantine concentration rising, and 45 min after i.p. injection, when ketamine but not memantine concentration should have substantially decreased. The behavioral effects of memantine and ketamine at low doses were similar at both time points, and differences in the drugs' effects at higher doses were similar at both time points [36]. The results suggested that the pharmacokinetic differences between the drugs do not make a major contribution to their differential behavioral effects in rodents. It appears likely that some of the observed differences between the effects of memantine and ketamine, for example sensitivity to transient inhibition of downstream effectors [41], could result from pharmacokinetic differences. However, it appears unlikely that the clinical and behavioral effects of memantine and ketamine differ predominantly because of the faster pharmacokinetics of ketamine.

A second possibility is that the differential clinical and behavioral effects of memantine and ketamine result from differences in their action at sites other than NMDARs. Multiple other sites of action have been reported for each drug (e.g., [26,71,72]). For example, memantine inhibits multiple acetylcholine receptors subtypes [73-76] and 5-HT$_3$ serotonin receptors [10,77], whereas ketamine binds to dopamine D2 and 5-HT$_2$ serotonin receptors [12,78] and to HCN1 channels [79]. Although multiple lines of evidence support the hypothesis that the actions of memantine and ketamine depend predominantly on NMDAR binding [10,70,80,81], there also is strong evidence supporting the importance of other sites of action [79]. It seems likely that some of the differences in the drugs' effects, especially at higher doses, depend on action at targets other than NMDARs.

A third possibility is that the effects of drug metabolites contribute to the differential pharmacological effects of memantine and ketamine. The (S)- and (R)-enantiomers of norketamine are major metabolites of ketamine, and inhibit NMDARs, although with lower potency than (S)- and (R)-ketamine [14,82,83]. Similar to ketamine, (R,S)-norketamine and (2S,6S)-hydroxynorketamine, another ketamine metabolite [83], can increase mTOR function [84]. Several ketamine metabolites potently inhibit α7-nicotinic acetylcholine receptor-mediated currents [85]. Although, to our knowledge, no active memantine metabolites have been reported, differences in the activity of metabolites of ketamine and potentially memantine at NMDARs or at non-NMDAR sites could underlie some of their differential clinical and behavioral effects.

A fourth possibility is that memantine and ketamine block overlapping but distinct populations of NMDARs. NMDARs play diverse roles in nervous system function, and differential inhibition of receptors involved in distinct functions could lead to divergent clinical and behavioral effects. Although memantine and ketamine bind to overlapping sites on NMDARs, there are multiple mechanisms by which they might inhibit distinct receptor subpopulations. In the next section we will focus on studies that address the hypothesis that memantine and ketamine inhibit distinct subpopulations of NMDARs.

Differential inhibition of NMDAR subpopulations by memantine and ketamine

Current understanding of the mechanisms of action of memantine and ketamine do not permit a confident determination of whether, and if so how, they inhibit distinct subpopulations of NMDARs. However, data pointing to an important dichotomy in the NMDAR subpopulations inhibited by memantine and ketamine have emerged.

Many recent studies suggest that the important NMDARs inhibited by memantine are predominantly extrasynaptic, whereas the important NMDARs inhibited by ketamine are synaptic. The significance of differential relative inhibition of synaptic and extrasynaptic NMDARs derives from a hypothesis particularly relevant to neurodegenerative diseases: that synaptic NMDAR stimulation activates cell survival pathways, whereas extrasynaptic NMDAR stimulation activates cell death pathways [86-88]. Activation of extrasynaptic NMDARs by ambient glutamate mediates tonic NMDAR current [89-91], and augmented extrasynaptic receptor activation has been hypothesized to compromise neuron health in nervous system disorders [86-88]. However, it is important to note that there is no consensus on the differential implications of synaptic and extrasynaptic NMDAR activation [6,24,92-95].

Memantine has been found to inhibit extrasynaptic NMDARs more potently than synaptic NMDARs ([96-102]; but see [63,93,94]). However, memantine inhibition of synaptic NMDARs can increase with increasing intensity of synaptic stimulation [93,103]. Memantine can restore long term potentiation impaired by tonic NMDAR activation following reduction of Mg^{2+} in hippocampal slices [104]; since tonic NMDAR current depends mainly on extrasynaptic NMDARs [89], these data are generally consistent with the idea that memantine preferentially inhibits extrasynaptic NMDARs. In Huntington's disease model mice, memantine reduced functional extrasynaptic NMDAR expression, reversed aberrant activation of cell death pathways by suppressing p38 MAPK activation and increasing nuclear CREB signaling, and reversed disease-associated deficits [98,100,102].

In contrast, the NMDAR subpopulation of central importance to the rapid anti-depressant effects of ketamine was proposed to be synaptic, and possibly a subgroup of NMDARs predominantly activated by spontaneous synaptic vesicle release [6,43,105,106]. Acute inhibition of synaptic NMDARs by ketamine at doses sufficient to produce antidepressant behavioral effects in rodents deactivated eukaryotic elongation factor 2 (eEF2) kinase, reducing eEF2 phosphorylation, relieved block of BDNF translation, and increased surface expression of AMPARs [105,106]. A recent study found that in the presence of physiological Mg^{2+}, ketamine inhibited synaptic NMDARs in hippocampal pyramidal neurons much more effectively than memantine [43]. The same study showed that in the absence of Mg^{2+}, inhibition of synaptic NMDARs by memantine and ketamine was indistinguishable, consistent with previous findings [63]. These results suggest that Mg^{2+}, which has been excluded in many basic studies of memantine and ketamine action on NMDARs, could play a key role by influencing relative inhibition of NMDAR subpopulations by memantine and ketamine.

194

Potential mechanisms of differential inhibition

We next will consider mechanisms by which a channel blocker could differentiate NMDAR subpopulations. There are at least three ways inhibitors could distinguish synaptic from extrasynaptic NMDARs: (1) by differential inhibition of NMDAR subtypes expressed synaptically versus extrasynaptically; (2) by differential inhibition based on the concentration of glutamate that activates receptors; (3) by differential inhibition based on the time course of receptor activation.

There is evidence for differential expression of NMDAR subunits by subcellular location. GluN2B-containing NMDARs have been reported to be preferentially localized extrasynaptically, and GluN2A-containing NMDARs to be preferentially localized synaptically in cortical and hippocampal neurons ([107-109]; but see [110,111]). However, neither memantine nor ketamine distinguish strongly between GluN2A- and GluN2B-containing NMDARs [14,16]. A caveat is that memantine and ketamine inhibition of triheteromeric receptors, which are highly expressed in the brain (see [4]), has not been characterized. Newly developed approaches for study of isolated triheteromeric receptors will facilitate determination of possible differential drug selectivity [112]. There also is evidence for preferential extrasynaptic expression of GluN2D-containing NMDARs in multiple brain regions [113,114], including hippocampus [115,116]. Because memantine and ketamine preferentially inhibit GluN2C- and GluN2D-containing NMDARs in physiological Mg^{2+} [16], extrasynaptic localization of GluN2D-containing NMDARs could underlie the drugs' enhanced inhibition of extrasynaptic receptors.

There also is evidence that memantine inhibits NMDARs more effectively at higher agonist concentrations ([117], but see [15,118]). However, this observation would not explain preferential inhibition of extrasynaptic receptors, since extrasynaptic NMDARs are activated by much lower glutamate concentrations than synaptic receptors.

Whether NMDAR inhibition by memantine and/or ketamine depends on the duration of agonist exposure has not been directly investigated. If memantine but not ketamine were to preferentially inhibit NMDARs tonically activated by the extracellular glutamate to which extrasynaptic receptors are exposed, then only memantine would preferentially inhibit extrasynaptic NMDARs. As described above, there are conflicting data on whether memantine distinguishes synaptic and extrasynaptic receptors in 0 Mg^{2+}, but evidence that differential actions of memantine and ketamine appear in the presence of physiological Mg^{2+} [43]. Although initially the powerful effect of Mg^{2+} on inhibition by channel blockers was suggested to affect memantine and ketamine similarly [16], subsequent data suggest that the effect of Mg^{2+} may differ among channel blockers [18]. Further characterization of memantine and ketamine inhibition of NMDAR responses in the presence of physiological Mg^{2+} is warranted.

If memantine and ketamine do inhibit distinct populations of NMDARs, then there must be an underlying difference in the drugs' mechanism of interaction with NMDARs. One difference that has been described is memantine's ability to bind to a superficial site on NMDARs to which ketamine does not bind. Memantine binding to the superficial site contributes to partial trapping of memantine, a phenomenon that has been proposed to

reduce inhibition of synaptic receptors [15,119-122]. The impact of the superficial memantine binding site on inhibition in the presence of Mg^{2+} is unexplored. Another possibility is that occupation of the channel by memantine or ketamine may differentially affect transition rates between NMDAR states (e.g., between open and closed, agonist-bound and agonist-unbound, and/or desensitized and undesensitized states) of blocked receptors [123-126]. The presence of a blocker in a channel can powerfully influence gating transitions, as suggested by Figure 1(b); the M3 α-helices, which surround the blockers, are centrally involved in channel gating [3]. "Foot-in-the-door" blockers, which do not permit channel closure when bound [127], provide an extreme example of how channel blockers can affect channel gating. Some NMDAR channel blockers act as foot-in-the-door blockers [124,128], but others accelerate channel closure [125] and agonist unbinding [126]. The effect of a channel blocker on transitions between blocked states influences many characteristics of inhibition, including dependence of inhibition on agonist concentration [129] and on duration of agonist presentation (NG Glasgow and JW Johnson, abstract in *Soc Neurosci Abstr* 2014, 501.08). Thus, there are biophysically plausible explanations for why, despite their similarities, memantine and ketamine could inhibit distinct populations of NMDARs.

Conclusions

The divergent clinical and behavioral effects of memantine and ketamine could be a consequence of multiple differences between the drugs. Their very different pharmacokinetics along with differences in their actions at binding sites other than NMDARs are likely to make some contribution to differences in the drugs' clinical and behavioral effects. There is considerable evidence, however, that the important NMDAR subpopulations inhibited by memantine and ketamine differ: many recent studies have attributed the beneficial effects of memantine to preferential inhibition of extrasynaptic NMDARs, whereas the rapid antidepressant effects of ketamine have been attributed to inhibition of synaptic NMDARs. Although the validity of this dichotomy has been questioned and a mechanistic basis for differential NMDAR inhibition by memantine and ketamine is not established, there are plausible biophysical explanations that remain to be tested. More extensive direct comparison of the effects of memantine and ketamine at multiple experimental levels will provide critical insight into the important mechanisms responsible for the clinical benefits of these NMDAR antagonists.

Acknowledgments

References and recommended reading

* of special interest

** of outstanding interest

1. Gladstone DJ, Black SE, Hakim AM. Heart, Stroke Foundation of Ontario Centre of Excellence in Stroke R. Toward wisdom from failure: Lessons from neuroprotective stroke trials and new therapeutic directions. Stroke; a journal of cerebral circulation. 2002; 33(8):2123–2136.

Curr Opin Pharmacol. Author manuscript; available in PMC 2016 February 01.

196

2. Muir KW. Glutamate-based therapeutic approaches: Clinical trials with nmda antagonists. Curr Opin Pharmacol. 2006; 6(1):53–60. [PubMed: 16359918]

3. Traynelis SF, Wollmuth LP, McBain CJ, Menniti FS, Vance KM, Ogden KK, Hansen KB, Yuan H, Myers SJ, Dingledine R. Glutamate receptor ion channels: Structure, regulation, and function. Pharmacological reviews. 2010; 62(3):405–496. [PubMed: 20716669]

4. Paoletti P, Bellone C, Zhou Q. NMDA receptor subunit diversity: Impact on receptor properties, synaptic plasticity and disease. Nat Rev Neurosci. 2013; 14(6):383–400. [PubMed: 23686171]

5. Lau A, Tymianski M. Glutamate receptors, neurotoxicity and neurodegeneration. Pflugers Archiv : European journal of physiology. 2010; 460(2):525–542. [PubMed: 20229265]

6. Kavalali ET, Monteggia LM. Synaptic mechanisms underlying rapid antidepressant action of ketamine. Am J Psychiatry. 2012; 169(11):1150–1156. [PubMed: 23534055]

7. Zhou Q, Sheng M. NMDA receptors in nervous system diseases. Neuropharmacology. 2013; 74:69–75. [PubMed: 23583930]

8. Glasgow NG, Retchless BS, Johnson JW. Molecular bases of nmda receptor subtype-dependent properties. J Physiol. 2014

9. Johnson JW, Kotermanski SE. Mechanism of action of memantine. Curr Opin Pharmacol. 2006; 6(1):61–67. [PubMed: 16368266]

10. Parsons CG, Stoffler A, Danysz W. Memantine: A NMDA receptor antagonist that improves memory by restoration of homeostasis in the glutamatergic system - too little activation is bad, too much is even worse. Neuropharmacology. 2007; 53(6):699–723. [PubMed: 17904591]

11. Rammes G, Danysz W, Parsons CG. Pharmacodynamics of memantine: An update. Curr Neuropharmacol. 2008; 6(1):55–78. [PubMed: 19305788]

12. Frohlich J, Van Horn JD. Reviewing the ketamine model for schizophrenia. J Psychopharmacol. 2014; 28(4):287–302. [PubMed: 24257811]

13. Yamakura T, Sakimura K, Shimoji K. The stereoselective effects of ketamine isomers on heteromeric N-methyl-d-aspartate receptor channels. Anesth Analg. 2000; 91(1):225–229. [PubMed: 10866917]

14. Dravid SM, Erreger K, Yuan H, Nicholson K, Le P, Lyuboslavsky P, Almonte A, Murray E, Mosely C, Barber J, French A, et al. Subunit-specific mechanisms and proton sensitivity of NMDA receptor channel block. J Physiol. 2007; 581(Pt 1):107–128. [PubMed: 17303642]

15. Gilling KE, Jatzke C, Hechenberger M, Parsons CG. Potency, voltage-dependency, agonist concentration-dependency, blocking kinetics and partial untrapping of the uncompetitive N-methyl-d-aspartate (NMDA) channel blocker memantine at human nmda (GluN1/GluN2a) receptors. Neuropharmacology. 2009; 56(5):866–875. [PubMed: 19371579]

16. Kotermanski SE, Johnson JW. Mg^{2+} imparts nmda receptor subtype selectivity to the alzheimer's drug memantine. J Neurosci. 2009; 29(9):2774–2779. [PubMed: 19261873]

17. Otton HJ, Lawson McLean A, Pannozzo MA, Davies CH, Wyllie DJ. Quantification of the Mg^{2+}-induced potency shift of amantadine and memantine voltage-dependent block in human recombinant GluN1/GluN2a NMDARs. Neuropharmacology. 2011; 60(2-3):388–396. [PubMed: 20955720]

18*. Nikolaev MV, Magazanik LG, Tikhonov DB. Influence of external magnesium ions on the NMDA receptor channel block by different types of organic cations. Neuropharmacology. 2012; 62(5-6):2078–2085. The powerful effect of Mg^{2+} on NMDAR inhibition by organic channel blockers was found to differ among channel blockers. [PubMed: 22261381]

19. Gass JT, Olive MF. Glutamatergic substrates of drug addiction and alcoholism. Biochemical pharmacology. 2008; 75(1):218–265. [PubMed: 17706608]

20. Winblad B, Gauthier S, Astrom D, Stender K. Memantine benefits functional abilities in moderate to severe alzheimer's disease. J Nutr Health Aging. 2010; 14(9):770–774. [PubMed: 21085908]

21. Wilkinson D. A review of the effects of memantine on clinical progression in alzheimer's disease. Int J Geriatr Psychiatry. 2012; 27(8):769–776. [PubMed: 21964871]

22. Krystal JH, D'Souza DC, Mathalon D, Perry E, Belger A, Hoffman R. NMDA receptor antagonist effects, cortical glutamatergic function, and schizophrenia: Toward a paradigm shift in medication development. Psychopharmacology (Berl). 2003; 169(3-4):215–233. [PubMed: 12955285]

23. Corazza O, Assi S, Schifano F. From "special k" to "special m": The evolution of the recreational use of ketamine and methoxetamine. CNS Neurosci Ther. 2013; 19(6):454–460. [PubMed: 23421859]

24. Krystal JH, Sanacora G, Duman RS. Rapid-acting glutamatergic antidepressants: The path to ketamine and beyond. Biol Psychiatry. 2013; 73(12):1133–1141. [PubMed: 23726151]

25. Prommer EE. Ketamine for pain: An update of uses in palliative care. J Palliat Med. 2012; 15(4): 474–483. [PubMed: 22500483]

26. Persson J. Ketamine in pain management. CNS Neurosci Ther. 2013; 19(6):396–402. [PubMed: 23663314]

27. Pringle A, Parsons E, Cowen LG, McTavish SF, Cowen PJ, Harmer CJ. Using an experimental medicine model to understand the antidepressant potential of the n-methyl-d-aspartic acid (nmda) receptor antagonist memantine. J Psychopharmacol. 2012; 26(11):1417–1423. [PubMed: 22596208]

28. Sani G, Serra G, Kotzalidis GD, Romano S, Tamorri SM, Manfredi G, Caloro M, Telesforo CL, Caltagirone SS, Panaccione I, Simonetti A, et al. The role of memantine in the treatment of psychiatric disorders other than the dementias: A review of current preclinical and clinical evidence. CNS drugs. 2012; 26(8):663–690. [PubMed: 22784018]

29. Alviar MJ, Hale T, Dungca M. Pharmacologic interventions for treating phantom limb pain. Cochrane database of systematic reviews. 2011; (12):CD006380. [PubMed: 22161403]

30. Bubenikova-Valesova V, Horacek J, Vrajova M, Hoschl C. Models of schizophrenia in humans and animals based on inhibition of NMDA receptors. Neurosci Biobehav Rev. 2008; 32(5):1014–1023. [PubMed: 18471877]

31. Moghaddam B, Krystal JH. Capturing the angel in "angel dust": Twenty years of translational neuroscience studies of NMDA receptor antagonists in animals and humans. Schizophrenia bulletin. 2012; 38(5):942–949. [PubMed: 22899397]

32. Creeley C, Wozniak DF, Labruyere J, Taylor GT, Olney JW. Low doses of memantine disrupt memory in adult rats. J Neurosci. 2006; 26(15):3923–3932. [PubMed: 16611808]

33. Koros E, Rosenbrock H, Birk G, Weiss C, Sams-Dodd F. The selective mGlu5 receptor antagonist mtep, similar to NMDA receptor antagonists, induces social isolation in rats. Neuropsychopharmacology. 2007; 32(3):562–576. [PubMed: 16794564]

34. More L, Gravius A, Nagel J, Valastro B, Greco S, Danysz W. Therapeutically relevant plasma concentrations of memantine produce significant l-N-methyl-d-aspartate receptor occupation and do not impair learning in rats. Behavioural pharmacology. 2008; 19(7):724–734. [PubMed: 18797249]

35. Smith JW, Gastambide F, Gilmour G, Dix S, Foss J, Lloyd K, Malik N, Tricklebank M. A comparison of the effects of ketamine and phencyclidine with other antagonists of the NMDA receptor in rodent assays of attention and working memory. Psychopharmacology. 2011; 217(2): 255–269. [PubMed: 21484239]

36*. Kotermanski SE, Johnson JW, Thiels E. Comparison of behavioral effects of the NMDA receptor channel blockers memantine and ketamine in rats. Pharmacology, biochemistry, and behavior. 2013; 109:67–76. The behavioral effects of memantine and ketamine were compared at two time points after administration; the weak time dependence observed suggested that pharmacokinetics play a minor role in the drugs' behavioral effects.

37*. Cottone P, Iemolo A, Narayan AR, Kwak J, Momaney D, Sabino V. The uncompetitive NMDA receptor antagonists ketamine and memantine preferentially increase the choice for a small, immediate reward in low-impulsive rats. Psychopharmacology (Berl). 2013; 226(1):127–138. The effects of memantine and ketamine on impulsive choice in rats were directly compared, and found to be remarkably similar. [PubMed: 23104264]

38. Wise LE, Lichtman AH. The uncompetitive N-methyl-D-aspartate (NMDA) receptor antagonist memantine prolongs spatial memory in a rat delayed radial-arm maze memory task. European journal of pharmacology. 2007; 575(1-3):98–102. [PubMed: 17850786]

39. Yuede CM, Dong H, Csernansky JG. Anti-dementia drugs and hippocampal-dependent memory in rodents. Behav Pharmacol. 2007; 18(5-6):347–363. [PubMed: 17762506]

40. Zoladz PR, Campbell AM, Park CR, Schaefer D, Danysz W, Diamond DM. Enhancement of long-term spatial memory in adult rats by the noncompetitive NMDA receptor antagonists, memantine and neramexane. Pharmacology, biochemistry, and behavior. 2006; 85(2):298–306.

41*. Sabino V, Narayan AR, Zeric T, Steardo L, Cottone P. mTOR activation is required for the anti-alcohol effect of ketamine, but not memantine, in alcohol-preferring rats. Behav Brain Res. 2013; 247:9–16. Both memantine and ketamine reduced ethanol consumption in alcohol-preferring rats. However, inhibition of mTOR reversed the effects of ketamine but not of memantine, suggesting that the drugs' effects depend on divergent pathways. [PubMed: 23466691]

42. Newman EL, Chu A, Bahamon B, Takahashi A, Debold JF, Miczek KA. NMDA receptor antagonism: Escalation of aggressive behavior in alcohol-drinking mice. Psychopharmacology (Berl). 2012; 224(1):167–177. [PubMed: 22588250]

43**. Gideons ES, Kavalali ET, Monteggia LM. Mechanisms underlying differential effectiveness of memantine and ketamine in rapid antidepressant responses. Proc Natl Acad Sci U S A. 2014; 111(23):8649–8654. Comparison of memantine and ketamine revealed that only ketamine demonstrated antidepressant-like effects in mice; ketamine inhibited synaptic NMDAR responses more effectively than memantine in the presence of Mg^{2+}; ketamine but not memantine affected downstream intracellular cascades associated with antidepressant action. [PubMed: 24912158]

44. Grant KA, Colombo G, Grant J, Rogawski MA. Dizocilpine-like discriminative stimulus effects of low-affinity uncompetitive NMDA antagonists. Neuropharmacology. 1996; 35(12):1709–1719. [PubMed: 9076750]

45. Swedberg MD, Ellgren M, Raboisson P. mGluR5 antagonist-induced psychoactive properties: MTEP drug discrimination, a pharmacologically selective non-NMDA effect with apparent lack of reinforcing properties. J Pharmacol Exp Ther. 2014; 349(1):155–164. [PubMed: 24472725]

46. Kocsis B, Brown RE, McCarley RW, Hajos M. Impact of ketamine on neuronal network dynamics: Translational modeling of schizophrenia-relevant deficits. CNS Neurosci Ther. 2013; 19(6):437–447. [PubMed: 23611295]

47. Zhang Y, Yoshida T, Katz DB, Lisman JE. NMDAR antagonist action in thalamus imposes delta oscillations on the hippocampus. Journal of neurophysiology. 2012; 107(11):3181–3189. [PubMed: 22423006]

48*. Hiyoshi T, Kambe D, Karasawa J, Chaki S. Differential effects of NMDA receptor antagonists at lower and higher doses on basal gamma band oscillation power in rat cortical electroencephalograms. Neuropharmacology. 2014; 85:384–396. Both memantine and ketamine were found to increase gamma oscillation power in rat cortical electroencephalogram recording, but only ketamine increased delta oscillations. [PubMed: 24907590]

49. Dedeurwaerdere S, Wintmolders C, Straetemans R, Pemberton D, Langlois X. Memantine-induced brain activation as a model for the rapid screening of potential novel antipsychotic compounds: Exemplified by activity of an mGlu2/3 receptor agonist. Psychopharmacology. 2011; 214(2):505–514. [PubMed: 21057775]

50. Lisman JE, Coyle JT, Green RW, Javitt DC, Benes FM, Heckers S, Grace AA. Circuit-based framework for understanding neurotransmitter and risk gene interactions in schizophrenia. Trends Neurosci. 2008; 31(5):234–242. [PubMed: 18395805]

51. Anticevic A, Cole MW, Repovs G, Savic A, Driesen NR, Yang G, Cho YT, Murray JD, Glahn DC, Wang XJ, Krystal JH. Connectivity, pharmacology, and computation: Toward a mechanistic understanding of neural system dysfunction in schizophrenia. Frontiers in psychiatry. 2013; 4:169. [PubMed: 24399974]

52. Schmitt HP. On the paradox of ion channel blockade and its benefits in the treatment of alzheimer disease. Med Hypotheses. 2005; 65(2):259–265. [PubMed: 15922097]

53. Kinney JW, Davis CN, Tabarean I, Conti B, Bartfai T, Behrens MM. A specific role for NR2A-containing nmda receptors in the maintenance of parvalbumin and GAD67 immunoreactivity in cultured interneurons. J Neurosci. 2006; 26(5):1604–1615. [PubMed: 16452684]

54. Behrens MM, Ali SS, Dao DN, Lucero J, Shekhtman G, Quick KL, Dugan LL. Ketamine-induced loss of phenotype of fast-spiking interneurons is mediated by NADPH-oxidase. Science. 2007; 318(5856):1645–1647. [PubMed: 18063801]

55. Zhou Z, Zhang G, Li X, Liu X, Wang N, Qiu L, Liu W, Zuo Z, Yang J. Loss of phenotype of parvalbumin interneurons in rat prefrontal cortex is involved in antidepressant- and propsychotic-like behaviors following acute and repeated ketamine administration. Mol Neurobiol. 2014

56. Lodge DJ, Behrens MM, Grace AA. A loss of parvalbumin-containing interneurons is associated with diminished oscillatory activity in an animal model of schizophrenia. J Neurosci. 2009; 29(8): 2344–2354. [PubMed: 19244511]

57. Volman V, Behrens MM, Sejnowski TJ. Downregulation of parvalbumin at cortical GABA synapses reduces network gamma oscillatory activity. J Neurosci. 2011; 31(49):18137–18148. [PubMed: 22159125]

58. Martina M, Comas T, Mealing GA. Selective pharmacological modulation of pyramidal neurons and interneurons in the CA1 region of the rat hippocampus. Front Pharmacol. 2013; 4:24. [PubMed: 23493925]

59. Monyer H, Burnashev N, Laurie DJ, Sakmann B, Seeburg PH. Developmental and regional expression in the rat brain and functional properties of four NMDA receptors. Neuron. 1994; 12(3):529–540. [PubMed: 7512349]

60. Standaert DG, Landwehrmeyer GB, Kerner JA, Penney JB Jr, Young AB. Expression of NMDAR2D glutamate receptor subunit mRNA in neurochemically identified interneurons in the rat neostriatum, neocortex and hippocampus. Brain Res Mol Brain Res. 1996; 42(1):89–102. [PubMed: 8915584]

61. Volbracht C, van Beek J, Zhu C, Blomgren K, Leist M. Neuroprotective properties of memantine in different in vitro and in vivo models of excitotoxicity. The European journal of neuroscience. 2006; 23(10):2611–2622. [PubMed: 16817864]

62. Wang C, Liu F, Patterson TA, Paule MG, Slikker W Jr. Preclinical assessment of ketamine. CNS Neurosci Ther. 2013; 19(6):448–453. [PubMed: 23462308]

63**. Emnett CM, Eisenman LN, Taylor AM, Izumi Y, Zorumski CF, Mennerick S. Indistinguishable synaptic pharmacodynamics of the N-methyl-d-aspartate receptor channel blockers memantine and ketamine. Mol Pharmacol. 2013; 84(6):935–947. In contrast to popular hypotheses, memantine and ketamine were found to affect synaptic NMDAR responses almost identically in the absence of Mg^{2+}; both drugs were neuroprotective in oxygen glucose deprivation experiments, although ketamine was slightly more effective. [PubMed: 24101301]

64. Gilmour G, Pioli EY, Dix SL, Smith JW, Conway MW, Jones WT, Loomis S, Mason R, Shahabi S, Tricklebank MD. Diverse and often opposite behavioural effects of NMDA receptor antagonists in rats: Implications for "NMDA antagonist modelling" of schizophrenia. Psychopharmacology (Berl). 2009; 205(2):203–216. [PubMed: 19421743]

65. Lord B, Wintmolders C, Langlois X, Nguyen L, Lovenberg T, Bonaventure P. Comparison of the ex vivo receptor occupancy profile of ketamine to several NMDA receptor antagonists in mouse hippocampus. Eur J Pharmacol. 2013; 715(1-3):21–25. [PubMed: 23872376]

66. Krystal JH, Karper LP, Seibyl JP, Freeman GK, Delaney R, Bremner JD, Heninger GR, Bowers MB Jr, Charney DS. Subanesthetic effects of the noncompetitive NMDA antagonist, ketamine, in humans. Psychotomimetic, perceptual, cognitive, and neuroendocrine responses. Arch Gen Psychiatry. 1994; 51(3):199–214. [PubMed: 8122957]

67. Nagels A, Kirner-Veselinovic A, Wiese R, Paulus FM, Kircher T, Krach S. Effects of ketamine-induced psychopathological symptoms on continuous overt rhyme fluency. Eur Arch Psychiatry Clin Neurosci. 2012; 262(5):403–414. [PubMed: 22189657]

68. Absalom AR, Lee M, Menon DK, Sharar SR, De Smet T, Halliday J, Ogden M, Corlett P, Honey GD, Fletcher PC. Predictive performance of the domino, hijazi, and clements models during low-dose target-controlled ketamine infusions in healthy volunteers. Br J Anaesth. 2007; 98(5):615–623. [PubMed: 17389691]

69. Hendrickson HP, Whaley EC, Owens SM. A validated liquid chromatographic/tandem mass spectrometric method for the determination of phencyclidine in microliter samples of rat serum. J Mass Spectrom. 2005; 40(1):19–24. [PubMed: 15584009]

70. Rogawski MA, Wenk GL. The neuropharmacological basis for the use of memantine in the treatment of alzheimer's disease. CNS Drug Reviews. 2003; 9(3):275–308. [PubMed: 14530799]

71. Lu CW, Lin TY, Wang SJ. Memantine depresses glutamate release through inhibition of voltage-dependent Ca^{2+} entry and protein kinase C in rat cerebral cortex nerve terminals: An NMDA receptor-independent mechanism. Neurochem Int. 2010; 57(2):168–176. [PubMed: 20493916]

72. McAllister J, Ghosh S, Berry D, Park M, Sadeghi S, Wang KX, Parker WD, Swerdlow RH. Effects of memantine on mitochondrial function. Biochemical pharmacology. 2008; 75(4):956–964. [PubMed: 18053965]

73. Buisson B, Bertrand D. Open-channel blockers at the human alpha4beta2 neuronal nicotinic acetylcholine receptor. Molecular Pharmacology. 1998; 53(3):555–563. [PubMed: 9495824]

74. Maskell PD, Speder P, Newberry NR, Bermudez I. Inhibition of human alpha 7 nicotinic acetylcholine receptors by open channel blockers of N-methyl-d-aspartate receptors. British Journal of Pharmacology. 2003; 140(7):1313–1319. [PubMed: 14645141]

75. Aracava Y, Pereira EF, Maelicke A, Albuquerque EX. Memantine blocks alpha7* nicotinic acetylcholine receptors more potently than N-methyl-d-aspartate receptors in rat hippocampal neurons. Journal of Pharmacology & Experimental Therapeutics. 2005; 312(3):1195–1205. [PubMed: 15522999]

76. Lee RH, Tseng TY, Wu CY, Chen PY, Chen MF, Kuo JS, Lee TJ. Memantine inhibits alpha3beta2-nachrs-mediated nitrergic neurogenic vasodilation in porcine basilar arteries. PLoS One. 2012; 7(7):e40326. [PubMed: 22792283]

77. Rammes G, Rupprecht R, Ferrari U, Zieglgansberger W, Parsons CG. The N-methyl-d-aspartate receptor channel blockers memantine, mrz 2/579 and other amino-alkyl-cyclohexanes antagonise 5-ht(3) receptor currents in cultured hek-293 and n1e-115 cell systems in a non-competitive manner. Neurosci Lett. 2001; 306(1-2):81–84. [PubMed: 11403963]

78. Kapur S, Seeman P. NMDA receptor antagonists ketamine and PCP have direct effects on the dopamine D(2) and serotonin 5-HT(2)receptors-implications for models of schizophrenia. Molecular psychiatry. 2002; 7(8):837–844. [PubMed: 12232776]

79. Chen X, Shu S, Bayliss DA. HCN1 channel subunits are a molecular substrate for hypnotic actions of ketamine. J Neurosci. 2009; 29(3):600–609. [PubMed: 19158287]

80. Lipton SA. Paradigm shift in neuroprotection by NMDA receptor blockade: Memantine and beyond. Nat Rev Drug Discov. 2006; 5(2):160–170. [PubMed: 16424917]

81. Nisijima K, Kuboshima K, Shioda K, Yoshino T, Iwamura T, Kato S. Memantine attenuates 3,4-methylenedioxymethamphetamine-induced hyperthermia in rats. Neurosci Lett. 2012; 531(2):198–203. [PubMed: 23142720]

82. Ebert B, Mikkelsen S, Thorkildsen C, Borgbjerg FM. Norketamine, the main metabolite of ketamine, is a non-competitive NMDA receptor antagonist in the rat cortex and spinal cord. Eur J Pharmacol. 1997; 333(1):99–104. [PubMed: 9311667]

83. Mion G, Villevieille T. Ketamine pharmacology: An update (pharmacodynamics and molecular aspects, recent findings). CNS Neurosci Ther. 2013; 19(6):370–380. [PubMed: 23575437]

84. Paul RK, Singh NS, Khadeer M, Moaddel R, Sanghvi M, Green CE, O'Loughlin K, Torjman MC, Bernier M, Wainer IW. (R,S)-ketamine metabolites (R,S)-norketamine and (2S,6S)-hydroxynorketamine increase the mammalian target of rapamycin function. Anesthesiology. 2014; 121(1):149–159. [PubMed: 24936922]

85. Moaddel R, Abdrakhmanova G, Kozak J, Jozwiak K, Toll L, Jimenez L, Rosenberg A, Tran T, Xiao Y, Zarate CA, Wainer IW. Sub-anesthetic concentrations of (R,S)-ketamine metabolites inhibit acetylcholine-evoked currents in alpha7 nicotinic acetylcholine receptors. Eur J Pharmacol. 2013; 698(1-3):228–234. [PubMed: 23183107]

86. Gladding CM, Raymond LA. Mechanisms underlying NMDA receptor synaptic/extrasynaptic distribution and function. Mol Cell Neurosci. 2011; 48(4):308–320. [PubMed: 21600287]

87. Hardingham GE, Bading H. Synaptic versus extrasynaptic NMDA receptor signalling: Implications for neurodegenerative disorders. Nat Rev Neurosci. 2010; 11(10):682–696. [PubMed: 20842175]

88. Parsons MP, Raymond LA. Extrasynaptic NMDA receptor involvement in central nervous system disorders. Neuron. 2014; 82(2):279–293. [PubMed: 24742457]

89. Le Meur K, Galante M, Angulo MC, Audinat E. Tonic activation of nmda receptors by ambient glutamate of non-synaptic origin in the rat hippocampus. J Physiol. 2007; 580(Pt. 2):373–383. [PubMed: 17185337]

90. Fleming TM, Scott V, Naskar K, Joe N, Brown CH, Stern JE. State-dependent changes in astrocyte regulation of extrasynaptic NMDA receptor signalling in neurosecretory neurons. J Physiol. 2011; 589(Pt 16):3929–3941. [PubMed: 21690192]

91. Povysheva NV, Johnson JW. Tonic NMDA receptor-mediated current in prefrontal cortical pyramidal cells and fast-spiking interneurons. Journal of neurophysiology. 2012; 107(8):2232–2243. [PubMed: 22236713]

92. Papouin T, Ladepeche L, Ruel J, Sacchi S, Labasque M, Hanini M, Groc L, Pollegioni L, Mothet JP, Oliet SH. Synaptic and extrasynaptic NMDA receptors are gated by different endogenous coagonists. Cell. 2012; 150(3):633–646. [PubMed: 22863013]

93*. Wroge CM, Hogins J, Eisenman L, Mennerick S. Synaptic NMDA receptors mediate hypoxic excitotoxic death. The Journal of neuroscience : the official journal of the Society for Neuroscience. 2012; 32(19):6732–6742. Reassessment of the roles of synaptic and extrasynaptic NMDARs in neurotoxicity and neuroprotection led to the conclusion that synaptic as well as extrasynaptic NMDAR activation mediates hypoxic excitotoxicity. [PubMed: 22573696]

94. Zhou X, Hollern D, Liao J, Andrechek E, Wang H. NMDA receptor-mediated excitotoxicity depends on the coactivation of synaptic and extrasynaptic receptors. Cell death & disease. 2013; 4:e560. [PubMed: 23538441]

95. Zhou X, Ding Q, Chen Z, Yun H, Wang H. Involvement of the GluN2A and GluN2B subunits in synaptic and extrasynaptic N-methyl-d-aspartate receptor function and neuronal excitotoxicity. J Biol Chem. 2013; 288(33):24151–24159. [PubMed: 23839940]

96. Leveille F, El Gaamouch F, Gouix E, Lecocq M, Lobner D, Nicole O, Buisson A. Neuronal viability is controlled by a functional relation between synaptic and extrasynaptic NMDA receptors. Faseb J. 2008; 22(12):4258–4271. [PubMed: 18711223]

97. Papadia S, Soriano FX, Leveille F, Martel MA, Dakin KA, Hansen HH, Kaindl A, Sifringer M, Fowler J, Stefovska V, McKenzie G, et al. Synaptic NMDA receptor activity boosts intrinsic antioxidant defenses. Nat Neurosci. 2008; 11(4):476–487. [PubMed: 18344994]

98. Okamoto S, Pouladi MA, Talantova M, Yao D, Xia P, Ehrnhoefer DE, Zaidi R, Clemente A, Kaul M, Graham RK, Zhang D, et al. Balance between synaptic versus extrasynaptic NMDA receptor activity influences inclusions and neurotoxicity of mutant huntingtin. Nat Med. 2009; 15(12):1407–1413. [PubMed: 19915593]

99*. Xia P, Chen HS, Zhang D, Lipton SA. Memantine preferentially blocks extrasynaptic over synaptic NMDA receptor currents in hippocampal autapses. The Journal of neuroscience : the official journal of the Society for Neuroscience. 2010; 30(33):11246–11250. Based on measurements using hippocampal autaptic cultures, memantine was found to inhibit extrasynaptic NMDARs more effectively than synaptic NMDARs. [PubMed: 20720132]

100. Milnerwood AJ, Gladding CM, Pouladi MA, Kaufman AM, Hines RM, Boyd JD, Ko RW, Vasuta OC, Graham RK, Hayden MR, Murphy TH, et al. Early increase in extrasynaptic NMDA receptor signaling and expression contributes to phenotype onset in huntington's disease mice. Neuron. 2010; 65(2):178–190. [PubMed: 20152125]

101. Kaufman AM, Milnerwood AJ, Sepers MD, Coquinco A, She K, Wang L, Lee H, Craig AM, Cynader M, Raymond LA. Opposing roles of synaptic and extrasynaptic NMDA receptor signaling in cocultured striatal and cortical neurons. J Neurosci. 2012; 32(12):3992–4003. [PubMed: 22442066]

102*. Dau A, Gladding CM, Sepers MD, Raymond LA. Chronic blockade of extrasynaptic NMDA receptors ameliorates synaptic dysfunction and pro-death signaling in huntington disease transgenic mice. Neurobiol Dis. 2014; 62:533–542. The neuroprotective effects of memantine were found to be associated with blockade of extrasynaptic NMDARs; signaling pathways involved in excitotoxicity were explored. [PubMed: 24269729]

103. Wild AR, Akyol E, Brothwell SL, Kimkool P, Skepper JN, Gibb AJ, Jones S. Memantine block depends on agonist presentation at the NMDA receptor in substantia nigra pars compacta dopamine neurones. Neuropharmacology. 2013; 73:138–146. [PubMed: 23727219]

104. Frankiewicz T, Parsons CG. Memantine restores long term potentiation impaired by tonic N-methyl-d-aspartate (NMDA) receptor activation following reduction of Mg^{2+} in hippocampal slices. Neuropharmacology. 1999; 38(9):1253–1259. [PubMed: 10471078]

105**. Autry AE, Adachi M, Nosyreva E, Na ES, Los MF, Cheng PF, Kavalali ET, Monteggia LM. NMDA receptor blockade at rest triggers rapid behavioural antidepressant responses. Nature. 2011; 475(7354):91–95. The mechanisms by which synaptic NMDAR inhibition by ketamine can lead to rapid and long-lasting antidepressant effects were explored. [PubMed: 21677641]

106. Nosyreva E, Szabla K, Autry AE, Ryazanov AG, Monteggia LM, Kavalali ET. Acute suppression of spontaneous neurotransmission drives synaptic potentiation. J Neurosci. 2013; 33(16):6990–7002. [PubMed: 23595756]

107. Tovar KR, Westbrook GL. The incorporation of NMDA receptors with a distinct subunit composition at nascent hippocampal synapses in vitro. J Neurosci. 1999; 19(10):4180–4188. [PubMed: 10234045]

108. Steigerwald F, Schulz TW, Schenker LT, Kennedy MB, Seeburg PH, Kohr G. C-terminal truncation of NR2A subunits impairs synaptic but not extrasynaptic localization of NMDA receptors. The Journal of neuroscience : the official journal of the Society for Neuroscience. 2000; 20(12):4573–4581. [PubMed: 10844027]

109. Groc L, Heine M, Cousins SL, Stephenson FA, Lounis B, Cognet L, Choquet D. NMDA receptor surface mobility depends on NR2A-2B subunits. Proceedings of the National Academy of Sciences of the United States of America. 2006; 103(49):18769–18774. [PubMed: 17124177]

110. Thomas CG, Miller AJ, Westbrook GL. Synaptic and extrasynaptic NMDA receptor NR2 subunits in cultured hippocampal neurons. Journal of neurophysiology. 2006; 95(3):1727–1734. [PubMed: 16319212]

111. Harris AZ, Pettit DL. Extrasynaptic and synaptic NMDA receptors form stable and uniform pools in rat hippocampal slices. The Journal of physiology. 2007; 584(Pt 2):509–519. [PubMed: 17717018]

112*. Hansen KB, Ogden KK, Yuan H, Traynelis SF. Distinct functional and pharmacological properties of triheteromeric GluN1/GluN2A/GluN2B NMDA receptors. Neuron. 2014; 81(5):1084–1096. An ingenious approach for study in isolation of triheteromeric NMDARs, which may be the predominant types of NMDARs in vertebrate nervous systems, is described. [PubMed: 24607230]

113. Momiyama A. Distinct synaptic and extrasynaptic NMDA receptors identified in dorsal horn neurones of the adult rat spinal cord. J Physiol. 2000; 523(Pt 3):621–628. [PubMed: 10718742]

114. Brickley SG, Misra C, Mok MH, Mishina M, Cull-Candy SG. NR2B and NR2D subunits coassemble in cerebellar golgi cells to form a distinct NMDA receptor subtype restricted to extrasynaptic sites. J Neurosci. 2003; 23(12):4958–4966. [PubMed: 12832518]

115. Lozovaya NA, Grebenyuk SE, Tsintsadze T, Feng B, Monaghan DT, Krishtal OA. Extrasynaptic NR2B and NR2D subunits of NMDA receptors shape 'superslow' afterburst epsc in rat hippocampus. J Physiol. 2004; 558(Pt 2):451–463. [PubMed: 15146049]

116. Harney SC, Jane DE, Anwyl R. Extrasynaptic NR2D-containing NMDARs are recruited to the synapse during LTP of NMDAR-EPSCs. J Neurosci. 2008; 28(45):11685–11694. [PubMed: 18987204]

117. Chen HS, Pellegrini JW, Aggarwal SK, Lei SZ, Warach S, Jensen FE, Lipton SA. Open-channel block of N-methyl-d-aspartate (NMDA) responses by memantine: Therapeutic advantage against NMDA receptor-mediated neurotoxicity. J Neurosci. 1992; 12(11):4427–4436. [PubMed: 1432103]

118. Gilling KE, Jatzke C, Parsons CG. Agonist concentration dependency of blocking kinetics but not equilibrium block of N-methyl-d-aspartate receptors by memantine. Neuropharmacology. 2007; 53(3):415–420. [PubMed: 17632186]

119. Blanpied TA, Boeckman FA, Aizenman E, Johnson JW. Trapping channel block of NMDA-activated responses by amantadine and memantine. J Neurophysiol. 1997; 77(1):309–323. [PubMed: 9120573]

120. Mealing GA, Lanthorn TH, Murray CL, Small DL, Morley P. Differences in degree of trapping of low-affinity uncompetitive N-methyl-d-aspartic acid receptor antagonists with similar kinetics of block. J Pharmacol Exp Ther. 1999; 288(1):204–210. [PubMed: 9862772]

121. Chen HSV, Lipton SA. Pharmacological implications of two distinct mechanisms of interaction of memantine with N-methyl-d-aspartate-gated channels. Journal of Pharmacology and Experimental Therapeutics. 2005; 314(3):961–971. [PubMed: 15901795]

122. Kotermanski SE, Wood JT, Johnson JW. Memantine binding to a superficial site on NMDA receptors contributes to partial trapping. J Physiol. 2009; 587(Pt 19):4589–4604. [PubMed: 19687120]

123. Antonov SM, Johnson JW. Voltage-dependent interaction of open-channel blocking molecules with gating of NMDA receptors in rat cortical neurons. J Physiol (Lond). 1996; 493(Pt 2):425–445. [PubMed: 8782107]

124. Sobolevsky AI, Koshelev SG, Khodorov BI. Probing of NMDA channels with fast blockers. J Neurosci. 1999; 19(24):10611–10626. [PubMed: 10594045]

125. Blanpied TA, Clarke RJ, Johnson JW. Amantadine inhibits NMDA receptors by accelerating channel closure during channel block. J Neurosci. 2005; 25(13):3312–3322. [PubMed: 15800186]

126. Yuan H, Erreger K, Dravid SM, Traynelis SF. Conserved structural and functional control of N-methyl-d-aspartate receptor gating by transmembrane domain m3. J Biol Chem. 2005; 280(33): 29708–29716. [PubMed: 15970596]

127. Neher E, Steinbach JH. Local anaesthetics transiently block currents through single acetylcholine-receptor channels. J Physiol (Lond). 1978; 277:153–176. [PubMed: 306437]

128. Benveniste M, Mayer ML. Trapping of glutamate and glycine during open channel block of rat hippocampal neuron NMDA receptors by 9-aminoacridine. J Physiol. 1995; 483(Pt 2):367–384. [PubMed: 7650609]

129. Johnson JW, Qian A. Interaction between channel blockers and channel gating of NMDA receptors. Biol Membr. 2002; 19(1):17–22.

130*. Karakas E, Furukawa H. Crystal structure of a heterotetrameric NMDA receptor ion channel. Science. 2014; 344(6187):992–997. See next reference. [PubMed: 24876489]

131*. Lee CH, Lu W, Michel JC, Goehring A, Du J, Song X, Gouaux E. NMDA receptor structures reveal subunit arrangement and pore architecture. Nature. 2014; 511(7508):191–197. References 130 and 131 are the first nearly complete NMDAR crystal structures published to date; the availability of improved structures will lead to better understanding of the mechanism of action of NMDAR ligands. [PubMed: 25008524]

132. Siegler Retchless B, Gao W, Johnson JW. A single GluN2 subunit residue controls NMDA receptor channel properties via intersubunit interaction. Nature neuroscience. 2012; 15(3):406–413. S401–402.

133. Pan J, Chen Q, Willenbring D, Mowrey D, Kong XP, Cohen A, Divito CB, Xu Y, Tang P. Structure of the pentameric ligand-gated ion channel glic bound with anesthetic ketamine. Structure. 2012; 20(9):1463–1469. [PubMed: 22958642]

134. Yamakura T, Mori H, Masaki H, Shimoji K, Mishina M. Different sensitivities of NMDA receptor channel subtypes to non-competitive antagonists. Neuroreport. 1993; 4(6):687–690. [PubMed: 8347808]

135. Kashiwagi K, Masuko T, Nguyen CD, Kuno T, Tanaka I, Igarashi K, Williams K. Channel blockers acting at N-methyl-d-aspartate receptors: Differential effects of mutations in the vestibule and ion channel pore. Mol Pharmacol. 2002; 61(3):533–545. [PubMed: 11854433]

136. Humphrey W, Dalke A, Schulten K. Vmd: Visual molecular dynamics. J Mol Graph. 1996; 14(1): 33–38. 27–38. [PubMed: 8744570]

Curr Opin Pharmacol. Author manuscript; available in PMC 2016 February 01.

204

Highlights

- Memantine and ketamine block open NMDAR channels via apparently similar Mechanisms

- Memantine is a very well-tolerated drug approved for treatment of Alzheimer's disease

- Ketamine has rapid antidepressant effects, but replicates symptoms of schizophrenia

- The drugs' differential effects may require inhibition of distinct NMDAR populations
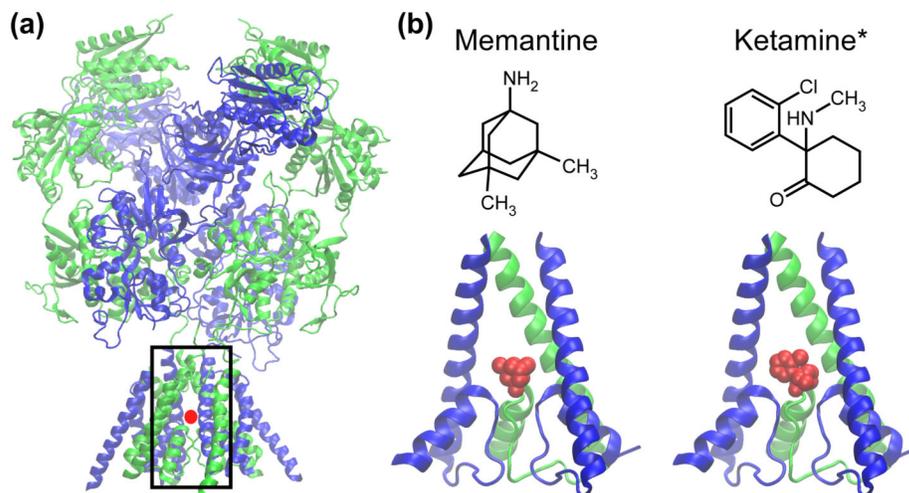
Figure 1.
Images of NMDAR channel blocked by memantine and ketamine. **(a)** Two nearly complete X-ray crystal structures of NMDARs composed of GluN1 and GluN2B subunits recently were published [130,131]. Here, one of the structures (Protein Data Bank (PDB) code 4TLM [131]) is shown with a red dot at the likely approximate location of memantine and ketamine binding sites. The black box indicates the area of the receptor blown up in (b). **(b)** Top, the structure of memantine (left) and ketamine (right). *, ketamine, which has two enantiomers ((S)- and (R)-ketamine), is depicted without chirality in this planar representation. Bottom, a view of the channel region of an NMDAR composed of GluN1 and GluN2A subunits with memantine (left) and with (R)-ketamine (right) blocking the channel. The structure of the NMDAR channel region is based on the homology model of [132]; the memantine structure is from www.edinformatics.com; the (R)-ketamine structure is from PDB code 4F8H [133]. There are no structures of NMDARs with a resolved channel blocker; memantine and ketamine are placed with the charged nitrogen close to the critical NMDAR channel asparagines [121,134,135]. GluN1 subunits are shown in green and GluN2 subunits in blue. Structural images were prepared using the molecular visualization program VMD [136].

BIBLIOGRAPHY

Abdallah CG, Averill LA and Krystal JH (2015) Ketamine as a promising prototype for a new generation of rapid-acting antidepressants. Ann N Y Acad Sci.

Akazawa C, Shigemoto R, Bessho Y, Nakanishi S and Mizuno N (1994) Differential expression of five N-methyl-D-aspartate receptor subunit mRNAs in the cerebellum of developing and adult rats. J Comp Neurol 347: 150-160.

Al-Hallaq RA, Conrads TP, Veenstra TD and Wenthold RJ (2007) NMDA Di-Heteromeric Receptor Populations and Associated Proteins in Rat Hippocampus. Journal of Neuroscience 27: 8334-8343.

Alviar MJ, Hale T and Dungca M (2011) Pharmacologic interventions for treating phantom limb pain. Cochrane Database Syst Rev: CD006380.

Amico-Ruvio Stacy A, Murthy Swetha E, Smith Thomas P and Popescu Gabriela K (2011) Zinc Effects on NMDA Receptor Gating Kinetics. Biophysical Journal 100: 1910-1918.

Amico-Ruvio SA, Paganelli MA, Myers JM and Popescu GK (2012) Ifenprodil effects on GluN2B-containing glutamate receptors. Mol Pharmacol 82: 1074-1081.

Amico-Ruvio SA and Popescu GK (2010) Stationary Gating of GluN1/GluN2B Receptors in Intact Membrane Patches. Biophysical Journal 98: 1160-1169.

Anitha M, Nandhu MS, Anju TR, Jes P and Paulose CS (2011) Targeting glutamate mediated excitotoxicity in Huntington's disease: neural progenitors and partial glutamate antagonist--memantine. Med Hypotheses 76: 138-140.

Antonov SM and Johnson JW (1996) Voltage-dependent interaction of open-channel blocking molecules with gating of NMDA receptors in rat cortical neurons. J Physiol 493 (Pt 2): 425-445.

Antonov SM and Johnson JW (1999) Permeant ion regulation of N-methyl-D-aspartate receptor channel block by Mg(2+). Proc Natl Acad Sci U S A 96: 14571-14576.

Arnth-Jensen N, Jabaudon D and Scanziani M (2002) Cooperation between independent hippocampal synapses is controlled by glutamate uptake. Nat Neurosci 5: 325-331.

Ascher P and Nowak L (1988) The role of divalent cations in the N-methyl-D-aspartate responses of mouse central neurones in culture. J Physiol 399: 247-266.

Auerbach A and Zhou Y (2005) Gating reaction mechanisms for NMDA receptor channels. J Neurosci 25: 7914-7923.

Autry AE, Adachi M, Nosyreva E, Na ES, Los MF, Cheng PF, Kavalali ET and Monteggia LM (2011) NMDA receptor blockade at rest triggers rapid behavioural antidepressant responses. Nature 475: 91-95.

Bading H (2013) Nuclear calcium signalling in the regulation of brain function. Nat Rev Neurosci 14: 593-608.

Banke TG, Dravid SM and Traynelis SF (2005) Protons trap NR1/NR2B NMDA receptors in a nonconducting state. J Neurosci 25: 42-51.

Banke TG and Traynelis SF (2003) Activation of NR1/NR2B NMDA receptors. Nat Neurosci 6: 144-152.

Barnham KJ, Masters CL and Bush AI (2004) Neurodegenerative diseases and oxidative stress. Nat Rev Drug Discov 3: 205-214.

Barria A and Malinow R (2005) NMDA Receptor Subunit Composition Controls Synaptic Plasticity by Regulating Binding to CaMKII. Neuron 48: 289-301.

Barygin OI, Gmiro VE, Kim K, Magazanik LG and Tikhonov DB (2009) Blockade of NMDA receptor channels by 9-aminoacridine and its derivatives. Neurosci Lett 451: 29-33.

Benveniste M, Mienville JM, Sernagor E and Mayer ML (1990) Concentration-jump experiments with NMDA antagonists in mouse cultured hippocampal neurons. J Neurophysiol 63: 1373-1384.

Berberich S, Punnakkal P, Jensen V, Pawlak V, Seeburg PH, Hvalby O and Kohr G (2005) Lack of NMDA receptor subtype selectivity for hippocampal long-term potentiation. J Neurosci 25: 6907-6910.

Bhatt JM, Prakash A, Suryavanshi PS and Dravid SM (2013) Effect of ifenprodil on GluN1/GluN2B N-methyl-D-aspartate receptor gating. Mol Pharmacol 83: 9-21.

Blanpied TA, Boeckman FA, Aizenman E and Johnson JW (1997) Trapping channel block of NMDA-activated responses by amantadine and memantine. J Neurophysiol 77: 309-323.

Blanpied TA, Clarke RJ and Johnson JW (2005) Amantadine inhibits NMDA receptors by accelerating channel closure during channel block. J Neurosci 25: 3312-3322.

Bolshakov KV, Gmiro VE, Tikhonov DB and Magazanik LG (2003) Determinants of trapping block of N-methyl-d-aspartate receptor channels. J Neurochem 87: 56-65.

Bolshakov KV, Kim KH, Potapjeva NN, Gmiro VE, Tikhonov DB, Usherwood PN, Mellor IR and Magazanik LG (2005) Design of antagonists for NMDA and AMPA receptors. Neuropharmacology 49: 144-155.

Bordji K, Becerril-Ortega J, Nicole O and Buisson A (2010) Activation of Extrasynaptic, But Not Synaptic, NMDA Receptors Modifies Amyloid Precursor Protein Expression Pattern and Increases Amyloid- Production. Journal of Neuroscience 30: 15927-15942.

Brigman JL, Wright T, Talani G, Prasad-Mulcare S, Jinde S, Seabold GK, Mathur P, Davis MI, Bock R, Gustin RM, Colbran RJ, Alvarez VA, Nakazawa K, Delpire E, Lovinger DM and Holmes A (2010) Loss of GluN2B-containing NMDA receptors in CA1 hippocampus and cortex impairs long-term depression, reduces dendritic spine density, and disrupts learning. J Neurosci 30: 4590-4600.

Burnashev N, Schoepfer R, Monyer H, Ruppersberg JP, Gunther W, Seeburg PH and Sakmann B (1992) Control by asparagine residues of calcium permeability and magnesium blockade in the NMDA receptor. Science 257: 1415-1419.

Burnashev N, Zhou Z, Neher E and Sakmann B (1995) Fractional calcium currents through recombinant GluR channels of the NMDA, AMPA and kainate receptor subtypes. J Physiol 485 (Pt 2): 403-418.

Chen HS and Lipton SA (1997) Mechanism of memantine block of NMDA-activated channels in rat retinal ganglion cells: uncompetitive antagonism. J Physiol 499 (Pt 1): 27-46.

Chen HS, Pellegrini JW, Aggarwal SK, Lei SZ, Warach S, Jensen FE and Lipton SA (1992) Open-channel block of N-methyl-D-aspartate (NMDA) responses by memantine: therapeutic advantage against NMDA receptor-mediated neurotoxicity. J Neurosci 12: 4427-4436.

Chen HSV and Lipton SA (2005) Pharmacological implications of two distinct mechanisms of interaction of memantine with N-methyl-D-aspartate-gated channels. Journal of Pharmacology and Experimental Therapeutics 314: 961-971.

Chen L, Durr KL and Gouaux E (2014) X-ray structures of AMPA receptor-cone snail toxin complexes illuminate activation mechanism. Science 345: 1021-1026.

Chen N, Moshaver A and Raymond LA (1997) Differential sensitivity of recombinant N-methyl-D-aspartate receptor subtypes to zinc inhibition. Mol Pharmacol 51: 1015-1023.

Chen N, Ren J, Raymond LA and Murphy TH (2001) Changes in agonist concentration dependence that are a function of duration of exposure suggest N-methyl-D-aspartate receptor nonsaturation during synaptic stimulation. Mol Pharmacol 59: 212-219.

Clarke RJ (2006) NMDA Receptor NR2 Subunit Dependence of the Slow Component of Magnesium Unblock. Journal of Neuroscience 26: 5825-5834.

Clarke RJ, Glasgow NG and Johnson JW (2013) Mechanistic and structural determinants of NMDA receptor voltage-dependent gating and slow Mg2+ unblock. J Neurosci 33: 4140-4150.

Clarke RJ and Johnson JW (2008) Voltage-dependent gating of NR1/2B NMDA receptors. The Journal of Physiology 586: 5727-5741.

Clements JD, Lester RA, Tong G, Jahr CE and Westbrook GL (1992) The time course of glutamate in the synaptic cleft. Science 258: 1498-1501.

Clements JD and Westbrook GL (1991) Activation kinetics reveal the number of glutamate and glycine binding sites on the N-methyl-D-aspartate receptor. Neuron 7: 605-613.

Collingridge GL, Isaac JT and Wang YT (2004) Receptor trafficking and synaptic plasticity. Nat Rev Neurosci 5: 952-962.

Collins S, Sigtermans MJ, Dahan A, Zuurmond WW and Perez RS (2010) NMDA receptor antagonists for the treatment of neuropathic pain. Pain Med 11: 1726-1742.

Cull-Candy SG and Leszkiewicz DN (2004) Role of distinct NMDA receptor subtypes at central synapses. Sci STKE 2004: re16.

Dau A, Gladding CM, Sepers MD and Raymond LA (2014) Chronic blockade of extrasynaptic NMDA receptors ameliorates synaptic dysfunction and pro-death signaling in Huntington disease transgenic mice. Neurobiol Dis 62: 533-542.

Dawe GB, Musgaard M, Andrews ED, Daniels BA, Aurousseau MR, Biggin PC and Bowie D (2013) Defining the structural relationship between kainate-receptor deactivation and desensitization. Nat Struct Mol Biol 20: 1054-1061.

Del Castillo J and Katz B (1957) Interaction at end-plate receptors between different choline derivatives. Proc R Soc Lond B Biol Sci 146: 369-381.

Delaney AJ, Sedlak PL, Autuori E, Power JM and Sah P (2013) Synaptic NMDA receptors in basolateral amygdala principal neurons are triheteromeric proteins: physiological role of GluN2B subunits. J Neurophysiol 109: 1391-1402.

Dilmore JG and Johnson JW (1998) Open channel block and alteration of N-methyl-D-aspartic acid receptor gating by an analog of phencyclidine. Biophys J 75: 1801-1816.

Dingledine R, Borges K, Bowie D and Traynelis SF (1999) The glutamate receptor ion channels. Pharmacol Rev 51: 7-61.

Doody R, Wirth Y, Schmitt F and Mobius HJ (2004) Specific functional effects of memantine treatment in patients with moderate to severe Alzheimer's disease. Dement Geriatr Cogn Disord 18: 227-232.

Dravid SM, Burger PB, Prakash A, Geballe MT, Yadav R, Le P, Vellano K, Snyder JP and Traynelis SF (2010) Structural Determinants of D-Cycloserine Efficacy at the NR1/NR2C NMDA Receptors. Journal of Neuroscience 30: 2741-2754.

Dravid SM, Erreger K, Yuan H, Nicholson K, Le P, Lyuboslavsky P, Almonte A, Murray E, Mosely C, Barber J, French A, Balster R, Murray TF and Traynelis SF (2007) Subunit-specific mechanisms and proton sensitivity of NMDA receptor channel block. J Physiol 581: 107-128.

Dravid SM, Prakash A and Traynelis SF (2008) Activation of recombinant NR1/NR2C NMDA receptors. The Journal of Physiology 586: 4425-4439.

Duman RS and Aghajanian GK (2012) Synaptic dysfunction in depression: potential therapeutic targets. Science 338: 68-72.

Durr KL, Chen L, Stein RA, De Zorzi R, Folea IM, Walz T, McHaourab HS and Gouaux E (2014) Structure and dynamics of AMPA receptor GluA2 in resting, pre-open, and desensitized states. Cell 158: 778-792.

Edmonds B and Colquhoun D (1992) Rapid decay of averaged single-channel NMDA receptor activations recorded at low agonist concentration. Proc Biol Sci 250: 279-286.

Ehlers MD, Fung ET, O'Brien RJ and Huganir RL (1998) Splice variant-specific interaction of the NMDA receptor subunit NR1 with neuronal intermediate filaments. J Neurosci 18: 720-730.

Ehlers MD, Zhang S, Bernhadt JP and Huganir RL (1996) Inactivation of NMDA receptors by direct interaction of calmodulin with the NR1 subunit. Cell 84: 745-755.

Emnett CM, Eisenman LN, Taylor AM, Izumi Y, Zorumski CF and Mennerick S (2013) Indistinguishable synaptic pharmacodynamics of the N-methyl-d-aspartate receptor channel blockers memantine and ketamine. Mol Pharmacol 84: 935-947.

Emre M, Tsolaki M, Bonuccelli U, Destee A, Tolosa E, Kutzelnigg A, Ceballos-Baumann A, Zdravkovic S, Bladstrom A and Jones R (2010) Memantine for patients with Parkinson's disease dementia or dementia with Lewy bodies: a randomised, double-blind, placebo-controlled trial. Lancet Neurol 9: 969-977.

Erreger K, Dravid SM, Banke TG, Wyllie DJ and Traynelis SF (2005) Subunit-specific gating controls rat NR1/NR2A and NR1/NR2B NMDA channel kinetics and synaptic signalling profiles. J Physiol 563: 345-358.

Erreger K, Geballe MT, Dravid SM, Snyder JP, Wyllie DJ and Traynelis SF (2005) Mechanism of partial agonism at NMDA receptors for a conformationally restricted glutamate analog. J Neurosci 25: 7858-7866.

Erreger K, Geballe MT, Kristensen A, Chen PE, Hansen KB, Lee CJ, Yuan H, Le P, Lyuboslavsky PN, Micale N, Jorgensen L, Clausen RP, Wyllie DJ, Snyder JP and

Traynelis SF (2007) Subunit-specific agonist activity at NR2A-, NR2B-, NR2C-, and NR2D-containing N-methyl-D-aspartate glutamate receptors. Mol Pharmacol 72: 907-920.

Erreger K and Traynelis SF (2008) Zinc inhibition of rat NR1/NR2A N-methyl-D-aspartate receptors. J Physiol 586: 763-778.

Fellin T, Pascual O, Gobbo S, Pozzan T, Haydon PG and Carmignoto G (2004) Neuronal synchrony mediated by astrocytic glutamate through activation of extrasynaptic NMDA receptors. Neuron 43: 729-743.

Ferrario CR, Ndukwe BO, Ren J, Satin LS and Goforth PB (2013) Stretch injury selectively enhances extrasynaptic, GluN2B-containing NMDA receptor function in cortical neurons. J Neurophysiol 110: 131-140.

Forsythe ID and Westbrook GL (1988) Slow excitatory postsynaptic currents mediated by N-methyl-D-aspartate receptors on cultured mouse central neurones. J Physiol 396: 515-533.

Foster KA, McLaughlin N, Edbauer D, Phillips M, Bolton A, Constantine-Paton M and Sheng M (2010) Distinct Roles of NR2A and NR2B Cytoplasmic Tails in Long-Term Potentiation. Journal of Neuroscience 30: 2676-2685.

Freudenthaler S, Meineke I, Schreeb KH, Boakye E, Gundert-Remy U and Gleiter CH (1998) Influence of urine pH and urinary flow on the renal excretion of memantine. Br J Clin Pharmacol 46: 541-546.

Freund TF, Buzsaki G, Leon A, Baimbridge KG and Somogyi P (1990) Relationship of neuronal vulnerability and calcium binding protein immunoreactivity in ischemia. Exp Brain Res 83: 55-66.

Garcia-Munoz M, Lopez-Huerta VG, Carrillo-Reid L and Arbuthnott GW (2015) Extrasynaptic glutamate NMDA receptors: key players in striatal function. Neuropharmacology 89: 54-63.

Gardoni F, Mauceri D, Malinverno M, Polli F, Costa C, Tozzi A, Siliquini S, Picconi B, Cattabeni F, Calabresi P and Di Luca M (2009) Decreased NR2B subunit synaptic levels cause impaired long-term potentiation but not long-term depression. J Neurosci 29: 669-677.

Gideons ES, Kavalali ET and Monteggia LM (2014) Mechanisms underlying differential effectiveness of memantine and ketamine in rapid antidepressant responses. Proc Natl Acad Sci U S A 111: 8649-8654.

Gilling KE, Jatzke C, Hechenberger M and Parsons CG (2009) Potency, voltage-dependency, agonist concentration-dependency, blocking kinetics and partial untrapping of the uncompetitive N-methyl-D-aspartate (NMDA) channel blocker memantine at human NMDA (GluN1/GluN2A) receptors. Neuropharmacology 56: 866-875.

Gilling KE, Jatzke C and Parsons CG (2007) Agonist concentration dependency of blocking kinetics but not equilibrium block of N-methyl-d-aspartate receptors by memantine. Neuropharmacology 53: 415-420.

Gladding CM and Raymond LA (2011) Mechanisms underlying NMDA receptor synaptic/extrasynaptic distribution and function. Molecular and Cellular Neuroscience 48: 308-320.

Gladding CM and Raymond LA (2011) Mechanisms underlying NMDA receptor synaptic/extrasynaptic distribution and function. Mol Cell Neurosci 48: 308-320.

Glasgow NG and Johnson JW (2014) Whole-cell patch-clamp analysis of recombinant NMDA receptor pharmacology using brief glutamate applications. Methods Mol Biol 1183: 23-41.

Glasgow NG, Siegler Retchless B and Johnson JW (2015) Molecular bases of NMDA receptor subtype-dependent properties. J Physiol 593: 83-95.

Gray John A, Shi Y, Usui H, During Matthew J, Sakimura K and Nicoll Roger A (2011) Distinct Modes of AMPA Receptor Suppression at Developing Synapses by GluN2A and GluN2B: Single-Cell NMDA Receptor Subunit Deletion In Vivo. Neuron 71: 1085-1101.

Groc L, Heine M, Cousins SL, Stephenson FA, Lounis B, Cognet L and Choquet D (2006) NMDA receptor surface mobility depends on NR2A-2B subunits. Proceedings of the National Academy of Sciences 103: 18769-18774.

Hamill OP, Marty A, Neher E, Sakmann B and Sigworth FJ (1981) Improved patch-clamp techniques for high-resolution current recording from cells and cell-free membrane patches. Pflugers Arch 391: 85-100.

Hansen KB, Ogden KK, Yuan H and Traynelis SF (2014) Distinct functional and pharmacological properties of Triheteromeric GluN1/GluN2A/GluN2B NMDA receptors. Neuron 81: 1084-1096.

Hardingham GE and Bading H (2010) Synaptic versus extrasynaptic NMDA receptor signalling: implications for neurodegenerative disorders. Nat Rev Neurosci 11: 682-696.

Hardingham GE, Fukunaga Y and Bading H (2002) Extrasynaptic NMDARs oppose synaptic NMDARs by triggering CREB shut-off and cell death pathways. Nature Neuroscience.

Harris AZ and Pettit DL (2007) Extrasynaptic and synaptic NMDA receptors form stable and uniform pools in rat hippocampal slices. The Journal of Physiology 584: 509-519.

Harris AZ and Pettit DL (2008) Recruiting extrasynaptic NMDA receptors augments synaptic signaling. J Neurophysiol 99: 524-533.

Hatton CJ and Paoletti P (2005) Modulation of Triheteromeric NMDA Receptors by N-Terminal Domain Ligands. Neuron 46: 261-274.

Herman MA and Jahr CE (2007) Extracellular glutamate concentration in hippocampal slice. J Neurosci 27: 9736-9741.

Hille B (2001). Ion channels of excitable membranes. Sunderland, Mass., Sinauer.

Huettner JE and Bean BP (1988) Block of N-methyl-D-aspartate-activated current by the anticonvulsant MK-801: selective binding to open channels. Proc Natl Acad Sci U S A 85: 1307-1311.

Iizuka A, Nakamura K and Hirai H (2015) Long-term oral administration of the NMDA receptor antagonist memantine extends life span in spinocerebellar ataxia type 1 knock-in mice. Neurosci Lett 592: 37-41.

Izumi Y, Tokuda K and Zorumski CF (2008) Long-term potentiation inhibition by low-level N-methyl-D-aspartate receptor activation involves calcineurin, nitric oxide, and p38 mitogen-activated protein kinase. Hippocampus 18: 258-265.

Jahr CE and Stevens CF (1990) A quantitative description of NMDA receptor-channel kinetic behavior. J Neurosci 10: 1830-1837.

Joe N, Scott V and Brown CH (2014) Glial regulation of extrasynaptic NMDA receptor-mediated excitation of supraoptic nucleus neurones during dehydration. J Neuroendocrinol 26: 35-42.

Johnson JW and Ascher P (1987) Glycine potentiates the NMDA response in cultured mouse brain neurons. Nature 325: 529-531.

Johnson JW, Glasgow NG and Povysheva NV (2015) Recent insights into the mode of action of memantine and ketamine. Curr Opin Pharmacol 20: 54-63.

Johnson JW and Kotermanski SE (2006) Mechanism of action of memantine. Curr Opin Pharmacol 6: 61-67.

Johnson JW and Qian A (2002) Interaction between channel blockers and channel gating of NMDA receptors. Biologicheskie Membrany 19: 17-22.

Kafi H, Salamzadeh J, Beladimoghadam N, Sistanizad M and Kouchek M (2014) Study of the neuroprotective effects of memantine in patients with mild to moderate ischemic stroke. Iran J Pharm Res 13: 591-598.

Kampa BM, Clements J, Jonas P and Stuart GJ (2004) Kinetics of Mg2+ unblock of NMDA receptors: implications for spike-timing dependent synaptic plasticity. J Physiol 556: 337-345.

Karakas E and Furukawa H (2014) Crystal structure of a heterotetrameric NMDA receptor ion channel. Science 344: 992-997.

Kashiwagi K, Masuko T, Nguyen CD, Kuno T, Tanaka I, Igarashi K and Williams K (2002) Channel blockers acting at N-methyl-D-aspartate receptors: differential effects of mutations in the vestibule and ion channel pore. Mol Pharmacol 61: 533-545.

Katagiri H, Tanaka K and Manabe T (2001) Requirement of appropriate glutamate concentrations in the synaptic cleft for hippocampal LTP induction. Eur J Neurosci 14: 547-553.

Kaufman AM, Milnerwood AJ, Sepers MD, Coquinco A, She K, Wang L, Lee H, Craig AM, Cynader M and Raymond LA (2012) Opposing Roles of Synaptic and Extrasynaptic NMDA Receptor Signaling in Cocultured Striatal and Cortical Neurons. J Neurosci 32: 3992-4003.

Kavalali ET and Monteggia LM (2015) How does ketamine elicit a rapid antidepressant response? Curr Opin Pharmacol 20: 35-39.

Kleckner NW and Dingledine R (1988) Requirement for glycine in activation of NMDA-receptors expressed in Xenopus oocytes. Science 241: 835-837.

Korinek M, Vyklicky V, Borovska J, Lichnerova K, Kaniakova M, Krausova B, Krusek J, Balik A, Smejkalova T, Horak M and Vyklicky L (2015) Cholesterol modulates open probability and desensitization of NMDA receptors. J Physiol 593: 2279-2293.

Kotermanski SE and Johnson JW (2009) Mg2+ imparts NMDA receptor subtype selectivity to the Alzheimer's drug memantine. J Neurosci 29: 2774-2779.

Kotermanski SE, Wood JT and Johnson JW (2009) Memantine binding to a superficial site on NMDA receptors contributes to partial trapping. J Physiol 587: 4589-4604.

Krupp JJ, Vissel B, Heinemann SF and Westbrook GL (1996) Calcium-dependent inactivation of recombinant N-methyl-D-aspartate receptors is NR2 subunit specific. Mol Pharmacol 50: 1680-1688.

Krupp JJ, Vissel B, Heinemann SF and Westbrook GL (1998) N-terminal domains in the NR2 subunit control desensitization of NMDA receptors. Neuron 20: 317-327.

Krupp JJ, Vissel B, Thomas CG, Heinemann SF and Westbrook GL (1999) Interactions of calmodulin and alpha-actinin with the NR1 subunit modulate Ca2+-dependent inactivation of NMDA receptors. J Neurosci 19: 1165-1178.

Krupp JJ, Vissel B, Thomas CG, Heinemann SF and Westbrook GL (2002) Calcineurin acts via the C-terminus of NR2A to modulate desensitization of NMDA receptors. Neuropharmacology 42: 593-602.

Krystal JH, D'Souza DC, Mathalon D, Perry E, Belger A and Hoffman R (2003) NMDA receptor antagonist effects, cortical glutamatergic function, and schizophrenia: toward a paradigm shift in medication development. Psychopharmacology (Berl) 169: 215-233.

Krystal JH, Karper LP, Seibyl JP, Freeman GK, Delaney R, Bremner JD, Heninger GR, Bowers MB, Jr. and Charney DS (1994) Subanesthetic effects of the noncompetitive NMDA antagonist, ketamine, in humans. Psychotomimetic, perceptual, cognitive, and neuroendocrine responses. Arch Gen Psychiatry 51: 199-214.

Krystal JH, Sanacora G and Duman RS (2013) Rapid-acting glutamatergic antidepressants: the path to ketamine and beyond. Biol Psychiatry 73: 1133-1141.

Kuner T and Schoepfer R (1996) Multiple structural elements determine subunit specificity of Mg2+ block in NMDA receptor channels. J Neurosci 16: 3549-3558.

Kupfer DJ, Frank E and Phillips ML (2012) Major depressive disorder: new clinical, neurobiological, and treatment perspectives. Lancet 379: 1045-1055.

Kussius CL, Kaur N and Popescu GK (2009) Pregnanolone sulfate promotes desensitization of activated NMDA receptors. J Neurosci 29: 6819-6827.

Kussius CL and Popescu GK (2009) Kinetic basis of partial agonism at NMDA receptors. Nat Neurosci 12: 1114-1120.

Kutsuwada T, Kashiwabuchi N, Mori H, Sakimura K, Kushiya E, Araki K, Meguro H, Masaki H, Kumanishi T, Arakawa M and et al. (1992) Molecular diversity of the NMDA receptor channel. Nature 358: 36-41.

Landwehrmeyer GB, Standaert DG, Testa CM, Penney JB, Jr. and Young AB (1995) NMDA receptor subunit mRNA expression by projection neurons and interneurons in rat striatum. J Neurosci 15: 5297-5307.

Lau A and Tymianski M (2010) Glutamate receptors, neurotoxicity and neurodegeneration. Pflügers Archiv - European Journal of Physiology 460: 525-542.

Lau A and Tymianski M (2010) Glutamate receptors, neurotoxicity and neurodegeneration. Pflugers Arch 460: 525-542.

Laurie DJ and Seeburg PH (1994) Regional and developmental heterogeneity in splicing of the rat brain NMDAR1 mRNA. J Neurosci 14: 3180-3194.

Le Meur K, Galante M, Angulo MC and Audinat E (2007) Tonic activation of NMDA receptors by ambient glutamate of non-synaptic origin in the rat hippocampus. J Physiol 580: 373-383.

Lee C-H, Lu W, Michel JC, Goehring A, Du J, Song X and Gouaux E (2014) NMDA receptor structures reveal subunit arrangement and pore architecture. Nature 511: 191-197.

Legendre P, Rosenmund C and Westbrook GL (1993) Inactivation of NMDA channels in cultured hippocampal neurons by intracellular calcium. J Neurosci 13: 674-684.

Lenaeus MJ, Burdette D, Wagner T, Focia PJ and Gross A (2014) Structures of KcsA in complex with symmetrical quaternary ammonium compounds reveal a hydrophobic binding site. Biochemistry 53: 5365-5373.

Lerma J, Zukin RS and Bennett MV (1990) Glycine decreases desensitization of N-methyl-D-aspartate (NMDA) receptors expressed in Xenopus oocytes and is required for NMDA responses. Proc Natl Acad Sci U S A 87: 2354-2358.

Lester RA, Clements JD, Westbrook GL and Jahr CE (1990) Channel kinetics determine the time course of NMDA receptor-mediated synaptic currents. Nature 346: 565-567.

Lester RA and Jahr CE (1992) NMDA channel behavior depends on agonist affinity. J Neurosci 12: 635-643.

Lester RA, Tong G and Jahr CE (1993) Interactions between the glycine and glutamate binding sites of the NMDA receptor. J Neurosci 13: 1088-1096.

Leveille F, El gaamouch F, Gouix E, Lecocq M, Lobner D, Nicole O and Buisson A (2008) Neuronal viability is controlled by a functional relation between synaptic and extrasynaptic NMDA receptors. The FASEB Journal 22: 4258-4271.

Leveille F, Papadia S, Fricker M, Bell KFS, Soriano FX, Martel MA, Puddifoot C, Habel M, Wyllie DJ, Ikonomidou C, Tolkovsky AM and Hardingham GE (2010) Suppression of the Intrinsic Apoptosis Pathway by Synaptic Activity. Journal of Neuroscience 30: 2623-2635.

Li S, Jin M, Koeglsperger T, Shepardson NE, Shankar GM and Selkoe DJ (2011) Soluble Abeta oligomers inhibit long-term potentiation through a mechanism involving excessive activation of extrasynaptic NR2B-containing NMDA receptors. J Neurosci 31: 6627-6638.

Limapichat W, Yu WY, Branigan E, Lester HA and Dougherty DA (2013) Key binding interactions for memantine in the NMDA receptor. ACS Chem Neurosci 4: 255-260.

Lipton P (1999) Ischemic cell death in brain neurons. Physiol Rev 79: 1431-1568.

Lipton SA (2004) Failures and successes of NMDA receptor antagonists: molecular basis for the use of open-channel blockers like memantine in the treatment of acute and chronic neurologic insults. NeuroRx 1: 101-110.

Lipton SA (2006) Paradigm shift in neuroprotection by NMDA receptor blockade: memantine and beyond. Nat Rev Drug Discov 5: 160-170.

Lipton SA (2006) Paradigm shift in neuroprotection by NMDA receptor blockade: Memantine and beyond. Nature Reviews Drug Discovery 5: 160-170.

Liu DD, Yang Q and Li ST (2013) Activation of extrasynaptic NMDA receptors induces LTD in rat hippocampal CA1 neurons. Brain Res Bull 93: 10-16.

Liu L, Wong TP, Pozza MF, Lingenhoehl K, Wang Y, Sheng M, Auberson YP and Wang YT (2004) Role of NMDA receptor subtypes in governing the direction of hippocampal synaptic plasticity. Science 304: 1021-1024.

Liu Y, Wong TP, Aarts M, Rooyakkers A, Liu L, Lai TW, Wu DC, Lu J, Tymianski M, Craig AM and Wang YT (2007) NMDA receptor subunits have differential roles in mediating excitotoxic neuronal death both in vitro and in vivo. J Neurosci 27: 2846-2857.

Lo FS, Blue ME and Erzurumlu RS (2015) Enhancement of postsynaptic GABAA and extrasynaptic NMDA receptor-mediated responses in the barrel cortex of Mecp2-null mice. J Neurophysiol: jn 00944 02015.

Lozovaya NA (2004) Extrasynaptic NR2B and NR2D subunits of NMDA receptors shape 'superslow' afterburst EPSC in rat hippocampus. The Journal of Physiology 558: 451-463.

Luo J, Wang Y, Yasuda RP, Dunah AW and Wolfe BB (1997) The majority of N-methyl-D-aspartate receptor complexes in adult rat cerebral cortex contain at least three different subunits (NR1/NR2A/NR2B). Mol Pharmacol 51: 79-86.

MacDermott AB, Mayer ML, Westbrook GL, Smith SJ and Barker JL (1986) NMDA-receptor activation increases cytoplasmic calcium concentration in cultured spinal cord neurones. Nature 321: 519-522.

Maki BA and Popescu GK (2014) Extracellular Ca(2+) ions reduce NMDA receptor conductance and gating. J Gen Physiol 144: 379-392.

Malenka RC and Bear MF (2004) LTP and LTD: an embarrassment of riches. Neuron 44: 5-21.

Martel M-A, Ryan Tomás J, Bell Karen FS, Fowler Jill H, McMahon A, Al-Mubarak B, Komiyama Noboru H, Horsburgh K, Kind Peter C, Grant Seth GN, Wyllie David JA and Hardingham Giles E (2012) The Subtype of GluN2 C-terminal Domain Determines the Response to Excitotoxic Insults. Neuron 74: 543-556.

Martel MA, Wyllie DJA and Hardingham GE (2009) In developing hippocampal neurons, NR2B-containing N-methyl-D-aspartate receptors (NMDARs) can mediate signaling to neuronal survival and synatpic potentiation, as well as neuronal death. Neuroscience 158: 334-343.

Massey PV, Johnson BE, Moult PR, Auberson YP, Brown MW, Molnar E, Collingridge GL and Bashir ZI (2004) Differential roles of NR2A and NR2B-containing NMDA receptors in cortical long-term potentiation and long-term depression. J Neurosci 24: 7821-7828.

Mayer ML, Vyklicky L, Jr. and Clements J (1989) Regulation of NMDA receptor desensitization in mouse hippocampal neurons by glycine. Nature 338: 425-427.

Mayer ML and Westbrook GL (1987) Permeation and block of N-methyl-D-aspartic acid receptor channels by divalent cations in mouse cultured central neurones. J Physiol 394: 501-527.

Mayer ML, Westbrook GL and Guthrie PB (1984) Voltage-dependent block by Mg2+ of NMDA responses in spinal cord neurones. Nature 309: 261-263.

McKay S, Bengtson CP, Bading H, Wyllie DJ and Hardingham GE (2013) Recovery of NMDA receptor currents from MK-801 blockade is accelerated by Mg2+ and memantine under conditions of agonist exposure. Neuropharmacology 74: 119-125.

Mealing GA, Lanthorn TH, Murray CL, Small DL and Morley P (1999) Differences in degree of trapping of low-affinity uncompetitive N-methyl-D-aspartic acid receptor antagonists with similar kinetics of block. J Pharmacol Exp Ther 288: 204-210.

Mealing GA, Lanthorn TH, Small DL, Murray RJ, Mattes KC, Comas TM and Morley P (2001) Structural modifications to an N-methyl-D-aspartate receptor antagonist result in large differences in trapping block. J Pharmacol Exp Ther 297: 906-914.

Medina I, Filippova N, Bakhramov A and Bregestovski P (1996) Calcium-induced inactivation of NMDA receptor-channels evolves independently of run-down in cultured rat brain neurones. J Physiol 495 (Pt 2): 411-427.

Medina I, Filippova N, Charton G, Rougeole S, Ben-Ari Y, Khrestchatisky M and Bregestovski P (1995) Calcium-dependent inactivation of heteromeric NMDA receptor-channels expressed in human embryonic kidney cells. J Physiol 482 (Pt 3): 567-573.

Meyerson JR, Kumar J, Chittori S, Rao P, Pierson J, Bartesaghi A, Mayer ML and Subramaniam S (2014) Structural mechanism of glutamate receptor activation and desensitization. Nature 514: 328-334.

Miller OH, Yang L, Wang CC, Hargroder EA, Zhang Y, Delpire E and Hall BJ (2014) GluN2B-containing NMDA receptors regulate depression-like behavior and are critical for the rapid antidepressant actions of ketamine. Elife 3: e03581.

Milnerwood AJ, Gladding CM, Pouladi MA, Kaufman AM, Hines RM, Boyd JD, Ko RW, Vasuta OC, Graham RK, Hayden MR, Murphy TH and Raymond LA (2010) Early increase in extrasynaptic NMDA receptor signaling and expression contributes to phenotype onset in Huntington's disease mice. Neuron 65: 178-190.

Milnerwood AJ, Kaufman AM, Sepers MD, Gladding CM, Zhang L, Wang L, Fan J, Coquinco A, Qiao JY, Lee H, Wang YT, Cynader M and Raymond LA (2012) Mitigation of augmented extrasynaptic NMDAR signaling and apoptosis in cortico-striatal co-cultures from Huntington's disease mice. Neurobiol Dis 48: 40-51.

Monyer H, Burnashev N, Laurie DJ, Sakmann B and Seeburg PH (1994) Developmental and regional expression in the rat brain and functional properties of four NMDA receptors. Neuron 12: 529-540.

Monyer H, Sprengel R, Schoepfer R, Herb A, Higuchi M, Lomeli H, Burnashev N, Sakmann B and Seeburg PH (1992) Heteromeric NMDA receptors: molecular and functional distinction of subtypes. Science 256: 1217-1221.

Muller T, Albrecht D and Gebhardt C (2009) Both NR2A and NR2B subunits of the NMDA receptor are critical for long-term potentiation and long-term depression in the lateral amygdala of horizontal slices of adult mice. Learn Mem 16: 395-405.

Neher E and Steinbach JH (1978) Local anaesthetics transiently block currents through single acetylcholine-receptor channels. J Physiol 277: 153-176.

Nikolaev MV, Magazanik LG and Tikhonov DB (2012) Influence of external magnesium ions on the NMDA receptor channel block by different types of organic cations. Neuropharmacology 62: 2078-2085.

Nosyreva E, Szabla K, Autry AE, Ryazanov AG, Monteggia LM and Kavalali ET (2013) Acute suppression of spontaneous neurotransmission drives synaptic potentiation. J Neurosci 33: 6990-7002.

Nowak L, Bregestovski P, Ascher P, Herbet A and Prochiantz A (1984) Magnesium gates glutamate-activated channels in mouse central neurones. Nature 307: 462-465.

Okamoto S, Pouladi MA, Talantova M, Yao D, Xia P, Ehrnhoefer DE, Zaidi R, Clemente A, Kaul M, Graham RK, Zhang D, Vincent Chen HS, Tong G, Hayden MR and Lipton SA (2009) Balance between synaptic versus extrasynaptic NMDA receptor activity influences inclusions and neurotoxicity of mutant huntingtin. Nature medicine 15: 1407-1413.

Orser BA, Pennefather PS and MacDonald JF (1997) Multiple mechanisms of ketamine blockade of N-methyl-D-aspartate receptors. Anesthesiology 86: 903-917.

Otton HJ, Lawson McLean A, Pannozzo MA, Davies CH and Wyllie DJ (2011) Quantification of the Mg2+-induced potency shift of amantadine and memantine voltage-dependent block in human recombinant GluN1/GluN2A NMDARs. Neuropharmacology 60: 388-396.

Palmer GC (2001) Neuroprotection by NMDA receptor antagonists in a variety of neuropathologies. Curr Drug Targets 2: 241-271.

Pan J, Chen Q, Willenbring D, Mowrey D, Kong XP, Cohen A, Divito CB, Xu Y and Tang P (2012) Structure of the pentameric ligand-gated ion channel GLIC bound with anesthetic ketamine. Structure 20: 1463-1469.

Paoletti P, Ascher P and Neyton J (1997) High-affinity zinc inhibition of NMDA NR1-NR2A receptors. J Neurosci 17: 5711-5725.

Paoletti P, Bellone C and Zhou Q (2013) NMDA receptor subunit diversity: impact on receptor properties, synaptic plasticity and disease. Nat Rev Neurosci 14: 383-400.

Papadia S, Soriano FX, Léveillé F, Martel M-A, Dakin KA, Hansen HH, Kaindl A, Sifringer M, Fowler J, Stefovska V, McKenzie G, Craigon M, Corriveau R, Ghazal P, Horsburgh K,

Yankner BA, Wyllie DJA, Ikonomidou C and Hardingham GE (2008) Synaptic NMDA receptor activity boosts intrinsic antioxidant defenses. Nature Neuroscience 11: 476-487.

Papouin T, Ladepeche L, Ruel J, Sacchi S, Labasque M, Hanini M, Groc L, Pollegioni L, Mothet JP and Oliet SH (2012) Synaptic and extrasynaptic NMDA receptors are gated by different endogenous coagonists. Cell 150: 633-646.

Papp E, Rivera C, Kaila K and Freund TF (2008) Relationship between neuronal vulnerability and potassium-chloride cotransporter 2 immunoreactivity in hippocampus following transient forebrain ischemia. Neuroscience 154: 677-689.

Parsons CG, Gilling KE and Jatzke C (2008) Blocking kinetics of memantine on NR1a/2A receptors recorded in inside-out and outside-out patches from Xenopus oocytes. J Neural Transm (Vienna) 115: 1367-1373.

Parsons CG, Quack G, Bresink I, Baran L, Przegalinski E, Kostowski W, Krzascik P, Hartmann S and Danysz W (1995) Comparison of the potency, kinetics and voltage-dependency of a series of uncompetitive NMDA receptor antagonists in vitro with anticonvulsive and motor impairment activity in vivo. Neuropharmacology 34: 1239-1258.

Parsons CG, Stoffler A and Danysz W (2007) Memantine: a NMDA receptor antagonist that improves memory by restoration of homeostasis in the glutamatergic system - too little activation is bad, too much is even worse. Neuropharmacology 53: 699-723.

Parsons CG, Stöffler A and Danysz W (2007) Memantine: a NMDA receptor antagonist that improves memory by restoration of homeostasis in the glutamatergic system - too little activation is bad, too much is even worse. Neuropharmacology 53: 699-723.

Parsons MP and Raymond LA (2014) Extrasynaptic NMDA receptor involvement in central nervous system disorders. Neuron 82: 279-293.

Partin KM, Fleck MW and Mayer ML (1996) AMPA receptor flip/flop mutants affecting deactivation, desensitization, and modulation by cyclothiazide, aniracetam, and thiocyanate. J Neurosci 16: 6634-6647.

Paupard MC, Friedman LK and Zukin RS (1997) Developmental regulation and cell-specific expression of N-methyl-D-aspartate receptor splice variants in rat hippocampus. Neuroscience 79: 399-409.

Payandeh J, Scheuer T, Zheng N and Catterall WA (2011) The crystal structure of a voltage-gated sodium channel. Nature 475: 353-358.

Persson J (2013) Ketamine in pain management. CNS neuroscience & therapeutics 19: 396-402.

Petralia RS, Wang YX, Hua F, Yi Z, Zhou A, Ge L, Stephenson FA and Wenthold RJ (2010) Organization of NMDA receptors at extrasynaptic locations. Neuroscience 167: 68-87.

Phelan MC (2006) Techniques for mammalian cell tissue culture. Curr Protoc Mol Biol Appendix 3: Appendix 3F.

Pittenger C, Sanacora G and Krystal JH (2007) The NMDA receptor as a therapeutic target in major depressive disorder. CNS Neurol Disord Drug Targets 6: 101-115.

Popescu G, Robert A, Howe JR and Auerbach A (2004) Reaction mechanism determines NMDA receptor response to repetitive stimulation. Nature 430: 790-793.

Povysheva NV and Johnson JW (2012) Tonic NMDA receptor-mediated current in prefrontal cortical pyramidal cells and fast-spiking interneurons. J Neurophysiol 107: 2232-2243.

Priestley T, Laughton P, Myers J, Le Bourdelles B, Kerby J and Whiting PJ (1995) Pharmacological properties of recombinant human N-methyl-D-aspartate receptors comprising NR1a/NR2A and NR1a/NR2B subunit assemblies expressed in permanently transfected mouse fibroblast cells. Mol Pharmacol 48: 841-848.

Pringle A, Parsons E, Cowen LG, McTavish SF, Cowen PJ and Harmer CJ (2012) Using an experimental medicine model to understand the antidepressant potential of the N-Methyl-D-aspartic acid (NMDA) receptor antagonist memantine. Journal of psychopharmacology 26: 1417-1423.

Prommer EE (2012) Ketamine for pain: an update of uses in palliative care. J Palliat Med 15: 474-483.

Qian A, Antonov SM and Johnson JW (2002) Modulation by permeant ions of Mg(2+) inhibition of NMDA-activated whole-cell currents in rat cortical neurons. J Physiol 538: 65-77.

Raman IM, Tong G and Jahr CE (1996) Beta-adrenergic regulation of synaptic NMDA receptors by cAMP-dependent protein kinase. Neuron 16: 415-421.

Rauner C and Kohr G (2010) Triheteromeric NR1/NR2A/NR2B Receptors Constitute the Major N-Methyl-D-aspartate Receptor Population in Adult Hippocampal Synapses. Journal of Biological Chemistry 286: 7558-7566.

Reisberg B, Doody R, Stoffler A, Schmitt F, Ferris S, Mobius HJ and Memantine Study G (2003) Memantine in moderate-to-severe Alzheimer's disease. N Engl J Med 348: 1333-1341.

Riebe I, Seth H, Culley G, Dosa Z, Radi S, Strand K, Frojd V and Hanse E (2016) Tonically active NMDA receptors - a signalling mechanism critical for interneuronal excitability in the CA1 stratum radiatum. Eur J Neurosci 43: 169-178.

Rosenmund C and Westbrook GL (1993) Rundown of N-methyl-D-aspartate channels during whole-cell recording in rat hippocampal neurons: role of Ca2+ and ATP. J Physiol 470: 705-729.

Rycroft BK and Gibb AJ (2004) Inhibitory interactions of calcineurin (phosphatase 2B) and calmodulin on rat hippocampal NMDA receptors. Neuropharmacology 47: 505-514.

Rycroft BK and Gibb AJ (2004) Regulation of single NMDA receptor channel activity by alpha-actinin and calmodulin in rat hippocampal granule cells. J Physiol 557: 795-808.

Sakimura K, Kutsuwada T, Ito I, Manabe T, Takayama C, Kushiya E, Yagi T, Aizawa S, Inoue Y, Sugiyama H and et al. (1995) Reduced hippocampal LTP and spatial learning in mice lacking NMDA receptor epsilon 1 subunit. Nature 373: 151-155.

Sani G, Serra G, Kotzalidis GD, Romano S, Tamorri SM, Manfredi G, Caloro M, Telesforo CL, Caltagirone SS, Panaccione I, Simonetti A, Demontis F and Girardi P (2012) The role of memantine in the treatment of psychiatric disorders other than the dementias: a review of current preclinical and clinical evidence. CNS drugs 26: 663-690.

Schell MJ, Molliver ME and Snyder SH (1995) D-serine, an endogenous synaptic modulator: localization to astrocytes and glutamate-stimulated release. Proc Natl Acad Sci U S A 92: 3948-3952.

Schneggenburger R (1996) Simultaneous measurement of Ca2+ influx and reversal potentials in recombinant N-methyl-D-aspartate receptor channels. Biophys J 70: 2165-2174.

Schorge S, Elenes S and Colquhoun D (2005) Maximum likelihood fitting of single channel NMDA activity with a mechanism composed of independent dimers of subunits. J Physiol 569: 395-418.

Sheng M, Cummings J, Roldan LA, Jan YN and Jan LY (1994) Changing subunit composition of heteromeric NMDA receptors during development of rat cortex. Nature 368: 144-147.

Shepherd JD and Huganir RL (2007) The cell biology of synaptic plasticity: AMPA receptor trafficking. Annu Rev Cell Dev Biol 23: 613-643.

Siegler Retchless B, Gao W and Johnson JW (2012) A single GluN2 subunit residue controls NMDA receptor channel properties via intersubunit interaction. Nat Neurosci 15: 406-413, S401-402.

Sigworth FJ and Neher E (1980) Single Na+ channel currents observed in cultured rat muscle cells. Nature 287: 447-449.

Sobolevskii AI and Khodorov BI (2002) Blocker studies of the functional architecture of the NMDA receptor channel. Neurosci Behav Physiol 32: 157-171.

Sobolevsky A and Koshelev S (1998) Two blocking sites of amino-adamantane derivatives in open N-methyl-D-aspartate channels. Biophys J 74: 1305-1319.

Sobolevsky AI, Koshelev SG and Khodorov BI (1998) Interaction of memantine and amantadine with agonist-unbound NMDA-receptor channels in acutely isolated rat hippocampal neurons. J Physiol 512 (Pt 1): 47-60.

Sobolevsky AI, Rosconi MP and Gouaux E (2009) X-ray structure, symmetry and mechanism of an AMPA-subtype glutamate receptor. Nature 462: 745-756.

Sobolevsky AI and Yelshansky MV (2000) The trapping block of NMDA receptor channels in acutely isolated rat hippocampal neurones. J Physiol 526 Pt 3: 493-506.

Sprengel R, Suchanek B, Amico C, Brusa R, Burnashev N, Rozov A, Hvalby O, Jensen V, Paulsen O, Andersen P, Kim JJ, Thompson RF, Sun W, Webster LC, Grant SG, Eilers J, Konnerth A, Li J, McNamara JO and Seeburg PH (1998) Importance of the intracellular domain of NR2 subunits for NMDA receptor function in vivo. Cell 92: 279-289.

Stout AK, Li-Smerin Y, Johnson JW and Reynolds IJ (1996) Mechanisms of glutamate-stimulated Mg2+ influx and subsequent Mg2+ efflux in rat forebrain neurones in culture. J Physiol 492 (Pt 3): 641-657.

Stroebel D, Carvalho S, Grand T, Zhu S and Paoletti P (2014) Controlling NMDA receptor subunit composition using ectopic retention signals. J Neurosci 34: 16630-16636.

Strong KL, Jing Y, Prosser AR, Traynelis SF and Liotta DC (2014) NMDA receptor modulators: an updated patent review (2013-2014). Expert Opin Ther Pat 24: 1349-1366.

Swanson GT and Heinemann SF (1998) Heterogeneity of homomeric GluR5 kainate receptor desensitization expressed in HEK293 cells. J Physiol 513 (Pt 3): 639-646.

Talantova M, Sanz-Blasco S, Zhang X, Xia P, Akhtar MW, Okamoto S, Dziewczapolski G, Nakamura T, Cao G, Pratt AE, Kang YJ, Tu S, Molokanova E, McKercher SR, Hires SA, Sason H, Stouffer DG, Buczynski MW, Solomon JP, Michael S, Powers ET, Kelly JW, Roberts A, Tong G, Fang-Newmeyer T, Parker J, Holland EA, Zhang D, Nakanishi N, Chen HS, Wolosker H, Wang Y, Parsons LH, Ambasudhan R, Masliah E, Heinemann SF, Pina-Crespo JC and Lipton SA (2013) Abeta induces astrocytic glutamate release, extrasynaptic NMDA receptor activation, and synaptic loss. Proc Natl Acad Sci U S A 110: E2518-2527.

Tang CM, Dichter M and Morad M (1990) Modulation of the N-methyl-D-aspartate channel by extracellular H+. Proc Natl Acad Sci U S A 87: 6445-6449.

Thomas CG, Miller AJ and Westbrook GL (2006) Synaptic and extrasynaptic NMDA receptor NR2 subunits in cultured hippocampal neurons. J Neurophysiol 95: 1727-1734.

Tong G and Jahr CE (1994) Regulation of glycine-insensitive desensitization of the NMDA receptor in outside-out patches. J Neurophysiol 72: 754-761.

Tong G, Shepherd D and Jahr CE (1995) Synaptic desensitization of NMDA receptors by calcineurin. Science 267: 1510-1512.

Tovar KR, McGinley MJ and Westbrook GL (2013) Triheteromeric NMDA Receptors at Hippocampal Synapses. J Neurosci 33: 9150-9160.

Tovar KR and Westbrook GL (1999) The incorporation of NMDA receptors with a distinct subunit composition at nascent hippocampal synapses in vitro. J Neurosci 19: 4180-4188.

Traynelis SF, Burgess MF, Zheng F, Lyuboslavsky P and Powers JL (1998) Control of voltage-independent zinc inhibition of NMDA receptors by the NR1 subunit. J Neurosci 18: 6163-6175.

Traynelis SF and Cull-Candy SG (1990) Proton inhibition of N-methyl-D-aspartate receptors in cerebellar neurons. Nature 345: 347-350.

Traynelis SF and Cull-Candy SG (1991) Pharmacological properties and H+ sensitivity of excitatory amino acid receptor channels in rat cerebellar granule neurones. J Physiol 433: 727-763.

Traynelis SF, Hartley M and Heinemann SF (1995) Control of proton sensitivity of the NMDA receptor by RNA splicing and polyamines. Science 268: 873-876.

Traynelis SF, Wollmuth LP, McBain CJ, Menniti FS, Vance KM, Ogden KK, Hansen KB, Yuan H, Myers SJ and Dingledine R (2010) Glutamate Receptor Ion Channels: Structure, Regulation, and Function. Pharmacological Reviews 62: 405-496.

Tu S, Okamoto S, Lipton SA and Xu H (2014) Oligomeric Abeta-induced synaptic dysfunction in Alzheimer's disease. Mol Neurodegener 9: 48.

Vance KM, Hansen KB and Traynelis SF (2012) GluN1 splice variant control of GluN1/GluN2D NMDA receptors. J Physiol 590: 3857-3875.

Vance KM, Hansen KB and Traynelis SF (2013) Modal gating of GluN1/GluN2D NMDA receptors. Neuropharmacology 71: 184-190.

Vargas-Caballero M and Robinson HP (2004) Fast and slow voltage-dependent dynamics of magnesium block in the NMDA receptor: the asymmetric trapping block model. J Neurosci 24: 6171-6180.

Varney MA, Jachec C, Deal C, Hess SD, Daggett LP, Skvoretz R, Urcan M, Morrison JH, Moran T, Johnson EC and Velicelebi G (1996) Stable expression and characterization of recombinant human heteromeric N-methyl-D-aspartate receptor subtypes NMDAR1A/2A and NMDAR1A/2B in mammalian cells. J Pharmacol Exp Ther 279: 367-378.

Vicini S, Wang JF, Li JH, Zhu WJ, Wang YH, Luo JH, Wolfe BB and Grayson DR (1998) Functional and pharmacological differences between recombinant N-methyl-D-aspartate receptors. J Neurophysiol 79: 555-566.

Villarroel A, Regalado MP and Lerma J (1998) Glycine-independent NMDA receptor desensitization: localization of structural determinants. Neuron 20: 329-339.

von Engelhardt J, Coserea I, Pawlak V, Fuchs EC, Kohr G, Seeburg PH and Monyer H (2007) Excitotoxicity in vitro by NR2A- and NR2B-containing NMDA receptors. Neuropharmacology 53: 10-17.

Vyklicky L, Jr., Vlachova V and Krusek J (1990) The effect of external pH changes on responses to excitatory amino acids in mouse hippocampal neurones. J Physiol 430: 497-517.

Vyklicky V, Smejkalova T, Krausova B, Balik A, Korinek M, Borovska J, Horak M, Chvojkova M, Kleteckova L, Vales K, Cerny J, Nekardova M, Chodounska H, Kudova E and Vyklicky L (2016) Preferential Inhibition of Tonically over Phasically Activated NMDA Receptors by Pregnane Derivatives. J Neurosci 36: 2161-2175.

Watanabe M, Inoue Y, Sakimura K and Mishina M (1992) Developmental changes in distribution of NMDA receptor channel subunit mRNAs. Neuroreport 3: 1138-1140.

Wild AR, Akyol E, Brothwell SL, Kimkool P, Skepper JN, Gibb AJ and Jones S (2013) Memantine block depends on agonist presentation at the NMDA receptor in substantia nigra pars compacta dopamine neurones. Neuropharmacology 73: 138-146.

Williams K (1996) Separating dual effects of zinc at recombinant N-methyl-D-aspartate receptors. Neurosci Lett 215: 9-12.

Wills TA, Klug JR, Silberman Y, Baucum AJ, Weitlauf C, Colbran RJ, Delpire E and Winder DG (2012) GluN2B subunit deletion reveals key role in acute and chronic ethanol sensitivity of glutamate synapses in bed nucleus of the stria terminalis. Proc Natl Acad Sci U S A 109: E278-287.

Winblad B, Jones RW, Wirth Y, Stoffler A and Mobius HJ (2007) Memantine in moderate to severe Alzheimer's disease: a meta-analysis of randomised clinical trials. Dement Geriatr Cogn Disord 24: 20-27.

Witt A, Macdonald N and Kirkpatrick P (2004) Memantine hydrochloride. Nat Rev Drug Discov 3: 109-110.

Wroge CM, Hogins J, Eisenman L and Mennerick S (2012) Synaptic NMDA receptors mediate hypoxic excitotoxic death. J Neurosci 32: 6732-6742.

Wu YN and Johnson SW (2015) Memantine selectively blocks extrasynaptic NMDA receptors in rat substantia nigra dopamine neurons. Brain Res 1603: 1-7.

Wyszynski M, Lin J, Rao A, Nigh E, Beggs AH, Craig AM and Sheng M (1997) Competitive binding of alpha-actinin and calmodulin to the NMDA receptor. Nature 385: 439-442.

Xia P, Chen HS, Zhang D and Lipton SA (2010) Memantine preferentially blocks extrasynaptic over synaptic NMDA receptor currents in hippocampal autapses. The Journal of neuroscience : the official journal of the Society for Neuroscience 30: 11246-11250.

Yamakura T, Mori H, Masaki H, Shimoji K and Mishina M (1993) Different sensitivities of NMDA receptor channel subtypes to non-competitive antagonists. Neuroreport 4: 687-690.

Yelshanskaya MV, Li M and Sobolevsky AI (2014) Structure of an agonist-bound ionotropic glutamate receptor. Science 345: 1070-1074.

Yuan H, Erreger K, Dravid SM and Traynelis SF (2005) Conserved structural and functional control of N-methyl-D-aspartate receptor gating by transmembrane domain M3. J Biol Chem 280: 29708-29716.

Yuan H, Hansen KB, Zhang J, Pierson TM, Markello TC, Fajardo KV, Holloman CM, Golas G, Adams DR, Boerkoel CF, Gahl WA and Traynelis SF (2014) Functional analysis of a de novo GRIN2A missense mutation associated with early-onset epileptic encephalopathy. Nat Commun 5: 3251.

Yuan H, Myers SJ, Wells G, Nicholson KL, Swanger SA, Lyuboslavsky P, Tahirovic YA, Menaldino DS, Ganesh T, Wilson LJ, Liotta DC, Snyder JP and Traynelis SF (2015) Context-dependent GluN2B-selective inhibitors of NMDA receptor function are neuroprotective with minimal side effects. Neuron 85: 1305-1318.

Zhang S, Ehlers MD, Bernhardt JP, Su CT and Huganir RL (1998) Calmodulin mediates calcium-dependent inactivation of N-methyl-D-aspartate receptors. Neuron 21: 443-453.

Zhao JP and Constantine-Paton M (2007) NR2A-/- mice lack long-term potentiation but retain NMDA receptor and L-type Ca2+ channel-dependent long-term depression in the juvenile superior colliculus. J Neurosci 27: 13649-13654.

Zhao X, Marszalec W, Toth PT, Huang J, Yeh JZ and Narahashi T (2006) In vitro galantamine-memantine co-application: mechanism of beneficial action. Neuropharmacology 51: 1181-1191.

Zhou Q and Sheng M (2013) NMDA receptors in nervous system diseases. Neuropharmacology 74: 69-75.

Zhou X, Ding Q, Chen Z, Yun H and Wang H (2013) Involvement of the GluN2A and GluN2B subunits in synaptic and extrasynaptic N-methyl-D-aspartate receptor function and neuronal excitotoxicity. J Biol Chem 288: 24151-24159.

Zhou X, Hollern D, Liao J, Andrechek E and Wang H (2013) NMDA receptor-mediated excitotoxicity depends on the coactivation of synaptic and extrasynaptic receptors. Cell Death Dis 4: e560.

Zhu S and Paoletti P (2015) Allosteric modulators of NMDA receptors: multiple sites and mechanisms. Curr Opin Pharmacol 20: 14-23.